VAPOR-LIQUID EQUILIBRIUM OF POLYMER SOLUTIONS DURING THERMAL DECOMPOSITION OF RIGID FOAMS

by

Nathan H. King

A dissertation submitted to the faculty of

Brigham Young University

in partial fulfillment of the requirements for the degree of

Doctor of Philosophy

Department of Chemical Engineering

Brigham Young University

August 2008

BRIGHAM YOUNG UNIVERSITY

GRADUATE COMMITTEE APPROVAL

of a dissertation submitted by

Nathan H. King

This dissertation has been read by each member of the following graduate committee and by majority vote has been found to be satisfactory.

Date	Thomas H. Fletcher, Chair
Date	W. Vincent Wilding
Date	Kenneth L. Erickson
Date	William G. Pitt
Date	John L. Oscarson

BRIGHAM YOUNG UNIVERSITY

As chair of the candidate's graduate committee, I have read the dissertation of Nathan H. King in its final form and have found that (1) its format, citations, and bibliographical style are consistent and acceptable and fulfill university and department style requirements; (2) its illustrative materials including figures, tables, and charts are in place; and (3) the final manuscript is satisfactory to the graduate committee and is ready for submission to the university library.

Date

Thomas H. Fletcher
Chair, Graduate Committee

Accepted for the Department

Larry L. Baxter
Graduate Coordinator

Accepted for the College

Alan R. Parkinson
Dean, Ira A. Fulton College of Engineering and Technology

ABSTRACT

VAPOR-LIQUID EQUILIBRIUM OF POLYMER SOLUTIONS DURING THERMAL DECOMPOSITION OF RIGID FOAMS

Nathan H. King

Department of Chemical Engineering

Doctor of Philosophy

Removable Epoxy Foam (REF) and other rigid foams experience severe changes in structure and properties when exposed to high heat. As thermal energy breaks network bonds in the foam many species are formed, including large polymer-like network fragments and smaller solvent-like molecules. During this process a liquid phase may form. The vapor-liquid equilibrium (VLE) behavior of the polymer solutions formed during initial decomposition can be highly non-ideal.

In this research VLE behavior of high-temperature polymer solutions was studied and a procedure was developed for predicting that behavior during decomposition of rigid foams. A high-temperature VLE facility was built and validated, and equilibrium pressures were measured at temperatures between 75 and 250ºC for six polymer/solvent systems: two polymers – polyethylene glycol and polystyrene – with each of three solvents – benzene, furan, and 4-isopropylphenol. Calculations from eighteen polymer

solution models were compared with experimental results to determine which model best described the VLE behavior. These models included six existing activity coefficient models used alone, as well as in combinations with the Peng-Robinson equation of state (EOS) through the Wong-Sandler mixing rules.

Because several of the models required values for polymer volumes, a comparison of the GCVOL and GCMCM group-contribution volume estimation methods was performed. GCMCM was found to give lower overall deviations from literature polymer volume data.

The models involving an equation of state required EOS parameter values for the pure polymers. A new method for determining these parameters was proposed. Models using parameters from the new method gave better agreement with equilibrium pressure data than models using parameters from the recommended method in the literature.

While agreement with equilibrium pressure data was similar for several models, some models predicted a liquid phase split under certain conditions. Data were not available to verify the presence of two liquid phases, but are needed to make an appropriate recommendation of the best model. If liquid phase splitting does not occur, it is recommended that the UNIFAC-ZM activity coefficient model be used alone. If phase splitting behavior is observed, it is recommended that the UNIFAC-FV activity coefficient model be used in combination with the Peng-Robinson EOS.

ACKNOWLEDGMENTS

The funding for this research was provided by Sandia National Laboratories and the Bill and Margaret Pope Professorship. In addition, as this project was most definitely not accomplished solely on the merits of my own abilities, I would like to give my thanks to several people who helped and influenced me along the way:

To Ken Erickson for all of his advice and collaboration. To Amy Sun for her suggestions and assistance with the modeling. To Jim Grossman for helping me to get the HT-VLE facility working.

To my advisor, Dr. Fletcher, for guiding me through this project and encouraging me in so many ways. To Dr. Wilding for being almost a co-advisor at points, and for helping me with the thermodynamics. To the BYU ChE faculty for helping me to become not only a better chemical engineer, but also a better person.

To my loving wife, Leslie, who was my greatest supporter, and to our children, Morgan and Emma, who learned to pronounce “dissertation” so they could pray for me. And lastly, but most importantly, to my Father in Heaven who has in so many ways answered those prayers.

TABLE OF CONTENTS

LIST OF TABLES

LIST OF FIGURES

NOMENCLATURE

A^{ex}	excess Helmholtz energy
A_k	group parameter for GCVOL volume estimation method
a	energy parameter for cubic equation of state
a_1	solvent activity
a_{ij}	cross-energy parameter for cubic equation of state
a_k	group parameter for GCMCM
a_m	energy parameter of mixture for cubic equation of state
a_{mn}	group interaction parameter for UNIFAC model
B_k	group parameter for GCVOL volume estimation method
b	volume parameter for cubic equation of state; proportionality constant for UNIFAC-FV model
b_{ij}	cross-volume parameter for cubic equation of state
b_m	volume parameter of mixture for cubic equation of state
C_k	group parameter for GCVOL volume estimation method
c	one-third of the external degrees of freedom per molecule; equation of state-specific constant for Wong-Sandler mixing rules
c_0	correlation intercept
c_P	pressure coefficient
c_T	temperature coefficient
D	intermediate calculation in the Wong-Sandler mixing rules
e_k	energy group parameter for GCMCM
F_V	vapor fraction
G^{ex}	excess Gibbs energy
i	species index
j	species index
K_i	ratio of mole fraction of species i in vapor to mole fraction in liquid
k	group index
k_{ij}	binary interaction parameter for Wong-Sandler mixing rules
L	liquid fraction
M_0	molecular weight parameter for GCMCM
M_r	molecular weight of polymer repeat unit
n	group index

MW	molecular weight
MW_c	critical molecular weight
MW_n	number-average molecular weight
MW_w	weight-average molecular weight
N_i	moles of species i
N_L	moles of liquid
N_V	moles of vapor
n	number of species in system; number of repeat units in polymer; number of data points; group index
n_k	number of groups of type k
n_i^L	moles of species i in the liquid phase
n_i^V	moles of species i in the vapor phase
P	pressure
P^*	characteristic pressure for GCMCM
P_c	critical pressure
P_i^{sat}	vapor pressure of species i
P_{PR}	pressure calculated from Peng-Robinson equation of state
Q	intermediate calculation in Wong-Sandler mixing rules
Q_k	group surface area parameter
q_i	species surface area parameter
R	universal gas constant
R_k	group volume parameter
r	free-volume correction factor for GCMCM
r_i	ratio of free-volume of species i to free-volume of smallest species; species volume parameter
T	temperature
T^*	characteristic temperature for GCMCM
T_c	critical temperature
V^*	characteristic volume for GCMCM
$\widetilde{V}$	specific volume
$\overline{V}$	molar volume
$\overline{V}_L$	molar volume of liquid phase
$\overline{V}_V$	molar volume of vapor phase
V^{ex}	excess volume
V_{tot}	total volume of system
v_i	molar volume of species i
v_i^{fv}	free-volume of species i

v_i^{hc}	hard-core volume of species i
$\breve{v}_i$	reduced volume of species i for UNIFAC-FV model
$\breve{v}_M$	reduced volume of mixture for UNIFAC-FV model
W_i	mass of species i
X_m	surface area fraction of group m
x_i	mole fraction of species i in liquid phase
y_i	mole fraction of species i in vapor phase
y_i^{norm}	normalized mole fraction of species i in vapor phase
Z	compressibility factor
z	coordination number
z_i	overall mole fraction of species i in system

Greek symbols:

α	non-randomness parameter of Freed-FV model; function describing temperature dependence of energy parameter, a
β_{ij}	interaction term of Freed-FV model
Γ_k	residual activity coefficient of group k
$\Gamma_k^{(i)}$	residual activity coefficient of group k in a solution of only species i
γ_i	mole fraction-based activity coefficient of species i
ε	molecular attraction energy
ε^*	characteristic energy for GCMCM
Θ_m	surface area fraction of group k for UNIFAC
θ_i	surface area fraction of species i
θ_k	surface area fraction of group k for GCMCM
κ	intermediate calculation for energy parameter, a
$v_k^{(i)}$	the number of groups of type in k species i
ϕ_i^{fv}	free-volume fraction of species i
ϕ_i^{vol}	volume fraction of species i
ϕ_i^L	liquid phase fugacity coefficient of pure species i
$\hat{\phi}_i^L$	partial fugacity coefficient of species i in liquid phase mixture
ϕ_i^{sat}	fugacity coefficient of pure species i at its vapor pressure
ϕ_i^V	vapor phase fugacity coefficient of pure species i
$\hat{\phi}_i^V$	partial fugacity coefficient of species i in vapor phase mixture
χ	Flory-Huggins energy parameter
Ψ_{mn}	group interaction parameter
ω	acentric factor

GLOSSARY OF ABBREVIATIONS

General abbreviations:

AAD	Average absolute deviation
AC	Aromatic carbon
ACM	Activity coefficient model
BHT	Butylated hydroxytoluene
BYU	Brigham Young University
DGEBA	Diglycidyl ether of bisphenol-A
DIPPR	Design Institute for Physical Properties
EOS	Equation of state
FTIR	Fourier-transfer infrared spectroscopy
GC/MS	Gas chromatograph/mass spectrometer
GPC	Gel permeation chromatography
HT-VLE	High-temperature vapor-liquid equilibrium facility
IPP	Isopropylphenol
LCST	Lower critical solution temperature
LLE	Liquid-liquid equilibrium
MSDS	Material safety data sheet
REF	Removable Epoxy Foam
TGA	Thermal gravimetric analyzer
VLE	Vapor-liquid equilibrium

Equation of state and activity coefficient model abbreviations:

FH	Flory-Huggins model
FV	Free-volume
GC-Flory	Group-contribution Flory equation of state
GCLF	Group-contribution lattice-fluid equation of state
GK-FV	Entropic-FV model modified by Georgios Kontogeorgis
MEFV	Modified Entropic-FV model
PR	Peng-Robinson equation of state
PRSV	Peng-Robinson equation of state modified by Stryjek and Vera
PSCT	Perturbed Soft-Chain Theory equation of state
SRK	Soave-Redlich-Kwong equation of state
SWP	Sako-Wu-Prausnitz equation of state
UNIFAC-FV	UNIversal Functional Activity Coefficient-FV model
UNIFAC-ZM	UNIFAC model modified by Zhong and Masuoka

Polymer abbreviations:

EVA18	Poly(ethylene-*co*-vinyl acetate), 18 wt% vinyl acetate
HDPE	High-density (linear) polyethylene
PA66	Polyamide 6,6 (also called nylon 6,6)
PBSA	Poly(butylene succinate-*co*-adipate)
PBS-br	Poly(butylene succinate) (branched)
PC	Bisphenol-A polycarbonate
PDMS	Polydimethylsiloxane
PEG	Poly(ethylene glycol)
PEI	Polyetherimide
PEO	Poly(ethylene oxide)
PEOx	Poly(2-ethyl-2-oxazoline)
PIB	Polyisobutylene
PPO	Poly(2,6-dimethylphenylene oxide)
PS	Polystyrene
PVPhKH	Poly(vinyl phenyl ketone hydrogenated)

CHEMICAL STRUCTURE INDEX

Small molecules:

Benzene 

Bisphenol-A 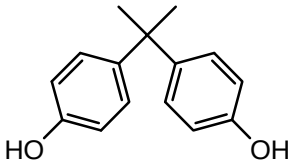

Diglycidyl ether of bisphenol-A 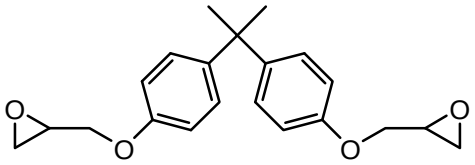

Dimethyldicyane 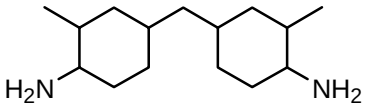

4-Ethylphenol 

Furan 

n-Hexanol 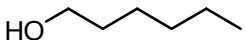

4-Isopropenylphenol 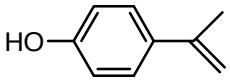

4-Isopropylphenol 

Methylfuran 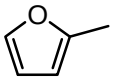

Nonylphenol 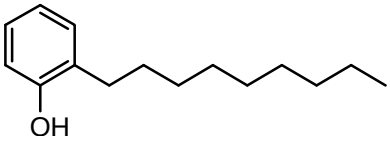

Octamethyl-
cyclotetrasiloxane 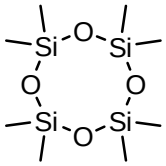

Pentaerythritol
triacrylate 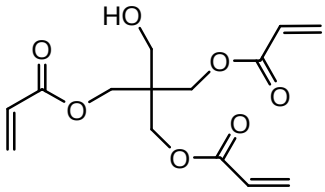

Perfluorohexane 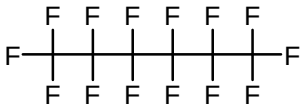

Phenol 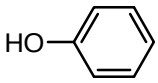

4-Tertbutylphenol 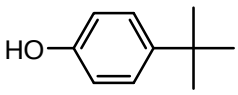

Toluene 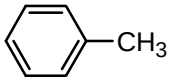

Polymers:

EVA 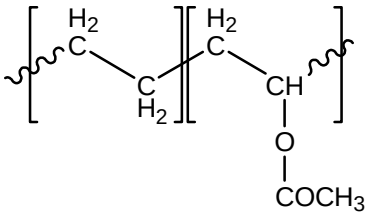

HDPE 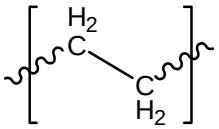

PA66 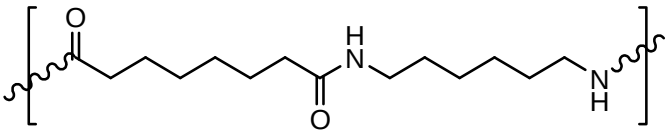

PBSA 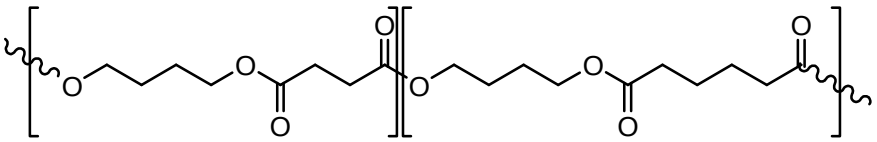

PBS 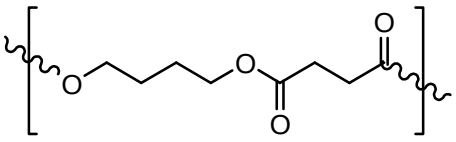

PC

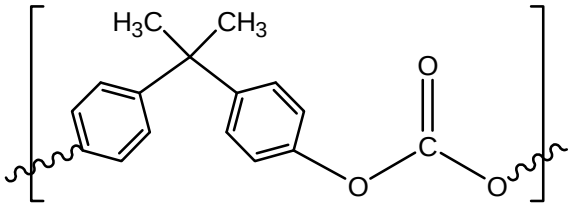

PDMS

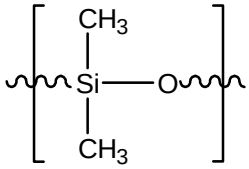

PEG / PEO

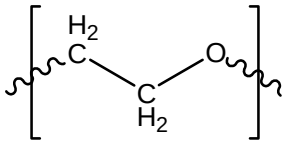

PEI

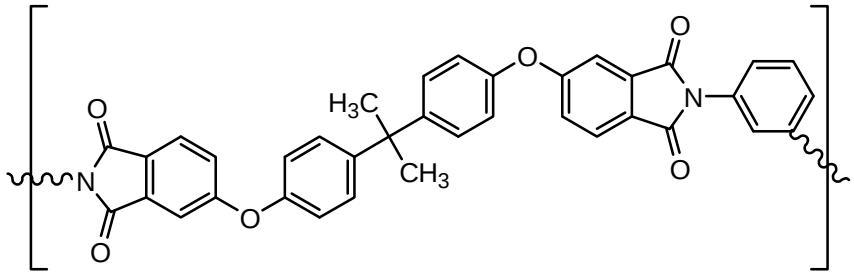

PEOx

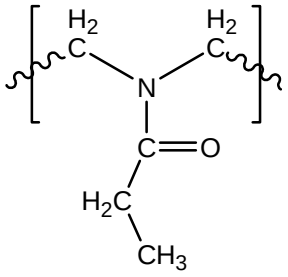

PIB

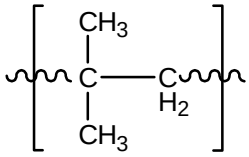

PPO

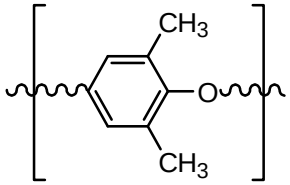

PS

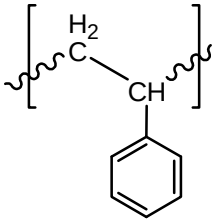

PVPhKH

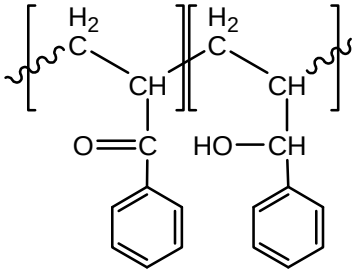

1 Introduction

The changing chemical and physical properties of cross-linked polymeric materials undergoing thermal degradation are important to the performance of many engineered systems. For example, foams found in airplanes, hotels, etc., experience severe changes in structure and properties when exposed to fire. As thermal energy breaks some of the network bonds in these foams or in other such cross-linked polymeric materials, many species are formed, including large polymer-like network fragments as well as smaller solvent-like molecules. The vapor-liquid equilibrium behavior of these degradation products will affect the composition and amounts of the phases present. These quantities will, in turn, strongly influence the physical properties of the system. If the system is enclosed, pressurization may also become a concern.

One type of system of interest to the funding source for this research involves the use of foam encapsulants to protect and isolate electronic and other sensitive devices from shock, vibration, and temperature. Many of the foam encapsulants currently used are rigid epoxy or polyurethane foams, but these can be very difficult to remove if repairs or equipment upgrades are necessary. A new foam has been developed at Sandia National Laboratories which is easily removed under mild conditions. The new foam, called Removable Epoxy Foam (REF), undergoes a reverse Diels-Alder reaction at temperatures above 90ºC to break cross-linking bonds in the molecular network, which

then allows the foam to be dissolved in a mild solvent. This reaction, along with other decomposition reactions at higher temperatures, creates a mixture which includes large polymer-like molecules and some small solvent-like molecules (Hobbs, 2003).

For a foam encapsulant to be used in systems where exposure to fire-like heat fluxes is possible, its physical properties and thermal decomposition behavior must be well understood. Models attempting to describe the decomposition of rigid polyurethane foam have been developed by Hobbs et al. (1999; 2003) and Clayton (2002). Hobbs has also done some modeling of the decomposition of REF (2003). These previous models generally assumed that the vapor-liquid interactions are ideal or can be described by a simple activity coefficient model. However, polymer solutions, such as may exist when REF or other cross-linked polymeric materials degrade, can exhibit highly non-ideal vapor-liquid equilibrium behavior. New models are needed to treat these non-idealities appropriately, as they influence the proportion of the initial mass that becomes part of the vapor phase, as well as the pressure of the system if it is closed. These models must be able to operate with little or no information other than the molecular structure of the mixture components. They also must be valid for use at high temperatures and pressures.

This research was a continuation of the studies done on REF by Dan Clayton. His work included the experimental characterization of REF by examining pyrolysis mass-release as a function of temperature, heating rate and pressure (Clayton, 2002). The present study focused on determining the vapor-liquid equilibrium behavior of polymer solutions that are similar to the initial REF decomposition products. A procedure was developed for predicting that behavior during thermal degradation of the actual foam. The results of this research serve as a basis for similar studies with other materials.

2 Background

This chapter describes the efforts to treat thermal decomposition of rigid polyurethane and epoxy foams, including REF. A description of the structure and decomposition behavior of REF is presented below, as well as how previous decomposition models have treated vapor-liquid equilibria of the initial products. Several polymer solution models available in the literature are then detailed and compared. Finally, existing polymer solution data and experimental methods for determining VLE behavior of polymer/solvent mixtures are discussed.

2.1 Removable Epoxy Foam

Removable Epoxy Foam was developed at Sandia National Laboratories as a more useful foam encapsulant to replace rigid polyurethane foams. Several researchers have studied its structure and tried to model its decomposition behavior. A description of REF and how vapor-liquid equilibrium of initial degradation products was treated in previous models is presented below.

2.1.1 REF Structure and Decomposition Behavior

Generally, epoxy foams are created by mixing a curing agent with an epoxy resin and allowing them to form a stable, highly cross-linked network. The cross-links form

from a ring-opening reaction between the epoxy resin and the curing agent, such as an amine or polyphenol that has a labile hydrogen. A versatile epoxy foam using diglycidyl ether of bisphenol-A (DGEBA) as the resin was developed by Russick and Rand (1998). This foam was modified by McElhanon et al. (2002) to make a removable epoxy foam by replacing some of the DGEBA with a resin incorporating a furan-maleimide Diels-Alder adduct. A hypothetical molecule representing the components of REF, adapted from Clayton (2002), is shown in Figure 2.1. A graphic representation of the repeating unit and an idealized two-dimensional REF network, adapted from Clayton (2002) and Hobbs (2003), is shown in Figure 2.2.

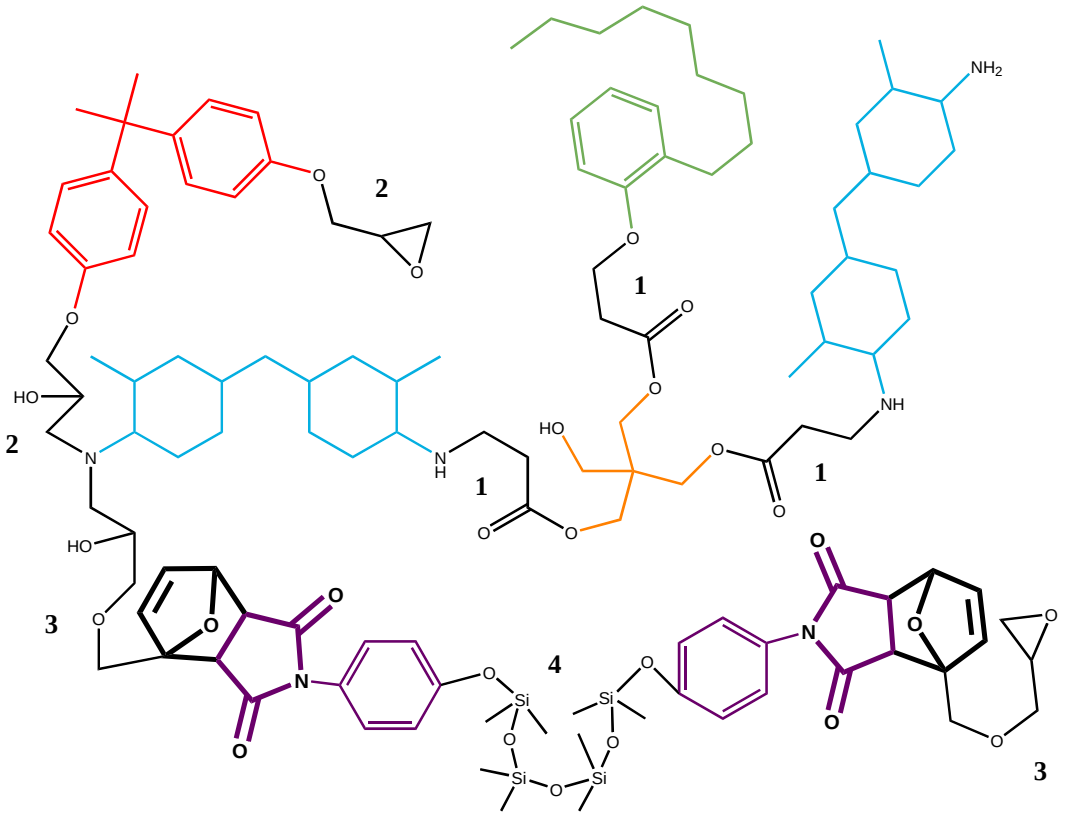

Figure 2.1 Representative REF molecule adapted from Clayton (2002) with Diels-Alder adducts shown in bold. Colors and numbers define building blocks and linkages.

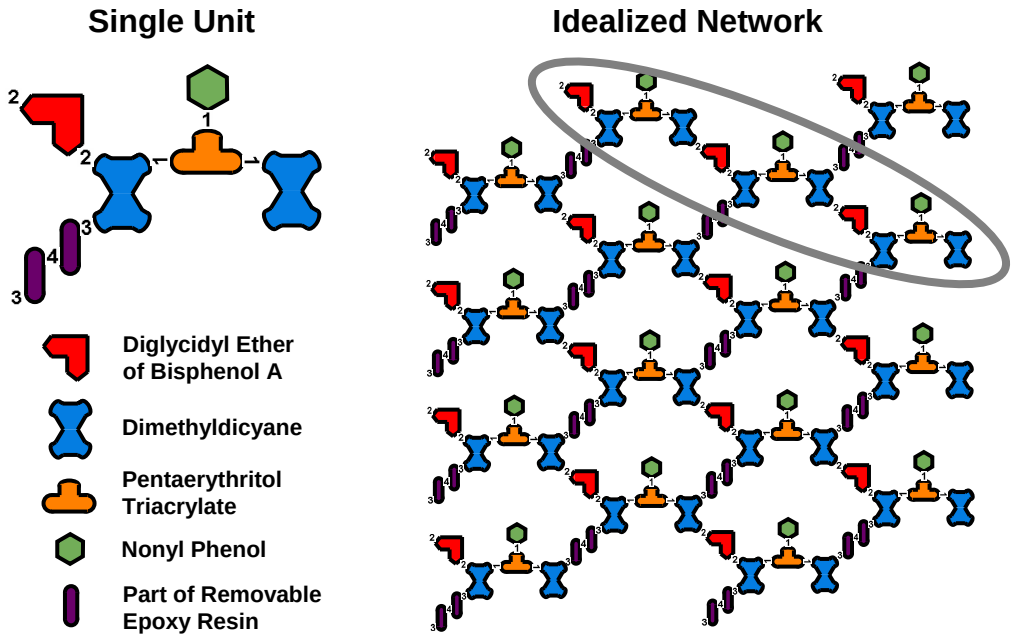

Figure 2.2 Graphic of a single REF unit and a two-dimensional idealized REF network (adapted from Clayton, 2002; Hobbs, 2003). Colors and numbers coincide with respective REF components and linkages shown in Figure 2.1. Circled portion of network represents initial polymer-like REF decomposition products.

The removability of REF results from the Diels-Alder reaction (a [4 + 2] cycloaddition between a diene and a dienophile) between a furan and a maleimide, as shown in Figure 2.3. The epoxy foam can be cured at temperatures between 20 and 60ºC, in which range the forward reaction is favored. The reverse reaction is favored at temperatures above 90ºC, allowing the cross-links in the foam network to be removed. The broken pieces of the network can then be dissolved in a mild solvent, such as *n*-butanol, and removed.

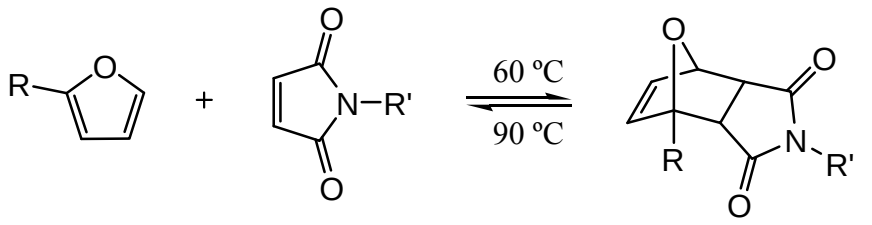

Furan Maleimide Diels-Alder Adduct

Figure 2.3 Reversible Diels-Alder reaction between furan and maleimide.

During thermal decomposition of REF, several solvent species evolve that contain a variety of chemical functional groups. Erickson et al. (2003) examined the decomposition of REF using a thermal gravimetric analyzer (TGA) and with online FTIR analysis. Mass-release derivative curves indicated three distinct stages of decomposition as shown in Table 2.1.

Table 2.1 Stages of mass-release during REF decomposition (Erickson et al., 2003).

Stage	**Temperature Range**	**Major Products Released**
1	Room temp. to 140ºC	perfluorohexane and siloxanes
2	140 to 300ºC	octamethylcyclotetrasiloxane
3	Above 300ºC	methylfuran, phenol, toluene, nonylphenol, bisphenol-A

In the temperature range up to 140ºC, the most abundant decomposition products were perfluorohexane (boiling point 58-60ºC) from the blowing agent and some siloxanes from the surfactant used in creating the foam structure. Between 140 and 300ºC, the major decomposition product was octamethylcyclotetrasiloxane (b.p. 175-176ºC), from the removable resin. Above 300ºC many organic products appeared including 2-methylfuran

(b.p. 63-66ºC), phenol (b.p. 182ºC), toluene (b.p. 111ºC), nonylphenol (b.p. 315ºC) and bisphenol-A (b.p. 360ºC). Nonylphenol and bisphenol-A were more abundant at temperatures above 350ºC.

2.1.2 Previous Foam Decomposition Models

Hobbs et al. (2003) developed the Chemical-structure-based PolyUrethane Foam (CPUF) model for the unconfined decomposition of the rigid foam based on the chemical percolation devolatilization (CPD) model of Grant et al. (1989). In the CPUF model it is assumed that the foam is made up of an infinite matrix of stable centers connected by labile chemical bonds. Percolation lattice statistics developed by Fisher and Essam (1961) are used to describe the fragmentation of the infinite matrix into the decomposition products as bonds break. Clayton (2002) developed the Mass-Transfer PolyUrethane Foam (MTPUF) model which extended the CPUF model to include flow and mass transfer effects under both confined and unconfined conditions.

In determining the vapor-liquid split, the CPUF and MTPUF models assume that the two fluid phases are in equilibrium with each other. A standard multicomponent isothermal flash calculation is performed using the Rachford-Rice equation:

$$0 = \sum_{i=1}^{n} \frac{z_i (K_i - 1)}{(K_i - 1) F_V + 1} \tag{2.1}$$

where

$$K_i \equiv \frac{y_i}{x_i} = \frac{\gamma_i P_i^{sat}}{P} \tag{2.2}$$

The vapor fraction, F_V, is the fraction of total moles in the system that are in the vapor phase, and it is determined iteratively from the Rachford-Rice equation. The variables z_i, y_i, and x_i are the species mole fractions in the overall system, and in the vapor and liquid phases, respectively; P is the system pressure; P_i^{sat} are the pure component vapor pressures of each species at the temperature of the system; γ_i are the activity coefficients of each species in the mixture. In the MTPUF model the vapor phase is treated as an ideal gas, and all γ_i are unity, meaning that the liquid phase is assumed to be an ideal solution. In the CPUF model, γ_i can be unity, or they can be calculated to lump Redlich-Kwong gas behavior with ideal solution behavior, or they can be calculated from the empirical Regular-solution model.

The MTPUF model corrects for some non-ideal behavior after determining the vapor-liquid split by using the compressibility factor, *Z*, in the equation:

$$P\overline{V} = ZRT \qquad \textbf{(2.3)}$$

Here, $\overline{V}$ is the molar volume; R is the universal gas constant; T is the system temperature. The compressibility factor is calculated using the Lee-Kesler equation of state. For confined cases, *Z* is used to correct the system pressure because the total mass of the system is known. For unconfined cases, *Z* is used to correct the final mass of the vapor phase because the pressure is fixed.

Hobbs also developed a Simple Removable Epoxy Foam (SREF) model based on the CPUF model, but for use with REF (2003). The vapor-liquid equilibrium calculation

in this model is performed in a similar manner to the calculation in the CPUF model. However, γ_i are estimated constants, and the presence of large polymer-like REF decomposition products that will not partition to the vapor phase is ignored.

Although the MTPUF model partially accounts for non-idealities in the vapor phase, and the CPUF and SREF models incorporate simple activity coefficient models, none of these models appropriately account for the non-idealities in the liquid phase due to the presence of large polymer-like decomposition products with a variety of functional groups, some of which may be polar. A model suitable for non-ideal vapor-liquid equilibrium in polymer solutions that resemble the decomposition products of REF is needed.

2.2 Polymer Solution VLE Models

A survey of the literature to find appropriate polymer solution models reveals two main categories: equations of state (EOS), and activity coefficient models (ACM). Several models important for polymer solution VLE are described and compared below. Both main categories, as well as the individual models in each, have strengths and limitations. These are mentioned, along with attempts to combine the capabilities of equations of state and activity coefficient models using excess energy mixing rules.

2.2.1 Equations of State

Equations of state are descriptions of pressure-volume-temperature (*PVT*) relationships. They can be used for pure substances as well as for mixtures. For accurate *PVT* prediction, they require information about the pure substances (often the critical

pressure and temperature) and some method of combining this information for mixtures. From an EOS, fugacity coefficients can be calculated to determine phase behavior. Many common equations of state for small molecules are simple two- or three-parameter cubic equations. Several non-cubic equations of state based on lattice-fluid theory or the van der Waals partition function have been proposed specifically for polymers and polymer solutions. Attempts have also been made to apply cubic equations of state to polymer solutions. Some significant equations of state are listed here.

GCLF

The GCLF EOS, proposed by High and Danner (1990), is the group-contribution version of the Panayiotou-Vera (1982) lattice-fluid EOS. This non-cubic EOS is based on statistics developed by Guggenheim (1952). Density is allowed to vary by changing the number of holes in the lattice. Parameters for seventeen groups of alkanes, cycloalkanes, arenes, ethers, water, ketones, and mono-chlorinated alkanes are available to calculate the two molecular parameters of the model. A binary interaction parameter is included to improve correlation of data, but can be set to zero. Thus, only the structure of the molecules in the mixture is required for prediction purposes.

GC-Flory

The GC-Flory EOS (Chen et al., 1990; Bogdanic and Fredenslund, 1994) was derived from a form of the van der Waals partition function. It is a modified group-contribution version of the Flory equation of state (Flory, 1970), which had previously been used successfully to correlate polymer solution data because it accounts for free-volume differences. Model parameters are available for 15 main groups and 32 sub-

groups. VLE data for binary mixtures of small molecules were used in a regression of the group interaction parameters, as opposed to using pure component data, with mixing and combining rules in a manner similar to most equations of state.

PSCT

The Perturbed Soft-Chain Theory (PSCT) equation of state (Morris et al., 1987) and its group-contribution version (Jin et al., 1986) are also derived from a form of the van der Waals partition function. They are based on a perturbation for chain-like molecules using a Lennard-Jones intermolecular potential energy function. It has been recommended (Kontogeorgis et al., 1994b) that for best results this model be used in a semi-group-contribution mode that uses molecular parameters for solvents and group parameters for polymers. All parameters were found by fitting pure component *PVT* data for small molecules. For this model, three molecular parameters (or *PVT* data from which they can be regressed) must be available for the solvent, but only the structure of the polymer is needed.

Cubic EOS

Some researchers have tried to use cubic equations of state to describe polymer solution behavior. Harismiadis et al. (1994) examined the use of the simple, two-parameter van der Waals equation of state for polymer solutions. They determined that if appropriate mixing and combining rules are used, cubic equations of state do not have inherent difficulties with size-asymmetric systems. In fact, the expression for the activity coefficient of the solvent from many common cubic equations of state is very similar to the expression from the Entropic-FV model, which is discussed below. Harismiadis and

coworkers used the method of Kontogeorgis et al. (1994a) to determine the energy and volume parameters, a and b, for the polymer (several methods for determining these parameters are compared later). The quadratic van der Waals one-fluid mixing rules were used for both EOS parameters for mixtures. The cross-volume parameter, b_{ij}, was calculated using the classical arithmetic mean combining rule, while the cross-energy parameter, a_{ij}, was calculated with the Berthelot combining rule. Using this method, solvent activity predictions for nearly athermal polymer solutions (low enthalpy of mixing) were good.

The SWP equation of state (Sako et al., 1989) is a three-parameter cubic EOS derived from the generalized van der Waals partition function that reduces to the Soave-Redlich-Kwong (SRK) equation of state when the third parameter, c ($3c$ is the number of external degrees of freedom per molecule) is set to unity. This third parameter extends the applicability of the equation of state to polymer systems. However, there is no adequate correlation for c, and it must be fit to polymer PVT data along with other polymer EOS parameters.

2.2.2 Activity Coefficient Models

Activity coefficient models use the activity coefficient, γ, to describe deviation of the behavior of species in real solutions from their behavior in an ideal solution ($RT\ln\gamma$, where R is the universal gas constant and T is the temperature, is the partial molar excess Gibbs energy). These models often divide the activity coefficient into separate terms resulting from different types of contributions to non-ideality. Generally, they can be written as follows:

$$\ln \gamma = \ln \gamma^{comb} + \ln \gamma^{res} \quad \textbf{(2.4)}$$

where γ^{comb} and γ^{res} are the combinatorial (or entropic) and residual (or enthalpic) terms, respectively. In effect, the combinatorial term describes deviations from ideality due to differences in size and shape between molecules in a mixture. The residual term describes deviations due to differences in intermolecular attractions.

Many activity coefficient models have been proposed for polymer solutions. The classical Flory-Huggins (FH) model (Flory, 1953) has formed the basis for most of these. It originally included only a combinatorial term:

$$\ln \gamma_i^{comb} = \ln\left(\frac{\phi_i^{vol}}{x_i}\right) + 1 - \frac{\phi_i^{vol}}{x_i} \quad \textbf{(2.5)}$$

where ϕ_i^{vol} is the volume fraction (sometimes segment fractions are used), and x_i is the mole fraction of species *i*. The FH model was derived from the expression for the entropy of mixing a polymer and a solvent on a lattice. Because this derivation assumed all lattice sites to be equal in size and did not allow for empty sites, the FH model cannot account for differences in free-volume. Free-volume can be thought of as the volume that is not occupied by the molecules themselves and is thus "accessible." Free-volume effects can be ignored for mixtures of small molecules because they have fairly similar free-volumes. However, polymers have significantly lower free-volumes than do most small molecules (except for water) (Elbro et al., 1990). In polymer solutions, solvent activities predicted by lattice-based entropy-of-mixing models neglecting free-volume

differences are lower than what is observed experimentally (Oishi and Prausnitz, 1978; Elbro et al., 1990).

Most of the effort put into improving polymer solution models has been focused on calculating the effect of the difference in free-volume between polymer and solvent on the non-ideality of the solution. When the polymer has a lower free-volume than the solvent, the free-volume correction to solvent activity is positive. Because free-volume is inherently related to the size and shape of the molecule, several models contain modified combinatorial terms that include free-volume effects, while other models have a separate free-volume term. Several important free-volume activity coefficient models are discussed here.

UNIFAC-FV

One of the earliest activity coefficient models to include an explicit free-volume term was UNIFAC-FV, developed by Oishi and Prausnitz (1978). It uses the combinatorial and residual terms of the original UNIFAC model proposed by Fredenslund et al. (1975), and adds a free-volume term derived from the Flory equation of state (Flory, 1970).

The UNIFAC model is based on group contributions. For the combinatorial term, which consists of the FH combinatorial term and a Staverman-Guggenheim shape correction, this means that volumes and surface areas of molecules are calculated by summing up the van der Waals volumes and surface areas of the individual functional groups that make up the molecules. For the residual term it means that interactions are calculated between pairs of functional groups instead of between pairs of molecules.

The new free-volume term was derived specifically for calculating solvent activities, and requires the specific volume of the polymer.

Entropic-FV and GK-FV

The Entropic-FV model, developed by Elbro et al. (1990), also uses the residual term from UNIFAC but contains a combined free-volume/combinatorial term that is very similar to the FH combinatorial term except with free-volume fractions in place of volume (or segment) fractions. It was derived from the generalized van der Waals partition function in the following form:

$$\ln \gamma_i^{comb+fv} = \ln\left(\frac{\phi_i^{fv}}{x_i}\right) + 1 - \frac{\phi_i^{fv}}{x_i} \qquad \textbf{(2.6)}$$

where ϕ_i^{fv} is the free-volume fraction of component *i*:

$$\phi_i^{fv} = \frac{x_i v_i^{fv}}{\sum_j x_j v_j^{fv}} \qquad \textbf{(2.7)}$$

The free-volume, v_i^{fv}, is defined as

$$v_i^{fv} = v_i - v_i^{hc} \qquad \textbf{(2.8)}$$

where v_i and v_i^{hc} are the molar and hard-core volumes of component *i* respectively. The hard-core volume is assumed to be the same as the van der Waals volume which can be calculated from values provided by Bondi (1968).

Later, Kontogeorgis et al. (1993) added a Staverman-Guggenheim correction term to account for differences in shape as the UNIFAC model does. The shape correction is always positive, and is generally small. This modification of the Entropic-FV model is called the GK-FV model.

MEFV

It has been noted by some authors (Bondi, 1968; Coutinho et al., 1995; Kouskoumvekaki et al., 2002) that the inaccessible volume is actually greater than the van der Waals volume due to the packing of the molecules. Kouskoumvekaki et al. (2002) reported better predictions of phase behavior in polymer solutions when the hard-core volume in the Entropic-FV model was multiplied by a factor of 1.2. This is comparable to the ratio of the molecular volume at 0 K and the van der Waals volume (Kouskoumvekaki et al., 2002). This model has been called the Modified Entropic-FV (MEFV) or EFV 1.2 model.

Freed-FV

The Freed-FV model (Radfarnia et al., 2005) is another Entropic-FV-based model. It adds a non-randomness factor based on Freed cluster lattice theory (Dudowicz et al., 1990) to the combinatorial/free-volume term. This modification is designed to

improve calculations of both solvent and polymer activities. The non-randomness factor in the activity coefficient expression for species *i* is

$$r_i\left[\sum_j \beta_{ji}\phi_j^{fv}\left(1-\phi_j^{fv}\right)-0.5\sum_{j\neq i}\sum_{k\neq i}\beta_{jk}\phi_j^{fv}\phi_k^{fv}\right] \qquad \textbf{(2.9)}$$

with

$$\beta_{ji}=\alpha\left(\frac{1}{r_j}-\frac{1}{r_i}\right) \qquad \textbf{(2.10)}$$

where r_i is the ratio of the free-volume of species *i* to the free-volume of the smallest solvent, and α, the non-randomness parameter, has been set to 0.2.

UNIFAC-ZM

The UNIFAC-ZM model of Zhong et al. (1996) does not include an explicit free-volume term, but modifies the volume fractions in the Flory-Huggins portion of the UNIFAC combinatorial term with a universal constant for all long-chain molecules. They found that the UNIFAC method of calculating the volume of a *n*-mer as *n* times the volume of the monomer resulted in volumes that were too large. From formulae for excluded volumes of overlapping spheres they found that the volume of a *n*-mer should be 0.6583*n* times the volume of the monomer. This has qualitatively the same effect as that created in the Entropic-FV model. In both cases, going from regular volume fractions (Flory Huggins/UNIFAC) to free-volume fractions (Entropic-FV) or modified volume fractions (UNIFAC-ZM) decreases the weight of polymer terms relative to solvent terms in the respective fractions. This is caused by polymer free-volumes being

smaller than solvent free-volumes or a polymer volume multiplier less than unity. The end result is that the solvent fraction, and thus the solvent activity, is increased, bringing them closer to experimental observations.

2.2.3 Comparison of Models

Prediction Capabilities

When evaluating VLE models, a distinction must be made between correlation and prediction. Some models describe phase behavior well by fitting one or more adjustable parameters to available VLE data. This allows the data to be interpolated and possibly extended. However, the predictive capability of a model with relation to a chemical system indicates its performance when no parameters have been adjusted to fit data from the system. Predictive VLE models are commonly compared using deviations between calculated and experimental values for solvent activities (or activity coefficients) or equilibrium pressure. Recommendations for the best model may vary depending on the system and its conditions.

In general, the free-volume activity coefficient models have been found to give better predictions than the group-contribution equations of state. Specifically, Danner and High (1993) compared predictions from three models (UNIFAC-FV, GCLF, and GC-Flory) with an extensive database including finite concentration data from sixteen classes of polymer solutions and infinite dilution data from 22 classes of polymer solutions. They recommended the UNIFAC-FV model as the best overall, and noted that while for some systems the GC-Flory EOS gave accurate results, it was inconsistent. In another study with similar findings, Kontogeorgis et al. (1994b) compared the PSCT, GCLF, and GC-Flory equations of state with the Flory-Huggins, UNIFAC, UNIFAC-FV, Entropic-

FV, and GK-FV activity coefficient models. Some of their results are shown in Figure 2.4 for a system of benzene and polyisobutylene (PIB) at 25ºC. They found the free-volume activity coefficient models to be simpler and more accurate at low pressures than the equations of state (although the GC-Flory EOS gave comparable results in some cases). At high pressures they recommended the PSCT EOS, though results were only satisfactory. They also noted that the shape correction term in the GK-FV model was not important for athermal systems, but may be important for polar systems.

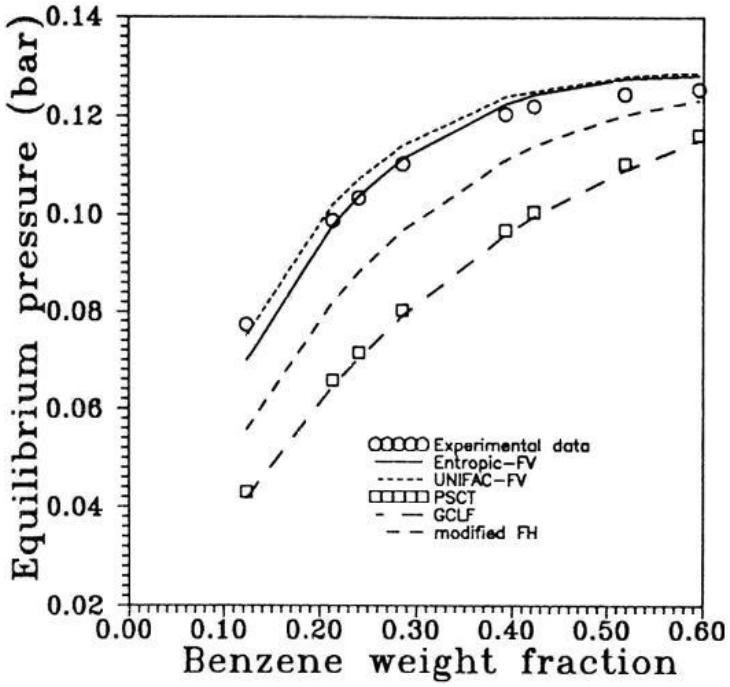

Figure 2.4 Experimental and predicted equilibrium pressure vs. solvent weight fraction for benzene/PIB (MW = 45,000) at 25ºC. From Kontogeorgis et al. (1994b).

Comparisons among the various free-volume activity coefficient models lead to somewhat less clear recommendations, though there is consensus that these are better than activity coefficient models that neglect free-volume effects. Pappa et al. (1999)

recommended using the Entropic-FV model over the UNIFAC-ZM model unless accurate polymer volumes are not available. In a study involving data from 142 systems of 16 polymers and 36 solvents, Wibawa et al. (2002) found that the UNIFAC-FV model was better than the Entropic-FV, GK-FV and UNIFAC-ZM models for athermal systems, while the Entropic-FV model was better for systems with aromatic and polar solvents. They later revised their recommendation (Wibawa et al., 2005) to say that the Entropic-FV model was also better for athermal systems except those containing PIB, for which the UNIFAC-FV model was better. Radfarnia et al. (2005) reported that the MEFV and Freed-FV models predicted solvent activity coefficients with absolute average deviations similar to or lower than those from the Entropic-FV model for athermal and non-athermal polymer solutions at finite and infinite dilution. Overall, several free-volume activity coefficient models, including the UNIFAC-FV model and the Entropic-FV based models, seem to have fairly similar VLE prediction capabilities.

In attempts to improve predictions, some studies have modified which UNIFAC group parameters are used. Because all of the successful free-volume activity coefficient models utilize these parameters, improvements resulting from these types of changes in one model signal possible improvements in the others, as well. Pappa et al. (1999) compared the use of the temperature-independent UNIFAC group interaction parameters of Hansen and coworkers (1991) with the use of their linearly temperature-dependent parameters (Hansen et al., 1992). Pappa and coworkers recommended using the temperature-dependent parameters; however, their calculations do not seem to show a significant difference between the two methods. They also noted that using the physical volume and surface area parameters for the OH group in the combinatorial term gives

much better results than using fitted parameters. Radfarnia et al. (2007) came to the same conclusion for OH, COO, and water group parameters. They also reported newly regressed values of OH, COO, and water group interaction parameters for the residual term that improved predictions of free-volume activity coefficient models for aqueous and alcohol polymer solutions.

Model Limitations

Many models that perform well in certain cases have limitations that make them unsuitable in others. This is so with many VLE models that require polymer specific parameters. Unless there is a simple way to obtain values for these parameters using only a knowledge of molecular structure, these models cannot be used to predict VLE during the decomposition of rigid foams where the "polymers" are large network fragments with many different functional groups instead of commercially available polymers with well-studied characteristics. Other limitations also exist and will be discussed here.

All of the models examined above are limited in some ways in their applicability and usefulness. In general, although the activity coefficient models appear to have better predictive capabilities, because they are not functions of pressure their use is restricted to low pressures and to the characterization of the liquid phase. The GC-Flory EOS was developed in a similar manner to activity coefficient models using data from binary mixtures at low pressure, and is confined to use at low pressure (Kontogeorgis et al., 1994b). The group-contribution equations of state do not have this limitation but are generally less accurate, and their group parameter tables are not nearly as large as those of UNIFAC, thus restricting the types of molecular structures that can be described. A

method for combining the strengths of activity coefficient models and equations of state is described later.

One problem encountered with the free-volume activity coefficient models (except UNIFAC-ZM) is the need for polymer molar volumes or densities. For commonly-encountered polymers, accurate volumes can be obtained from the Tait correlation with parameters from Rodgers (1993); otherwise the volume must be estimated. Results from free-volume models can be very sensitive to the values used. For example, Pappa et al. (1999) reported that for the Entropic-FV model, percent errors in weight fraction based activity coefficients at infinite dilution were two to three times larger than errors in polymer volumes. Some models are more sensitive than others. Model sensitivity to polymer volumes, along with polymer volume estimation methods, is discussed below.

Various other factors must also be taken into account when deciding whether to use a specific polymer solution VLE model:

- At some temperatures the GC-Flory EOS cannot find a liquid-like root for the solvent and thus fails (Danner and High, 1993).
- The GCLF EOS is very sensitive to the values of its binary interaction parameters (Harismiadis et al., 1994).
- Predictions from the UNIFAC-ZM model become worse with increasing temperature (Pappa et al., 1999). This is also the case with the MEFV model (Kouskoumvekaki et al., 2002).

- The UNIFAC-FV model cannot be used to predict the activity of the polymer because it uses a parameter regressed only for solvents (Kouskoumvekaki et al., 2002; Radfarnia et al., 2005).
- Solvent activities are often underestimated by the Entropic-FV model (Kouskoumvekaki et al., 2002).

Estimation of Polymer Volumes

Several researchers have noted the sensitivity of free-volume activity coefficient models to the accuracy of the polymer molar volume, as mentioned above. The UNIFAC-FV and MEFV models are more sensitive to errors in polymer volume than the Entropic-FV and Freed-FV models, as can be seen in Figure 2.5 from Radfarnia et al. (2005). Thus it is important to evaluate group-contribution volume estimation methods.

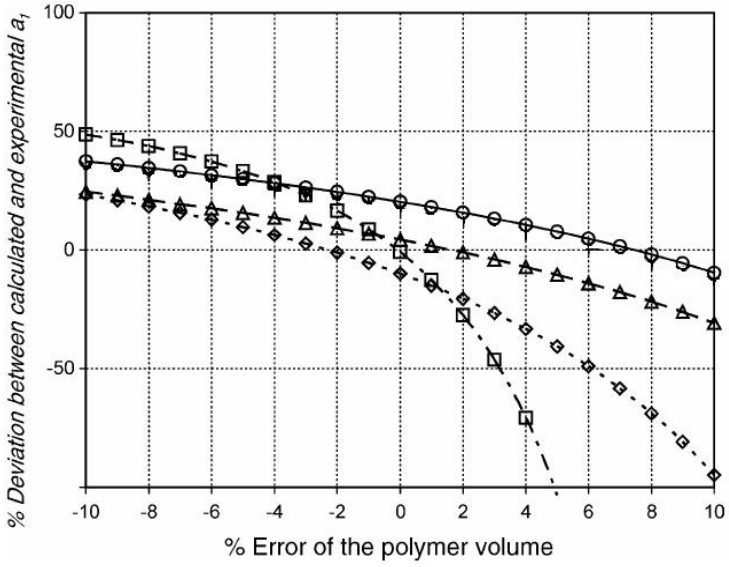

Figure 2.5 Effect of polymer molar volume error on the deviation of calculated solvent activities (a_1) of several free-volume activity coefficient models for the system pentane/PIB (MW = 1,000,000) at 35ºC. UNIFAC-FV:□, Entropic-FV:○, MEFV:◊, Freed-FV:Δ. From Radfarnia et al. (2005).

Polymer volume estimation methods in the literature include that of van Krevelen (Van Krevelen and Hoftyzer, 1972), as well as GCVOL (Elbro et al., 1991) and GCMCM (Sato et al., 1998). The van Krevelen method was developed for polymers at 25ºC. GCVOL, the most commonly used method, was developed to predict densities of solvents and polymers as a function of temperature. Density data for linear polyethylene and a large number of solvent molecules was used to obtain parameters for its 36 group volume increments. The temperature dependence of the volume increments was described by a simple polynomial function. Ihmels (Ihmels and Gmehling, 2003) later used a database of 1040 compounds to revise the existing group parameters and extend GCVOL to include 60 groups. One limitation of the GCVOL method is that it is not a function of pressure. Because liquid volumes are being predicted, though, errors associated with the lack of pressure-dependence may be small compared to other errors. In contrast, GCMCM is actually an equation of state for polymer melts based on the cell model of Prigogine (1957). It has parameters for only 20 groups, regressed from density data for 32 homopolymers. However, it can be used to describe a large majority of the structures that can be described even by the extended GCVOL method (many of the GCVOL groups are combinations of other groups, created to impart more accuracy).

A few authors have compared the use of these volume estimation methods in free-volume activity coefficients. Using the original GCVOL to estimate polymer volumes was shown by Radfarnia et al. (2005) to give better results than using volumes estimated by the method of van Krevelen. Wibawa et al. (2002) reported much lower errors in polymer volumes predicted by GCMCM than by GCVOL. However, this conclusion was based on some of the same experimental data that was used in the regression of the

GCMCM group parameters. There is evidence, though, that GCMCM can be used with good success for other polymers. It was shown by Sato et al. (2000) to predict the volume of three complex biopolymers with errors under 3%. Overall, a decisive comparison of GCVOL and GCMCM resulting in a clear recommendation of the best group-contribution polymer volume estimation method does not seem to exist in the literature at the current time.

2.2.4 Combined Activity Coefficient Models and Equations of State

All of the VLE models discussed so far have advantages and disadvantages. In general, activity coefficient models can describe the behavior of complex mixtures, but only at liquid densities, well below the critical temperature. Equations of state can be used over the entire density range and over a large range of temperatures. However, using the normal van der Waals one-fluid mixing rules only leads to good results for simple mixtures. Because the EOS mixing rules essentially perform the same function as activity coefficient models – describing how pure component properties relate to mixture properties – much effort has been put into developing mixing rules that can extend the capabilities of an equation of state to more complex mixtures. The excess energy family of mixing rules, specifically, has been very effective in this regard.

Excess Energy Mixing Rules

In essence, an excess energy mixing rule is developed by equating the excess energy as calculated by an equation of state with that from an activity coefficient model. Huron and Vidal (1979) were the first to successfully combine an equation of state with an activity coefficient model in this manner. They equated the excess Gibbs energy, G^{ex},

from an EOS with that from an ACM at infinite pressure. In order that G^{ex} from the EOS not be infinite, they had to assume that the excess volume, V^{ex}, was zero, and thus that the EOS volume parameter for the mixture was a linear combination of the pure component volume parameters. This mixing rule was useful but suffered from several limitations, including the fact that the parameters of the ACM needed different values when the model was used alone than when it was combined with an equation of state (Wong et al., 1992). While the excess Gibbs energy is a function of pressure, activity coefficient models do not vary with pressure. Thus, parameters regressed from data at low pressure do not correctly describe behavior at high pressure, which is what an activity coefficient model is meant to do in the Huron-Vidal mixing rule.

In an attempt to develop a mixing rule that could use existing activity coefficient model parameters, Michelsen (1990a) modified the Huron-Vidal mixing rule by equating G^{ex} from the EOS and ACM at zero pressure. The assumption was that while the excess Gibbs energy at low pressure was not similar to that at high pressure, it was similar to that at zero pressure. However, problems with this mixing rule arose at temperatures where no liquid root for the equation of state exists. Several further modifications made use of various extrapolations to higher temperatures, including the MHV1 (Michelsen, 1990b), and MHV2 (Dahl and Michelsen, 1990) mixing rules, as well as another by Kalospiros and Tassios (1995), developed specifically for polymer solutions.

Wong and Sandler (1992) took a different approach by matching the excess Helmholtz energy, A^{ex}, from the equation of state and activity coefficient model at infinite pressure. By using A^{ex} instead of G^{ex}, they did not have to assume that V^{ex} was zero as Huron and Vidal had done, and were free to choose a non-linear mixing rule for the EOS

volume parameter. They therefore chose to use a quadratic mixing rule, which at low densities produces a second virial coefficient with quadratic composition dependence, consistent with statistical mechanical theory. In order to use an activity coefficient model in their mixing rule, they had to make assumptions about the relationship between G^{ex} at low pressure and A^{ex} at infinite pressure. Since V^{ex} is small away from the critical point and A^{ex} is much less pressure-dependent than G^{ex}, they assumed that

$$G^{ex}(P = low) \approx A^{ex}(P = low) \approx A^{ex}(P = \infty) \qquad \textbf{(2.11)}$$

Thus existing activity coefficient model parameters developed at low pressure could be used directly in their mixing rule without change. There is one binary interaction parameter, k_{ij}, in the mixing rules (see equations in appendix) that was originally fit to data. However Wong et al. (1992) recommended that the value of this parameter be obtained by fitting the combined EOS+ACM to the ACM alone at low pressure. Thus, no additional information was needed. This approach is an attempt to account for errors related to the assumptions in Equation 2.11. They found the value of k_{ij} to be largely independent of the activity coefficient model used, suggesting that it was indeed related to the difference between G^{ex} at low pressure and A^{ex} at infinite pressure. With this method, the activity coefficient model could be used to make good phase equilibrium calculations at temperatures over 200ºC higher than the temperature at which the ACM parameters were obtained, and at much higher pressures.

Orbey et al. (1993) pointed out other strengths of the Wong-Sandler mixing rules. They noted that having the correct composition dependence at low density is important

even for high densities because the fugacity coefficient involves an integral of the partial derivative of pressure with respect to composition from zero density to the density of interest. They also created a completely predictive model by combining UNIFAC with the Peng-Robinson equation of state, as modified by Stryjek and Vera (PRSV, Stryjek and Vera, 1986) through the Wong-Sandler mixing rules. For ease of calculation, values of k_{ij} were obtained by fitting the EOS+ACM to the ACM at the concentration mid-point only, instead of fitting it over the entire composition range. Even using the temperature-independent parameters of UNIFAC, they were able to obtain good VLE predictions over wide ranges of temperature and pressure. They also found that using the UNIFAC parameters for VLE in this method gave liquid-liquid equilibria (LLE) predictions comparable to predictions from UNIFAC alone using the LLE parameter table. When used alone, UNIFAC with VLE parameters often gives poor LLE predictions.

Orbey and Sandler (1994) were the first to apply the Wong-Sandler mixing rules to polymer solutions. They used the PRSV equation of state and the Flory-Huggins ACM to correlate VLE for concentrated polymer solutions. They noted that the χ parameter in the FH model was almost composition- and temperature-independent when used in this manner, in contrast to its normal behavior. Orbey et al. (1998a) explained the reduction in sensitivity of ACM parameters using the relationship between the excess Gibbs and Helmholtz energies

$$G^{ex} = A^{ex} + PV^{ex} \qquad \textbf{(2.12)}$$

Activity coefficient models are meant to describe G^{ex} but they cannot account for changes in the PV^{ex} term with temperature and composition without changing the values of the parameters. Thus, when an ACM is used in the Wong-Sandler mixing rules where it is actually only describing A^{ex}, its parameters are less sensitive. ACM parameters are also less sensitive when used in the zero-reference-pressure excess energy mixing rules because the ACM is only meant to describe the mixture behavior at zero pressure, while the effects of temperature and pressure are accounted for by the equation of state.

This same reduction in parameter sensitivity has been noted for other activity coefficient models and with other excess energy mixing rules. This can be attributed to the fact that the ACM parameters are only used to describe mixture behavior at the specific conditions at which G^{ex} from the ACM and EOS is equated, while the effects of changing temperature and pressure are accounted for by the equation of state. However, Orbey and Sandler (1995) found that the Wong-Sandler mixing rules were more accurate than the MHV1 and MHV2 mixing rules when extrapolated over a large range of temperatures and when using binary data for ternary systems. Later Orbey and Sandler (1997) stated that for any zero-reference-pressure excess energy mixing rule, there is a similar infinite-reference-pressure mixing rule that has a better theoretical basis and performs equally well or better.

Several other researchers have applied excess energy mixing rules to polymer solutions with good results. Kalospiros and Tassios (1995) used a modified and translated PR EOS combined with the Entropic-FV model through their modification of the Huron-Vidal mixing rules and got generally better predictions than from the PSCT and GCLF equations of state. Orbey and coworkers (1998a) used an infinite-reference-

pressure mixing rule with the PRSV equation of state and the FH and NRTL activity coefficient models. Later (1998b), they used the SRK equation of state with the FH model through a zero-reference-pressure mixing rule to correlate moderately non-ideal polymer solutions and found that the FH model correlated data better when combined with the EOS than by itself. Haghtalab and Espanani (2004) combined the PRSV EOS with a modification of the NRTL model through the Wong-Sandler mixing rules to predict VLE for several types of polymer solutions. They stated that the choice of an appropriate activity coefficient model is a major part of achieving good results.

Some authors, however, have noted that limitations seem to exist in the application of excess energy mixing rules to asymmetric systems. Coutsikos et al. (1995) reported that the zero-reference-pressure mixing rules fail to predict VLE in very asymmetric systems such as those containing light gases. They also noted that in the Wong-Sandler mixing rules, k_{ij} is used to compensate for the difference between A^{ex} at infinite pressure and G^{ex} at low pressure. However, for asymmetric systems, a single value of k_{ij} cannot reproduce G^{ex} from the ACM. This is because A^{ex} at infinite pressure may not be similar to A^{ex} at low pressure (one of the assumptions of Wong and Sandler) in asymmetric systems. Kontogeorgis and Vlamos (2000) showed that excess energy mixing rules include the difference of the combinatorial terms of the ACM and the EOS itself. This should theoretically be zero, but is not for asymmetric systems. Orbey et al. (2002) confirmed in a study of carbon dioxide and *n*-alkanes that the MHV2 model fails for such asymmetric systems, but also concluded that the Wong-Sandler mixing rules, as well as another set of infinite-reference-pressure mixing rules, give acceptable

predictions of VLE behavior at higher temperatures and pressures using parameters obtained at low temperature and pressure.

Thus the use of excess energy mixing rules has potential for polymer solutions, but must be further evaluated. One advantage of the EOS+ACM method is that the same model can be used to describe non-ideal mixtures in the liquid and vapor phases. However, with polymer solutions where the polymer can be assumed to be present only in the liquid phase a γ-ϕ approach could be used to predict VLE, with the ACM alone being used for the liquid phase and the EOS alone being used for the vapor phase. The main benefits, then, of the EOS+ACM method for polymer solutions may be the ability to use ACM parameters regressed at low temperature and pressure at much higher temperatures and pressures, and the ability to account for situations in which oligomers or low-molecular weight polymers may be in the vapor phase in small amounts.

EOS Parameters for Polymers

One issue that becomes important when using excess energy mixing rules to combine a cubic equation of state with an activity coefficient model is how to obtain values for the EOS parameters for the pure polymer. The energy and volume parameters of a cubic equation of state, a and b, are determined for small molecules using correlations involving critical properties. This is not possible for polymers, for which critical properties cannot be measured.

Several methods for determining the cubic equation of state parameters of pure polymers have been proposed. Kontogeorgis et al. (1994a) used two polymer density data points at different temperatures (preferably at the lowest and highest temperatures of

concern), and at essentially zero pressure, to solve simultaneously for the parameters *a* and *b*. The Tait correlation was used to calculate densities for most of the common polymers. When these constants were not available for a specific polymer, and there were no experimental data, the density was estimated using GCVOL. The EOS parameters determined in this manner were assumed to be temperature independent and were found to be proportional to molecular weight. Thus *a/MW* and *b/MW* for each polymer are constant. This simple method, however, was found to predict volumetric behavior poorly at high pressures and result in unrealistically high polymer vapor pressures at high temperatures (Louli and Tassios, 2000).

Orbey and Sandler (1994) calculated the EOS parameters by arbitrarily assigning the pure polymer a low vapor pressure of 10^{-7} MPa. They set the fugacity coefficients of the pure polymer liquid and 'vapor' equal, and solved for *a* and *b*. This approach requires a value for the liquid molar volume at the temperature of interest. In cases where this temperature was below the glass transition temperature, Orbey and Sandler used the molar volume of the glassy polymer. Although Kontogeorgis and coworkers allowed the polymer vapor pressure to be exactly zero, the use of the isofugacity constraint by Orbey and Sandler makes the latter method more thermodynamically consistent (Orbey et al., 1998a).

Another method for determining *a* and *b* of the pure polymer, based on free-volume theory, was proposed by Kalospiros and Tassios (1995). Their method led to good results and low polymer vapor pressures, but required such properties as the thermal expansion coefficient and molar volume of the glassy state, as well as an experimental value for the volume at a temperature above the glass transition temperature.

Orbey et al. (1998a) proposed an empirical correlation for b based on the degree of polymerization, the specific volume of the polymer, and its weight-average molecular weight. The a parameter is then calculated by setting the pressure in the equation of state to zero and solving for a in terms of temperature, molar volume of the polymer and b. Using this method a is a linear function of temperature, but b is temperature independent. This method resulted in very low vapor pressures for the polymer, and has the correct liquid molar volume built in.

Later, Orbey et al. (1998b) suggested using common values of the critical temperature and pressure for all polymers of T_c = 1800 K and P_c = 10 bar. The parameters a and b could then be calculated in the same manner as with solvents, assuming α, a function describing the temperature dependence of a, to be identically equal to one (thus removing any temperature dependence for the polymer). This method, however, often led to large errors in the liquid volume of the polymer (Louli and Tassios, 2000).

Finally, Louli and Tassios (2000) presented a method similar to that of Kontogeorgis et al. (1994a), but instead of using the polymer density at only two temperatures, the values of a and b for the polymer were fit over a wide range of PVT data. Polymer densities were obtained from the Tait correlation. The polymer EOS parameters obtained in this manner resulted in predicted polymer vapor pressures that were several orders of magnitude lower than those predicted using parameters obtained from any of the other methods described above. Errors in liquid volumes, compared in Figure 2.6 with errors using parameters obtained from other methods, were much smaller as well.

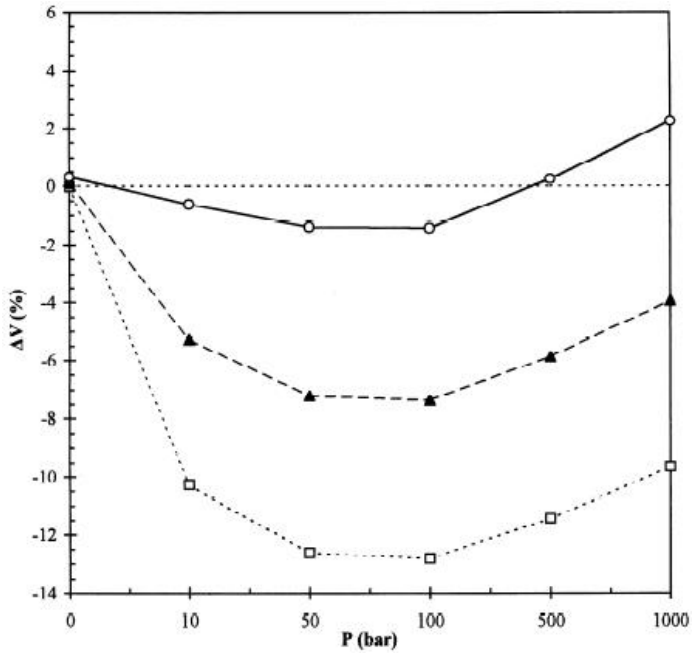

Figure 2.6 Percent error in PR EOS volume calculations for PIB (*MW* = 50,000) vs. pressure at 65ºC using parameters obtained following different methods. Method of Louli and Tassios (2000): ○, Orbey & Sandler (1994):▲, Kontogeorgis et al. (1994a):□. Error using method of Orbey et al. is larger than 90% and is not shown. Figure from Louli & Tassios.

2.3 Experimental Data and Methods in the Literature

A search of the literature was conducted in order to determine the scope of available polymer solution data as well as to learn about experimental methods appropriate for determining VLE behavior of polymer/solvent systems.

2.3.1 VLE and PVT Data

Much of the available polymer solution VLE data has been compiled by Hao et al. (1992) and by Wohlfarth (1994). There is also a relatively large collection of data on copolymer solutions by Wohlfarth (2001). The great majority of these existing data was collected at temperatures lower than 100ºC. In general, data have been collected for a

small number of commercially important polymers and solvents. No data could be found for systems containing many of the relatively low molecular weight products of REF decomposition such as phenol, furan, and bisphenol-A.

Polymer *PVT* data needed for the free-volume activity coefficient models are available for over 170 polymers, including some copolymers and blends, in a compilation by Zoller and Walsh (1995). Coefficients of the Tait equation, fit to specific volume data for 43 of the most common homopolymers and 13 common copolymers, are given by Rodgers (1993).

2.3.2 Experimental VLE Methods

Danner and High (1993) provide a comprehensive review of experimental methods for measuring polymer-solvent phase equilibrium. The most common methods are gravimetric sorption, piezoelectric sorption, and differential vapor pressure measurements. Inverse gas chromatography is also used somewhat but is limited to low concentrations of solvent.

An experimental apparatus for the gravimetric sorption method, as described by Lieu and Prausnitz (1999), is shown in Figure 2.7. In the gravimetric sorption method, pure polymer is hung from a quartz spring or electronic microbalance and then exposed to solvent vapors at constant temperature (and thus at constant pressure, since the solvent is the only species in the vapor phase). Equilibration of the system may take up to a few days. The weight fraction of solvent absorbed by the polymer can be determined from the measured change in mass. Tanbonliong and Prausnitz (1997) developed a similar apparatus that can be used for ternary systems (two solvents).

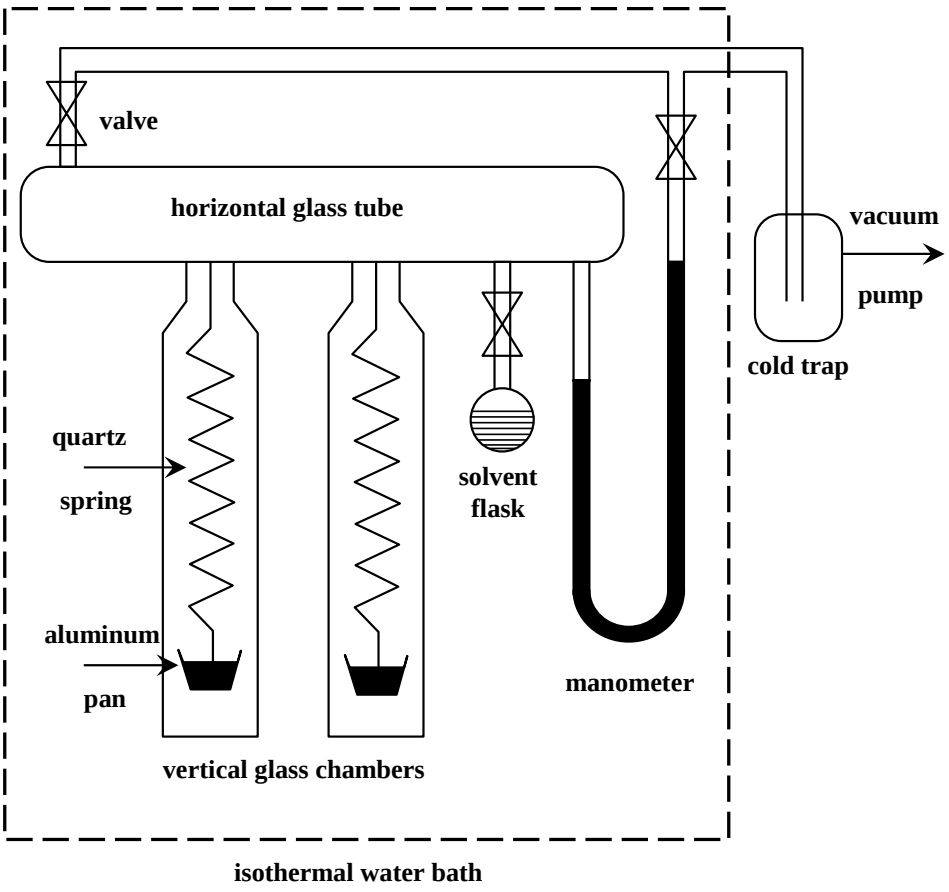

Figure 2.7 Schematic of gravimetric sorption method of measuring polymer solution VLE. From Lieu and Prausnitz (1999).

The piezoelectric sorption is similar to gravimetric sorption in that the pure polymer is exposed to solvent vapors at constant temperature and allowed to equilibrate. However, in this method, the polymer is coated on a quartz crystal, and the mass of absorbed solvent is determined by the change in the crystal's vibrational frequency. A description of this method is given by Saeki (1981). Measurements made by this method can be very accurate, but temperatures are limited to the polymer's melting point because it must exist as a solid film on the crystal surface. Both sorption techniques are generally

limited to low pressures and to solutions that contain more than 50 wt% polymer (Danner and High, 1993).

Differential vapor pressure measurements can also be used as a measure of polymer solution equilibria. In this method the difference in vapor pressure of a polymer/solvent solution of known composition and the pure solvent is measured at constant temperature. Bawn et al. (1950) state that this method can be used over almost the whole range of concentration. An apparatus for measuring differential vapor pressure is described by Haynes et al. (1989). A similar technique measuring the absolute pressure over the polymer/solvent solution is described by Surana et al. (1997) and is shown in Figure 2.8. This pressure can then be compared with correlations for the vapor pressure of the pure solvent.

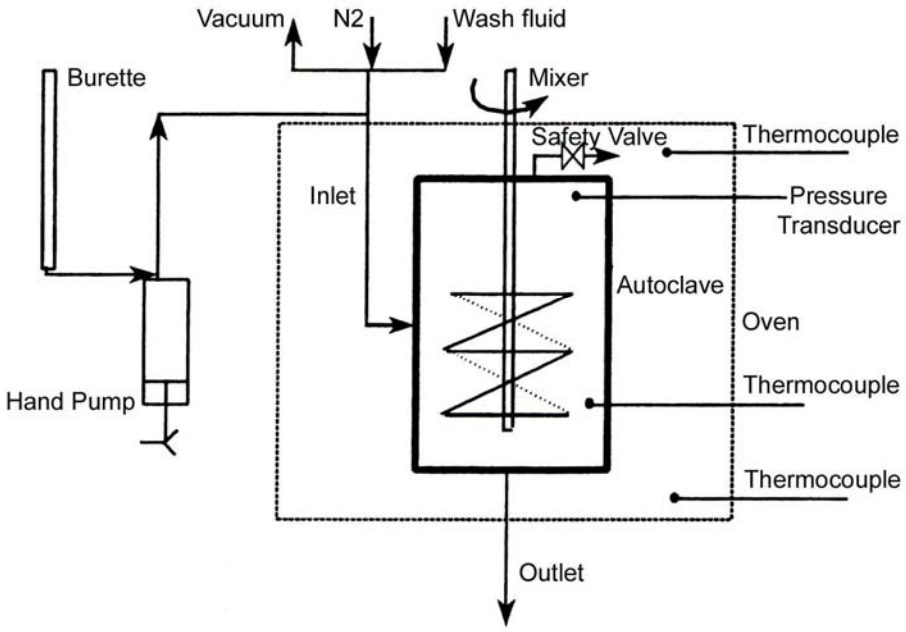

Figure 2.8 Schematic of absolute vapor pressure method of measuring polymer solution VLE from Surana et al. (1997).

Results from the gravimetric and piezoelectric sorption methods have the potential to be more accurate than results from the vapor pressure method because measurements of mass and quartz crystal frequencies are often more accurate than measurements of pressure. However, because of the temperature and concentration limitations of the two sorption methods the vapor pressure method is the only one of these three that is suited to the study of vapor-liquid equilibrium of REF decomposition products.

2.4 Summary of Literature Review

In this chapter, existing work and methods related to this research have been reviewed. Current models for the decomposition of rigid foams assume ideal vapor-liquid equilibrium behavior, or treat it simply in manner that is not appropriate for the mixtures of large, polymer-like components and small, solvent-like species that may exist. A suitable procedure for predicting VLE of these initial decomposition products is needed.

There is a general consensus in the literature that the free-volume activity coefficient models are better than other types of models at describing VLE behavior of polymer solutions. Results from the different free-volume ACMs are similar and further study is needed to determine which is best for specific situations. Most of these models (UNIFAC-ZM is an exception) require values of the liquid volume, which may be unknown. Two polymer volume estimation methods exist, but there is no definitive comparison of their abilities. One problem with activity coefficient models is that they may not work well at high temperatures and pressures away from the conditions at which

their parameters were determined. The ACMs can be combined with a simple cubic equation of state through excess energy mixing rules, in which case the sensitivity of their parameters to temperature and composition is reduced, and thus their range of applicability is increased. The use of an equation of state requires parameters for the pure polymer. There are many ways to evaluate polymer EOS parameters, but the best method in the literature involves fitting them to *PVT* data.

Experimental VLE data at temperatures up to a few hundred degrees Celsius are needed for polymer solutions with components similar to the decomposition products of REF and other rigid foams. Very few data for any polymer solutions exist at temperatures above 100ºC, and for several species that are observed during foam decomposition no data are available. The vapor pressure method of measuring polymer solution VLE is the most applicable for these high temperatures and for use over the entire range of composition.

3 Research Objectives

The main objectives of this research were to measure the vapor-liquid equilibrium behavior of some high-temperature (around 75-250ºC) polymer solutions similar to initial decomposition products of REF and other rigid foams, and to develop a procedure for predicting VLE behavior during thermal decomposition of the actual foams. In order to predict this behavior with the information constraints involved, a model was needed that required no polymer-specific information other than molecular structure, and that was valid for use at high temperatures and pressures. Experiments were performed to measure the vapor pressure of selected polymer/solvent mixtures at high temperatures. These experiments were then used to evaluate appropriate polymer solution models available in the literature, as well as to explore novel combinations of these models. With this information a procedure was developed to estimate polymer solution VLE in order to create an appropriate submodel for use in a larger foam decomposition and pressurization model developed at Sandia National Laboratories. This research was divided into the three tasks discussed below.

3.1 Tasks

Task 1. Measurement of VLE Behavior of Representative Solvents and Polymers

a. Identify solvents and polymers that were representative of the initial REF decomposition products.
b. Design and build a high-temperature vapor-liquid equilibrium facility.
c. Measure the equilibrium pressure of the selected polymer solutions over a range of compositions and at temperatures between 75 and 250ºC.

Task 2. VLE Submodel Development

a. Select individual models from the literature, as well as combinations of these models, that show potential for describing high-temperature polymer solution VLE behavior.
b. Develop a modular computer program for calculating vapor-liquid equilibria of multi-component solutions in order to evaluate different polymer solution models.

Task 3. Application to Degradation of Rigid Foams

a. Obtain appropriate VLE model parameters.
b. Compare data collected in Task 1c with predictions from models selected in Task 2a to develop the best procedure for predicting VLE of initial decomposition products of REF and other rigid foams.
c. Make sample predictions of VLE behavior of REF decomposition products.

3.2 Approach

Task 1a. Identification of Representative Solvents and Polymers

Solvents and polymers representative of the initial REF decomposition products were identified through discussions with Dr. Ken Erickson of Sandia National Laboratories, and by examination of the structure of REF as identified by Clayton (2002). First, important functional groups present in REF and its degradation products were identified. These included aromatic rings, phenols, siloxanes, amines, ethers, and furans. Polymers and solvents containing some of these functional groups were then chosen based on availability and safety of use. Two polymers were chosen: polyethylene glycol (PEG), a polyether, and polystyrene (PS), which has aromatic functionality. The solvents chosen were benzene, furan, and isopropylphenol.

Task 1b. High-temperature Vapor-Liquid Equilibrium Facility

Because of the high temperatures involved and the desire to be able to explore VLE behavior of polymer solutions across the entire composition range, the vapor pressure method of measurement was chosen. A high-temperature vapor-liquid equilibrium (HT-VLE) facility similar to the apparatus of Surana et al. (1997) was designed and built at Brigham Young University (BYU).

Task 1c. Equilibrium Pressure Measurements of Representative Polymer Solutions

The HT-VLE facility was validated by measuring the vapor pressure curves of several pure solvents and comparing them with vapor pressure correlations found in the literature. Experiments were next performed for a system of toluene and PEG to establish safe operating procedures and a valid experimental method. VLE experiments

were then performed for systems involving the components selected in Task 1a. A matrix of the experimental systems is shown in Table 3.1.

Table 3.1 Matrix of experimental systems.

	Polymer	
Solvent	PEG	PS
Toluene	x	-
Benzene	x	x
Furan	x	x
Isopropylphenol	x	x

Task 2a. Selection of Polymer Solution Models from Literature

The literature was reviewed to select a few polymer solution models which showed the most promise in predicting the vapor-liquid equilibrium of REF decomposition products. Group-based models that could also be applicable to other materials were desirable. The models needed to be capable of performing well at high temperatures. Also, because very little or no experimental data is available for the VLE of REF decomposition products, preference was given to group-contribution models or other models which require few substance-specific parameters that must be determined experimentally. Candidate models chosen for evaluation were the UNIFAC-FV, Entropic-FV, GK-FV, MEFV, Freed-FV, and UNIFAC-ZM activity coefficient models by themselves and combined with the Peng-Robinson (PR) equation of state through excess energy mixing rules of Wong and Sandler (1992). Because many of the free-volume activity coefficient models require polymer volumes, which are not available

experimentally for most complex polymers, the GCMCM and GCVOL volume estimation methods were compared.

Task 2b. Computer Program Development

A computer program was developed to predict the vapor-liquid equilibrium of high-temperature polymer solutions. The algorithm of the program was general enough that any of the polymer solution models selected from the literature could be incorporated. Initially, a program capable of calculating VLE for solutions with one solvent and one polymer was developed. The capabilities of this program were then extended to include the calculation of VLE for solutions of more than two components.

The computer program was built around a bubble point subroutine that solves for the pressure and composition of the vapor in equilibrium with a liquid of a given composition at a specified temperature by satisfying the isofugacity condition for each species. Additional constraints of total system volume and number of moles allow for calculation of the liquid phase composition from the overall composition. Model calculations were compared with pressure measurements from the HT-VLE facility.

Task 3a. Determination of Model Parameters

All necessary parameters for each model selected in Task 2a were determined. Of the free-volume activity coefficient models, the Entropic-FV-based models have no adjustable parameters if all of the group-contribution parameters are available (for the terms taken from UNIFAC, as well as for estimating unknown polymer volumes). The UNIFAC-FV model has two parameters with constant values suggested by Oishi and Prausnitz, but they admit that different values may be needed, especially for estimating

polymer activities. However, obtaining other values for the UNIFAC-FV parameters is beyond the scope of this work.

For the Peng-Robinson EOS, the unknown parameters include the energy and co-volume parameters for polymers. From the literature the best way to determine these parameters is to fit them to *PVT* data for the pure polymer following the method of Louli and Tassios (2000). For the two polymers chosen for the experiments in this research, parameters for the Tait equation were available. However, *PVT* data and/or parameters for the Tait equation are not available for the large, polymer-like network fragments that exist in the initial stages of foam decomposition. Thus, *PVT* data were obtained from a volume estimation method. A new method for determining the polymer EOS parameters was also developed in this work.

The Wong-Sandler mixing rules need a value for the binary interaction parameter, which may or may not be treated as adjustable. In this work, the method of Wong et al. (1992) was used: the value of the interaction parameter was determined without using any data by adjusting it to fit the excess Gibbs energy calculated by the combined EOS+ACM to that from the ACM alone over the entire composition range.

Task 3b. Determination of Recommended Procedure for VLE Prediction

Predictions from the polymer solution models chosen as part of Task 2a (using the parameters determined in Task 3a) were compared with experimental polymer solution VLE data from the literature and from the HT-VLE facility to determine which model best describes VLE of REF decomposition products. Preliminary comparisons were performed with low temperature data for simple polymer solutions from the literature to test the method. Final comparisons were performed with the data collected in this

research for high-temperature polymer solutions representative of REF decomposition products.

Task 3c. Sample VLE Predictions of REF Decomposition Products

Predictions of the VLE behavior of a sample mixture of initial REF decomposition products were performed following the recommended procedure from Task 3b. Solvents in the mixture were chosen from the low-molecular weight species seen during REF decomposition (see Table 2.1). The polymer-like degradation products were defined as having the repeating unit shown in Figure 3.1.

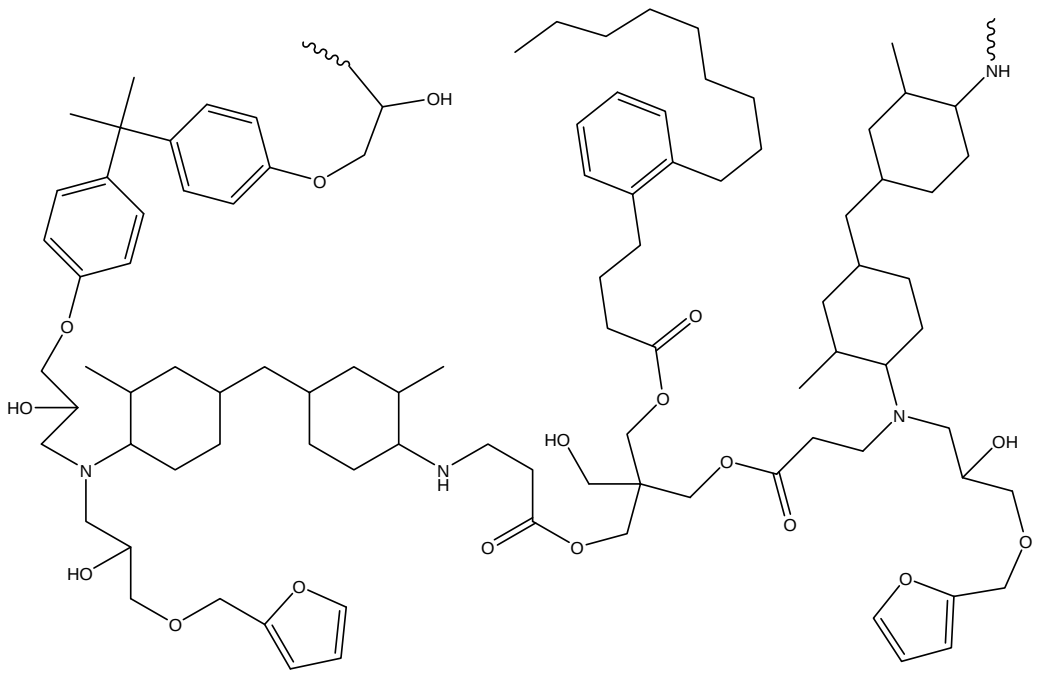

Figure 3.1 Representative structure of the repeating unit of the polymer-like decomposition products of REF. Wavy bonds represent connections to other repeat units.

The structure is different from the representative unit of REF itself, presented earlier in Figure 2.1, mainly because of the reverse Diels-Alder reactions that occur in the early stages of decomposition of the foam network. Also, the epoxide and amine groups which Clayton (2002) chose to show as unreacted are here shown to have reacted to form the linkages pictured in the idealized network of Figure 2.2. From discussions with Dr. Ken Erickson, the molecular weight of the polymer-like products was chosen to be around 5000-10,000 g/mol.

4 Experimental Method

During this research a few types of experimental data were collected. The most important were the equilibrium pressure data of polymer solutions. Supporting data included the measurement of the system volume of the HT-VLE facility and the decomposition temperatures of the polymers used in the VLE experiments. Descriptions of the equipment and materials used in this work, as well as the methods followed, are presented here.

4.1 Equipment

As a part of this work a high-temperature vapor-liquid equilibrium facility was designed and built at BYU. A thermogravimetric analyzer was also used to determine polymer decomposition temperatures. Both of these are described below.

4.1.1 High-Temperature Vapor-liquid Equilibrium Facility

The HT-VLE facility is shown schematically in Figure 4.1. It consisted of a Parr model 4742 pressure vessel (22 mL) heated inside a Mellen series SV07 vertical split-tubular furnace. Attached to the top of the vessel was a gage block that supplied connections for an inlet/vacuum/pressure relief line, as well as for temperature and pressure measurements.

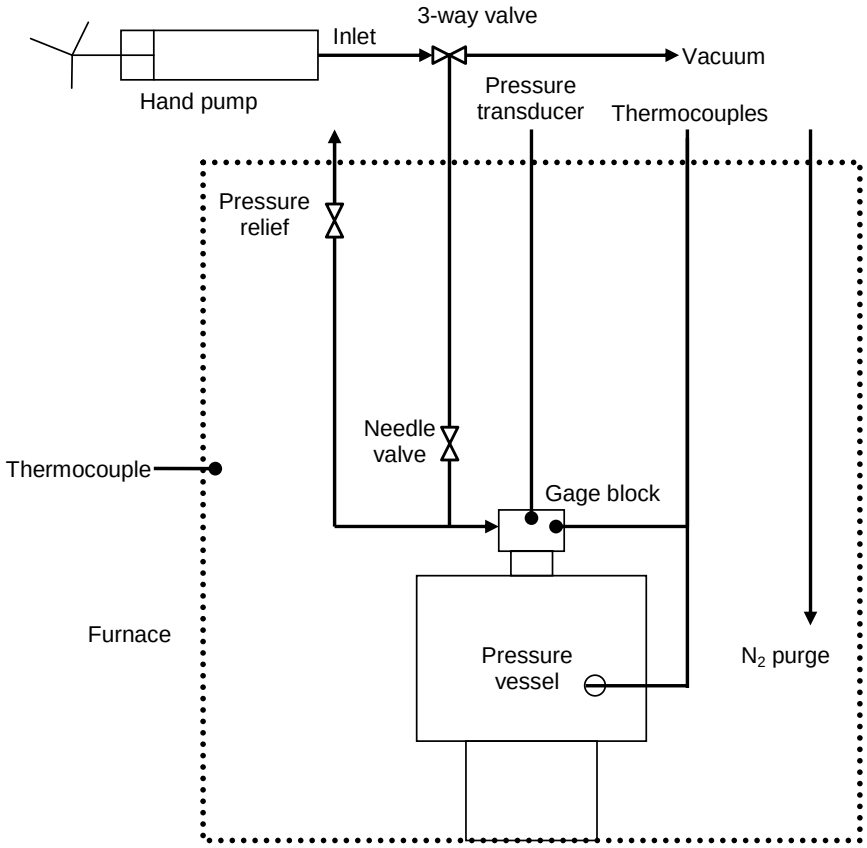

Figure 4.1 Schematic of the high-temperature vapor-liquid equilibrium facility at Brigham Young University.

The inlet/vacuum/pressure relief line contained a tee, with one side leading to a burst disk assembly and the other to a needle valve which could be used to close off the system during an experiment. A line from the needle valve extended out the top of the furnace to a three-way valve, which was connected to a 100 mL Ruska series 2200 positive displacement hand pump on one side and a vacuum line on the other. For safety, a nitrogen purge line was positioned inside the furnace next to the vessel and a snorkel was located over the furnace to dilute and remove any escaping vapors. The furnace was hinged in the middle so as to allow all connections to be made with the pressure vessel

while it was still outside the furnace. The vessel assembly could then be placed inside, and the furnace closed around it.

Measurements in the gage block were made using a type K grounded thermocouple probe and Kulite XTEH-10L-190 series "super high temperature" pressure transducers. The transducers had a maximum operating temperature of 538ºC and pressure ranges of either 0-50 or 0-300 psia. Pressure readings from the 0-50 psia transducers had an average standard deviation of about 0.1-0.2 psi, while those from the 0-300 psia transducers had an average standard deviation of about 1.0-1.5 psi. The transducers were powered by a Lambda model LP-412A-FM power supply set to 10.00 V. For some experiments another type K thermocouple was also placed against the side of the vessel wall through an access hole in the vessel lid. Data were collected and recorded using an Agilent 34970A data acquisition unit and LabVIEW 7.

During initial testing of the HT-VLE facility it was discovered that an effective seal could not be created between the pressure transducer and the gage block using the original nickel-plated copper crush rings provided with the Kulite transducers. Because of incorrect sizing, the crush ring would not remain properly seated during installation of the pressure transducer and was damaged every time. After suggestions were given to the manufacturer, resized crush rings were designed to replace the old ones. These new crush rings were able to create an effective seal.

4.1.2 Thermogravimetric Analyzer

Decomposition temperatures for the polymers used in this research were obtained from a high-pressure TGA, which measured mass as a function of time and temperature as a sample was heated. The TGA at Brigham Young University, shown schematically in

Figure 4.2, was built by Deutsche Montan Technologie and is capable of operating at temperatures up to 1100ºC and pressures up to 100 bar. A microbalance measures the mass of a small sample basket that hangs from a chain into an electrically heated reactor. Inert or reaction gases flow past the basket and through a valve that controls the pressure. The flow rate and composition of these gases are managed by mass flow controllers. Data, including the time, temperature, pressure, flow rates, and mass are recorded using LabVIEW.

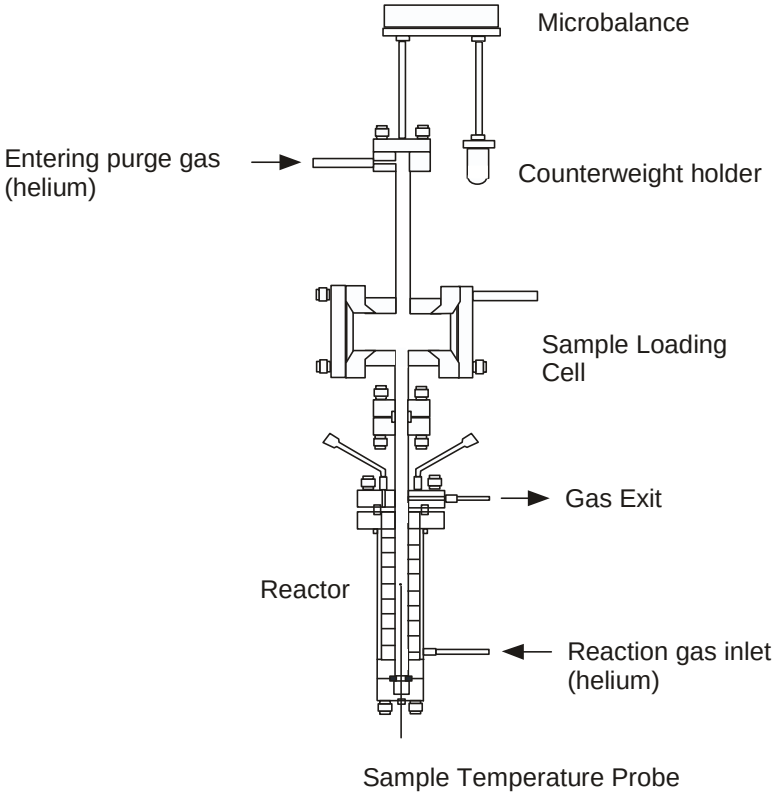

Figure 4.2 Schematic of the high-pressure thermogravimetric analyzer at Brigham Young University (Clayton, 2002).

4.2 Materials

The chemicals for this research were acquired from a variety of sources and were used as received, without further purification. The solvents used in this work are listed in Table 4.1 along with their sources and purities.

Table 4.1 Solvents used in this research, including their source and purity.

Solvent	Source	Purity	Notes
1-Hexanol	Spectrum	98%	Minimum purity
Toluene	Fisher-Scientific	99.8%	HPLC-grade
Benzene	OmniSolv	99.95%	
Furan	Aldrich	99%	Inhibited with 0.025 wt% BHT
4-Isopropylphenol	Acros Organics	98%	

Molecular biology-grade PEG 8000 was obtained as a powder from Fisher-Scientific with a molecular weight range of 7000-9000. Polystyrene was obtained in bead form from Aldrich with a bimodal molecular weight distribution. To allow for better mixing the polystyrene was powdered in a crucible before each run. The technical data sheet for the polystyrene listed a number-average molecular weight of 1300 and a weight-average molecular weight of 37,400. The polystyrene was analyzed by gel permeation chromatography (GPC) with PS molecular weight standards at BYU. The two peaks of the molecular weight distribution were found to be centered at molecular weights of about 1050 and 72,000, with 58 wt% of the PS associated with the first peak, and 42 wt% associated with the second peak.

Three of these chemicals, the two polymers and 4-isopropylphenol, are solids at room temperature but become liquids at relatively low temperatures. According to

technical data sheets and MSDS, the PS obtained has a midpoint glass transition temperature of 64ºC, the PEG melts in the range from 59-63ºC, and 4-isopropylphenol melts between 59 and 61ºC.

4.3 HT-VLE Facility Calibration and Testing

Because the HT-VLE facility was built as part of this research, its component measurements needed to be verified before use. The thermocouples and pressure transducers were therefore calibrated or tested as described below.

4.3.1 Thermocouples

In order to ensure that the combination of the thermocouples and the reference junction in the data acquisition unit gave accurate temperature readings, the boiling and freezing points of distilled water were measured. The ambient pressure was measured with a mercury barometer and was corrected for the density of mercury at the ambient temperature. The correct boiling point of water at the ambient pressure was obtained from a database of pure chemical properties maintained by the Design Institute for Physical Properties (DIPPR) (Rowley et al., 2005). Distilled water was then heated on a hot plate while mixing it with a magnetic stir bar. Once the water was boiling, the thermocouples were placed just above the surface (water occasionally touched them as it was stirred) to avoid measuring the temperature of super-heated water. The boiling point measured by different thermocouples was only 0.0-0.3ºC lower than value from DIPPR, which has an error of <0.2%. Before measuring the freezing point, a mixture of distilled water and crushed ice was stirred for ten minutes. The thermocouples were then lowered into the mixture. The freezing point measured by the thermocouples was only 0.1-0.3ºC

too low. From these calibrations the temperature readings were deemed accurate enough and were used in later VLE experiments without correction.

4.3.2 Pressure Transducers

The Kulite pressure transducers were calibrated with a Paroscientific Model 740 Digiquartz digital pressure transducer. A Kulite pressure transducer was attached to the vessel and placed in the furnace. An extra tee was connected to the three-way valve to allow the Digiquartz transducer outside of the furnace to be exposed to the same pressure as the Kulite transducer inside the furnace. The entire system could be evacuated, exposed to the atmosphere, or pressurized with nitrogen. Calibration measurements for the 0-300 psia transducer (identified by alpha code Z66-96) were taken under vacuum, at ambient pressure, and at pressure intervals of 10 psi up to about 190 psia (the limit of the regulator on the nitrogen tank). This was repeated with the Kulite transducer at different temperatures in intervals of 50ºC from 100-250ºC. Calibration measurements for the 0-50 psia transducer (alpha code B77-61) were taken at 10-psi pressure intervals, and at temperature intervals of 50ºC from 125-275ºC. The calibration coefficients for these transducers are reported in the appendix.

The calibration of the Digiquartz transducer was checked using an Omega PCL-200 pressure calibrator. Calibration measurements were taken at room temperature from ambient pressure up to about 80 psia. The readings from the Digiquartz transducer were all within about 0.1 psi of those from the Omega pressure calibrator.

It became apparent after several experiments that the zero-point offset of the Kulite pressure transducers varied somewhat over time. The reason for the variation is not entirely known, but it was limited to a few psi at most. The data from some

experiments, after being adjusted by the pressure calibration, still included values of pressure that were several psi from zero during the period of evacuation of the vessel before solvent was introduced to the system. This was not an artifact of the pressure calibration because it was not consistent from run to run. In fact, values of the offset regressed from different sets of calibration measurements for the same temperature and over the same pressure range taken several days apart were significantly different, even though values of the gain regressed from these sets of data were the same. Thus, the zero-point offset used in correcting the pressure readings from each experimental run was determined from the readings taken during evacuation of the vessel before addition of the solvent, if those readings were available. In the cases where this information was not available, the pressure readings happened to be higher than the vapor pressure of the pure solvent at the lowest recorded temperatures (around 35-40ºC). Since the vapor pressure was generally only a few psia at those temperatures, the correct experimental pressure was closely bracketed by the vapor pressure and by zero pressure. Thus, the offset was determined as the change required to bring the pressure readings down to the vapor pressure of the pure solvent at the lowest recorded temperature.

4.4 Experimental Procedure

In this section is given a description of the procedures followed for measuring the system volume of the HT-VLE facility, the equilibrium pressure of polymer solutions, and the decomposition temperatures of the polymers used in this study.

4.4.1 System Volume Measurement

It is important in designing VLE experiments to know when the equilibrium state of the system has been completely specified. For example, according to the Gibbs phase rule for a system of two components and two phases, there are two degrees of freedom, meaning that the equilibrium state is fixed when the values of two relevant variables are specified. However, the Gibbs phase rule only applies to independent intensive variables of the individual phases. Thus for a two-component, two-phase system, specifying the temperature and the liquid mole fraction of a component completely fixes the equilibrium state, whereas specifying temperature and the overall composition of the system does not. The latter is the case of the HT-VLE facility, in which the phase compositions are not measured. Therefore, the value of another variable must be known. A suitable choice, as will be shown here, is to specify the total volume of the system.

In a two-component, two-phase system, one set of relevant variables that can be used to fix the state of a system is temperature, T, pressure, P, and the mole fraction of one component in the liquid and vapor phases, x_1 and y_1, respectively. If any two of these four are specified, the other two can be calculated from the equilibrium relationships

$$x_1\hat{\phi}_1^L = y_1\hat{\phi}_1^V \tag{4.1}$$

$$x_2\hat{\phi}_2^L = y_2\hat{\phi}_2^V \tag{4.2}$$

where $\hat{\phi}_i^L$ and $\hat{\phi}_i^V$ are the partial fugacity coefficients of component *i* in the liquid and vapor phase mixtures, respectively. The fugacity coefficients are functions of *T*, *P*, and x_i (for the liquid phase coefficients) or y_i (for the vapor phase coefficients). When the total volume, V_{tot}, and overall composition in terms of the moles of each component, N_1 and N_2, are specified, the state of the system is fixed and the values of *P*, x_i, and y_i can be calculated using the equilibrium relationships above along with the following species mole balance and total volume balance equations:

$$N_1 = x_1 L(N_1 + N_2) + y_1(1 - L)(N_1 + N_2) \quad \textbf{(4.3)}$$

$$V_{tot} = \overline{V}_L L(N_1 + N_2) + \overline{V}_V(1 - L)(N_1 + N_2) \quad \textbf{(4.4)}$$

where *L* is the liquid fraction, or the fraction of total moles in the liquid phase, and $\overline{V}_L$ and $\overline{V}_V$ are the molar volumes of the mixtures in the liquid and vapor phases. The molar volumes are functions of *T*, *P*, and x_i (for the liquid volume) or y_i (for the vapor volume).

As more components are added to the system, each component adds two more independent variables, x_i and y_i. However, each new component also adds two more independent equations – another equilibrium relationship and another species mole balance – so the state of the system is still fixed. Thus, in order to compare model calculations with VLE data collected from the HT-VLE facility for systems with any number of components, the total experimental volume was needed.

The experimental volume (the volume available to a mixture during an experiment) consists of the volume inside the pressure vessel itself, as well as the volume in the attached equipment including the gage block, the pressure relief assembly up to the burst disk, and the tubing up to the needle valve inside the furnace. The volume was determined by using the properties of a one-component system at constant temperature. In a one-component system the pressure remains constant (at the vapor pressure) with changes in volume as long as the liquid and vapor phases are both present. Changes in the total volume change the relative amounts of the two phases. Only when the system becomes liquid-full or vapor-full does the pressure begin to increase or decrease, respectively. Because pressure increases dramatically with increases in the density of a liquid, the liquid-full point represents the most sensitive volume measurement.

The experimental volume was measured using the Ruska hand pump (containing toluene) connected to the Digiquartz pressure transducer. First, the pressure vessel and attached equipment were evacuated for approximately half an hour. Next, the hand pump was turned until toluene began to drip from its attachment tubing and then it was connected to the three-way valve. The three-way valve was opened to the hand pump, which was turned until the tubing between the three-way valve and the needle valve was full of toluene. The hand pump was then turned a little more to achieve a pressure significantly above the room-temperature vapor pressure of toluene to establish a liquid-full point for use as a baseline before opening the needle valve. The pressure and volume displacement of the hand pump were recorded. Toluene was then introduced into the system by opening the needle valve. Pressure and volume displacement measurements were recorded at intervals while the hand pump was turned. The point at which the hand

pump was turned enough to re-condense all of the toluene in the system and achieve the same pressure as the baseline reading was used to find the volume of the system.

4.4.2 Equilibrium Pressure Measurements Using HT-VLE Facility

A description of the procedure used to obtain equilibrium pressure measurements of polymer solutions in the HT-VLE facility is as follows:

1. A known mass of polymer was added to the pressure vessel.
2. The gage block and connections were attached to the vessel, and the entire assembly was placed in the furnace at room temperature.
3. The vacuum pump was turned on and the needle valve inside the furnace was opened for approximately 20 minutes to evacuate the vessel. The valve was then closed.
4. The furnace was heated to about 70ºC.
5. The needle valve was opened for approximately another 20 to 30 minutes to the vacuum line to degas the polymer. The needle valve was then closed.
6. The three-way valve above the furnace was switched from the vacuum line to the hand pump, and solvent was introduced into the tubing between the three-way valve and the needle valve. The pressure in the hand pump was increased to about 50 psia and then the pressure and hand pump displacement were recorded.
7. The needle valve was opened again and the hand pump turned to introduce solvent into the vessel. The needle valve was closed again.
8. The hand pump was turned some more to bring the pressure back up to the same level as before the needle valve was opened. The volume of solvent

introduced into the vessel was found from the difference between the new hand pump displacement and the previously recorded value at the same pressure.

9. Solvent remaining in the tubing between the valves was allowed to evaporate or was removed by collecting it in a single test tube cold-trap inserted in the vacuum line.
10. A cold-trap consisting of three test tubes in series surrounded by dry ice was then inserted in the vacuum line. The trap was evacuated for several minutes and then clamped off from the vacuum pump.
11. The needle valve was opened to the evacuated cold-trap for 5-10 seconds to degas the solvent in the vessel. The valve was then closed.
12. The change in mass of the cold trap was determined to calculate the mass of solvent removed.
13. The system was then heated to the maximum temperature for that run and allowed to equilibrate for 24 to 48 hours.
14. Finally, the system was cooled in one of the following two ways while the pressure and temperature were recorded: (a) experiments with the initial chemical systems were performed with a furnace cooling rate of 2ºC/hr, or (b) to save time overall but allow for more equilibration time at each temperature, later experiments were allowed to cool in steps of 25ºC with approximately 20 hours of soaking time between steps.

A matrix of the chemical systems examined in this work is given in Table 3.1. The procedure above was used for runs at several different compositions for each system,

mostly at or below 50 wt% solvent. Each experimental run lasted approximately a week to ten days. For the experiments involving isopropylphenol, the procedure had to be modified because it is a solid at room temperature. In these cases, known masses of both isopropylphenol and polymer were added to the vessel before placing it in the furnace. The vessel was evacuated at room temperature for approximately thirty minutes before closing the needle valve and heating the furnace to 80ºC. The vessel was allowed to sit overnight in order for any gases absorbed in the polymer or isopropylphenol to be released. The needle valve was then opened and the system was evacuated for about five more minutes. At this furnace temperature, the vessel temperature was only about 73ºC, at which temperature the vapor pressure of isopropylphenol was about 0.02 psia. Because this was a factor of almost 500 smaller than the vapor pressure of benzene and a factor of over 2000 smaller than the vapor pressure of furan, the mass of isopropylphenol lost during the degassing procedure was negligible.

4.4.3 Polymer Decomposition Temperature Measurements Using TGA

Measurements of the decomposition temperature of PEG and PS were made using the TGA in the following manner. Around 5-10 mg of polymer were placed in the sample basket and lowered into the reactor section of the TGA. The TGA was sealed and helium was introduced to the reactor section at a flow rate of about 1.3 slpm (helium at about 0.9 slpm was used as a purge gas to protect the microbalance). Helium was used because of its high thermal conductivity and low density. A heating rate of 3.3ºC/min was maintained by the electric heaters. The sample temperature probe was located just below the sample basket. Because of the small sample mass and low heating rate, the temperature measured by the sample temperature probe was assumed to be the same as

the actual sample temperature. Time, temperature, and sample mass were recorded by LabVIEW. Because constant mass flow rates of gas were used, the velocity of the helium flowing up around the sample basket increased with increasing temperature. Thus, the TGA results were adjusted for buoyancy effects using the results of an empty basket run under the same conditions of heating rate and helium flow rates. The results were also normalized using the initial mass of the polymer. The derivative of the mass with respect to time was taken to determine mass-release rates. The temperature of the peak mass-release rate was treated as the decomposition temperature of the polymer.

4.5 Summary of Experimental Method

In this chapter descriptions of the HT-VLE facility and the TGA at BYU were given along with an account of the materials used in this study. The calibration of the thermocouples and pressure transducers in the HT-VLE facility was explained. The experimental procedures used to measure the system volume and polymer decomposition temperatures were presented along with a detailed description of the procedure used to measure the equilibrium pressures of high-temperature polymer solutions.

5 Experimental Results

The experimental results obtained in this research are presented and discussed in this chapter. First, measurements of the system volume and polymer decomposition temperatures are given, followed by a validation of the HT-VLE facility. Finally, results for each polymer/solvent chemical system are presented.

5.1 System Volume

The volume accessible to the mixture in the pressure vessel during an experiment was measured several times at room temperature. Results for two runs are shown in Figure 5.1. Before opening the needle valve to allow toluene to enter the system, the pressure was brought up to 50.0 psia. After the needle valve was opened the pressure dropped to a value near the vapor pressure of toluene (0.55 psia at 25ºC). From the figure it can be seen that the pressure in the system remained relatively constant near the vapor pressure of toluene as the hand pump was turned. Once the system neared the liquid-full point, the pressure began to rise dramatically. The experimental volume was determined from the point at which the pressure again reached the baseline pressure of 50.0 psia. A relatively high baseline pressure was used to reduce the effects of having a small amount of non-condensable gases in the system. The system was found to have an accessible volume of 29.25 ± 0.01 mL.

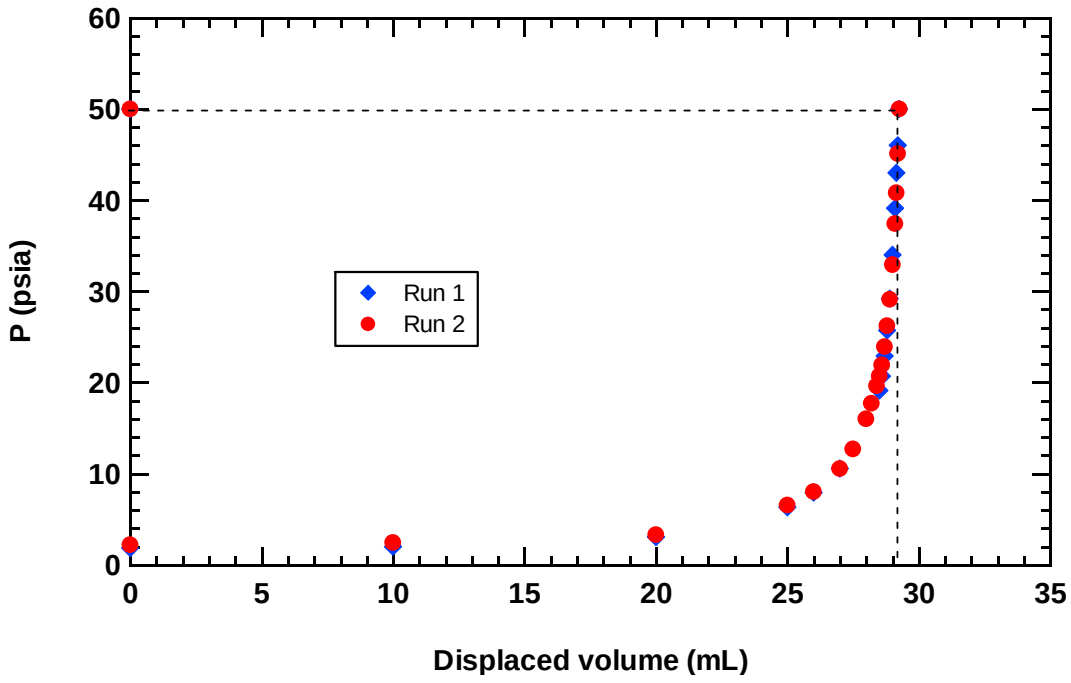

Figure 5.1 Pressure and displaced volume of a hand pump containing toluene during measurement of accessible experimental volume in the HT-VLE facility. Dashed lines indicate baseline pressure and volume of system.

5.2 Polymer Decomposition Temperatures

The results of the TGA experiments used to determine the decomposition temperature of the PEG and PS used in this work are shown in Figure 5.2 and Figure 5.3, respectively. Three runs were performed for each polymer. All runs were performed with a heating rate of 3.3ºC. Two of the three PEG runs gave almost identical results with a peak mass-release rate near 367ºC. The PEG used in the other run had been left exposed to the atmosphere overnight and had a peak mass-release rate at a temperature of a few degrees lower. It may be that the PEG absorbed some moisture from the air that caused it to decompose at a lower temperature. As for the PS, all three runs had peak mass-release rates at about 398ºC. Two of the runs showed some noise that may have been caused by low pressure in the helium tanks supplying the reactor and purge gases.

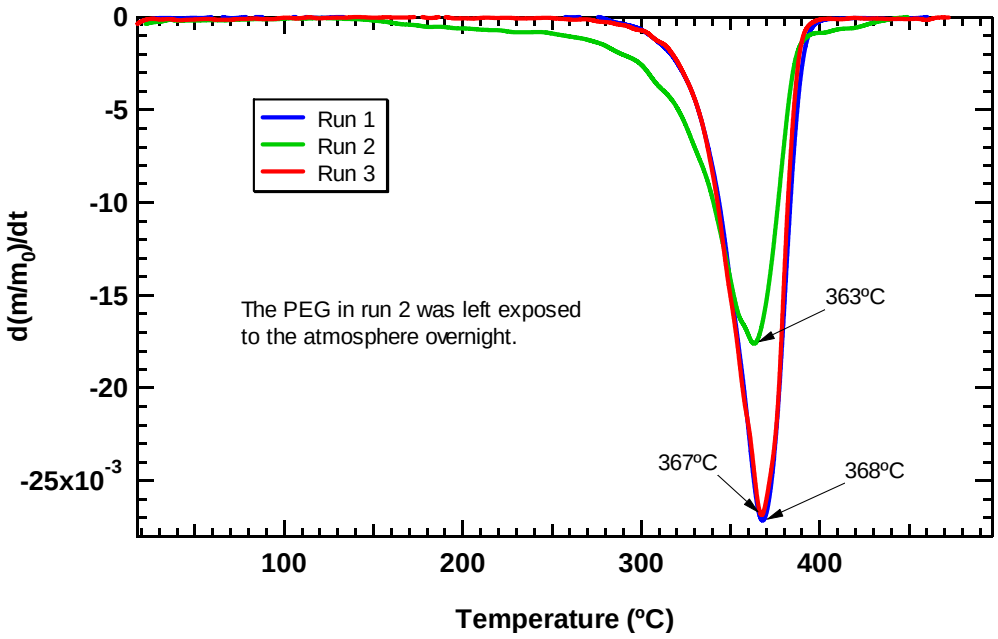

Figure 5.2 Normalized PEG mass-release rates versus temperature obtained using a TGA. The peak mass-release rate represents the decomposition temperature.

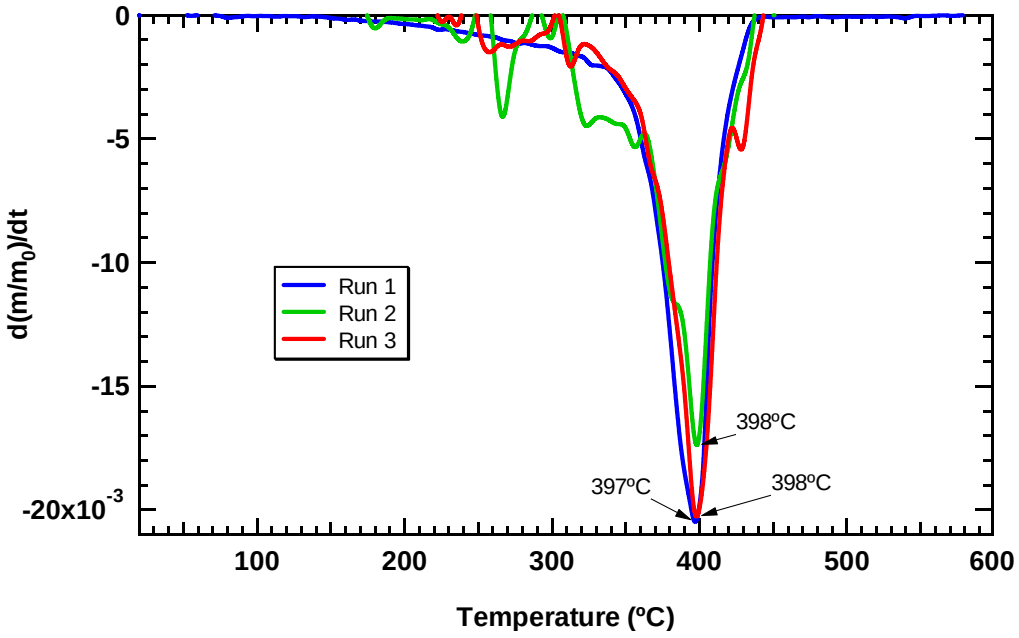

Figure 5.3 Normalized PS mass-release rates versus temperature obtained using a TGA. The peak mass-release rate represents the decomposition temperature.

Although the locations of the peak mass-release rates for both polymers were between 350 and 400ºC, there was some noticeable mass loss at temperatures as low as about 300ºC. For this reason, VLE experiments were limited to temperatures below 300ºC.

5.3 HT-VLE Facility Validation

Several steps were taken to ensure that the HT-VLE facility was working properly and that experimental data collected from it would be valid. First, the vapor pressures of some pure solvents were measured and compared with literature correlations to validate the equipment. Next, preliminary experiments with polymer solutions were carried out to find the conditions that allowed for sufficient thermal and mass-transfer equilibrium in the system and to validate the experimental method. Finally, some duplicate experiments were conducted to confirm repeatability.

5.3.1 Measurement of Pure Solvent Vapor Pressures

In an attempt to show that all the components of the HT-VLE facility were functioning correctly and that data collected from the facility would match data from the literature, the vapor pressures of some pure solvents such as hexanol, toluene, benzene, and furan were measured and compared with correlations from the DIPPR database. Initial results showed that even after applying the pressure calibration, vapor pressures measured in the HT-VLE facility were systematically lower than those calculated from DIPPR correlations. A sample vapor pressure curve measured at BYU for hexanol is plotted along with the DIPPR vapor pressure correlation in Figure 5.4.

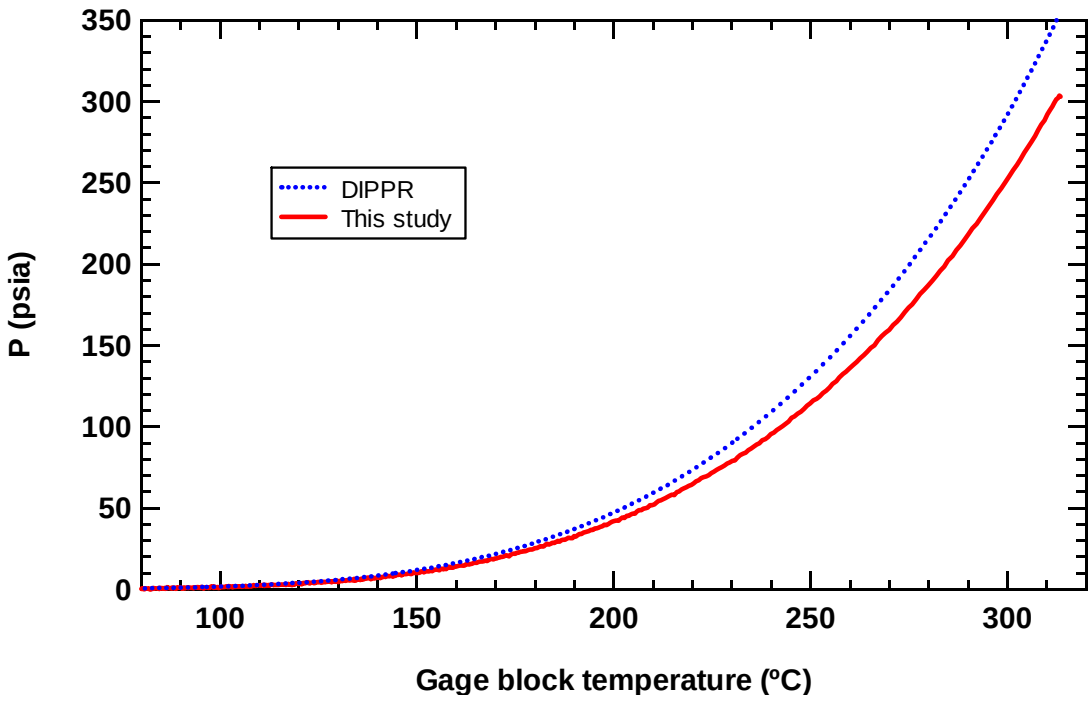

Figure 5.4 Vapor pressure of pure hexanol vs. temperature of gage block.

Several possible explanations of the large deviation were explored without success until finally a temperature mapping of the furnace was conducted. Measurements of the steady-state temperature profile inside the furnace showed that the temperature of the pressure vessel was several degrees lower than that of the gage block. This explained why the vapor pressure calculated from the gage block temperature was consistently higher than the measured pressure. For this reason, the thermocouples measuring the wall temperature of the pressure vessel were added to the setup. Because the thermal conductivity of the stainless steel vessel is on the order of 500 times larger than that of air, the range of any steady-state temperature profile within the vessel would be very small compared to that of the air in the furnace. Therefore the temperature of the thermocouple on the vessel wall was assumed to be the same as the temperature of the

vessel contents. The small cross section of the connection between the vessel and the gage block, however, allowed these components of the HT-VLE facility to be at different steady-state temperatures. A correlation between the temperatures of the gage block and vessel was obtained to correct data that had already been collected. This correlation is given in the appendix.

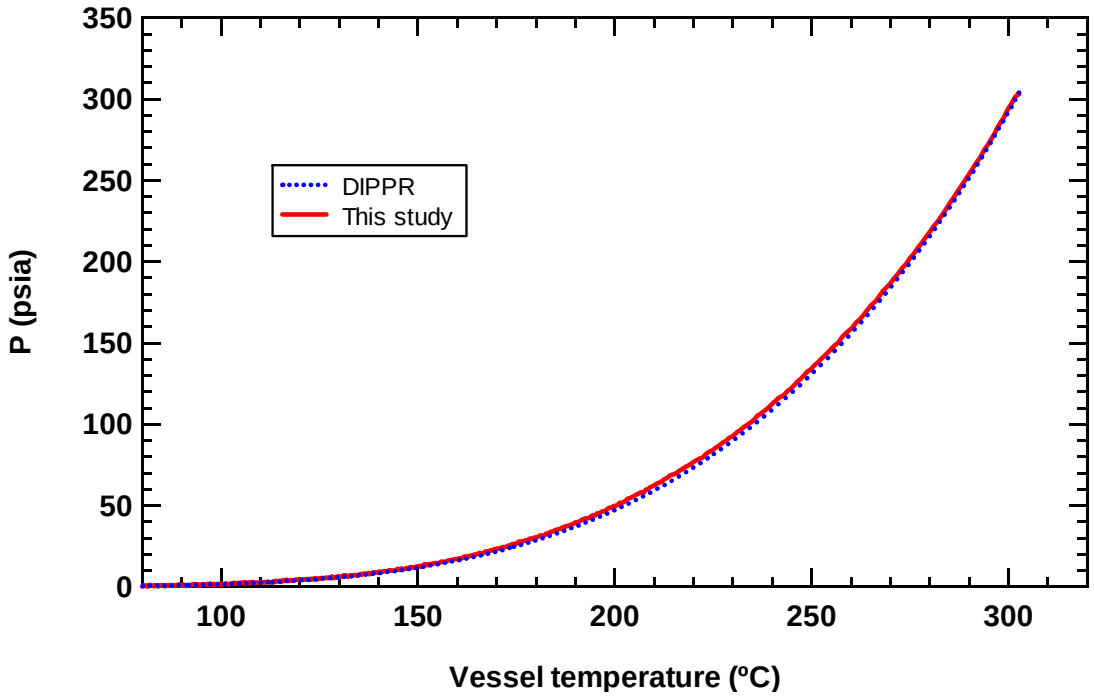

Figure 5.5 Vapor pressure of pure hexanol vs. temperature of pressure vessel.

A plot of the vapor pressure of hexanol vs. the vessel temperature is shown in Figure 5.5. Reported temperatures in subsequent plots of experimental data refer to vessel temperatures except where indicated. The use of the vessel temperature reduced the maximum deviation between the hexanol vapor pressures measured in this study and obtained from DIPPR from over 50 psi to less than 4 psi, which is only slightly larger

than the level of noise in the pressure transducer readings. Similar results were obtained for benzene, furan, and IPP and are presented in section 5.4.1. These results indicate that valid measurements of pure component vapor pressures can be obtained from the HT-VLE facility.

5.3.2 Experimental Method Validation

The experimental method for measuring the equilibrium pressure of polymer solutions was validated in a few ways. Experiments were conducted to determine if there were any leaks in the system or chemical reactions. Care was also taken to ensure that the data collected were at conditions of thermal and mass-transfer equilibrium.

Data from two thermal cycles, five days apart, of a mixture of PEG and benzene are shown in Figure 5.6. The fact that the second pressure vs. temperature curve lies directly on top of the first indicates that there were no significant leaks or chemical reactions taking place.

Because of the large thermal mass of the pressure vessel, it was necessary to perform a study of cool-down rates to determine what rate would allow the system to be essentially at thermal equilibrium. The initial experiments conducted with PEG and toluene to establish an appropriate experimental method showed significant differences in the pressure measured during heating and cooling. Data from one run are shown in Figure 5.7. In this case the furnace was allowed to heat-up and cool-down at its maximum rate. Thermal lag caused the pressure measured during cool-down to be much greater than the pressure measured during heat-up. The true equilibrium pressure is bracketed by the heating and cooling curves.

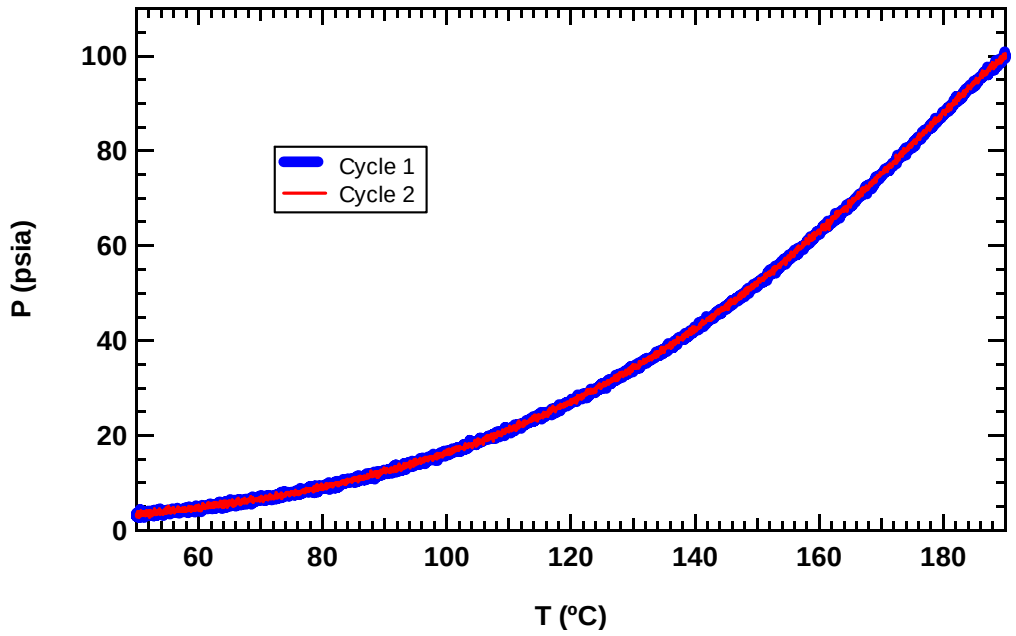

Figure 5.6 Pressure measured during the cool-down portion of two thermal cycles, five days apart, of a mixture of PEG and benzene. The curve representing the first thermal cycle was thickened to show that it lies directly underneath the curve representing the second cycle.

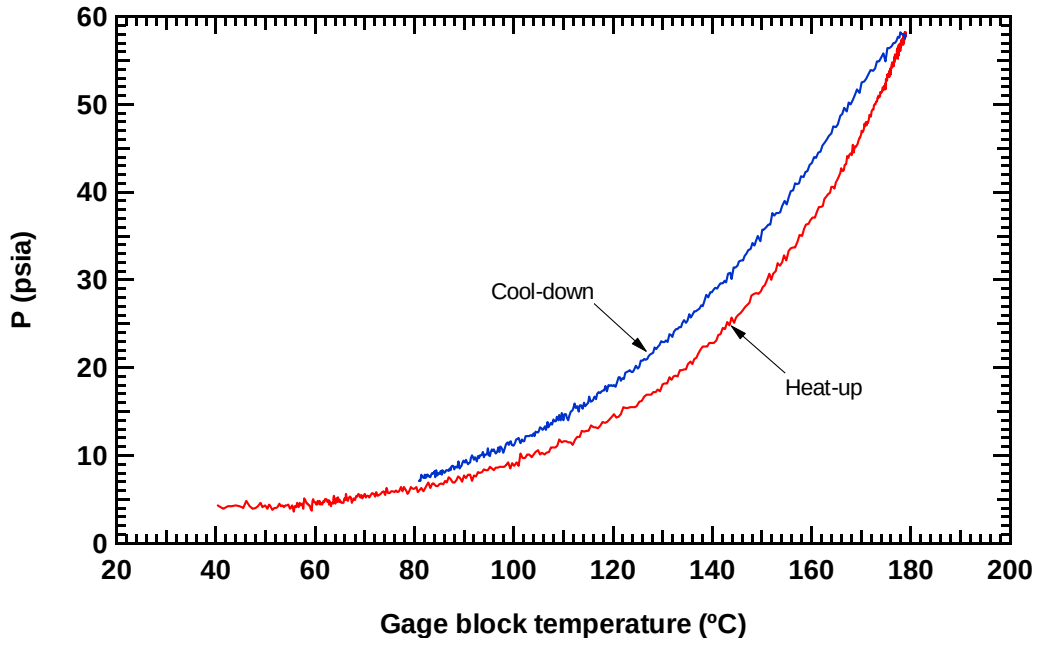

Figure 5.7 Pressure vs. temperature of a mixture of PEG and toluene during heat-up and cool-down.

It was determined that the temperature during cool-down should be controlled, and different cooling rates were examined. Data for three cooling rates are shown in Figure 5.8. Because the pressure vs. temperature curves collected during faster cool-downs are noticeably above that of the 2ºC/hr cool-down, these higher rates were not used. However, the data collected during the 2ºC/hr cool-down are within 1 psi of the pressure measured at temperature points at which the system was allowed to equilibrate for 12-24 hours. It was thus assumed that a 2ºC/hr cool-down gives pressures that are essentially the equilibrium values.

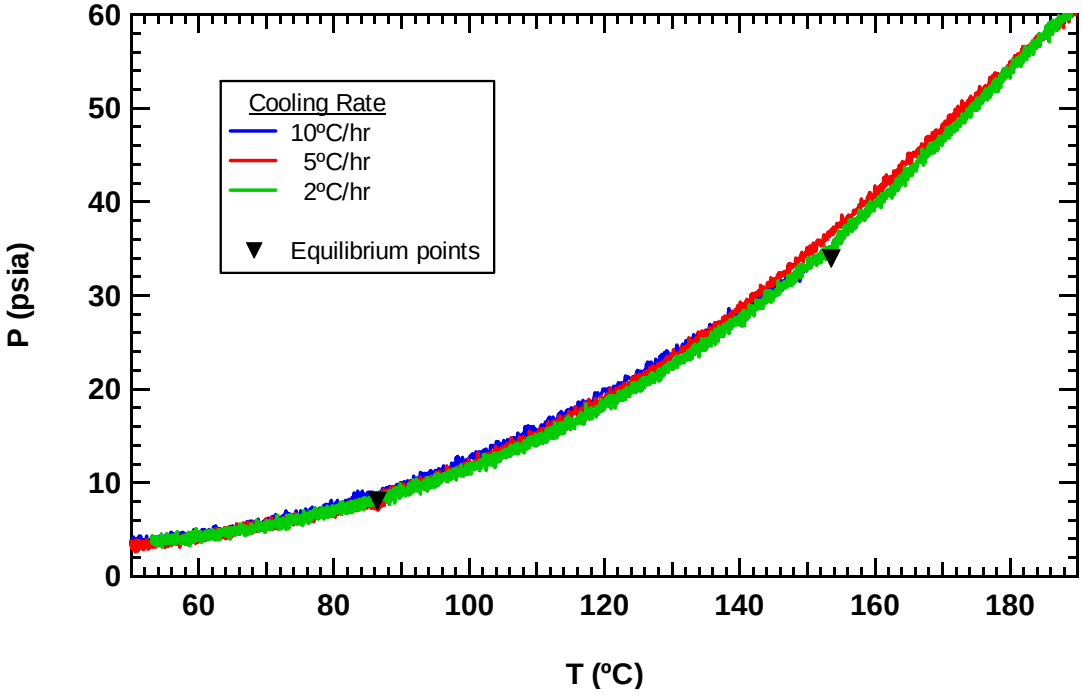

Figure 5.8 Pressure measured during the cooling portion of three thermal cycles of the same PEG/benzene mixture with different furnace cool-down rates. Points at which the mixture was allowed to equilibrate for 12-24 hours are shown for comparison.

Another area of concern in VLE measurements of polymer solutions is whether mass-transfer equilibrium between the phases is achieved. While the pressure measured during heat-up of the furnace was normally below the equilibrium value because of the thermal lag of the vessel, in some cases where the weight percent of solvent was relatively high the measured pressure would swing above the equilibrium value at higher temperatures as in Figure 5.9. In cases such as this, the solvent does not have enough time to mix with the polymer during heat up, so a solvent-rich layer of liquid may exist that leads to a higher pressure that decreases as mass-transfer equilibrium is slowly achieved.

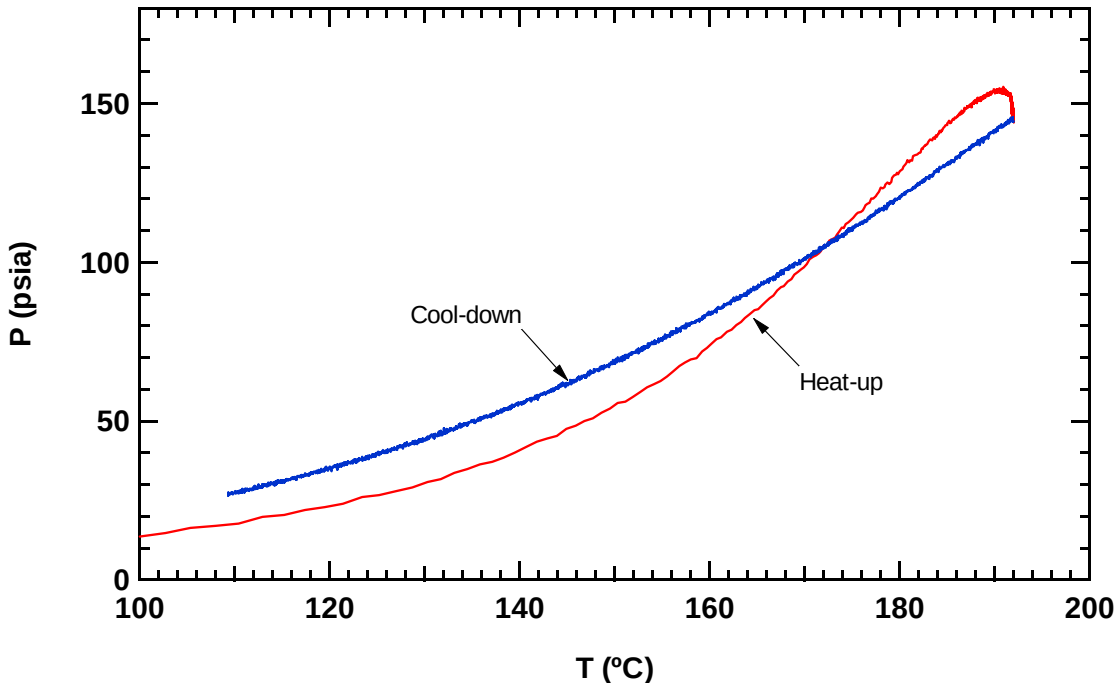

Figure 5.9 Pressure measured during heat-up and cool-down of a PEG/benzene mixture (58.3 wt% benzene).

Polymer solution data from the literature were often collected after one or more days of equilibration time to allow polymer and solvent to go from a completely unmixed state to the equilibrium state. This is one of the reasons that the cool-down portion of the thermal cycle was selected to approximate the equilibrium curve as opposed to the heat-up portion. This method allows the polymer and solvent to mix at the maximum temperature of the run where diffusion rates are higher and initial equilibrium can be achieved more quickly. Although the polymer solution data in the literature were generally collected at much lower temperatures than in this study, the experimental method used here still allowed one to two days for initial equilibrium to be achieved. Only incremental changes in phase composition were then needed as the solutions were allowed to slowly cool. The equilibrium points shown in Figure 5.8 provide evidence that the assumption of mass-transfer equilibrium between phases is good during cool-down.

The experiments described above show that the experimental method used in this research was valid and allowed for appropriate thermal and mass-transfer equilibrium to be achieved.

5.3.3 Duplicate Experiments

The last measure that needed to be taken to validate the use of the HT-VLE facility was to show that results were reasonable and reproducible. Data at 190ºC from the first several experimental runs at different compositions of the PEG/benzene system are shown as orange circles in Figure 5.10. Surprisingly, these data points did not follow the normal concave-down shape that is characteristic of the literature data on the PEG/benzene system at lower temperatures (see Figure 5.11 below for example). The

results of two more runs, including an attempted duplicate, are shown as red triangles in Figure 5.10. Obviously, something was in error since these latter points did not fall on the same curve as the previous data. After further investigation a problem was discovered that the cold-trap allowed some solvent vapors to escape through the vacuum line. Thus, the solvent weight percent in each run was lower than had been calculated from the change in mass of the cold-trap during solvent degassing. The problem was corrected so that no solvent would escape the cold-trap and new experiments were performed. Results are shown as blue diamonds in Figure 5.10, including two approximate duplicates.

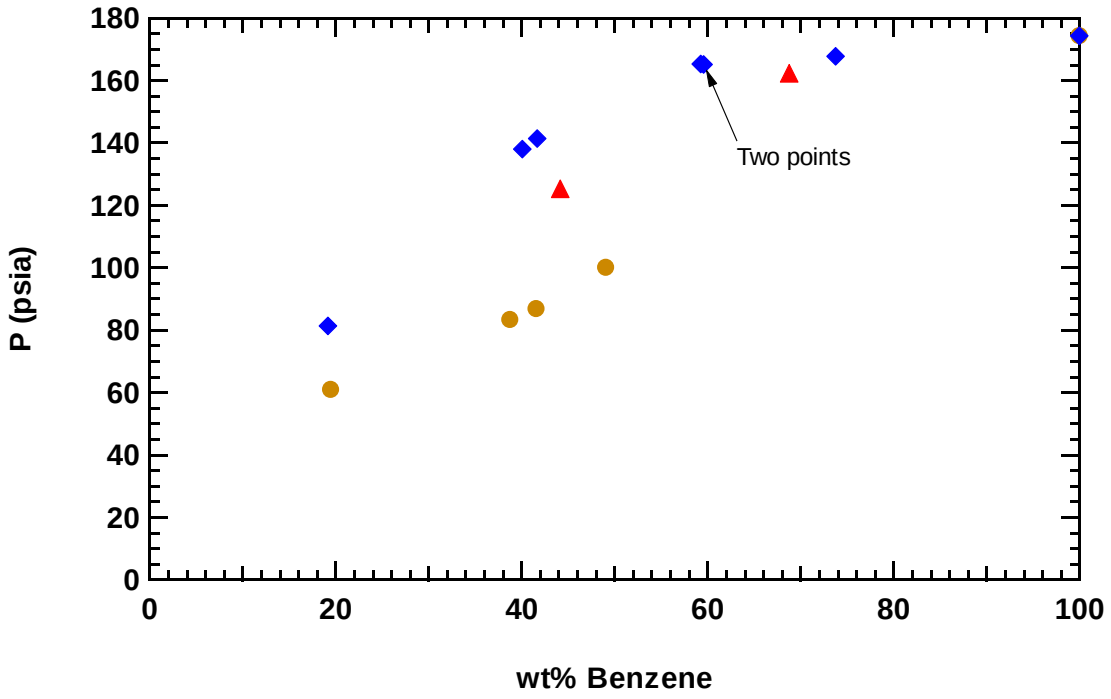

Figure 5.10 PEG/benzene at 190ºC. Initial experiments (orange circles) showed unexpected shape; additional experiments (red triangles) did not fall on the same curve; cold-trap was modified to prevent escape of solvent vapors and new data were collected (blue diamonds).

The new data were reproducible and a curve through the points had the appropriate shape. As further validation, the data collected at 70ºC were compared with data from the DECHEMA data series (pg. 134, Hao et al., 1992), shown in Figure 5.11. These literature data were presented in the form of solvent activities, which were multiplied by the pressure of pure benzene measured in this study to obtain the values of pressure plotted here (the conversion from activities makes the assumption that the vapor phase is ideal – a good assumption at these pressures).

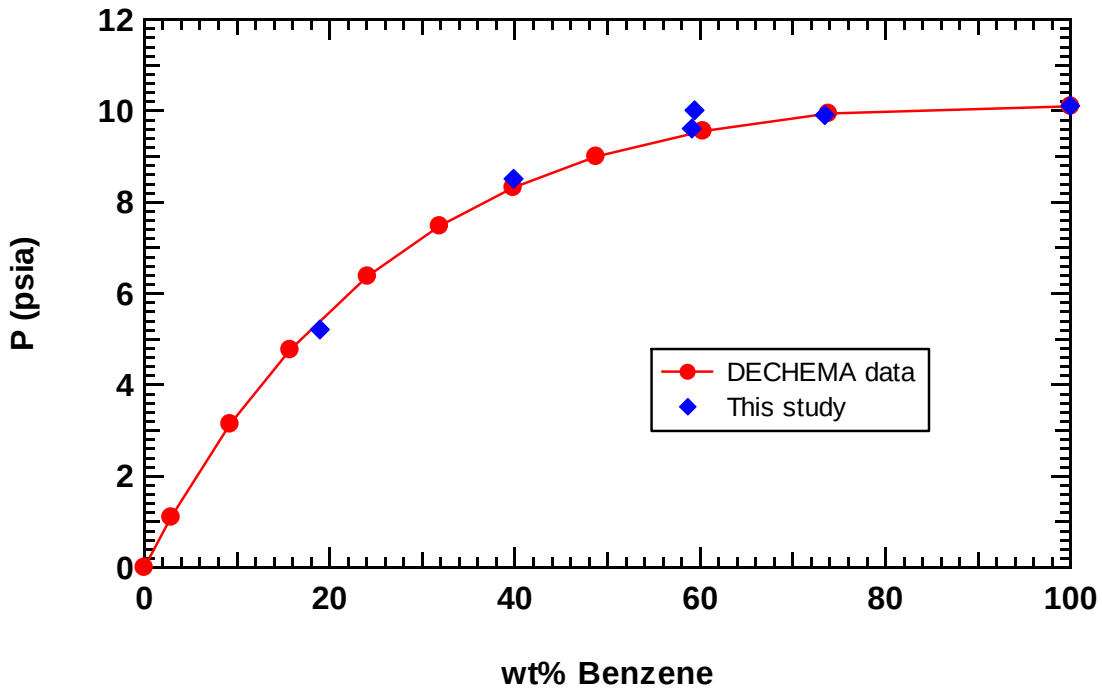

Figure 5.11 Comparison of data collected in this study for the PEG/benzene system at 70ºC with data from the DECHEMA data series (pg. 134, Hao et al., 1992). The number-average molecular weight of the PEG (actually PEO) from the DECHEMA data was 5700.

The results given in this section have shown that polymer solution data collected from the HT-VLE facility at BYU are reproducible and agree well with data in the literature at low temperatures.

5.4 Experimental Results and Discussion

This section contains the experimental results obtained in this work. Also included is a discussion of the data. The results for pure solvent vapor pressure measurements are presented first, followed by the results for each polymer/solvent system in the order in which the experiments were performed.

5.4.1 Pure Solvent Data

The pure solvent vapor pressures measured in this study are presented in Figure 5.12. To reduce the noise evident in the pressure readings, the experimental curves shown in the figure are half-hour pressure averages (meaning they span a temperature range of about 1ºC). As shown earlier for hexanol (Figure 5.5), the pressures measured in the HT-VLE facility are within 1 psi of the DIPPR vapor pressure correlation for benzene, and a correlation for IPP derived by fitting the Antoine equation to data in the range of 117-234ºC from Nesterova et al. (1990). The differences between the DIPPR correlation and the measured pressures for pure furan are somewhat larger, but are still only about 3%. All values of pure solvent vapor pressures presented later, as well as the values used in model calculations, are those measured in this study.

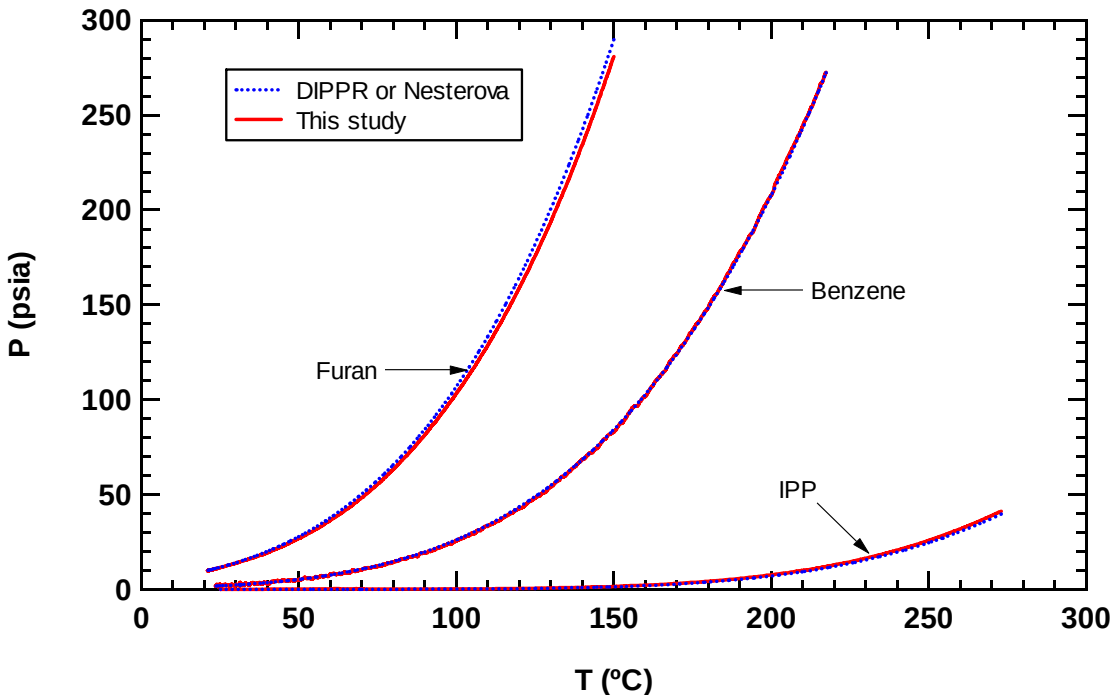

Figure 5.12 Pure solvent vapor pressures measured in HT-VLE facility compared with DIPPR correlations for benzene and furan and a correlation developed by fitting the Antoine equation to data from Nesterova et al. (1990) for IPP.

5.4.2 Finding Liquid Compositions

Only the overall compositions were measured for the polymer solution data collected in the HT-VLE facility. VLE behavior is not completely characterized by overall compositions. In fact, the same overall composition can lead to different equilibrium pressures at the same temperature, depending on the volume of the system. In contrast, all systems with the same liquid composition will have the same equilibrium pressure at the same temperature, even if the amounts of the phases are different.

The liquid compositions, although expected to be fairly close to the overall compositions, were not measured in this work and thus needed to be calculated. This was done by calculating the volume of liquid in the pressure vessel (initially by assuming

everything to be in the liquid phase) and subtracting it from the total system volume to get the volume of vapor. The vapor was assumed to be pure solvent. The measured pressure for each data point was used in the Peng-Robinson equation of state to calculate the vapor molar volume of the pure solvent, and this value was used along with the total vapor volume to find the amount of solvent in the vapor phase. This amount was subtracted from the total amount of solvent in the system to obtain the liquid composition, and the calculation process was repeated until the amount of solvent in the liquid phase converged.

The differences between overall and liquid compositions were significant in some cases and negligible in others. These differences ranged from a maximum of 7.9 wt% solvent difference for PEG/furan at 190ºC (overall composition of 30.2 wt% furan) to a minimum of essentially zero for PS/IPP at 200ºC. These differences were larger at higher temperatures for the same solvent, and for solvents with higher vapor pressures at the same temperature. They were also somewhat larger for experimental runs that had smaller mixture amounts in the pressure vessel.

Unless otherwise noted, all polymer solution compositions given below are reported as liquid compositions. Because one experimental run with constant overall composition experiences different equilibrium pressures at different temperatures, the reported liquid compositions are different at different temperatures even for the same run. This is the reason that the polymer solution data seen below are observed to be at slightly lower solvent weight percents at higher temperatures than at lower temperatures.

The liquid volumes that were needed to calculate the liquid compositions were found from the Tait equation for the two polymers, from DIPPR correlations for benzene

and furan, and from GCVOL for IPP. The mixture volume was assumed to be the sum of the volumes of the pure species (i.e., negligible volume change on mixing). Although this was not necessarily the case, it was found that even at the highest measured equilibrium pressures, changing the estimated liquid volume by over 10% resulted in less than 0.5% change in the predicted difference of overall and liquid compositions.

5.4.3 PEG/Benzene Data

A summary of the valid data for the PEG/benzene system is presented in Figure 5.13. The points represent half-hour pressure averages centered on the respective temperature listed in the legend. Data in tabulated form for this and other chemical systems studied here can be found in the appendix. In all, fifteen runs were conducted on the PEG/benzene system, of which the first nine have compositions that are not well known because of the problem with the cold-trap. The last six runs resulted in very good data, including two pairs of approximate replicates at about 40 and 60 wt% benzene. The pressures measured during the runs at 59.3 and 59.6 wt% benzene, in particular, were within 0.5 psi of each other. In addition, the data collected in this study matched well with data in the literature at 70ºC, as shown previously. In all of the runs the combined mass of PEG and benzene was about 8-10 g, except for the run at 73.8 wt% benzene, which contained only about 5 g of material. From measurements of the mass of the pressure vessel and its contents at different points during the experimental setup, as well as at the end of each run, the possible errors in composition were found to be generally less than 0.5 wt%.

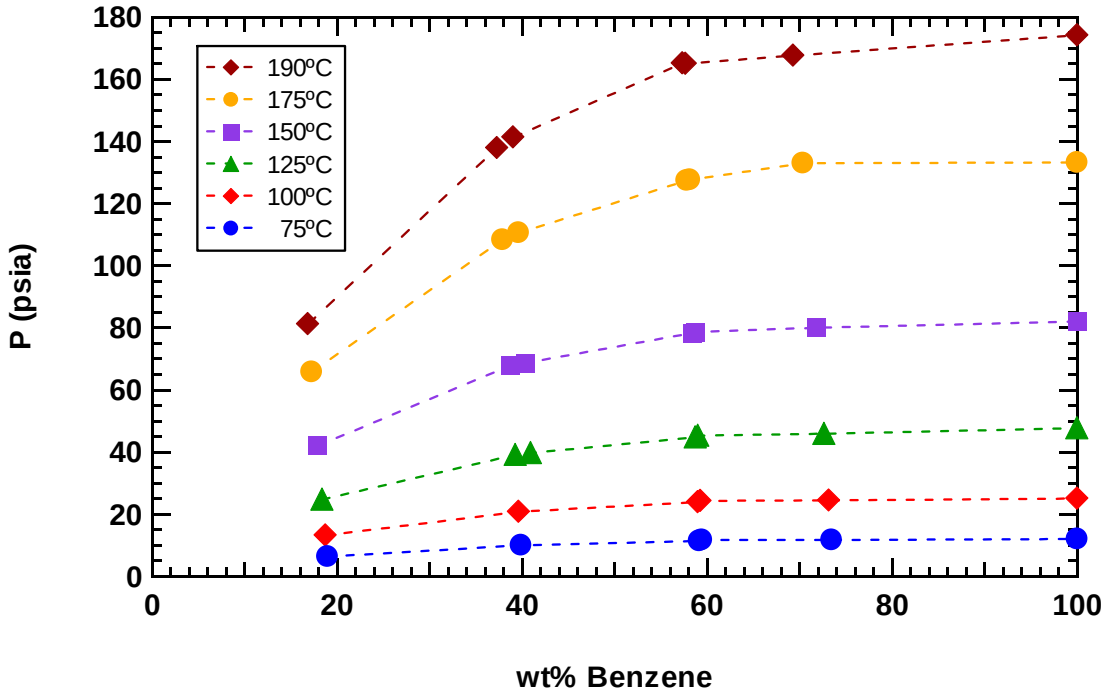

Figure 5.13 PEG/benzene data collected in the HT-VLE facility at BYU. Dotted lines serve to connect data points at the same temperature.

5.4.4 PEG/Furan Data

Data for the PEG/furan system are given in Figure 5.14. Measurements at high solvent weight percents and the highest temperatures could not be taken because of the limitations on the safe operating range of the pressure transducer. Replicates were attempted at compositions around 20 and 30 wt% furan, but the amount of furan removed during solvent degassing was difficult to control. However, the relative results of these two pairs of data points compare reasonably well.

The possible composition errors for this system were somewhat larger than for the PEG/benzene system, averaging about 1.0 wt%. This may be due to the fact that furan is more volatile than benzene and more solvent was lost upon opening the vessel at the end of the run, before the vessel mass was measured again.

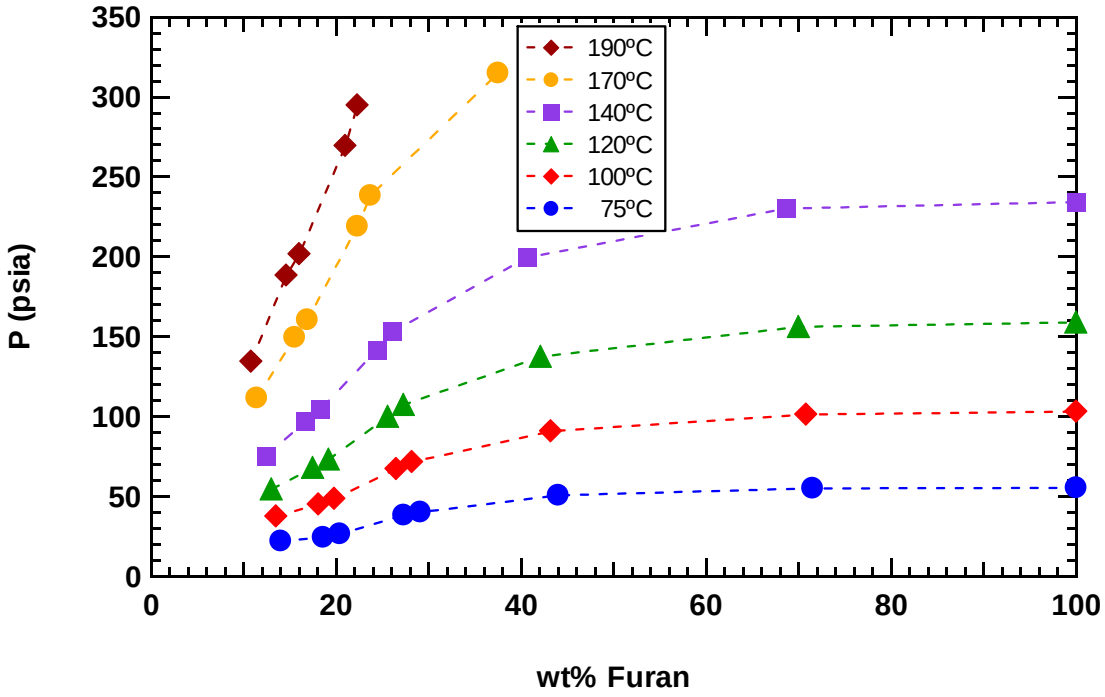

Figure 5.14 PEG/furan data collected in the HT-VLE facility at BYU. Dotted lines serve to connect data points at the same temperature.

The last two runs (at compositions of 21.2 and 19.4 wt % furan) were performed somewhat later than the rest and made use of a new calibration of the pressure transducer. They were also the first runs to employ a cool-down in 25ºC steps with 20 hours of equilibration time between each step, instead of the 2ºC/hr cool-down employed for previous experiments. All remaining experiments were conducted using the 25ºC temperature step method. In the case of experiments following this method, data points represent the one-hour average of the pressure readings at the end of the equilibration time for each step.

Also of note for the PEG/furan system was that most of the mixtures experienced a color change to dark brown. Of concern was whether reactions were taking place that would significantly alter the chemical composition of the mixtures. However, GC/MS

analysis of the volatile species for a few samples indicated the presence of almost pure furan, with very small amounts of BHT and benzene (less than BHT). It was concluded that the color change was most likely due to oxidation of the BHT inhibitor and that any changes in mixture composition due to reaction were negligible.

5.4.5 PS/Benzene and PS/Furan Data

Equilibrium pressures for the PS/benzene and PS/furan systems are shown in Figure 5.15 and Figure 5.16, respectively.

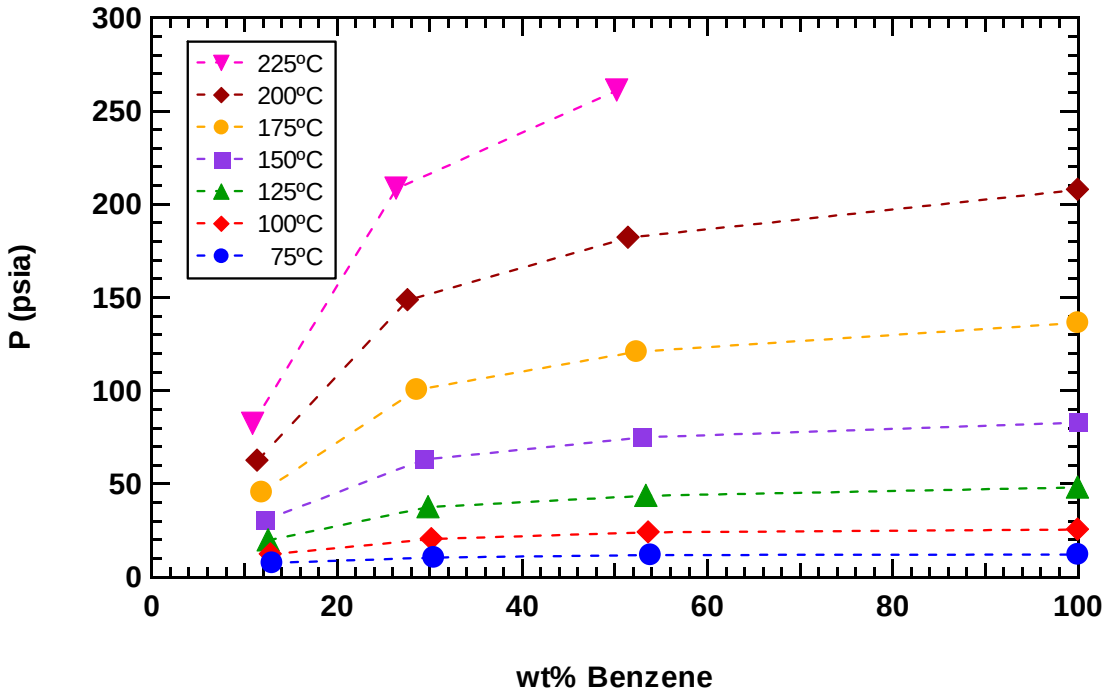

Figure 5.15 PS/benzene data collected in the HT-VLE facility at BYU. Dotted lines serve to connect data points at the same temperature.

From experiments with the previous systems it became obvious that most of the useful information came from data collected at compositions lower than about 50 wt%

solvent, so later efforts were focused on this region. The experimental data collected for these systems, as well as the IPP systems, included temperature readings from the wall of the pressure vessel. Thus the vessel temperature did not need to be calculated from the gage block temperature with the correlation derived from the furnace temperature profile.

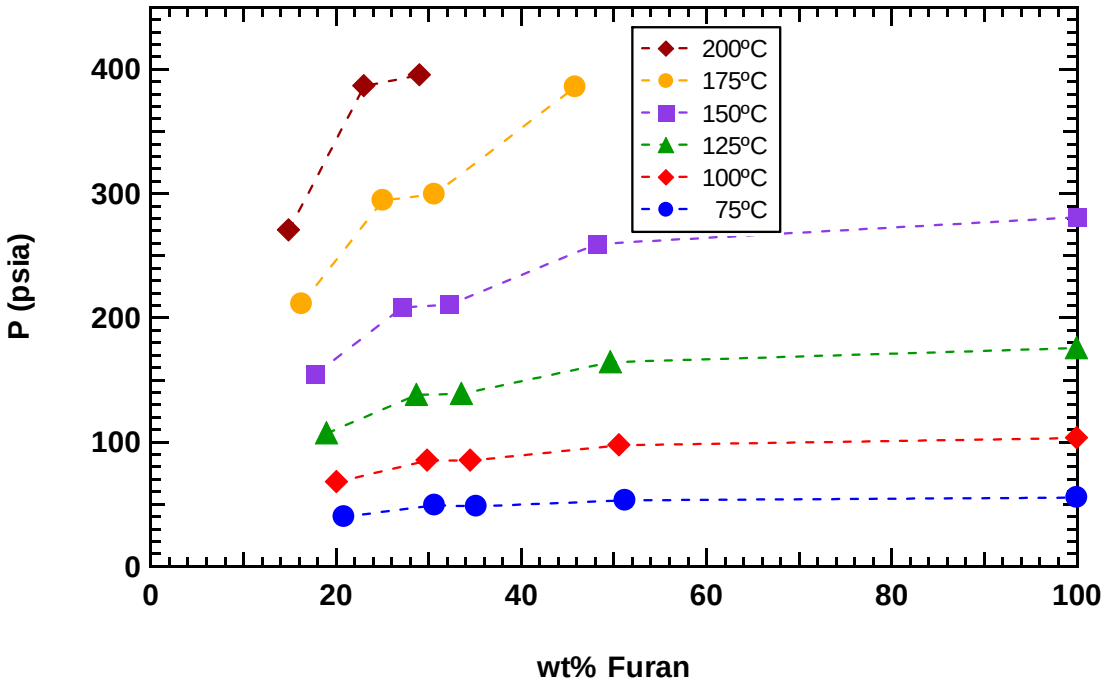

Figure 5.16 PS/furan data collected in the HT-VLE facility at BYU. Dotted lines serve to connect data points at the same temperature.

5.4.6 PEG/IPP and PS/IPP Data

Data for the IPP systems were more difficult to collect than for the others since care was needed to avoid what seemed to be a slow IPP decomposition reaction. Decomposition of IPP at high temperatures (above about 250ºC) necessitated using increasing temperature steps instead of starting at the maximum temperature of the run and cooling the mixture. The initial temperature at which the mixtures were allowed to

equilibrate was still high enough (150ºC) to allow for good diffusion of the mixture species, but longer equilibration times were allowed (up to two days for each step) to ensure that mass-transfer equilibrium was achieved. Several experimental runs, however, showed signs of IPP decomposition even at the initial temperature steps. Sample data from runs with and without decomposition at the low temperature steps are shown below.

Figure 5.17 shows the vessel temperature and pressure during a successful run (no low-temperature decomposition) as functions of elapsed time. Equilibrium was reached at several temperatures, but at 250ºC there was some decomposition. At 275ºC decomposition was occurring fairly rapidly, as evidenced by the rise in pressure. The residual pressure after cool-down was noticeably higher than at the beginning of the run.

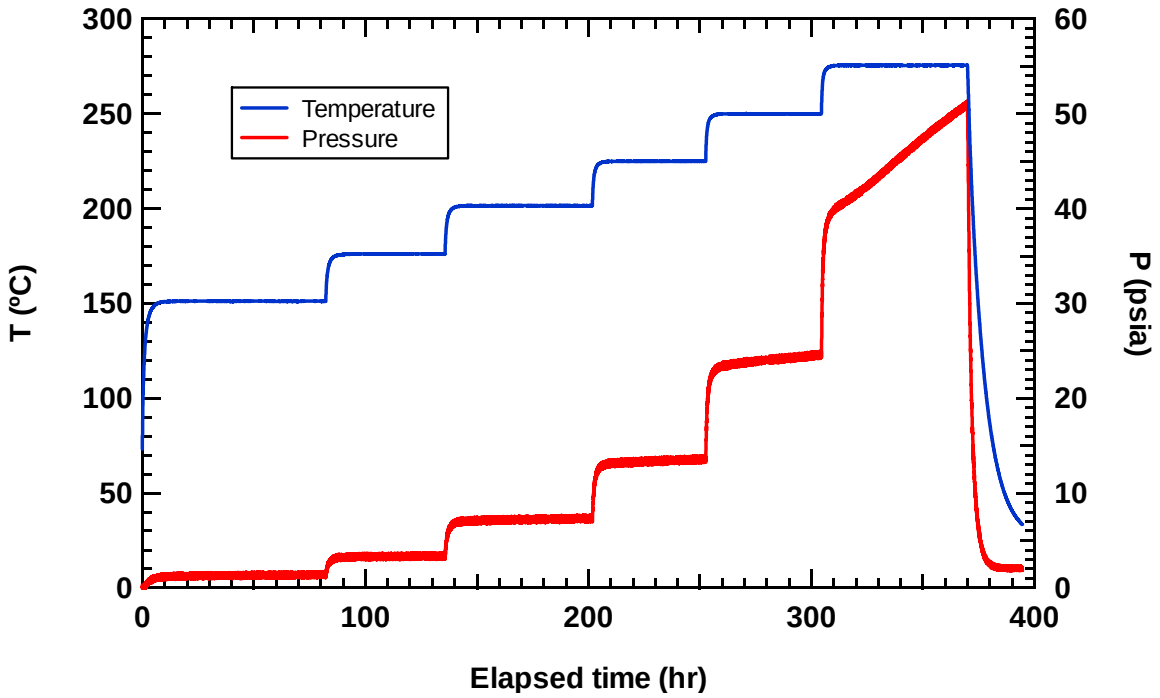

Figure 5.17 Experimental data for a successful run with a mixture of PS/IPP at 50.0 overall wt% IPP.

Figure 5.18 shows the results of an unsuccessful run. From the beginning of the run the measured pressure increased steadily. The reason that the decomposition started at the beginning of the run is not known. Low-temperature IPP decomposition does not seem to be a function of the amount of IPP or the identity of the polymer, because successful runs were achieved at the same conditions as unsuccessful runs. It may be the case that during unsuccessful runs the needle valve leaked enough to allow a small amount of air into the vessel, causing decomposition at lower temperatures. The needle valve did seem to have problems sealing completely, sometimes, after several thermal cycles to temperatures around 300ºC.

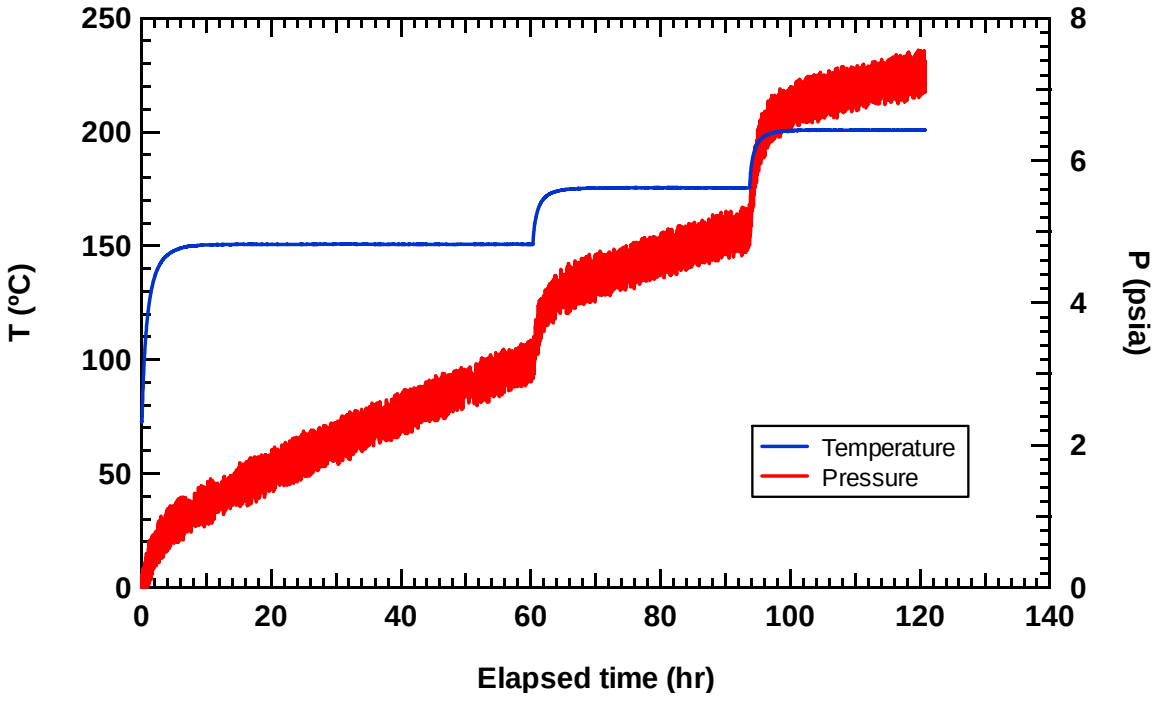

Figure 5.18 Experimental data for an unsuccessful run with a mixture of PEG/IPP at 18.6 overall wt% IPP. The measured pressure shows evidence of slow decomposition even during the first temperature steps.

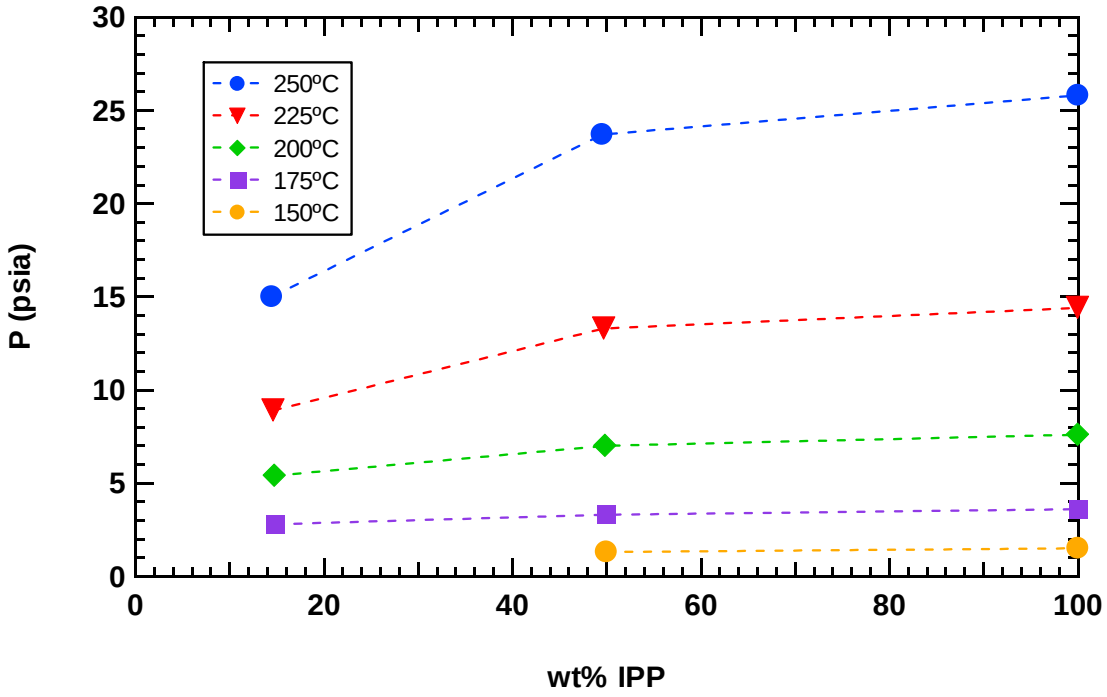

Figure 5.19 PS/IPP data collected in the HT-VLE facility at BYU. Dotted lines serve to connect data points at the same temperature.

The data from successful runs for the PS/IPP and PEG/IPP systems are presented in Figure 5.19 and Figure 5.20, respectively. For these systems the 0-50 psia pressure transducer was used because of its higher sensitivity. It is interesting to note that the data for the PS/IPP systems follow the same trends seen in the previous systems, but the trend in the limited data available for the PEG/IPP system seems to be very different. The pressure is closer to being linear over the range of IPP weight percent. The reason for this different trend is not known, but modeling results presented in chapter 9 support it at least qualitatively.

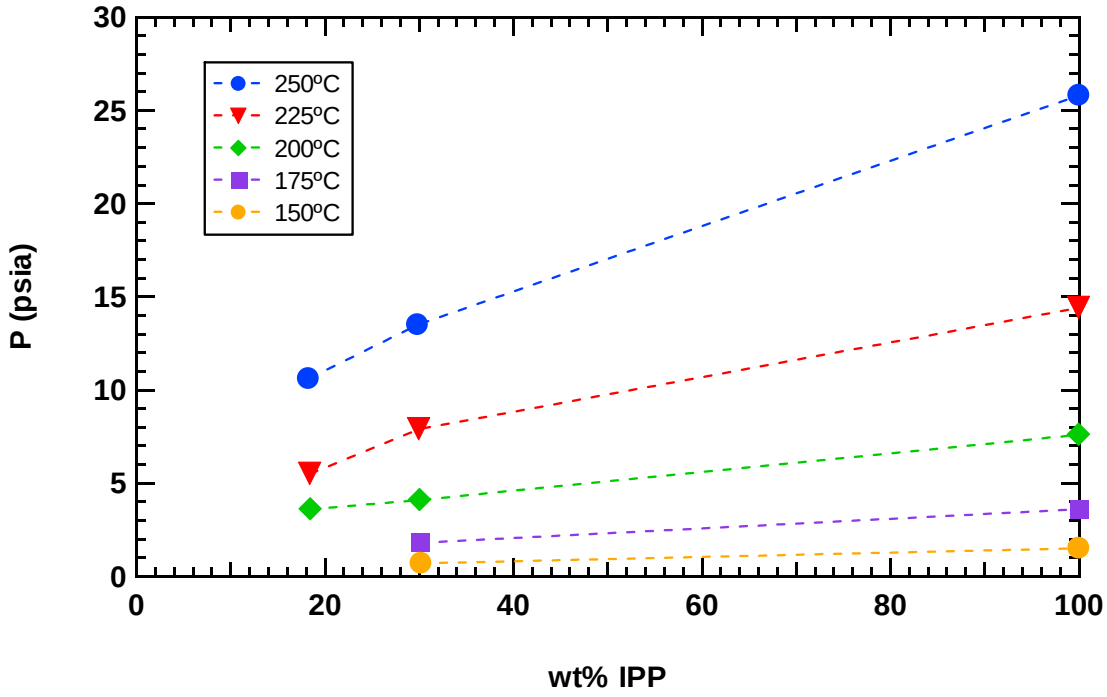

Figure 5.20 PEG/IPP data collected in the HT-VLE facility at BYU. Dotted lines serve to connect data points at the same temperature.

5.5 Summary of Experimental Results

This chapter included the presentation of several important experimental measurements. The reported system volume was 29.25 mL. The decomposition temperatures of PEG and PS were found to be 367 and 398ºC, respectively. However, evidence of some decomposition at lower temperatures limited later VLE experiments to temperatures below 300ºC.

The HT-VLE facility components were validated by comparing readings of pure solvent vapor pressures with literature correlations for hexanol, benzene, furan, and IPP. The largest average difference was about 3% for the vapor pressure of furan, while the measured vapor pressures of benzene and IPP were consistently within 1 psi of the

literature values. In the process of this comparison, the difference in temperature between the gage block and pressure vessel was found to be significant.

The experimental method for measuring the equilibrium pressure of high-temperature polymer solutions was also validated. After correcting a problem with the cold-trap, data were shown to be reproducible. In addition, care was taken to show that the data were collected under conditions of thermal and mass-transfer equilibrium. Next, data collected at 70ºC in the HT-VLE facility for PEG/benzene were compared with data from the literature and were found to be in very good agreement.

For purposes of correctly characterizing the VLE behavior, liquid compositions were calculated from the overall compositions of each run conducted in the HT-VLE facility. This was done using the volume available to the mixture in the pressure vessel, correlations for the volume of the liquid components, and the Peng-Robinson equation of state for the pure solvents. The amount of solvent in the vapor phase at each temperature was calculated through an iterative process and then subtracted from the overall amount in the vessel to obtain the liquid composition.

Equilibrium pressure data were collected at temperatures between 75 and 250ºC for six polymer/solvent systems – combinations of PS and PEG with benzene, furan, and IPP. Data trends for most of the systems were consistent with trends seen in literature data for the benzene systems (and other polymer/solvent systems) at lower temperatures. The equilibrium pressures for the PEG/IPP system, however, were closer to being linear over the composition range. The data collected in this study were unique in that data were not previously available in the literature for the benzene systems at temperatures above 70ºC, nor were any data available for the furan or IPP systems.

6 Estimating Liquid Molar Volumes

Almost all of the free-volume activity coefficient models require the use of liquid molar volumes of the pure species during calculation of mixture properties. For most solvents and some common polymers correlations of liquid molar or specific volume data exist in the literature (e.g. the Tait equation for polymers, and correlations from the DIPPR database for solvents). For complex polymers such as the polymer-like initial decomposition products of REF experimental data are not available. In this chapter is an evaluation of different volume estimation methods available in the literature for use in estimating polymer volumes (volumes refer to molar or specific volumes, which are used interchangeably). Attention is then given to estimating solvent volumes in cases when they are not available. This chapter also includes the group assignments necessary to estimate the volume of the polymer-like REF decomposition products, as well as of the solvent, IPP. Recommendations for estimating unknown volumes are summarized.

6.1 Polymer Volumes

Two group-contribution methods for polymer volume estimation, GCVOL (Elbro et al., 1991) and GCMCM (Sato et al., 1998), have been used in the literature on free-volume ACMs. These methods have been described previously. Most studies in the literature have made use of the GCVOL method to estimate the specific volume of

polymers for which no Tait parameters are available. As mentioned earlier, a few studies used the GCMCM method, but only one compared the two methods and the comparison was only carried out for polymers that were used in the regression of GCMCM group parameters. Thus, no definitive comparison of these two methods exists in the literature.

In this study, an evaluation of GCMCM and GCVOL was made by comparing estimated polymer volumes with polymer volumes correlated by the Tait equation using parameters from Rodgers (1993), or with experimental volumes from the literature. The revised GCVOL parameters of Ihmels and Gmehling (2003) were used. The polymers used in this evaluation, and the sources and ranges of data, are listed in Table 6.1.

The polymers used were selected for various reasons, some because of their structure and some because they were not used in developing the volume estimation methods. PEO and PS were included because they were used in the experimental part of this research. PEO is essentially the same polymer as PEG, but with different end groups. PDMS was selected because it has siloxane groups like REF (although these will generally not be a part of the polymer-like decomposition products as a result of the reverse Diels-Alder reactions). PA66 was used because of its nitrogen groups and also because it was the polymer with the largest volume errors for the GCMCM method. EVA18 was chosen because it is a copolymer. PC was included because it is a polymer of bisphenol-A. PBSA, PEOx, and PVPhKH were selected specifically because they (along with others listed below) were not used in the regression of GCMCM parameters. PBS-br was chosen because it is branched. PPO was included for its main-chain aromatic rings. Finally, PEI, ER6, and CE were selected because they are very similar structurally to components of REF. CE is an epoxy network like REF.

Table 6.1 Summary of *PVT* data used for comparison of volume estimation methods.

Polymer	Symbol	Range of data used		Data Type	Source
		T (ºC)	P (bar)		
Poly(ethylene oxide)	PEO	88-224	1-300	Tait eqn.	(Rodgers, 1993)
Polystyrene	PS	115-196	1-300	Tait eqn.	(Rodgers, 1993)
Polydimethylsiloxane	PDMS	25-70	1-300	Tait eqn.	(Rodgers, 1993)
Bisphenol-A polycarbonate	PC	151-340	1-300	Tait eqn.	(Rodgers, 1993)
Polyamide 6,6	PA66	246-298	1-300	Tait eqn.	(Rodgers, 1993)
Poly(ethylene-*co*-vinyl acetate)[a]	EVA18	112-219	1-300	Tait eqn.	(Rodgers, 1993)
Poly(butylene succinate)[b]	PBS-br	120-220	1-500	Table	(Sato et al., 2000)
Poly(butylene succinate-*co*-adipate)[c]	PBSA	120-220	1-500	Table	(Sato et al., 2000)
Poly(2-ethyl-2-oxazoline)	PEOx	40-220	100	Table	(Maldonado-Santoyo et al., 2004)
Poly(vinyl phenyl ketone hydrogenated)[d]	PVPhKH	40-221	100	Table	(Maldonado-Santoyo et al., 2004)
Poly(2,6-dimethylphenylene oxide)	PPO	210-330	0-400	Table	(Zoller and Walsh, 1995)
Polyetherimide	PEI	222-359	0-400	Table	(Zoller and Walsh, 1995)
Epoxy resin of diglycidyl ether of bisphenol-A[e]	ER6	76-196	1-400	Figure	(Dlubek et al., 2007)
Cured epoxy of DGEBA and triethylene-tetramine[f]	CE	39-141	100	Figure	(Brostow et al., 2004)

[a] 18 wt% (7 mol%) vinyl acetate
[b] Branched structure
[c] 20 mol% butylene adipate
[d] 23 mol% units with ketone, balance hydrogenated to alcohol
[e] DGEBA oligomer of 6 units on average
[f] Not in molten state; no information about mole ratio of DGEBA to triethylene-tetramine provided in source, ratio assumed to be 1

The group assignments (including how many of each group) that were used to describe the structure of each polymer for both volume estimation methods are presented in Table 6.2. The parameters for each group are given in the appendix. In general, it was more difficult to describe the structures of polymers containing aromatic rings in the chain using GCVOL than using GCMCM. Often GCVOL did not have an appropriate group, so substitutions were made. Different possibilities could make large differences in error. When the structure of a polymer included an aromatic carbon with no hydrogen attached (an AC group), the ACH group (an aromatic carbon with attached hydrogen) was used in GCVOL, and the molecular weight of the repeating unit was increased by the weight of the extra hydrogen. This was found to be better than trying to subtract a hydrogen from another group somewhere else in the molecule (e.g. using a CH_2 group to represent a CH_3 group). It was also found to be generally better to avoid representing aromatic carbons using groups containing non-aromatic carbons. For example, the structure of PC has two aromatic carbons with no attached hydrogens that could not be properly fit into any existing GCVOL groups. If the C group was used to represent the aromatic carbon, the average error increased from 3.5% to over 10%. However, this was sometimes unavoidable using GCVOL, such as in the structures of PC, PPO, and PEI where ether oxygens have no linkages other than with aromatic carbons or carboxyl groups. In these cases the CO (ether) group was used in GCVOL to represent the ACO (aromatic carbon with attached ether oxygen) group. They could not be treated separately because GCVOL has no lone oxygen group.

Table 6.2 Comparison of deviations between values of polymer specific volume from the Tait equation or experimental data and values predicted by GCMCM or GCVOL.

	GCMCM			GCVOL		
Polymer	Group assignments	AAD%[a]	Max. dev.%	Group assignments	AAD%[a]	Max. dev.%
PEO[b]	2:CH_2, 1:O	0.81	1.14	1:CH_2, 1:CH_2O	1.21	4.18
PS[b]	1:CH_2, 5:ACH, 1:ACCH	0.42	0.44	1:CH_2, 5:ACH, 1:ACCH	7.91	10.14
PDMS[b]	2:CH_3, 1:SiO	0.02	0.04	2:CH_3, 1:SiO	2.33	4.80
PC[b,c,d]	2:CH_3, 1:C, 1:COO, 8:ACH, 3:AC, 1:ACO	0.17	0.27	2:CH_3, 9:ACH, 1:ACC, 1:ACCOO, 1:CO	3.54	10.17
PA66[b]	10:CH_2, 2:CO, 2:NH	2.59	2.98	8:CH_2, 2:CH_2CO, 2:NH	12.28	15.93
EVA18	0.07:CH_3, 1.93:CH_2, 0.07:CH, 0.07:COO	1.92	2.08	1.93:CH_2, 0.07:CH, 0.07:CH_3COO	1.45	2.79
PBS-br	6:CH_2, 2:COO	1.04	2.08	4:CH_2, 2:CH_2COO	2.28	6.95
PBSA	6.4:CH_2, 2:COO	1.20	1.97	4.4:CH_2, 2:CH_2COO	2.30	6.95
PEOx[e]	1:CH_3, 3:CH_2, 1:CO, 1:NH	8.26	10.19	1:CH_3, 2:CH_2, 1:CH_2CO, 1:N	2.25	5.21
PVPhKH[d]	1:CH_2, 1:CH, 5:ACH, 0.77:ACCH, 0.23:ACCO, 0.77:OH	3.64	8.21	1:CH_2, 0.77:CH, 6:ACH, 0.77:CHOH, 0.23:CHCO	3.78	4.64
PPO[c,d,f]	2:CH_3, 2:ACH, 3:AC, 1:ACO	12.74	13.23	3:ACH, 2:$ACCH_3$, 1:CO	2.73	7.56
PEI[c,d,e,g]	2:CH_3, 1:C, 4:CO, 18:ACH, 10:AC, 2:ACO, 2:NH	8.43	9.47	2:CH_3, 1:C, 28:ACH, 4:CHO, 2:CO, 2:N	28.41	30.52
ER6[c,d]	2:CH_3, 2:CH_2, 1:CH, 1:C, 8:ACH, 2:AC, 2:ACO, 1:OH	0.40	0.72	2:CH_3, 2:CH_2, 9:ACH, 1:ACC, 1:CHOH, 2:CO	13.23	15.73
CE[c,d,h]	2:CH_3, 8:CH_2, 1:CH, 1:C, 8:ACH, 2:AC, 2:ACO, 4:NH, 1:OH	10.29	11.76	2:CH_3, 6:CH_2, 9:ACH, 1:ACC, 1:CHOH, 2:CO, 2:CH_2NH_2, 2:NH	7.40	7.80
Overall		3.71			6.51	
Overall w/o polymers used in GCMCM regression		5.32			7.09	

[a] Average absolute percent deviation over *T* and *P* ranges listed in Table 6.1
[b] Polymer included in the determination of GCMCM group parameters
[c] GCVOL does not have ACO (ether) group, so CO (ether) was used
[d] GCVOL does not have AC group, so ACH group was used and *MW* of repeating unit was increased by weight of extra hydrogen
[e] GCMCM does not have N group, so NH group was used and *MW* was increased accordingly
[f] For GCMCM, if ACO group is replaced with O and C groups (similar to GCVOL, where CO is used to represent the ACO group) AAD% decreases to 5.91
[g] GCVOL does not have CO (carbonyl) group, so CHO (aldehyde) group was used and *MW* was increased according
[h] GCMCM does not have NH_2 group, so NH group was used and *MW* was decreased accordingly

Table 6.2 also gives the average and maximum deviations of the estimated polymer volumes from experimental values or those calculated from the Tait equation over the temperature and pressure ranges listed in Table 6.1. For most polymers evaluated here, using the GCMCM method resulted in slightly smaller average deviations and significantly lower maximum deviations. The average deviation in polymer volumes overall was 3.71% for GCMCM, compared to 6.51% for GCVOL. When the polymers used in the regression of the GCMCM parameters were excluded, the average overall deviation was 5.32% for GCMCM and 7.09% for GCVOL.

One of the reasons for the larger differences in maximum volume errors between the two methods, relative to the average errors, is shown in Figure 6.1. This figure gives a comparison of errors in temperature sensitivity, calculated here as the difference between the specific volumes at the highest and lowest temperatures of the temperature range for each polymer divided by the size of the range. The figure shows that, overall, errors in the temperature sensitivity were smaller for GCMCM than for GCVOL. Of the fourteen polymers examined here, the only exceptions were PVPhKH and CE. In general, the GCVOL method greatly overestimated the temperature sensitivity of polymer volumes. This means that the predictions from GCVOL were not only off by a constant amount, but that the whole characterization of the polymer volume behavior was incorrect. Thus, for estimating polymer volumes, GCMCM is recommended.

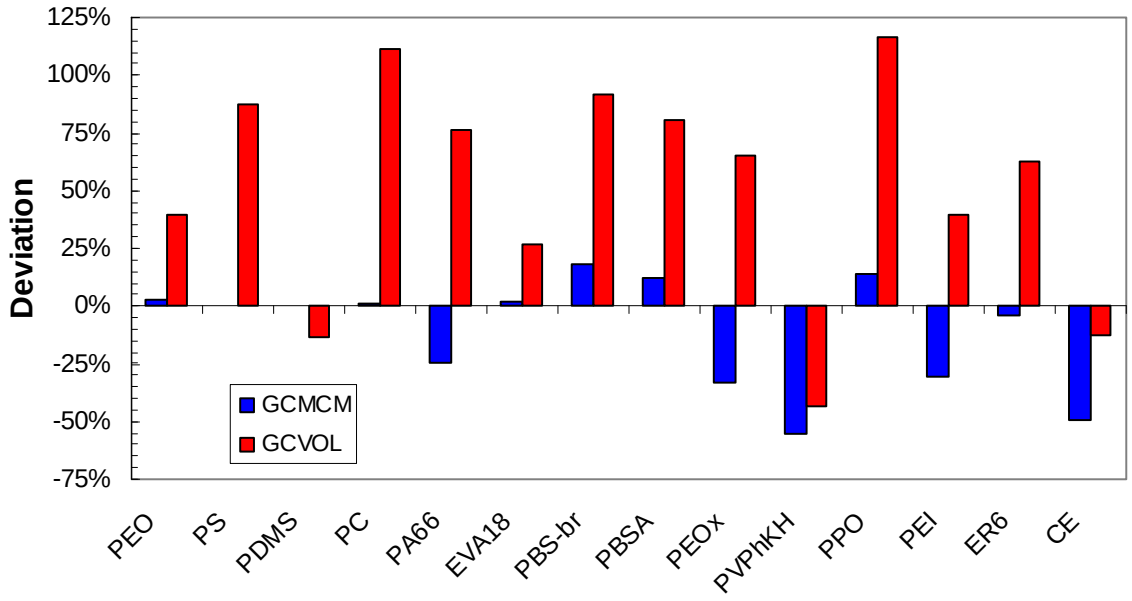

Figure 6.1 Deviations between estimated and experimental temperature sensitivities of polymer volumes. Temperature sensitivities were calculated as the total change in specific volume over the temperature ranges listed in Table 6.1. Deviations averaged over pressure ranges.

6.2 Solvent Volumes

For most solvents, correlations of liquid volumes are available in the DIPPR database. When they are not available, as in the case of IPP, the GCVOL method can be used to estimate the volume. The GCVOL method was developed specifically for use with small and large molecules. In fact, all of the information used in the regression of its group parameters comes from data on small molecules. A large table of groups that are applicable to solvents is available from the work of Ihmels and Gmehling (2003).

A comparison of liquid solvent volumes calculated from correlations in the DIPPR database and predicted by GCVOL is presented in Figure 6.2. The solvents shown are furan and benzene, as well as two solvents similar to IPP that are in the DIPPR database (4-ethylphenol and 4-tertbutylphenol). The GCVOL predictions were

satisfactory for most of these solvents at temperatures that were not close to the critical temperature of the solvent. The large deviations in the specific volume of furan may result from the fact that there was not an appropriate group in GCVOL to describe the oxygen. An ACOH group (aromatic carbon with attached OH) was used here for the sole reason that it gave better results than using the non-aromatic ether CHO group. The GCVOL method was originally specified for use only up to the normal boiling point of a solvent and was not able to reproduce the sharp rise in specific volume that occurred as the critical point was neared. However, deviations between GCVOL and DIPPR were less than 5% up to temperatures that are 80% of the critical temperature for benzene, and up to 90% of the critical temperature for ethylphenol and tertbutylphenol.

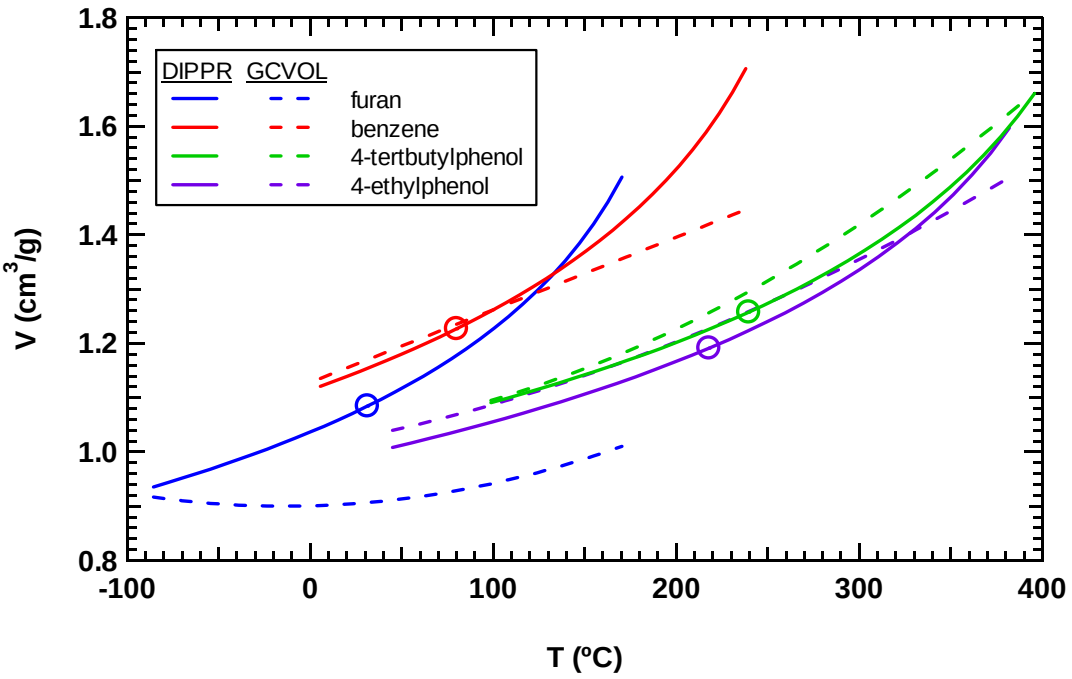

Figure 6.2 Comparison between solvent volumes, at temperatures from the melting point up to about 90% of the value (on an absolute scale) of the critical temperature, calculated from correlations in the DIPPR database (Rowley et al., 2005) and those predicted by the GCVOL method. Circles indicate the normal boiling point of each solvent.

6.3 Group Assignments Necessary to Calculate Liquid Volumes in This Work

The group assignments for the polymer-like decomposition products of REF were based on the structure shown previously in Figure 3.1, and are given in Table 6.3 along with specific volumes estimated for 1 bar at 100 and 300ºC. Although GCMCM is the method recommended for use with polymers, information for GCVOL is also provided for comparison purposes. While both methods predicted roughly the same volume at 100ºC, the GCVOL prediction was 6% higher at 300ºC. As shown previously, the temperature sensitivity estimated using GCVOL is likely too large.

Table 6.3 Group assignments and predicted specific volumes (at 1 bar) for GCMCM and GCVOL for polymer-like decomposition products of REF.

Method	Group assignments	$\widetilde{V}$ at 100ºC (cm^3/g)	$\widetilde{V}$ at 300ºC (cm^3/g)
GCMCM[a,b]	7:CH_3, 43:CH_2, 16:CH, 2:C, 3:COO, 18:ACH, 4:AC, 4:ACO, 4:NH, 5:OH, 2:O	0.9209	1.0364
GCVOL[c,d,e]	7:CH_3, 23:CH_2, 1:C, 19:ACH, 2:$ACCH_2$, 1:ACC, 1:CH_2OH, 4:CHOH, 3:CH_2COO, 2:CH_2O, 4:CO, 12:CH_2 (cyclic), 12:CH (cyclic), 2:NH, 2:N	0.9162	1.1022

[a] GCMCM does not have N group, so NH group was used and *MW* was increased accordingly
[b] ACO (ether) was used to represent part of furan
[c] GCVOL does not have AC group, so ACH group was used and *MW* was increased accordingly
[d] GCVOL does not have ACO (ether) group, so CO (ether) was used
[e] CO (ether) was used to represent part of furan

Because there is no correlation for the liquid volume of IPP in the DIPPR database, GCVOL group assignments and specific volume predictions at 100 and 300ºC are given in Table 6.4. No pressure is given with the GCVOL volume predictions because the GCVOL method has no pressure dependence.

Table 6.4 Group assignments and specific volumes for GCVOL for IPP.

Group assignments	$\widetilde{V}$ at 100ºC (cm^3/g)	$\widetilde{V}$ at 300ºC (cm^3/g)
2:CH_3, 4:ACH, 1:ACCH, 1:ACOH	1.0776	1.4372

6.4 Recommendations for Estimating Liquid Volumes

This study contained the first comprehensive comparison of the GCMCM and GCVOL methods for use in predicting polymer volumes. Overall, the GCMCM method is recommended. Although the overall average deviation of the GCVOL method was only slightly larger than that from GCMCM (7.09% vs. 5.32% when results for polymers used the regression of GCMCM parameters were excluded), there were several other factors that also discouraged the use of GCVOL for predicting polymer volumes. The first was that the predicted temperature sensitivity was generally too high. In addition, the quality of GCVOL predictions did not seem to be consistent from polymer to polymer. There were several polymers for which GCVOL predictions differed from literature values by more than 10%, notably for PA66, PEI, and ER6. Such cases for GCMCM predictions were fewer and not as severe.

GCVOL is recommended, however, as a method for estimating solvent volumes when no other information is available. It should not be used at temperatures higher than approximately 80% of the solvent critical temperature, though. Also, predicted volumes may have large errors when appropriate group assignments are not available.

7 Polymer EOS Parameters

Excess energy mixing rules are used to calculate mixture parameters for equations of state from pure component parameters and from information on mixing from an activity coefficient model. For small molecules the pure component parameters are generally calculated from correlations involving critical properties. However, for polymers the critical properties cannot be measured because decomposition occurs at temperatures below the critical point. Thus some other method must be used to determine their equation of state parameters. Acceptable values of these parameters should lead to a good fit of liquid volumes, as well as the prediction of essentially zero vapor pressures.

The EOS parameters needed in this work are those of the Peng-Robinson equation of state, a cubic EOS usually written in the form of

$$P = \frac{RT}{\overline{V} - b} - \frac{a}{\overline{V}^2 + 2\overline{V}b - b^2} \qquad \textbf{(7.1)}$$

where a is the energy parameter and b is the volume parameter. The first term on the right side of the equation gives the repulsive contribution to the equation of state. The denominator of this term represents the free-volume (b is the excluded molar volume).

The second term is the attractive contribution. A problem with the parameters of the EOS in this form is that *a* and *b* are known to vary significantly with molecular size, as does the molar volume, $\overline{V}$. However, it is desirable to have parameters whose values are constant for a given polymer, and not dependent on the molecular weight. One option is to modify the equation to replace $\overline{V}$ with the specific volume, $\widetilde{V}$, which for polymers does not vary significantly with molecular weight. The Peng-Robinson EOS can then be written as

$$P = \frac{1}{MW}\left[\frac{RT}{\widetilde{V} - b/MW} - \frac{a/MW}{\widetilde{V}^2 + 2\widetilde{V}\,b/MW - (b/MW)^2}\right] \qquad \textbf{(7.2)}$$

7.1 Method of Louli and Tassios

Of the methods for determining polymer EOS parameters in the literature, that of Louli and Tassios (2000) was found to give the best fit of specific volumes and the lowest predicted polymer vapor pressures. Their method involves fitting the equation of state to *PVT* data over a wide range of temperature and pressure. Like the proponents of most other methods they assume *a/MW* and *b/MW* to be constants for a given polymer, regardless of molecular weight. Using this method for PIB (*MW* = 50,000) they reported matching experimental specific volume data to within a few percent and predicting polymer vapor pressures below 10^{-13} bar even at temperatures above 200ºC.

As one alternative in this research, the method of Louli and Tassios was followed to find appropriate EOS parameters for polymers. Values for *a/MW* and *b/MW* were obtained by fitting the Peng-Robinson equation of state to experimental specific volumes

correlated by the Tait equation using parameters from Rodgers (1993). The regression was accomplished by using the optimization program, OptdesX (Parkinson et al., 1994), to minimize the objective function

$$F = \sum_{n} \left(\frac{\tilde{V}_{calc} - \tilde{V}_{data}}{\tilde{V}_{data}} \right)^2 \Big/ n \qquad \textbf{(7.3)}$$

where $\tilde{V}_{calc}$ and $\tilde{V}_{data}$ are the calculated and experimental specific volumes and n is the number of points. This objective function represents the mean squared fractional error in specific volume. Because the function was found to depend only weakly on the value of *a/MW* in relevant regions of the parameter space (making it difficult to find the minimum), it was sensitized to this parameter by replacing *a/MW* with exp(*A*) in Equation 7.2 (an implicit equation for $\tilde{V}_{calc}$). The value of *A* was varied to find the minimum in the objective function and then used to calculate the value of *a/MW*.

Table 7.1 Values of parameters for Peng-Robinson EOS obtained in this work (assuming *MW* = 50,000) compared with values reported by Louli and Tassios (2000).

	This work			Louli & Tassios		
Polymer	*a/MW* [a]	*b/MW* [b]	AAD% [c]	*a/MW* [a]	*b/MW* [b]	AAD% [c]
PIB	2,010,000	1.0908	1.20	2,307,400	1.0882	1.21
HDPE	1,163,000	1.1910	2.07	1,280,756	1.2066	2.30
PEO	3,535,000	0.9631	2.51	2,278,342	0.9497	2.63
PS	5,090,000	0.9933	1.08	1,315,409	0.9549	2.99

[a] Units of (cm^6·bar/mol·g), so *a* has units of (cm^6·bar/mol^2)
[b] Units of (cm^3/g), so *b* has units of (cm^3/mol)
[c] Based on using parameters of Louli & Tassios with *T* and *P* ranges used in this work and with *MW* = 50,000; original AAD% reported by Louli & Tassios for PIB, HDPE, PEO, PS were 1.40, 2.77, 2.48, 2.17

Values of the PR EOS parameters for a few polymers obtained in this work are compared in Table 7.1 with values reported by Louli and Tassios. There is good agreement for PIB and HDPE but not for PEO or PS. Some reasons are discussed below.

7.1.1 Effects of Molecular Weight and Data Range

The EOS parameter values obtained from fitting *PVT* data depend on several things including the range of the data, the molecular weight assumed for calculations, and the choice of objective function to be minimized. The ranges of data used by Louli and Tassios were the temperature and pressure ranges given with the Tait parameters for each polymer. For validation purposes, the complete ranges given with the Tait parameters for PIB and linear polyethylene (high-density polyethylene, HDPE) were also used in this work. For PEO and PS, the same temperature ranges were used in this work as by Louli and Tassios, but the pressure ranges were limited to 1-150 bar, which is more reasonable for VLE applications. It can be seen in Table 7.1 that agreement between the parameters obtained in this work and by Louli and Tassios is much better for PIB and HDPE than for PEO and PS. Because for PIB and HDPE the data ranges used were the same, and because figures in the article by Louli and Tassios suggest that they also used a molecular weight of 50,000 at least for PIB, the relatively small differences in parameters may be the result of different objective functions. The large differences in the PEO parameters and especially in the PS parameters may be partially the result of the different pressure ranges used, but is likely more attributable to the use of different molecular weights during parameter regression. This will be discussed in greater detail below.

Although the Tait equation is not a function of molecular weight, specific volumes predicted by the Peng-Robinson EOS do vary with molecular weight even when

a/MW and *b/MW* are constant. Louli and Tassios do not report the molecular weights used in their parameter regressions, nor do they mention that values for molecular weight are needed. They report parameter values as being independent of molecular weight. However, different combinations of *a/MW* and *b/MW* are obtained when different values of molecular weight are assumed. Sample results for PIB parameters are shown in Table 7.2. As can be seen, even though the values vary widely, each set of parameters obtained (even when using an artificially low value of $MW = 1$) gives a good fit of the *PVT* data at the molecular weight of the fit. In general, larger values of molecular weight used during the fit lead to larger values of *a/MW* and *b/MW*, although most of the change in these parameters is observed below molecular weights around 10,000.

Table 7.2 Results of fitting Peng-Robinson EOS parameters to *PVT* data correlated by the Tait equation for PIB (range of data: 53-110ºC, 1-1000 bar).

MW used for *PVT* fit	*a/MW*	*b/MW*	AAD% at *MW* of fit	AAD% at $MW = 1000$[a]	AAD% at $MW = 100{,}000$[a]
1	469,000	0.9466	1.31	8.72	12.78
500	845,000	1.0425	0.54	1.23	4.24
5000	1,488,000	1.0808	0.92	1.40	1.39
50,000	2,010,000	1.0908	1.20	1.84	1.23

[a] AAD% when *MW* different from that used in fit is used in specific volume calculations

The values of the polymer EOS parameters obtained when fitting *PVT* data also depend on the range of data used in the fit. As an example, Figure 7.1 shows a comparison of specific volume calculations from the Peng-Robinson EOS, using the parameters obtained assuming $MW = 5000$, with some of the same data used in the fit.

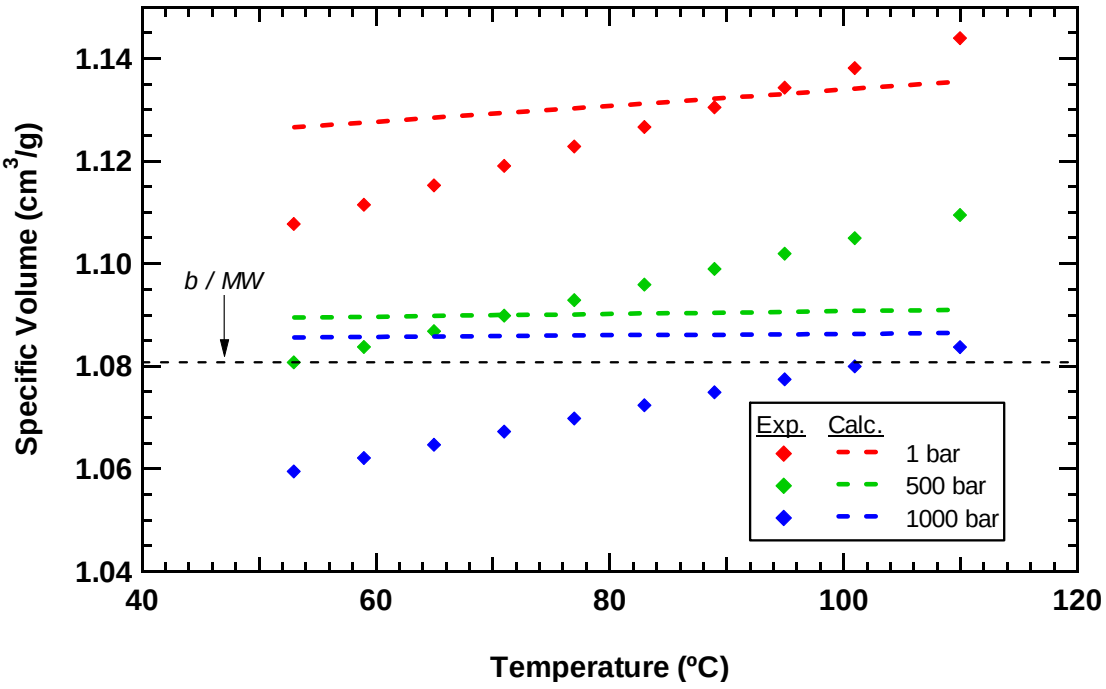

Figure 7.1 Experimental specific volume data for PIB correlated by the Tait equation compared with calculations from the Peng-Robinson EOS using a/MW = 1,488,000, b/MW = 1.0808, and MW = 5000.

Although the average error is not large, the EOS calculations do not recreate the temperature and pressure dependence of the data very well. The calculated temperature sensitivity is very small and there is little sensitivity to pressure at high pressures. To a large degree the EOS calculations are an average of the experimental specific volumes over the range of the fit. Thus, polymer EOS parameters should be fit to data in a temperature and pressure range that is similar to the range in which the parameters will be used. Another implication is that using larger temperature ranges will lead to larger errors in EOS calculations of the specific volume at the extremes of the range.

7.1.2 Implications of Different Parameter Values

Because the method of Louli and Tassios is based on fitting the EOS parameters to *PVT* data, and because different sets of EOS parameters can give similar goodness of fit, other effects of the choice of parameter sets must be examined. Important considerations include the sensitivity of calculated specific volumes to *MW*, temperature and pressure, as well as how realistically polymer vapor pressures are predicted.

Larger values of the polymer EOS parameters lead to less sensitivity in specific volume calculations with changes in molecular weight, a desirable characteristic in the region of molecular weight relevant to polymers because experimentally measured specific volumes do not vary much in this region. The AAD% in PIB specific volumes for calculations at different molecular weights listed in Table 7.2 is an example. The average error in volumes calculated at MW = 1000 and MW = 100,000 is 1.23 and 4.24, respectively, using the parameters fit at MW = 500, but 1.84 and 1.23 using the parameters fit at MW = 50,000. The reason for this is that at larger values of a/MW the specific volume begins to collapse to the value of b/MW.

However, this same phenomenon leads to the loss of almost all temperature and pressure sensitivity. Temperature, in particular, has the largest physically real influence on polymer volumes. Figure 7.1 shows EOS calculations of the specific volume of PIB using the parameters fit at MW = 5000. In low-pressure calculations there is some temperature dependence, but at higher pressures where the volume begins to collapse toward the value of b/MW the specific volume is basically constant with changes in temperature. At these conditions the pressure sensitivity is also reduced to levels below

what is seen experimentally. Larger values of the EOS parameters cause the calculated specific volumes to begin to collapse to the value of *b/MW* at even lower pressures.

The choice of parameters also affects polymer vapor pressure predictions. From Equation 7.2 it can be seen that P, and thus the vapor pressure, P^{sat}, is inversely proportional to MW when a/MW and b/MW are taken to be constant. So, for example, increasing the molecular weight used in calculations by a factor of ten results in a factor-of-ten decrease in P^{sat}. Thus, the same molecular weight must be used to compare P^{sat} calculations in order to isolate the effect of changes in parameter values. Table 7.3 shows the predicted vapor pressure for PIB of a molecular weight of 1000 at 25 and 300ºC using each set of EOS parameters listed in Table 7.2. (As a note, when the largest set of parameters is used, the predicted vapor pressure for MW = 50,000 at 200ºC is 3.4×10^{-12} bar, which compares well with the vapor pressure of about 10^{-13} bar calculated by Louli and Tassios.) It is evident from Table 7.3 that some of the parameter sets, even though they fit the *PVT* data well, lead to unrealistically high values for the polymer vapor pressure. These high vapor pressures are of most concern at low values of molecular weight and at high temperatures.

Table 7.3 PIB vapor pressures predicted by the Peng-Robinson EOS (at MW = 1000) using different sets of parameters.

a/MW	*b/MW*	P^{sat} (bar) at 25ºC	P^{sat} (bar) at 300ºC
469,000	0.9466	9.1×10^{-4}	3.4×10^{-1}
845,000	1.0425	5.1×10^{-7}	8.5×10^{-3}
1,488,000	1.0808	5.7×10^{-13}	9.0×10^{-6}
2,010,000	1.0908	6.2×10^{-19}	2.7×10^{-8}

To show that the vapor pressures predicted by the smaller EOS parameters are indeed unrealistically high, vapor pressures of the *n*-alkane series from C_9 to C_{36} at 300ºC are shown in Figure 7.2. Linear extrapolation of these data to a molecular weight of 1000 gives a vapor pressure of 1.7×10^{-4} bar. As evidenced by the negative curvature in the data, this value is conservatively high (by comparison, extrapolation of a quadratic fit gives a vapor pressure of 6.4×10^{-6} bar). Although the vapor pressure for branched molecules is generally higher than for linear molecules of the same type and molecular weight, branched C_9 alkanes have a vapor pressure of at most 40% higher than that of *n*-nonane at 300ºC (Rowley et al., 2005). The vapor pressures calculated at 300ºC using the first two sets of parameters in Table 7.3 are 2000 and 50 times greater, respectively, than even the conservatively high linearly extrapolated value. Thus, it is reasonable to conclude that these parameter values are not suitable.

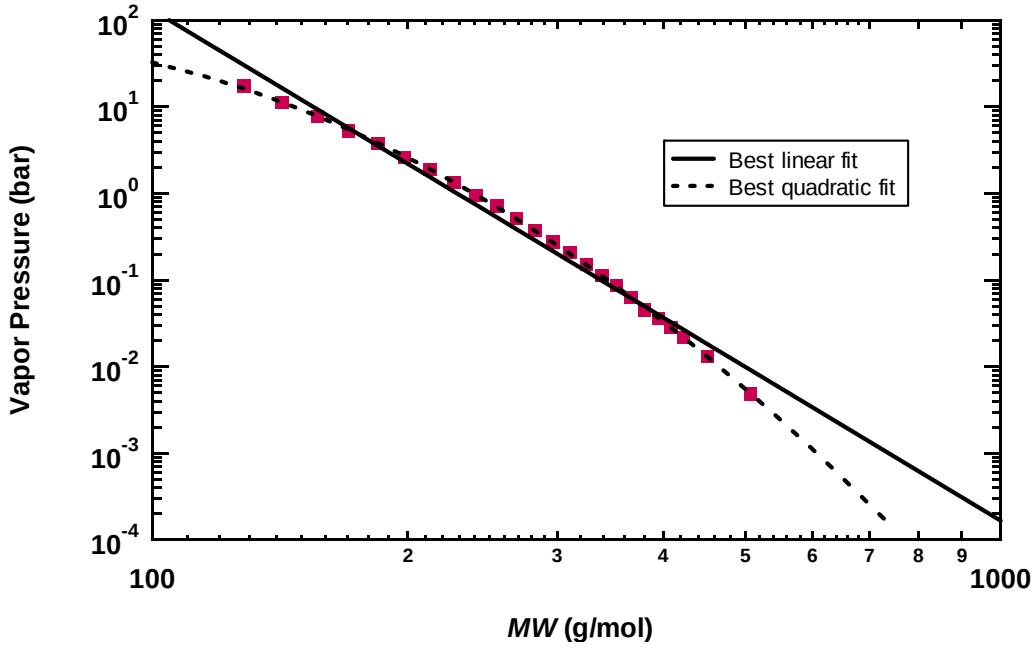

Figure 7.2 Vapor pressures of *n*-alkane series from C_9 to C_{36} at 300ºC (data from Rowley et al., 2005).

To get an order of magnitude estimate of appropriate values for polymer EOS parameters, the minimum value of *a/MW* that would result in a predicted vapor pressure at *MW* = 1000 and 300ºC of at most 1.0×10^{-4} bar was determined for values of *b/MW* from 0.7 to 1.2. A linear fit of the obtained parameter pairs is very good ($R^2 > 0.999$). For predicted polymer vapor pressures to be sufficiently low, then, the following relationship between the EOS parameters should be satisfied:

$$a/MW \geq 1.11\times10^{6}\, b/MW + 7.54\times10^{4} \qquad \textbf{(7.4)}$$

This equation can be used either to evaluate sets of polymer EOS parameters found previously, or as a constraint during the parameter regression. In optimization cases where *a/MW* is forced by the constraint to be larger, the optimum value of *b/MW* may also change slightly, but the goodness of fit of the *PVT* data should not change significantly.

7.1.3 Recommendations Concerning the Method of Louli and Tassios

Louli and Tassios showed that by regressing polymer EOS parameters from a large range of *PVT* data, they could get a good fit of those data as well as predict low polymer vapor pressures. However, they neglected to address some important considerations in this process – the effects of the molecular weight and of the temperature and pressure ranges of the data used during the fit. First, because the specific volume calculated from the Peng-Robinson EOS with constant *a/MW* and *b/MW* is somewhat of an average of the data these parameters were fit to, it is recommended that the *PVT* data

used in the fit be in the same temperature and pressure ranged as those in which these parameters will be used. The temperature and pressure range used during regression should always be reported along with the values of the parameters. It should also be recognized that larger specific volume errors will result from using broader temperature ranges. In addition, to maintain at least some temperature and pressure dependence in specific volume calculations from the EOS, but also to reduce sensitivity to changes in molecular weight, it is recommended that the parameters be fit assuming MW = 10,000. In most cases this procedure will result in parameters that lead to appropriately low polymer vapor pressures by satisfying Equation 7.4. When that is not so, the parameters can be refit using this equation as a constraint without sacrificing much in the goodness of fit of the *PVT* data. These recommendations help to clarify and improve upon the method of Louli and Tassios. Recommended parameter values for PEO and PS obtained using the procedure described here, for the range from 100 to 300ºC and 1 to 150 bar, are given in Table 7.4.

Table 7.4 Recommended values of PR EOS parameters determined by fitting *PVT* data, correlated by Tait equation, with MW = 10,000 (data range: 100-300ºC, 1-150 bar).

Polymer	*a/MW*	*b/MW*
PEO	1,690,000	0.9719
PS	2,030,000	0.9960

7.2 New Method for Obtaining Polymer EOS Parameters

Although most methods for obtaining polymer EOS parameters assume that *a/MW* and *b/MW* are constant for a given polymer, and the method of Louli and Tassios

in particular has been shown to give satisfactory results, there are reasons to believe that a better choice of polymer parameters exists. Primary among these is the fact that assuming different values for *MW* during parameter regression leads to different values of *a/MW* and *b/MW*, in violation of the initial assumption. Upon reexamination of the form of the Peng-Robinson equation of state, the obvious choice of volume parameter remains *b/MW*, as it represents the excluded volume in mass units rather than mole units. However, the units of *a* ($cm^6 \cdot bar/mol^2$) seem to suggest using a/MW^2 instead of *a/MW* as the energy parameter. Preliminary theoretical considerations imply the same thing. In the statistical mechanical development of lattice-based equations of state $a = \varepsilon b$, where ε is the molecular attraction energy. If this attraction energy is assumed to be proportional to surface area, as is commonly done, and the polymer is roughly assumed to be a long cylinder, then the surface area and ε are proportional to *MW*. Because the molecular volume, related to *b* through Avogadro's number, is also proportional to *MW*, *a* should be proportional to MW^2. Based on this choice for the energy parameter the Peng-Robinson equation of state can be written as

$$P = \frac{1}{MW}\left[\frac{RT}{\tilde{V} - b/MW}\right] - \frac{a/MW^2}{\tilde{V}^2 + 2\tilde{V}\,b/MW - \left(b/MW\right)^2} \qquad \textbf{(7.5)}$$

It can be seen from Equations 7.2 and 7.5 that neither parameter option for *a* completely removes the dependence of specific volume on molecular weight. In fact, there is no simple choice of EOS parameters that will do so.

7.2.1 Choice of Energy Parameter

In an attempt to gain insight into which form of the energy parameter is most appropriate, the *n*-alkane series was examined. The behavior of this series should approach the behavior of linear polyethylene. Trends in EOS parameters, as calculated from critical properties using the normal correlations for small molecules, are shown in Figure 7.3. Although a/MW and a/MW^2 both appear to be leveling off at larger molecular weights, it is not clear from the figure which, if either, will lead to constant values at high molecular weights.

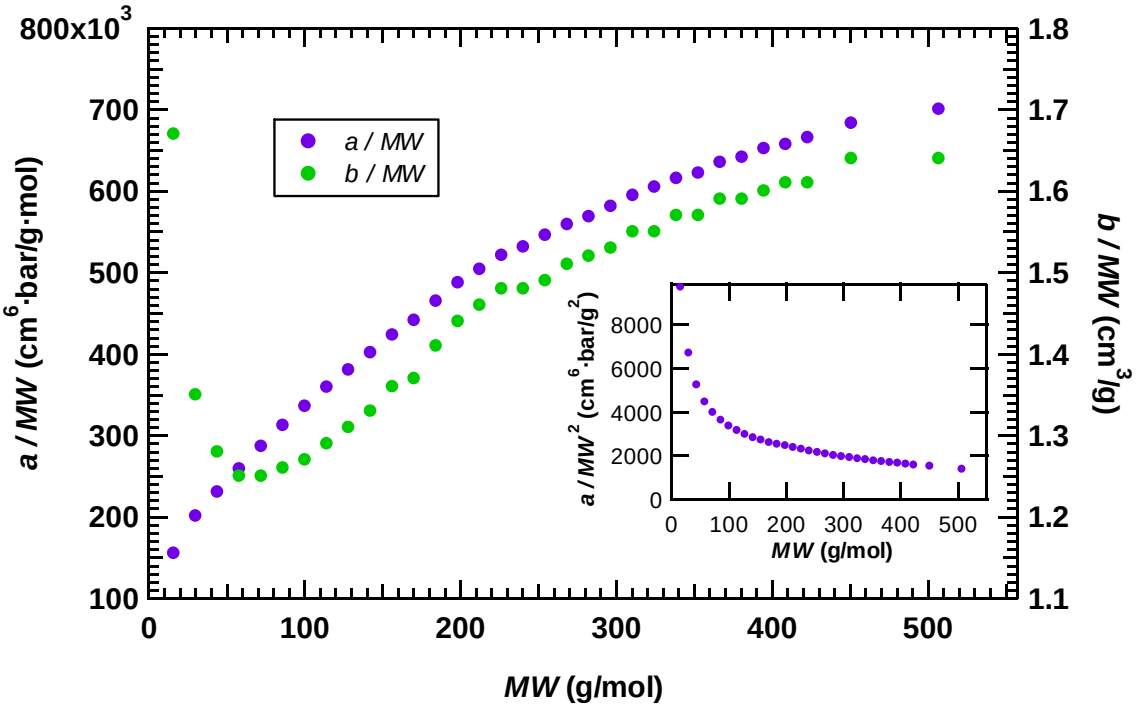

Figure 7.3 Trends in a/MW and b/MW with molecular weight as calculated using critical properties from the DIPPR database (Rowley et al., 2005) for *n*-alkanes from C_1 to C_{36} (α, the function describing the temperature dependence of a, was taken to be unity). Inset plot shows a/MW^2 trend.

Because each choice of energy parameter leads to a different relationship between molecular weight and specific volume calculated by the EOS, and because the Tait equation does not consider any relationship between the two, it is useful to investigate the experimental volume behavior exhibited by the *n*-alkane series and by polyethylene. Figure 7.4 shows that the specific volume is essentially constant with changes in molecular weight in the region of molecular weight relevant to polymers. In fact, there is only a difference of 2.6% between the specific volume of polyethylene of MW = 126,000 and polyethylene wax of MW = 1190 (sometimes considered to be an oligomer rather than a polymer). The specific volume only changes significantly at molecular weights below about mid-range in the plotted *n*-alkane series. The specific volume begins to increase rapidly with decreasing molecular weight because of two reasons: first, liquids of the smaller *n*-alkanes have a lower density of strong covalent bonds (short distance between atoms) and a higher density of weak intermolecular attractions (larger distance between atoms) than liquids of the longer *n*-alkanes. Also, the smaller *n*-alkanes have larger ratios of CH_3 to CH_2 groups. The CH_3 groups (at the chain ends) are much more bulky than the CH_2 groups.

In contrast to experimental behavior, the relationships between calculated specific volume and molecular weight when a/MW and a/MW^2 are assumed constant are presented in Figure 7.5a and b, respectively. In the case of constant a/MW, the specific volume is essentially equal to the value of b/MW at high molecular weights. At a value of MW that depends on pressure (see Point 1 in Figure 7.5a), the specific volume then experiences a sharp increase with decreasing molecular weight before again becoming insensitive to changes in molecular weight at low MW (see Point 2 in Figure 7.5a). The

size of this sharp increase is larger at higher temperatures. The specific volume in the case of constant a/MW^2 is also equal to b/MW at high molecular weights, but experiences a more dramatic upswing (that again varies with pressure and temperature) with decreasing molecular weight at low MW (see Point 3 in Figure 7.5b). Using larger parameter values in the case of constant a/MW reduces the size of the sharp increase in volume, and in the case of constant a/MW^2 causes the volume upswing to shift to lower molecular weights.

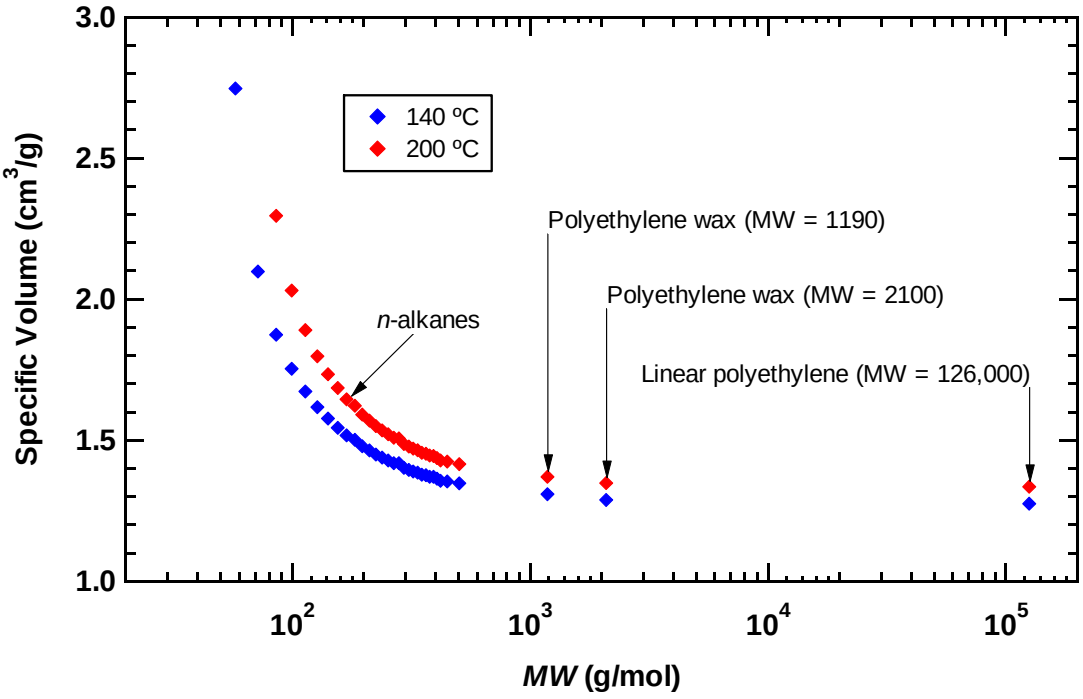

Figure 7.4 Specific volume of liquid at 140 and 200ºC and at 1 bar for *n*-alkanes from C_4 to C_{36} (data from Rowley et al., 2005) and for polyethylene of molecular weights over a couple of orders of magnitude (data from Zoller and Walsh, 1995).

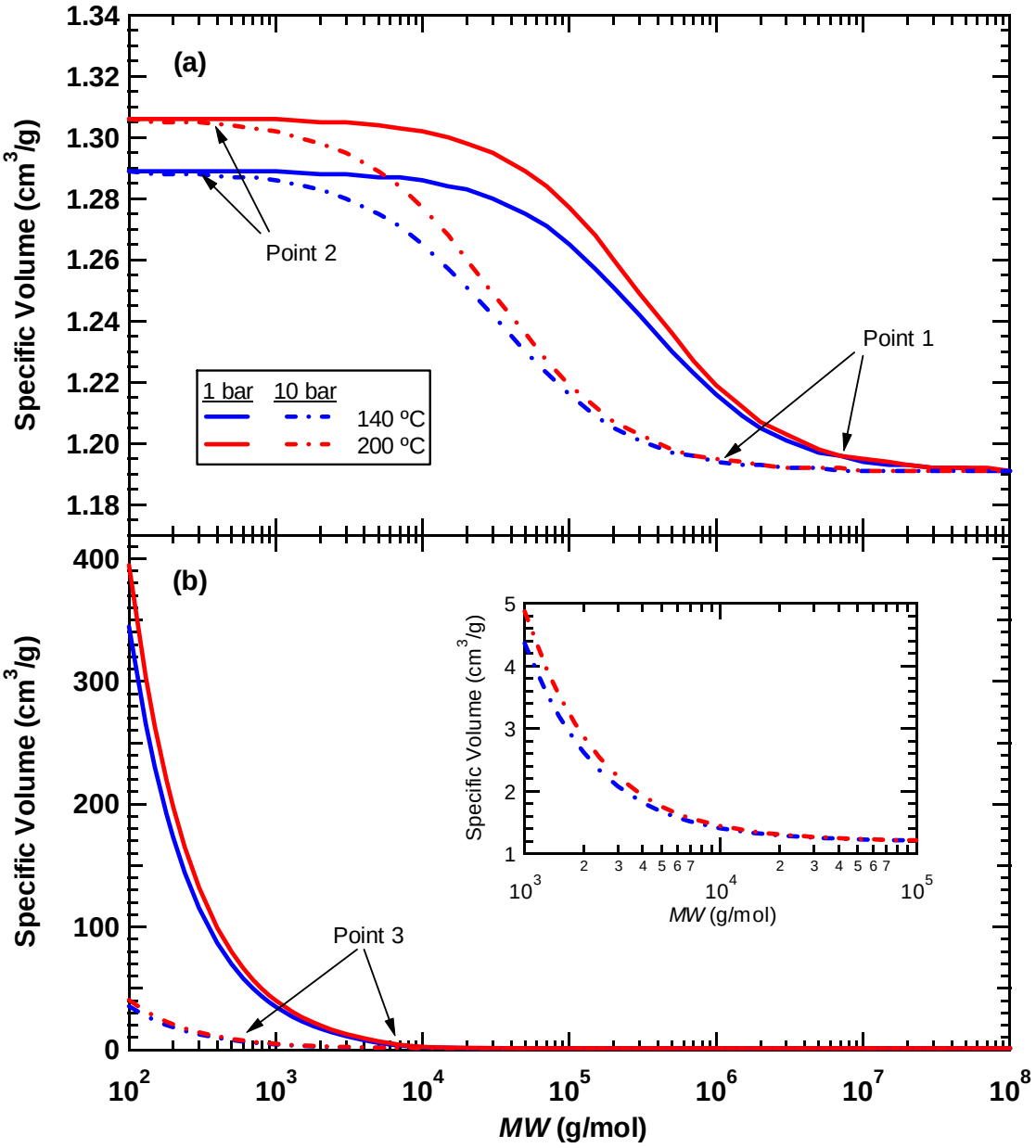

Figure 7.5 Variation of specific volume with molecular weight as predicted by PR EOS assuming (a) constant a/MW, and (b) constant a/MW^2. Inset in (b) shows enlarged view of 10-bar curve. Parameters were fit in the range from 140 to 203ºC and from 0 to 1960 bar to *PVT* data for HDPE, correlated by the Tait equation. Used MW = 50,000 for fit. Parameter values: b/MW = 1.1910 (both cases), a/MW = 1,163,000, a/MW^2 = 23.28. Labeled points are referenced in the text.

Figure 7.5a explains some of the problems with using a constant value for *a/MW* that were noted in the discussion of the method of Louli and Tassios. Temperature sensitivity at a given molecular weight can be seen to vary from a maximum at low pressures to zero at high pressures (see the difference in slope of calculated volume with temperature at different pressures in Figure 7.1). Also, using larger values of EOS parameters reduces the sensitivity of specific volume to all variables by compressing the volume jump. Fitting the EOS to *PVT* data essentially finds the size of the volume jump that gives temperature and pressure sensitivities that most closely match the data at the molecular weight of the fit. Because these calculated sensitivities vary with molecular weight, the specific volume behavior is not correct at other molecular weights.

Using a constant value of a/MW^2 also has its problems, however. Figure 7.5b shows that the qualitative trend in specific volume with molecular weight seems to be the same as that seen experimentally (Figure 7.4), but with vastly different quantitative values. Under the same conditions of 140ºC and 1 bar for $MW = 100$ (heptane), the equation of state predicts a specific volume of 345 cm^3/g compared to the DIPPR database value of 1.75 cm^3/g (Rowley et al., 2005). This is a result of fitting the equation in a region of molecular weight where the specific volume is basically constant. Other undesirable effects include a very large sensitivity to changes in pressure and almost total insensitivity to temperature in regions of molecular weight relevant to polymers.

Each of the polymer energy parameter choices discussed here has strengths and weaknesses with regard to specific volume. Using constant *a/MW* gives an erroneous trend with changes in molecular weight and does not give the correct temperature and pressure dependence. However, using constant *a/MW* does give some temperature and

pressure dependence, and calculated values are guaranteed to always be reasonably close to experimental values even at largely different molecular weights. Using constant a/MW^2 gives the correct shape of the specific volume vs. molecular weight curve, but leads to unrealistic specific volumes at low molecular weights and a total loss of temperature and pressure sensitivity at higher molecular weights. With constant values of either of these parameters, the cubic equation of state is not flexible enough to match the correct specific volume behavior.

7.2.2 Overcoming Problems Associated with Using a / MW^2

The problem of unrealistically large specific volumes at relevant molecular weights can be alleviated by using a larger value for a/MW^2 in order to shift the volume upswing seen in Figure 7.5b to smaller molecular weights. Each value of a/MW^2 corresponds with a critical molecular weight, MW_c, below which the calculated specific volume begins to rise rapidly. In turn, any value chosen for MW_c has an associated value of a/MW^2. Using a value of a/MW^2 greater than or equal to this will ensure that reasonable specific volumes are obtained at molecular weights above the chosen MW_c. Defining the critical molecular weight as the point above which the difference between the calculated specific volume and b/MW is less than 4% leads to the following correlation:

$$a/MW^2 \geq \exp\left[15.09 - \ln\left(MW_c\right)\right] \qquad \textbf{(7.6)}$$

As temperature, pressure, and the value of *b/MW* also affect the value of a/MW^2 that corresponds to MW_c, it must be noted that Equation 7.6 was determined assuming T = 300ºC, P = 0 bar, and b/MW = 1.4 cm^3/g (an approximate upper limit for this parameter). These values were used because the difference between the calculated specific volume and *b/MW* increases with increasing temperature, decreasing pressure, and increasing value of *b/MW*. Thus, the specific volume difference at MW_c should be less than 4% under all relevant conditions. Generally, the percent difference slightly more than doubles at a molecular weight that is half of the defined critical value, and is over 35 times greater at a molecular weight that is one-eighth of the critical value.

To overcome the lack of temperature and pressure sensitivity in the specific volume when large values of a/MW^2 are used, *b/MW* can be made to depend on these variables. This approach is not common, but some justification for it can be found by remembering that *b/MW* represents the excluded volume of the polymer. If the polymer is imagined as a long thread that is constantly coiling and bending and sweeping out the volume near it, it is logical to assume that the excluded volume would increase with temperature as the kinetic energy of the molecule increases, and it would decrease with pressure as those movements are confined. Because the specific volume of polymers is generally linear with temperature, and the temperature sensitivity is fairly similar at different pressures, *b/MW* can be fit to specific volume data using the linear equation

$$b/MW = c_0 + c_T T + c_P P \qquad \textbf{(7.7)}$$

where c_0 is the hypothetical value of *b/MW* at zero temperature and pressure, and c_T and c_P are the temperature and pressure coefficients.

7.2.3 Recommended Procedure and Comparison with Method of Louli and Tassios

Theoretical and practical considerations suggest that *a/MW* is not the best choice of energy parameter for polymers. An alternative method for obtaining polymer EOS parameters to that of Louli and Tassios, developed in this work, makes use of the parameter a/MW^2. It has been shown that any value of a/MW^2 greater than the value associated with the chosen critical value of molecular weight causes the calculated specific volume to collapse to the value of *b/MW*. For simplicity, a constant value of 2500 for a/MW^2 (corresponding to a value of MW_c of approximately 1460) is recommended for all polymers. The coefficients for *b/MW* are found by fitting *PVT* data using Equation 7.7. Recommended parameter values for PEO and PS obtained using this method with data correlated by the Tait equation in the range from 100 to 300ºC and 1 to 150 bar are given in Table 7.5.

Table 7.5 Recommended values of PR EOS parameters obtained using newly proposed method. *PVT* data correlated by the Tait equation (range: 100-300ºC, 1-150 bar).

Polymer	a/MW^{2a}	c_0 [b]	c_T [b]	c_P [b]
PEO	2500	0.6869	6.84×10^{-4}	-8.99×10^{-5}
PS	2500	0.7901	5.06×10^{-4}	-7.81×10^{-5}

[a] Units of ($cm^6 \cdot bar/g^2$)
[b] For *b / MW* in (cm^3/g), *T* in (K), and *P* in (bar)

Some important results of using these parameters compared with the parameters obtained using the method of Louli and Tassios are presented in Table 7.6. The new method results in lower predicted polymer vapor pressures. At molecular weights above MW_c the new method also gives a significantly better fit of the original specific volume data. Because the temperature sensitivity is more correct in this method, maximum errors in specific volume are much lower than using the method of Louli and Tassios, and dependence of the parameter values on the range of the data used is greatly reduced. Finally, the parameter regression is simpler (because it involves a linear instead of a cubic equation) and no assumption need be made about the molecular weight of the polymer. As a note, the average errors given in the table for the new method at MW = 1000 and MW = 10,000 in part reflect the difference between the volume calculated by the equation of state at that molecular weight and the value of b/MW. The average error for MW = 100,000 is essentially the error associated with fitting the PVT data using a linear equation.

Table 7.6 Comparison of specific volume errors and predicted polymer vapor pressures from PR EOS with parameters obtained from two different methods (values in Table 7.4 and Table 7.5). PVT data correlated by Tait equation (range: 100-300ºC, 1-150 bar).

	Method of Louli & Tassios				New Method			
	AAD% in $\widetilde{V}$			P^{sat} (bar)	AAD% in $\widetilde{V}$			P^{sat} (bar)
Polymer	MW=10^3	MW=10^4	MW=10^5	300ºC, MW=10^3	MW=10^3	MW=10^4	MW=10^5	300ºC, MW=10^3
PEO	3.37	3.44	3.84	1.1×10^{-7}	3.16	0.29	0.12	7.1×10^{-11}
PS	2.42	2.44	2.84	2.6×10^{-9}	3.25	0.32	0.09	7.3×10^{-11}

7.3 Parameters for Polymer-like REF Decomposition Products

To this point in the discussion the experimental *PVT* values used in the regression of the polymer equation of state parameters were obtained from data correlated by the Tait equation with coefficients from Rodgers (1993). These coefficients are available for homopolymers commonly used in industrial processes, as well as for some copolymers and polymer blends. However, no coefficients for the Tait equation are available for more complicated polymers or, obviously, for the polymer-like decomposition products of REF. In such cases experimental data are replaced with specific volume predictions from GCMCM.

In order to compare the effect of using GCMCM predictions instead of experimental *PVT* data correlated by the Tait equation, EOS parameters for PEO and PS were obtained following the method of Louli and Tassios and compared to the parameters obtained previously at the same molecular weight and using the same data range (listed in Table 7.4). These new parameters are given in Table 7.7, along with the AAD% in relation to GCMCM and to the Tait equation. The values of AAD% in relation to the Tait equation are almost exactly the same as those obtained using the parameters fit to the Tait equation: 3.44 and 2.44 for PEO and PS, respectively. Because GCMCM predicts a slightly larger specific volume span than occurs experimentally for these polymers, the AAD% in relation to GCMCM is actually larger than the AAD% in relation to the Tait equation.

Table 7.7 Peng-Robinson EOS parameters for PEO and PS from method of Louli & Tassios using GCMCM volume predictions (range: 100-300ºC and 1-150 bar). All equation of state calculations used MW = 10,000.

Polymer	a/MW	b/MW	AAD% from GCMCM	AAD% from Tait eqn.
PEO	1,619,000	0.9826	3.95	3.54
PS	1,970,000	0.9926	2.59	2.44

Using GCMCM predicted volumes with the new method for obtaining polymer EOS parameters was also examined and yields the results in Table 7.8. The relatively large value of AAD% in relation to the Tait equation for PEO results from the temperature sensitivity predicted by GCMCM being higher than that seen experimentally. The values of AAD% in relation to the Tait equation using the parameters fit to the Tait equation are 0.29 and 0.32 for PEO and PS. By chance, using the PS parameters fit to GCMCM volume predictions gives a better fit at MW = 10,000 of data correlated by the Tait equation than using the parameters that were fit to that data. Such is not the case at higher molecular weights, where the volume calculated by the equation of state more closely matches the value of b/MW.

Table 7.8 Peng-Robinson EOS parameters for PEO and PS from new method using GCMCM volume predictions (range: 100-300ºC and 1-150 bar). All equation of state calculations used MW = 10,000.

Polymer	a/MW^2	c_0	c_T	c_P	AAD% from GCMCM	AAD% from Tait eqn.
PEO	2500	0.6490	7.94×10^{-4}	-9.78×10^{-5}	0.54	1.61
PS	2500	0.7741	5.34×10^{-4}	-7.87×10^{-5}	0.32	0.21

Thus it can be seen that using volume predictions from GCMCM is a reasonable substitute for using experimental data and in some cases may be the only option. In this manner EOS parameters for the polymer-like decomposition products of REF were obtained using the method of Louli and Tassios, as well as the new method proposed in this work. They are presented in Table 7.9.

Table 7.9 Peng-Robinson EOS parameters for polymer-like degradation products of REF from two methods. Parameters were fit to GCMCM volume predictions (range: 100-300ºC and 1-150 bar). All equation of state calculations used MW = 10,000.

Method	Parameter	Value	AAD% from GCMCM
Louli & Tassios	a/MW	1,862,000	2.84
	b/MW	0.9427	
New method	a/MW^2	2500	0.34
	c_0	0.7135	
	c_T	5.53×10^{-4}	
	c_P	-5.95×10^{-5}	

7.4 Summary of Methods for Obtaining Polymer EOS Parameters

A review of the literature showed that the method of Louli and Tassios (2000) for obtaining polymer EOS parameters resulted in the lowest predicted polymer vapor pressures, as well as the smallest deviations in subsequent liquid volume calculations using the EOS. The method of Louli and Tassios involves assuming a/MW and b/MW to be constant for a given polymer, regardless of molecular weight, and fitting these two parameters to a range of *PVT* In this chapter, the effects of molecular weight and *PVT* data range on parameter values determined by this method were studied and found to be

significant. It was recommended that, when using the method of Louli and Tassios, polymer EOS parameters should be fit assuming a molecular weight of around 10,000 and using *PVT* data in the same temperature and pressure range over which the parameters will be used. A correlation between *a/MW* and *b/MW* was given to ensure that polymer vapor pressure predicted by the EOS would be realistically small.

A new method for obtaining polymer EOS parameters was also proposed in this chapter. In the new method, a/MW^2 was assumed to be constant for a given polymer instead of *a/MW*. Some theoretical justification for this assumption was found. A value of 2500 $cm^6 \cdot bar/g^2$ was recommended for a/MW^2 in most cases. It was also recommended that *b/MW* be fit to *PVT* data as a linear function of temperature and pressure. When using parameters obtained following this new method, deviations between data and volumes calculated by the EOS were generally an order of magnitude smaller than those obtained using polymer parameters from the method of Louli and Tassios. Predicted polymer vapor pressures were acceptably small in both cases.

Values of the polymer EOS parameters from both methods were reported for PEG, PS, and for the polymer-like decomposition products of REF. It was also found that *PVT* data for use in fitting these parameters could be substituted with GCMCM volume predictions when experimental data or Tait parameters are not available.

8 Modeling Method

This chapter gives a description of the models examined in this work and the method by which they were compared to the experimental data from the HT-VLE facility. Details are then presented for the computer code created to calculate VLE of multicomponent polymer solutions. Finally, an explanation is included of how the necessary model parameters and information were obtained.

8.1 Method of Model Comparison

Six different free-volume activity coefficient models (ACM) were evaluated in this work: Entropic-FV, Freed-FV, GK-FV, MEFV, UNIFAC-FV, and UNIFAC-ZM. Each ACM was used in three different ways for a total of eighteen distinct models. Descriptions of these models and the conditions used to compare them to experimental data are given below.

8.1.1 Description of Model Types

The three types of ACM usage were designated as follows:

- ACM alone
- ACM + EOS Method 1
- ACM + EOS Method 2

The first ACM usage type, "ACM alone", consisted of calculating the activity coefficient of the solvent(s) in the mixture and the vapor pressure of the pure solvent(s) to obtain the system pressure. The following equilibrium relationship was used:

$$x_i \gamma_i P_i^{sat} \phi_i^{sat} = y_i \hat{\phi}_i^V P \qquad \textbf{(8.1)}$$

where ϕ_i^{sat} is the fugacity coefficient of pure species *i* at its vapor pressure. While the equilibrium relationship presented earlier in Equation 4.1 is exact, Equation 8.1 neglects a term called the Poynting factor, involving an integral of the liquid volume from the vapor pressure to the system pressure. This factor is close to unity except at very large pressures, and the assumption made by neglecting it was very good under all the conditions encountered in this study. The above relationship can be written for each species and summed to eliminate y_i, giving the system pressure. The vapor phase mole fractions can then be computed as well. The necessary equations are

$$P = \sum x_i \gamma_i P_i^{sat} \frac{\phi_i^{sat}}{\hat{\phi}_i^V} \qquad \textbf{(8.2)}$$

$$y_i = \frac{x_i \gamma_i P_i^{sat} \dfrac{\phi_i^{sat}}{\hat{\phi}_i^V}}{P} \qquad \textbf{(8.3)}$$

Further simplifications can be made if there is only one solvent in the mixture. In that case the vapor phase is essentially a pure species and the partial fugacity coefficient

of the solvent (designated by the subscript 1), $\hat{\phi}_1^V$, reduces to ϕ_1^V, the vapor phase fugacity coefficient of the pure solvent. The pressure is then given by

$$P = x_1 \gamma_1 P_1^{sat} \frac{\phi_1^{sat}}{\phi_1^V} \qquad \textbf{(8.4)}$$

If the ratios of fugacity coefficients in Equations 8.1 to 8.4 are neglected (thus assuming ideal gas behavior), the ACM can truly be used alone to calculate the VLE behavior of the system. ACMs are generally written so as to give γ_i as a function of temperature and liquid composition. All that are needed in addition are vapor pressure values. If ideal gas conditions are not assumed, an equation of state is needed to calculate the fugacity coefficients. The Peng Robinson (PR) EOS of Equation 7.1 (or its equivalent forms) was used in this study to calculate the ratio of fugacity coefficients for the pure solvent at its vapor pressure and at the system pressure. This ratio is a function of the system pressure, *P*, and so Equation 8.4 had to be solved iteratively. Convergence was achieved quickly with a successive substitution method when the initial guess for pressure was taken as $P = x_1 \gamma_1 P_1^{sat}$.

The effect of using the PR EOS to account for deviations from ideal gas behavior is shown in Figure 8.1 for the PEG/furan system at 75 and 175ºC. The correction was negligible at 75ºC but important at 175ºC. In general, assuming ideal gas behavior resulted in larger errors at higher pressures. Thus, it was more important to account for the real behavior of the vapor phase at higher temperatures and for solvents with higher vapor pressures.

Although an equation of state was used to calculate the solvent fugacity coefficients in the vapor, this method was still called designated as "ACM alone" because no EOS calculations were performed for polymer mixtures in this type of ACM usage.

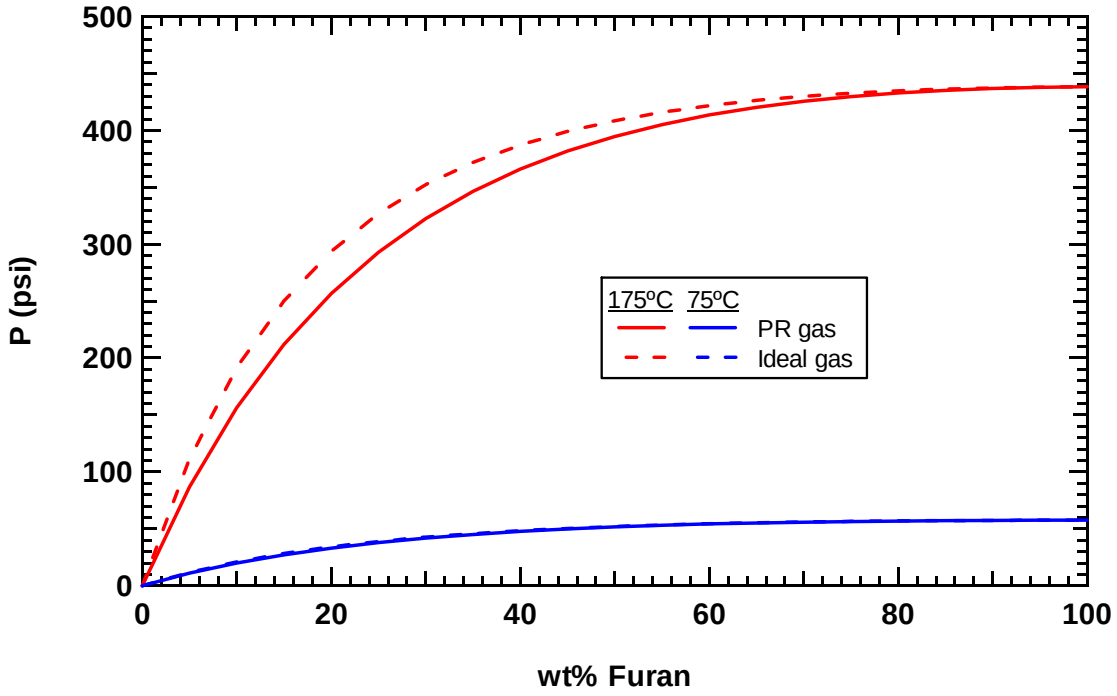

Figure 8.1 Pressure calculations for the PEG/furan system at 75 and 175ºC using the Entropic-FV ACM and assuming either ideal gas behavior or using the PR EOS to calculate the behavior of the solvent in the vapor phase.

The other two ACM usage types, "ACM + EOS Method 1" and "ACM + EOS Method 2" consisted of combining the ACM with the PR EOS through the Wong-Sandler mixing rules. In both these cases the pressure was calculated directly from the combined ACM + EOS, and no vapor pressure values were needed (except as guess values) because the information was built into the EOS parameters. The difference between the two types of models was in the EOS parameters used for the polymer. "Method 1" used polymer

EOS parameters obtained from the method of Louli and Tassios (2000) (see section 7.1), and "Method 2" used parameters obtained from the new method described in section 7.2.

8.1.2 Conditions Used During Model Comparisons

Calculations for all of the eighteen models were made at 21 liquid compositions and at three temperatures for each polymer/solvent system in this study in order to compare the results with the experimental data collected from the HT-VLE facility. Compositions used were in increments of 5 wt% from 0 to 100 wt% solvent, with the lowest and highest compositions being adjusted to 0.0001 and 99.9999 wt%, respectively. The temperatures that were used varied by polymer/solvent system and were chosen out of consideration of the available data. For PEG/benzene, calculations were made at 75, 150, and 190ºC. For PEG/furan, the temperatures were 75, 140, and 170ºC. For PS/benzene, calculations were made at 100, 175, and 225ºC and for PS/furan they were made at 100, 150, and 175ºC. For PEG/IPP and PS/IPP, the temperatures were 200, 225, and 250ºC. The deviations between predicted and measured pressures were found as a percentage of the pure solvent vapor pressure.

Values of molecular weight were needed for each polymer in order to make the model calculations. The molecular weight used for PEG was 8000. The PS was assumed to be made up of two different molecular weight components, simplified from the GPC findings mentioned earlier. Unless otherwise noted, the PS was taken to be a mixture of 52 wt% of a component with MW = 1050 and 48 wt% of a component with MW = 72,000. The number-average molecular weight of this mixture was 1637.

8.2 Computer Code

The object of the computer code (written modularly so that the different models could easily be tested) was to calculate predicted pressures and phase compositions given the system temperature and overall composition. Subroutines were written for each of the six free-volume activity coefficient models. These subroutines could be used directly to calculate results for the "ACM alone" models given the liquid composition. The overall algorithm described below was used to find the correct liquid composition from the overall composition. For the "ACM + EOS" models, bubble point and volume root-finding algorithms were also needed to compute VLE behavior.

8.2.1 Overall Algorithm

The overall algorithm of the computer code was a method of successive substitution to find the correct liquid composition from the overall composition, by making use of the system volume. With the system temperature, T, total volume, V_{tot}, and overall composition specified, the mixture was initially assumed to be all liquid. The composition and pressure of the vapor in equilibrium with this liquid were then calculated. The amounts of each species in the vapor phase were calculated from the vapor composition and the volume available in the system for the vapor. These amounts were then subtracted from what was in the liquid and the process was repeated. A more detailed description of the algorithm is given below.

The first actual step in the code was to ensure that the system was in the two-phase region under the specified conditions. This was done by calculating the total volume at the dew point and bubble point pressures. The dew point pressure is defined as

the pressure at which the first drop of liquid appears as pressure increases at constant temperature. The bubble point pressure is defined as the pressure at which the first bubble of vapor appears as pressure decreases at constant temperature. For the system to be in the two-phase region V_{tot} needed to be in between the volume calculated for the specified mixture to be essentially all liquid and the volume calculated for the mixture to be essentially all vapor. With a polymer in the mixture, the dew point pressure was basically zero and the corresponding volume very large, so in essence the algorithm checked to make sure the specified total volume was bigger than what was required to contain all of the mixture as a liquid.

After the system was found to be in the two-phase region, initial guesses for the composition and amount of the liquid phase were obtained from $x_i = z_i$ and $N_L = \sum N_i$, where N_i is the total moles of species *i* in the system and N_L is the total number of moles in the liquid phase. The algorithm then continued with the following steps (the arrow indicates the computational loop):

- The bubble point algorithm described in section 8.2.2 below was used to calculate *P* and y_i given *T* and x_i
- The volume root-finding algorithms described in section 8.2.3 were used to calculate $\overline{V}_L$ and $\overline{V}_V$ from *T*, *P*, and x_i or y_i, respectively
- N_V, the total number of moles in the vapor phase, was calculated from

$$N_V = \frac{V_{tot} - \overline{V}_L N_L}{\overline{V}_V} \qquad \textbf{(8.5)}$$

- n_i^V and n_i^L, the number of moles of each species *i* in the vapor and liquid phases, respectively, were calculated from

$$n_i^V = y_i N_V \quad \textbf{(8.6)}$$

$$n_i^L = N_i - n_i^V \quad \textbf{(8.7)}$$

- New estimates of N_L and x_i were obtained from

$$N_L = \sum n_i^L \quad \textbf{(8.8)}$$

$$x_i = \frac{n_i^L}{N_L} \quad \textbf{(8.9)}$$

- Iteration occurred until N_L stopped changing

8.2.2 Bubble Point Algorithm

The bubble point algorithm used in this code was a standard bubble point pressure algorithm similar to the one given by Sandler (Sandler, 1999). Like the outer calculation loop described in the overall algorithm, it was also a successive substitution method. The dew point algorithm was very similar.

Initial guesses for pressure, K_i (the ratio of y_i to x_i), and y_i were obtained assuming ideal solution behavior from

$$P = \sum x_i P_i^{sat} \tag{8.10}$$

$$K_i = \frac{P_i^{sat}}{P} \tag{8.11}$$

$$y_i = K_i x_i \tag{8.12}$$

The algorithm proceeded with two nested loops (designated by solid and dotted-line arrows) as follows:

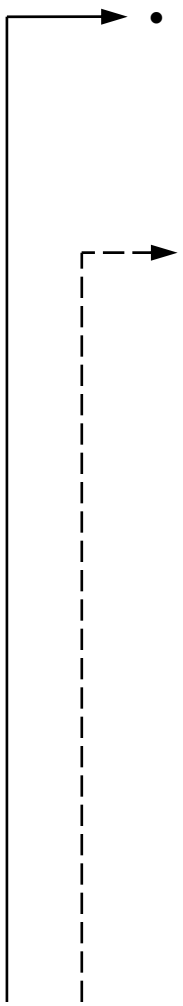

- Liquid fugacity coefficients, $\hat{\phi}_i^L$, were calculated from T, P, and x_i (equations for fugacity coefficients from the PR EOS fugacity are given in the appendix)
  - The vapor mole fractions were normalized (y_i was already normalized from the initial guess, but in later iterations y_i did not sum to one until the correct pressure was found)

$$y_i^{norm} = \frac{y_i}{\sum y_i} \tag{8.13}$$

  - Vapor fugacity coefficients, $\hat{\phi}_i^V$, were calculated from T, P, and y_i^{norm} (using the equations for fugacity coefficients from the PR EOS in the appendix)

- New estimates of K_i and y_i were obtained (Equation 8.14 comes from rearranging the equilibrium relationship of Equation 4.1 and substituting for the definition of K_i)

$$K_i = \frac{\hat{\phi}_i^L}{\hat{\phi}_i^V} \tag{8.14}$$

$$y_i = K_i x_i \tag{8.15}$$

- Iteration occurred until y_i stopped changing

- A new estimate of the pressure was found from

$$P = P\sum y_i \tag{8.16}$$

- Iteration occurred until the sum of y_i was equal to 1

8.2.3 Finding Volume Roots of the PR EOS

The molar volume needed to be calculated several times during the overall and bubble point algorithms. The correct volume was found as a root of the equation

$$P_{PR}(\overline{V}, T) - P = 0 \tag{8.17}$$

where P_{PR} is the pressure calculated by the PR EOS. Depending on the specified pressure, there could be one or three roots: the liquid and vapor molar volumes and a middle, non-physical root that is the result of using a cubic equation to try to model both liquid and vapor phases. The derivative of the pressure at both physical roots is negative, while the derivative at the non-physical root is positive.

Liquid root

A plot of pressure vs. molar volume calculated from the PR EOS for pure furan at 100ºC is given in Figure 8.2 with the liquid root circled. The negative pressures shown are a result of the form of the equation and are not physical.

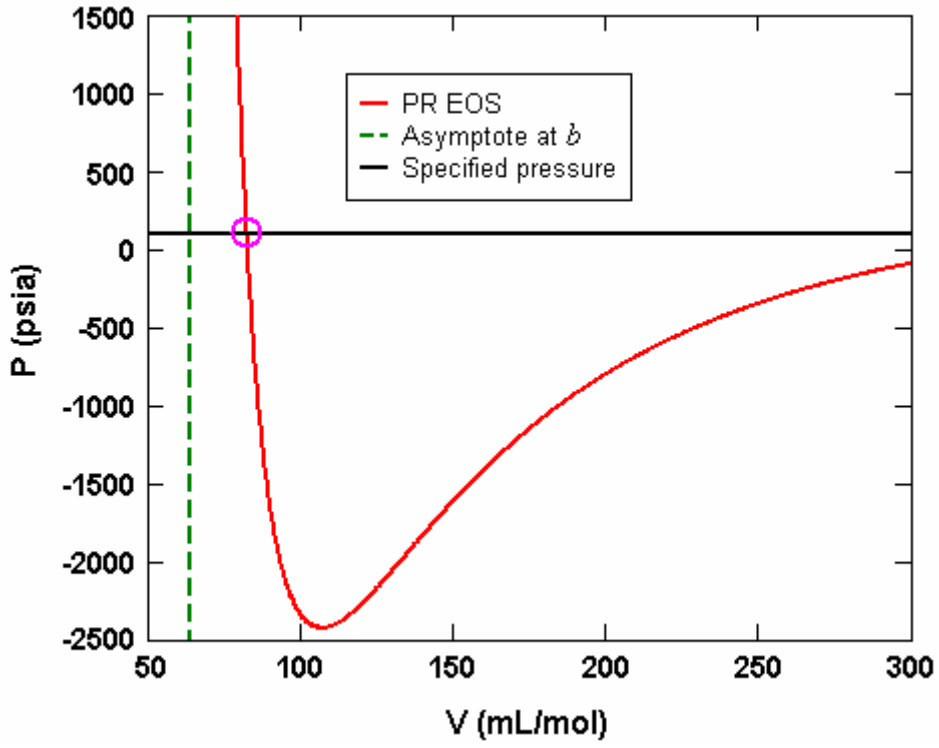

Figure 8.2 Pressure vs. molar volume for PR EOS for pure furan at 100ºC. Vertical asymptote is shown at *b*. Liquid volume root at 100 psi is circled. Maximum value of abscissa corresponds to about 5*b*.

Cubic equations of state, when plotted in this fashion, have a vertical asymptote at $\overline{V} = b$. Starting a numerical search for a root of Equation 8.17 at a molar volume just larger than b would guarantee convergence of Newton's method to the liquid root, because the function has positive curvature in that region. However, the slope is so steep (almost vertical) that Newton's method converges very slowly. In this work the bisection method was used. The left volume bound was set to a value just larger than b (the sign of the function was checked to ensure that it was close enough – it should be positive). The right bound was found by increasing the molar volume in increments of $0.1b$ until the function became negative. Because the function was generally very steep in this region, the bisection method then converged quickly on the liquid root.

In rare cases when the specified pressure, P, was located just above the local minimum of the cubic EOS, a change in molar volume of $0.1b$ could step over the liquid and the non-physical roots and never result in a negative function value. However, the derivative was checked as the right bound was moved, and if it became positive the liquid root was known to be bounded. The bisection method would then converge on one of these two roots. The function derivative was checked at the location of the root that was found, and if it was positive (meaning the non-physical root was found) the right bound was set equal to the left bound and the left bound was reinitialized at a value just larger than b. The bisection method then found the liquid root.

Vapor root

A different portion of the pressure vs. volume curve calculated from the PR EOS for furan at 100ºC is shown in Figure 8.3 with the vapor root circled. To find the vapor molar volume, bounds were determined from the competing terms of the cubic EOS. For

the PR EOS, the left and right bounds of the vapor molar volume lay on the curves described by Equations 8.18 and 8.19.

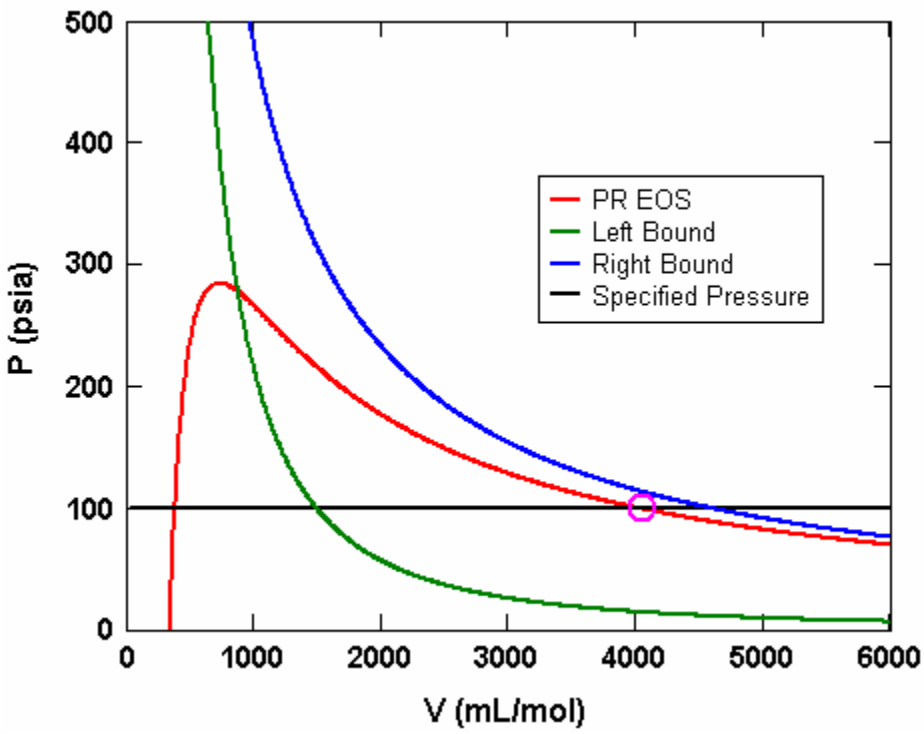

Figure 8.3 Pressure vs. molar volume for PR EOS for pure furan at 100ºC. Curves representing left and right bounds for vapor root are shown. Vapor volume root at 100 psi is circled. Maximum value of abscissa corresponds to about 100*b*.

$$P = \frac{a}{\overline{V}^2 + 2b\overline{V} - b^2} \qquad \textbf{(8.18)}$$

$$P = \frac{RT}{\overline{V} - b} \qquad \textbf{(8.19)}$$

Solving these equations for $\overline{V}$ gives $\sqrt{2b^2 + a/P} - b$ and RT/P, respectively. A subroutine from Sandia National Laboratories, called zeroin, was used to find the vapor root. The method in zeroin is an efficient combination of bisection and the secant rule.

8.3 Model Parameters and Information

In order to make calculations from the models examined in this study, several parameter values, as well as UNIFAC group assignments, were needed. Methods for obtaining polymer EOS parameters were described previously. To calculate EOS parameters for solvents, critical properties were needed. Because the DIPPR database does not have values of the critical properties for IPP, these properties had to be estimated. In addition, values of k_{ij} for the Wong-Sandler mixing rules were needed for each binary system. UNIFAC group assignments for the species involved in this work are also presented.

8.3.1 Critical Properties for IPP

The critical temperature and pressure of IPP were estimated by using MATHCAD to fit them to vapor pressure data from Nesterova et al. (1990). The acentric factor, ω, was also needed and is defined as

$$\omega \equiv -1.0 - \log_{10}\left(\frac{P^{sat}}{P_c}\right)_{T=0.7T_c} \qquad \textbf{(8.20)}$$

The vapor pressures calculated from the PR EOS by setting the vapor and liquid fugacity coefficients equal were compared with experimental vapor pressures. The critical properties were used in correlations to calculate the EOS parameters, a and b. The sum of squared errors between the calculated and experimental vapor pressures was minimized by varying T_c and P_c. The results of this minimization are given in Table 8.1. The values of the critical properties obtained here for IPP had a root-mean-squared deviation from the experimental values of less than 0.03 psi. They also appeared reasonable when compared with the critical properties of similar molecules that are available in the DIPPR database. These values are also shown in Table 8.1.

Table 8.1 Critical properties of IPP found in this work. T_c and P_c were fitted to vapor pressure data from Nesterova et al. (1990), and ω was calculated. Critical properties of similar molecules that are in the DIPPR database are included for comparison.

	T_c (K)	P_c (bar)	ω
IPP	741.6	48.47	0.4957
4-isopropenylphenol	742.7	39.36	0.5240
4-ethylphenol	716.5	42.90	0.5154
4-tertbutylphenol	734.0	33.40	0.5094

8.3.2 Values of k_{ij} for Wong-Sandler Mixing Rules

The method of Wong et al. (1992) was used to find values of the binary interaction parameters for the Wong-Sandler mixing rules (see appendix for mixing rule equations). This method involved fitting the excess Gibbs energy calculated from the combined ACM + EOS to that calculated from the ACM alone at low pressure over the entire composition range. No experimental data were needed. The binary interaction

parameters serve to adjust for the difference between A^{ex} at infinite pressure and G^{ex} at low pressure, which was assumed to be zero in the derivation of the mixing rules. In the case of these mixing rules $k_{ji} = k_{ij}$.

The excess Gibbs energy is calculated from activity coefficients by

$$\frac{G^{ex}}{RT} = \sum x_i \ln\gamma_i \qquad \textbf{(8.21)}$$

Activity coefficients are calculated from the combined ACM + EOS by

$$\gamma_i = \frac{\hat{\phi}_i^L}{\phi_i^L} \qquad \textbf{(8.22)}$$

where $\hat{\phi}_i^L$ is the partial fugacity coefficient of species *i* in the liquid mixture, and ϕ_i^L is the liquid phase fugacity coefficient of pure species *i*.

Figure 8.4 gives an example of the effect of the value of k_{ij} on the excess Gibbs energy. Values of G^{ex}/RT from the Entropic-FV ACM for PS/furan at 75ºC were compared with values of G^{ex}/RT calculated from the same ACM combined with the PR EOS using the Wong-Sandler mixing rules with various values of k_{ij}. In this case a value of 0.998 minimized the deviations. The molecular weight of PS used in these calculations was 72,000. Under these conditions the match between ACM and ACM + EOS was very sensitive to the value of k_{ij}. At lower polymer molecular weights the value of k_{ij} that gave the best match is lower, but there was also less sensitivity to the value of k_{ij}.

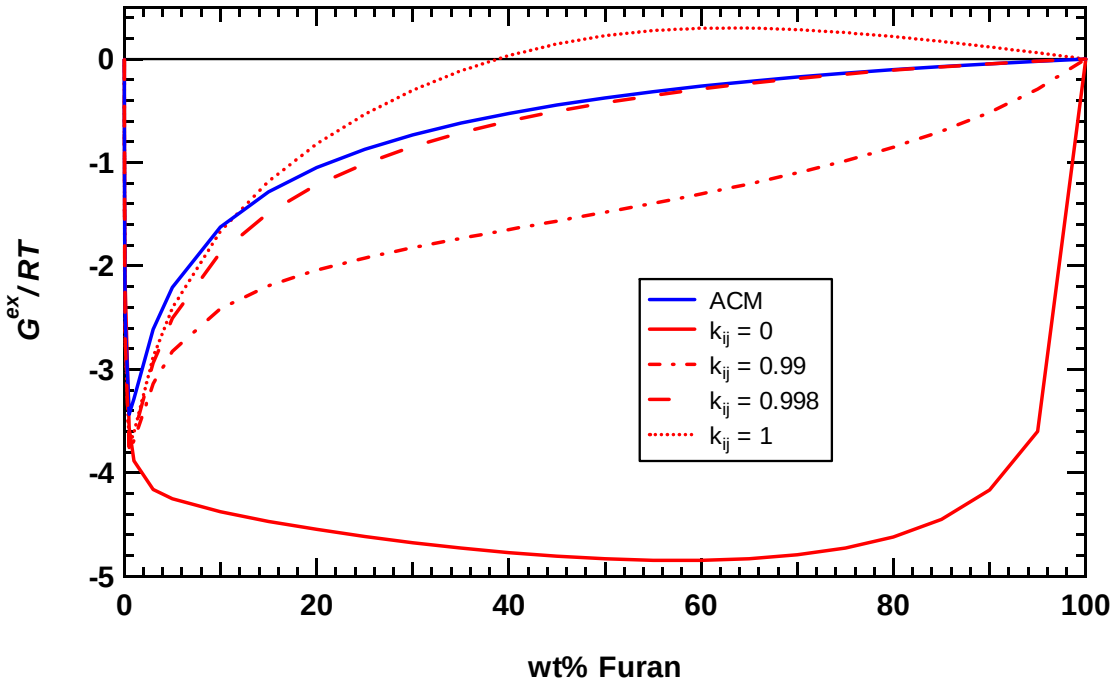

Figure 8.4 G^{ex}/RT for PS/furan system at 75ºC calculated from the Entropic-FV ACM alone, and from the same ACM combined with the PR EOS using different values of k_{ij} in the Wong-Sandler mixing rules. Polymer EOS parameters were determined using the new method from this work and molecular weight used for PS was 72,000.

Values of k_{ij} were found at various temperatures using several activity coefficient models to determine important effects. Table 8.2 shows some of these values for the PEG/benzene system. There was very little variation between values obtained using different ACMs, and only a small dependency on temperature, consistent with the findings of Wong et al. (1992). Values of k_{ij} were also found to vary with the molecular weight of the polymer, and to be more sensitive to temperature at lower polymer molecular weights. However, this higher sensitivity of the value of k_{ij} to temperature was offset by the finding that model calculations were less sensitive to the value of k_{ij} at lower polymer molecular weights. Thus, it was assumed that, for a given polymer/solvent

system and polymer molecular weight, a constant value of k_{ij} could be used at all temperatures.

Table 8.2 Values of k_{ij} for the PEG/benzene system (polymer MW = 8000) that minimize the deviation between G^{ex}/RT calculated from various ACMs alone and calculated from the ACM + PR EOS.

	27ºC	100ºC	150ºC	200ºC
Entropic-FV	-	0.979	0.978	0.976
Freed-FV	0.980	0.979	-	0.976
MEFV	-	0.979	-	0.977

Recommended values of k_{ij} are given in Table 8.3. They were obtained using the Entropic-FV ACM at 150ºC for systems with benzene and furan, or 200ºC for systems with IPP. The values presented here also show how k_{ij} varies with polymer molecular weight. Values closer to unity were needed for higher molecular weights. In actuality, the values are probably more dependent on the relative size of the two molecules. The value of k_{ij} was found to be 0.969 for the interaction between PS of MW = 1050 and of MW = 72,000. That is fairly similar to the value found for PEG and IPP, which had a molecular weight ratio close to that of the two PS molecular weights.

Table 8.3 Recommended values of k_{ij} for Wong-Sandler mixing rules.

	PEG	PS		
	MW = 8000	MW = 1050	MW = 72,000	MW = 1637
Benzene	0.978	0.850	0.998	0.903
Furan	0.982	0.876	0.998	0.921
IPP	0.976	0.860	0.998	0.918

8.3.3 UNIFAC Group Assignments

All of the ACMs in this study made use of the UNIFAC residual (or enthalpic) term for the activity coefficient. Thus, information about the UNIFAC interaction parameters was needed. The ACMs also made use of the UNIFAC group volumes and surface areas either for volume and surface area fractions (in the case of UNIFAC-FV and UNIFAC-ZM), or for calculating hard-core volumes (for the other four ACMs, which are based on the Entropic-FV model). As with the GCVOL and GCMCM group-contribution liquid volume estimation methods, the structure of each molecule was divided into various functional groups, for which the necessary parameters are known. The UNIFAC group assignments for each species (or for the repeating unit in the case of polymers) involved in the systems studied in the HT-VLE facility are presented in Table 8.4. The group assignments for the species in a hypothetical mixture of initial REF decomposition products are presented in Table 8.5. The volume, surface area, and interaction parameters for each group are given in the appendix.

Table 8.4 UNIFAC group assignments for each species (or for the repeating unit, in the case of polymers) involved in the systems studied in the HT-VLE facility.

Species involved in HT-VLE facility experiments	
Benzene	6:ACH
Furan	3:ACH, 1: CHO (ether)[a]
IPP	2:CH_3, 4:ACH, 1:ACCH, 1:ACOH
PEG	1:CH_2, 1:CH_2O
PS	1:CH_2, 5:ACH, 1:ACCH

[a] An appropriate UNIFAC group was not available for the furan oxygen so the non-aromatic CHO (ether) group was used to represent the furan oxygen and its neighboring aromatic carbon with attached hydrogen

Table 8.5 UNIFAC group assignments for each species (or for the repeating unit, in the case of polymers) in a hypothetical mixture of initial REF decomposition products.

Toluene	5:ACH, 1:$ACCH_3$
Bisphenol-A	2:CH_3, 1:C, 8:ACH, 2:AC, 2:ACOH
REF polymer[a,b]	7:CH_3, 31:CH_2, 15:CH, 2:C, 12:ACH, 4:AC, 2:$ACCH_2$, 5:OH, 3:CH_2COO, 2:CH_2O, 1:CH_2NH, 1:CHNH, 2:CH_2N, 2:furfural[c]

[a] From structure in Figure 3.1
[b] UNIFAC interaction parameters were not available for the interactions between the amine and furfural groups, so they were set to zero. These interactions, however, are only a very small fraction of the total number of interactions.
[c] An appropriate UNIFAC group was not available for the furan oxygen, so the furfural group (furan with attached aldehyde) was used to represent the furan ring and the neighboring CH_2O group, in effect representing the CH_2O with a CHO (aldehyde). The molecular weight of the repeating unit was according increased by the mass of the additional hydrogen.

8.4 Summary of Modeling Methods

In this chapter a description was given of eighteen distinct models (six activity coefficient models used in three different ways) and the method by which they were compared with the experimental data from the HT-VLE facility that were reported earlier. The algorithms used in the computer code written for this study were then presented. Finally, information necessary to perform the model calculations, including values of critical properties for IPP, values of k_{ij} (the Wong-Sandler binary interaction parameters), and UNIFAC group assignments for each species were reported.

9 Modeling Results

This section describes the validation of the modeling approach and algorithms used in this study. Results are then presented that compare the model predictions of the eighteen different models examined here with the data collected in the HT-VLE facility. These results are discussed and recommendations are given. Finally, sample VLE calculations of a mixture of some REF decomposition products are presented.

9.1 Modeling Method Validation

Two approaches were used to validate different aspects of the modeling method. First, preliminary calculations were made to verify the ability of activity coefficient models combined with an equation of state through the Wong-Sandler mixing rules to predict VLE behavior for polymer solutions. Work was then performed to validate the algorithms used in the computer code for VLE of multicomponent solutions.

Figure 9.1 shows a comparison of some literature data for PEG/benzene at 70ºC with calculations from two ACMs combined with the PR EOS. This comparison served two purposes. It verified the findings of Orbey and Sandler (1994), who were the first to apply an ACM + EOS model to polymer solutions, and it served to compare the abilities of two very different activity coefficient models. The UNIFAC-FV ACM combined with the Peng-Robinson EOS was able to give very good predictions of the experimental data.

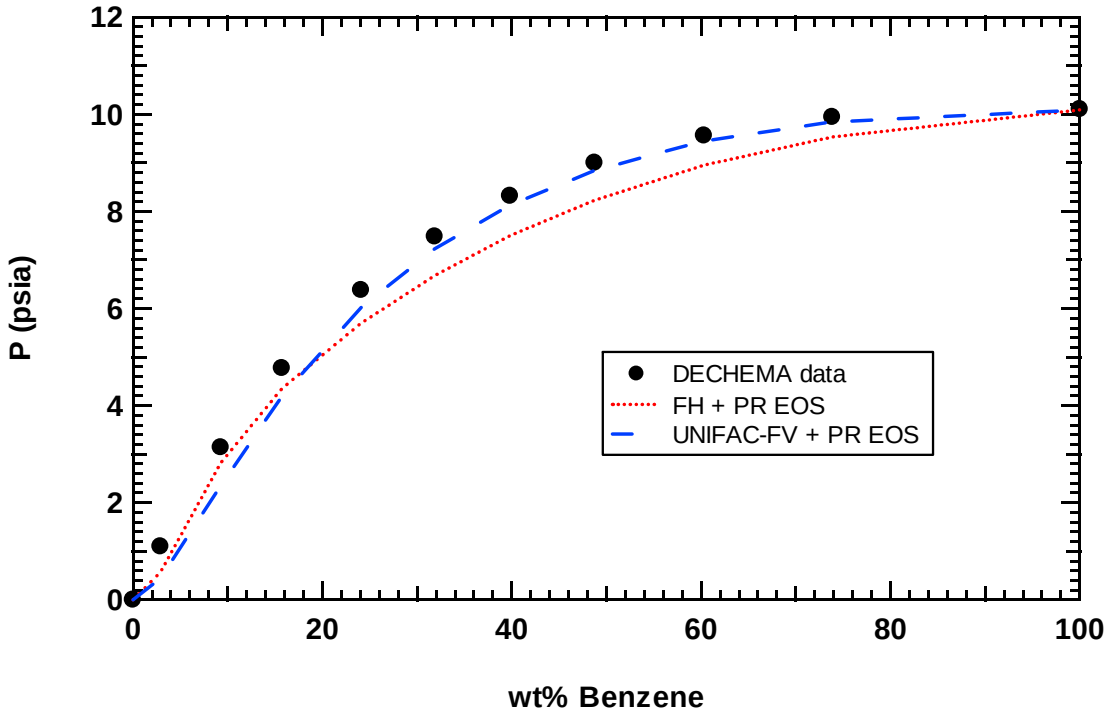

Figure 9.1 Comparison of equilibrium pressures predicted by two models with data from the DECHEMA data series (pg. 134, Hao et al., 1992) for PEG/benzene at 70ºC. For the FH + PR EOS model, $k_{ij} = 0.771$ and $\chi = 0$. For the UNIFAC-FV + PR EOS model, $k_{ij} = 0.779$. EOS parameters for polymer were $a = 260$ m^6·Pa/mol^2 and $b = 0.00464$ m^3/mol from Orbey and Sandler (1994).

After the computer code was written, it was used to calculate equilibrium pressures for a series of mixtures of benzene, cyclohexane, and tertpentanol. The purpose of these calculations was to validate the algorithms used, showing that experimental data for multicomponent solutions could be reproduced. The results are shown in Figure 9.2. For these calculations the NRTL activity coefficient model was used because parameters fit to the experimental data were given with the data. Therefore, it was known that the ACM (at least alone) fit the data very well, and the algorithm could be validated by the quality of the results. The calculated pressures agreed well with the measured pressures.

Also, the calculated vapor mole fractions were within 0.02, on average, of the measured mole fractions. These small differences were most likely a result of combining the NRTL ACM with an equation of state with k_{ij} set to 0. Because there were no polymers in this mixture, the appropriate value of k_{ij} would have been small, and the calculated equilibrium pressures were also not as sensitive to that value. Thus it was verified that the computer code algorithms were working correctly.

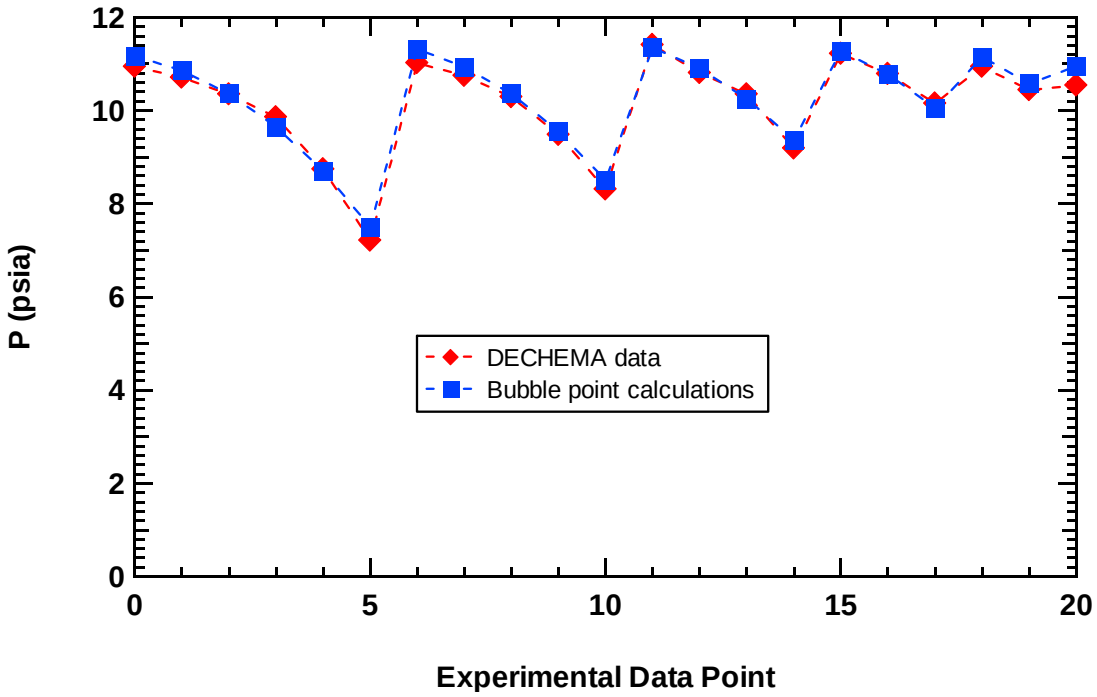

Figure 9.2 Comparison of equilibrium pressures calculated using the bubble point algorithm for the benzene/cyclohexane/tertpentanol system at 70ºC with data from the DECHEMA data series (pg. 734, Gmehling et al., 1982). Each experimental data point represents a different liquid composition, with the points covering almost the entire range of composition of all three components. The model used in the bubble point calculations was the NRTL ACM combined with the PR EOS through the Wong-Sandler mixing rules with $k_{ij} = 0$. NRTL parameters were given with the data.

9.2 Effect of Polymer Molecular Weight

After the modeling methods were validated, calculations were performed with several ACM + EOS models over a range of temperatures for the PS/benzene system with PS of different molecular weights to explore the effect of molecular weights on polymer solution VLE behavior. In all cases, model predictions resulted in very low computed vapor phase polymer mass fractions. They were generally less than 10^{-10} even for the lowest molecular weight of 1050 and at the highest temperatures. Predicted polymer mass fractions in the vapor reached values as small as 10^{-250} for higher molecular weights.

The molecular weight of the polymer also affected the predicted equilibrium pressure. Figure 9.3 shows some pressures predicted by the Entropic-FV + Peng Robinson EOS model for the PS/benzene system at 190º at molecular weights of 1050 and 72,000. Also included are predictions for the 52/48 wt% mixture of these two molecular weights that was used for all subsequent model calculations on systems with PS. The number-average molecular weight, MW_n, of this hypothetical mixture was 1637. It can be seen from the figure that the equilibrium pressures predicted using this average molecular weight were similar but not equal to those predicted for the mixture of the two molecular weights of PS. However, if information is not available about the molecular weight distribution of the polymer, or if it is known to be fairly narrow (as in the case of most unimodal molecular weight distributions), it is recommended that the number-average molecular weight of the polymer be used in model calculations.

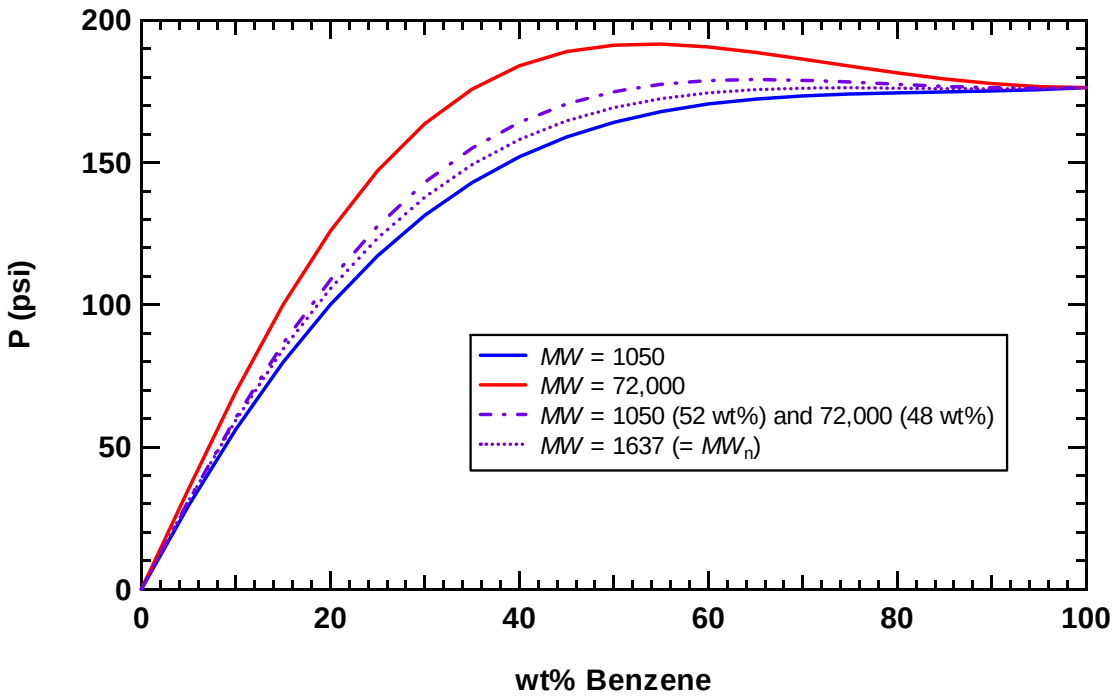

Figure 9.3 Computed pressure of PS/benzene system at 190ºC for different molecular weights of PS. Calculations were made using Entropic-FV ACM + PR EOS with polymer EOS parameters from the new method described in this work. Values of k_{ij} for each molecular weight given in Table 8.3.

Another interesting effect of the polymer molecular weight was that larger molecular weights tended to lead more to a liquid phase split, where the liquid phase separates into two liquid phases of different compositions. A local maximum in the pressure, when plotted as in Figure 9.3, generally indicates the existence of an azeotrope. An azeotrope occurs when the liquid and vapor compositions in equilibrium with each other are the same. That was obviously not the case for polymer solutions which had essentially no polymer in the vapor phase. However, calculations made at compositions close to the pure solvent showed that there was also a small local minimum. The presence of a local maximum and local minimum in pressure calculated by an EOS or

ACM is a prediction of the existence of two liquid phases. One would be almost pure solvent, and the other would be a mixture of polymer and solvent that would be higher in polymer concentration than the overall composition of the combined liquid phases. Since they would be in equilibrium, the pressure at both liquid compositions must be essentially equal to the vapor pressure of the pure solvent. A more detailed discussion is presented in the next section.

9.3 Results and Discussion

Each of the eighteen models described in detail in the last chapter (six ACMs in each of three usage types) were used to calculate equilibrium pressures over the entire composition range for all of the polymer/solvent systems for which equilibrium pressure data were reported in Chapter 5. The average absolute deviations (AAD%) for each model were calculated from the following equation using the HT-VLE facility data for each chemical system at the temperatures given in section 8.1.2:

$$AAD\% = 100\% \cdot \sum_{n} \frac{\left|P_{calc} - P_{data}\right|}{P^{sat}} \Big/ n \qquad \textbf{(9.1)}$$

where P^{sat} is the vapor pressure of the pure solvent at the temperature of each data point.

Table 9.1 lists the average absolute deviations from the data collected in the HT-VLE facility for each polymer/solvent system. Overall values of the AAD% for each model are also shown. The results shown here will be discussed below using examples from the model calculations performed. All of the modeling results are also given in the appendix.

Table 9.1 Summary of AAD% between system pressure calculations from several models and data collected at BYU for each polymer/solvent system.

Usage Type	ACM	PEG			PS			Overall
		Benzene	Furan	IPP	Benzene	Furan	IPP	
ACM alone	Entropic-FV	2.26	7.89	14.67	4.25	4.32	6.45	6.64
	Freed-FV	2.58	6.16	15.46	5.59	4.12	9.70	7.27
	GK-FV	3.33	10.63	13.96	4.51	4.54	4.84	6.97
	MEFV	3.64	12.00	14.20	5.22	7.96	5.20	8.04
	UNIFAC-FV	2.64	5.76	15.51	5.53	11.67	7.63	8.12
	UNIFAC-ZM	3.01	3.52	11.92	3.81	9.62	4.09	6.00
ACM + EOS Method 1	Entropic-FV	12.04	29.41	4.50	9.46	10.51	5.24	11.86
	Freed-FV	9.54	26.10	5.01	6.56	6.40	5.00	9.77
	GK-FV	12.83	31.78	4.71	10.03	10.75	6.14	12.71
	MEFV	12.98	32.58	4.55	11.39	13.04	5.87	13.40
	UNIFAC-FV	9.90	19.78	4.64	6.14	2.77	5.00	8.04
	UNIFAC-ZM	12.87	24.06	6.06	6.85	4.13	6.49	10.08
ACM + EOS Method 2	Entropic-FV	5.34	8.80	13.48	7.85	4.46	10.16	8.35
	Freed-FV	2.79	6.19	14.28	5.49	3.39	9.86	7.00
	GK-FV	6.16	11.10	12.88	8.46	4.63	9.69	8.82
	MEFV	6.26	11.97	13.22	9.38	6.07	9.67	9.43
	UNIFAC-FV	3.85	2.30	13.79	4.62	5.81	10.47	6.81
	UNIFAC-ZM	6.24	3.64	10.55	5.25	6.08	9.28	6.84

One thing evident from Table 9.1 is that no one model had the smallest deviations from the experimental data for all of the polymer/solvent systems, nor was there one model that seemed to be extremely better overall than the others. A typical comparison is shown in Figure 9.4. In this figure, model predictions from the three types of models involving the Freed-FV ACM are compared with experimental data for the PEG/benzene system. The equilibrium pressures calculated from the "ACM alone" and from the "ACM + EOS Method 2" models were similar to each other in their overall shape as well as in their deviation from the data. The pressures calculated from the "ACM + EOS Method 1" model, however, were quite different from the data at all three temperatures.

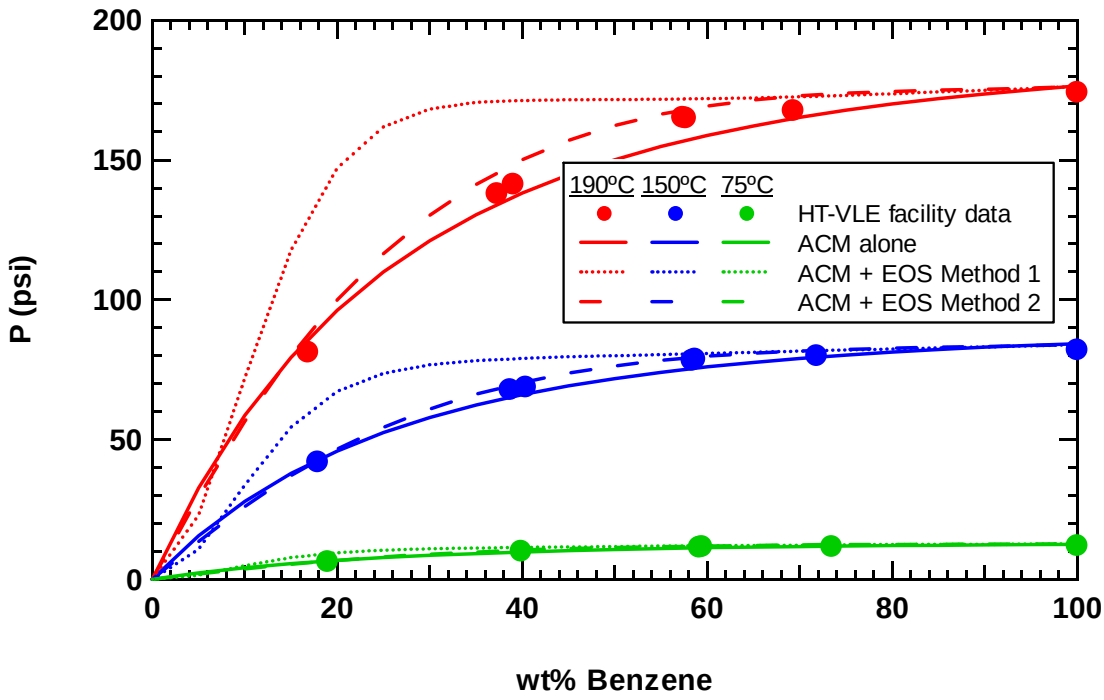

Figure 9.4 Comparison of data from this work for the PEG/benzene system with calculations from the three models using the Freed-FV ACM.

Table 9.2 gives the overall average deviations for each of the three model types. The deviations for the models using a combined ACM + EOS with the polymer EOS parameters obtained from the method of Louli and Tassios (ACM + EOS Method 1) were noticeably larger than the deviations for the other two types of models. In fact, the "ACM alone" model type had the lowest overall average deviation by a small margin. However, the "ACM + EOS Method 2" models had an overall average deviation that was similar to that of the "ACM alone" models. The former also had a somewhat smaller standard deviation, indicating that the quality of the results was slightly more consistent from ACM to ACM and from system to system.

Table 9.2 Overall AAD% for each type of ACM usage. Each usage type represents six models. Standard deviations were calculated from individual values of AAD% listed in Table 9.1 for each polymer/solvent system for each model.

ACM Usage Type	Usage type AAD%	St. dev.
ACM alone	7.17	4.10
ACM + EOS Method 1	10.98	8.16
ACM + EOS Method 2	7.87	3.41

Additional model predictions are shown in Figure 9.5. These predictions are from the three models involving the UNIFAC-FV ACM for the PEG/furan system. Again, it is seen that the combined ACM + EOS model using the parameters from the method of Louli and Tassios resulted in larger deviations from the experimental data than the combined model using the parameters from the new method described in this work. Also, in this case the "ACM + EOS Method 2" model clearly followed the data better than the "ACM alone" model. For other systems, though, the reverse was true.

It was mentioned earlier that the experimental data for the PEG/IPP system followed significantly different trends from the data for the other systems. It is interesting to note that this behavior was captured at least somewhat qualitatively by all of the models examined here, if not quantitatively. Figure 9.6 shows calculations from the three UNIFAC-ZM models for this system. While the experimental data and model predictions for other systems showed equilibrium pressures that were close to the pure solvent vapor pressure even for compositions as low as 50 to 60 wt% solvent, predictions for the PEG/IPP system showed the pressure dropping even for small amounts of polymer. PEG and IPP may experience some specific intermolecular attractions that are as important, if not more so, than the effects of the difference in molecular size.

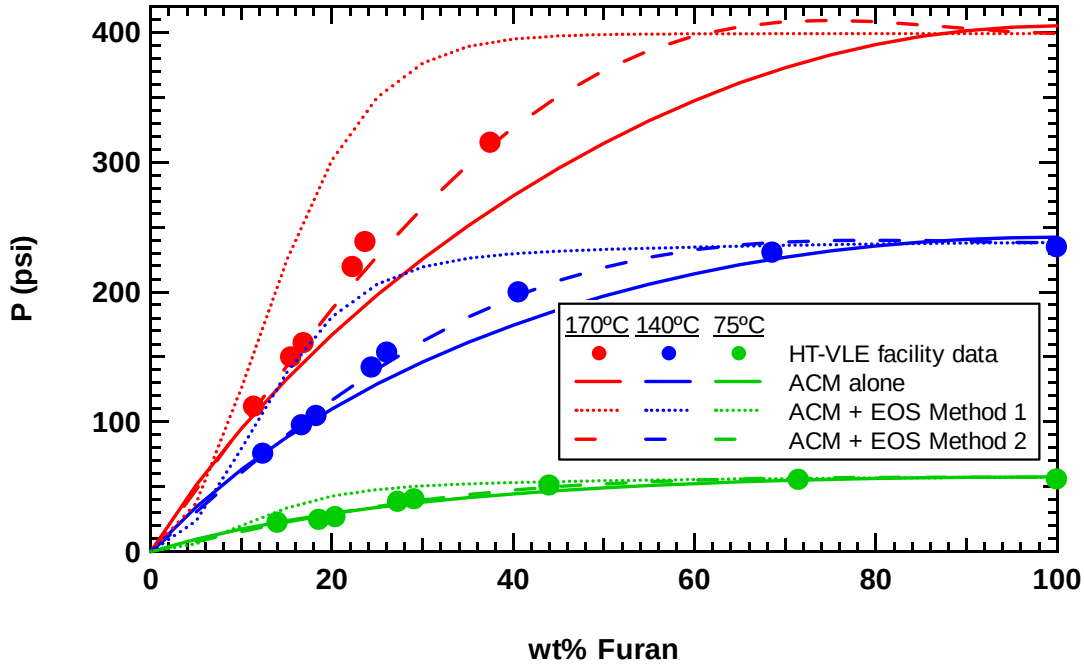

Figure 9.5 Comparison of data from this work for the PEG/furan system with calculations from the three models using the UNIFAC-FV ACM.

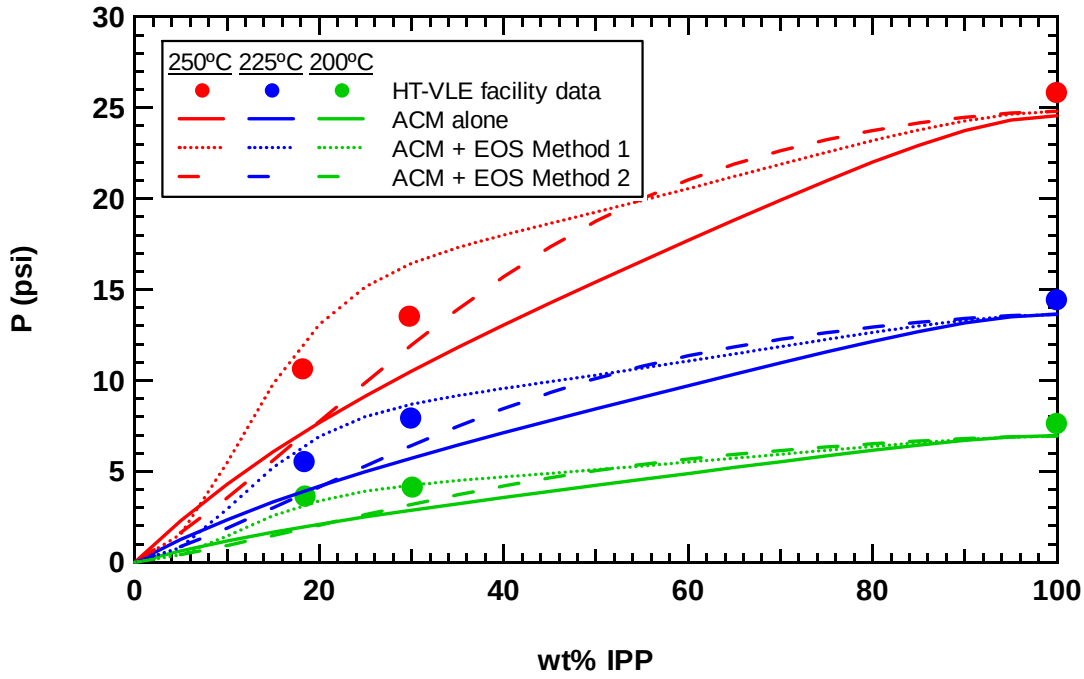

Figure 9.6 Comparison of data from this work for the PEG/IPP system with calculations from the three models using the UNIFAC-ZM ACM.

An important difference was found between the "ACM alone" models and the "ACM + EOS Method 2" models. Figure 9.7 shows a comparison of predictions from two of the UNIFAC-ZM models and the experimental data for the PS/furan system. It is evident that the "ACM + EOS Method 2" model predicted a liquid phase split. Circles are used to show the approximate compositions of the two liquid phases that were predicted to exist for mixtures where the concentration of furan was higher than about 60 wt%. Under no circumstances examined in this study did any of the "ACM alone" models predict this type of behavior. Since liquid compositions were not measured in the HT-VLE facility, there are no data to support either case.

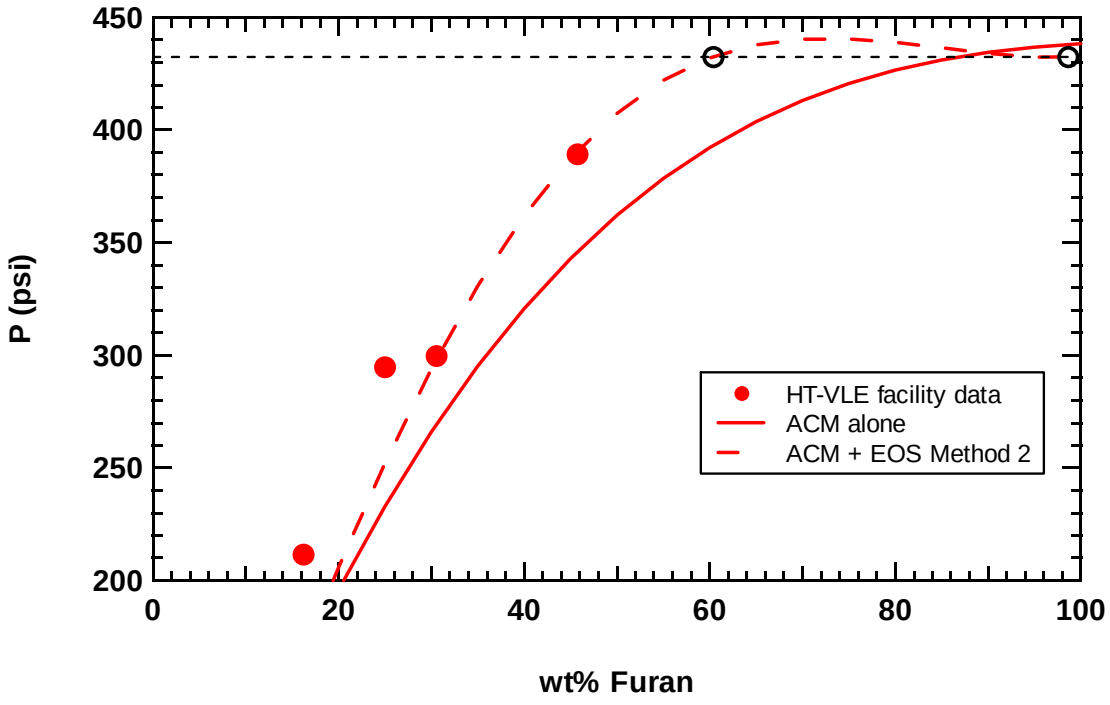

Figure 9.7 Comparison of data from this work for the PS/furan system with calculations from the two of the models that use the UNIFAC-ZM ACM. The black dotted line represents the possibility of a liquid/liquid phase split predicted by ACM + EOS model at high furan concentrations. Circles show approximate compositions of two liquid phases.

The propensity for an ACM + EOS model to predict a liquid phase split was greater at higher temperatures, indicative of the existence of a Lower Critical Solution Temperature (LCST). The LCST is the temperature above which the two species are no longer completely miscible. The propensity for a predicted phase split was also higher for larger polymer molecular weights, in agreement with theory (see Danner and High, 1993; Rodriguez et al., 2003).

Table 9.3 is a summary of the overall average deviations between predictions from each model and the entire HT-VLE facility data set, grouped by model type and then ordered by increasing overall AAD%. These values were reported in Table 9.1, but are repeated here in this order for ease of study.

Table 9.3 Overall AAD% for each model (from Table 9.1), grouped by ACM usage type and then ordered by increasing AAD%.

ACM alone		ACM + EOS Method 1		ACM + EOS Method 2	
ACM	AAD%	ACM	AAD%	ACM	AAD%
UNIFAC-ZM	6.00	UNIFAC-FV	8.04	UNIFAC-FV	6.81
Entropic-FV	6.64	Freed-FV	9.77	UNIFAC-ZM	6.84
GK-FV	6.97	UNIFAC-ZM	10.08	Freed-FV	7.00
Freed-FV	7.27	Entropic-FV	11.86	Entropic-FV	8.35
MEFV	8.04	GK-FV	12.71	GK-FV	8.82
UNIFAC-FV	8.12	MEFV	13.40	MEFV	9.43

To determine the predictive capabilities of each model, it was more useful to examine the overall average deviations between each model and the entire data set than to examine the average deviations from the data for each polymer/solvent system. The end points of the equilibrium pressure vs. composition curve were fixed at essentially zero at the pure polymer end, and at the vapor pressure of the pure solvent at the other end (this

value varied between model types only because the ACMs used a correlation from the DIPPR database for the vapor pressure, and the ACM + EOS models got that information indirectly from the solvent critical properties). Therefore, the variation between the models ensured that there was almost always one model that fit each data set very well by chance. Using overall averages indicated the quality of the predictive capabilities of the each model in general, rather than whether a model happened to match the experimental data for a particular system very well.

The model with the lowest overall average deviation was, surprisingly, the UNIFAC-ZM ACM used alone, at 6.00%, but several other models had average deviations that were not much larger. Among these were the UNIFAC-FV and UNIFAC-ZM ACMs combined with the PR EOS using the new polymer parameters from this study, at 6.81 and 6.84%, respectively. It is interesting to note that results from the UNIFAC-FV ACM were among the best when it was combined with an equation of state, but were the worst when it was used alone. In contrast, the Entropic-FV model fared poorly when used in combination with an equation of state. The fact that polymer volumes were estimated by GCMCM may be part of the reason why the Entropic-FV results were not as good as others have found them to be. This is consistent with the findings of Pappa et al. (1999) who recommended using the Entropic-FV ACM when accurate volumes were known, but recommended using UNIFAC-ZM otherwise. The modifications of the Entropic-FV model in the GK-FV and MEFV ACMS only seemed to lead to higher deviations for the polymer/solvent systems studied here. In fact, the three MEFV models had, on average, the highest deviations from the data.

9.4 Model Recommendations

In recommending a model for use in predicting high-temperature polymer solution VLE, it is noted that some further work is needed to determine whether the combined ACM + EOS models were correct in predicting liquid phase splitting under some conditions, or if the ACM models used alone were correct in predicting complete miscibility over the entire range of conditions studied in this research. If no phase splitting is seen, the UNIFAC-ZM ACM used alone is recommended as the best model. If there is the possibility of phase splitting, then the UNIFAC-FV ACM + PR EOS with polymer EOS parameters from the new method should be used. In addition, the pressures encountered in this study were not especially high, even though the experiments were conducted at high temperatures. Significantly higher pressures could be encountered during rigid foam decomposition. At higher pressures, using combined ACM + EOS models may have additional advantages over using ACMs alone because the ACMs are not functions of pressure.

The recommended procedure for using the UNIFAC-FV ACM + PR EOS model to predict VLE of polymer solutions during decomposition of rigid foams is as follows:

1. Identify species and their structures (and molecular weights for polymers)
2. Obtain liquid volume correlations for solvents or make GCVOL group assignments
3. Obtain Tait equation parameters, if available, or make GCMCM group assignments for polymers
4. Obtain critical properties for solvents or fit them to vapor pressure data

5. Calculate *a* and *b* for solvents from critical properties using correlations for Peng-Robinson equation of state
6. Determine *a* and *b* for polymers using the new method developed in this work
7. Make UNIFAC group assignments for all species
8. Find k_{ij} for each pair of species in the system by fitting G^{ex}/RT from ACM + EOS to G^{ex}/RT from ACM alone over the entire composition range
9. Use the computer code written in this study with the UNIFAC-FV ACM + PR EOS model to determine equilibrium pressures and phase compositions, given the temperature and either the liquid composition or the overall amounts of each species and the system volume.

If the UNIFAC-ZM ACM is used alone to make VLE predictions, several of the steps in the above procedure are not necessary. Solvent and polymer liquid volumes (steps 2 and 3) are not needed. Solvent critical properties and EOS parameters for each species are not needed (steps 4-6), but vapor pressures for each solvent are needed. Finally, values of k_{ij} do not need to be found (step 8), because no mixing rules are used.

9.5 VLE of Initial REF Decomposition Products

Sample VLE calculations were made for a system of toluene, bisphenol-A, and the polymer-like decomposition products of REF (with the structure shown in Figure 3.1). The molecular weight of the "polymer" was assumed to be 7500. The values of k_{ij} were found to be 0.965 for toluene/REF polymer, 0.942 for bisphenol-A/REF polymer, and 0.19 for toluene/bisphenol-A. The calculations were performed at several compositions using the UNIFAC-FV ACM + PR EOS with polymer parameters

determined using the new method from this work. Equilibrium pressures predicted at 200 and 280ºC are presented in Figure 9.8 and Figure 9.9, respectively. In these figures the "polymer" weight percent is the remainder of the mixture after reading the weight percent of toluene and bisphenol-A from the plot. Thus, the "polymer" concentration is lower at the right side of the plots than at the left, and it is also lower on curves representing higher bisphenol-A concentrations.

The polymer-like REF decomposition products had the same type of effect on the equilibrium pressure as the polymers studied in the HT-VLE facility. The vapor pressure of bisphenol-A was negligible compared to that of toluene, so the differences in pressure at different concentrations of bisphenol-A were a combination of the effects of a lower "polymer" concentration, and of interactions between bisphenol-A and toluene. Generally, the addition of bisphenol-A decreased the equilibrium pressure for a given toluene concentration. It is interesting to note that at low toluene concentrations the predictions for 20 wt% bisphenol-A resulted in higher pressures than predictions for 0 wt% bisphenol-A. This effect was more pronounced at 200ºC than at 280ºC. It may be that at high "polymer" concentrations (on the left side of the plots on the blue and red curves) the effect of removing some "polymer" was more important than the interactions between bisphenol-A and toluene, and thus the equilibrium pressure on the 20 wt% bisphenol-A curve was higher than on the 0 wt% curve. However, at lower "polymer" concentrations (on the right side of the plots or on the green and purple curves) the interactions between bisphenol-A and toluene may have been more important, causing the predicted equilibrium pressure on the 20 wt% (and higher) curves to be lower than on the 0 wt% curve.

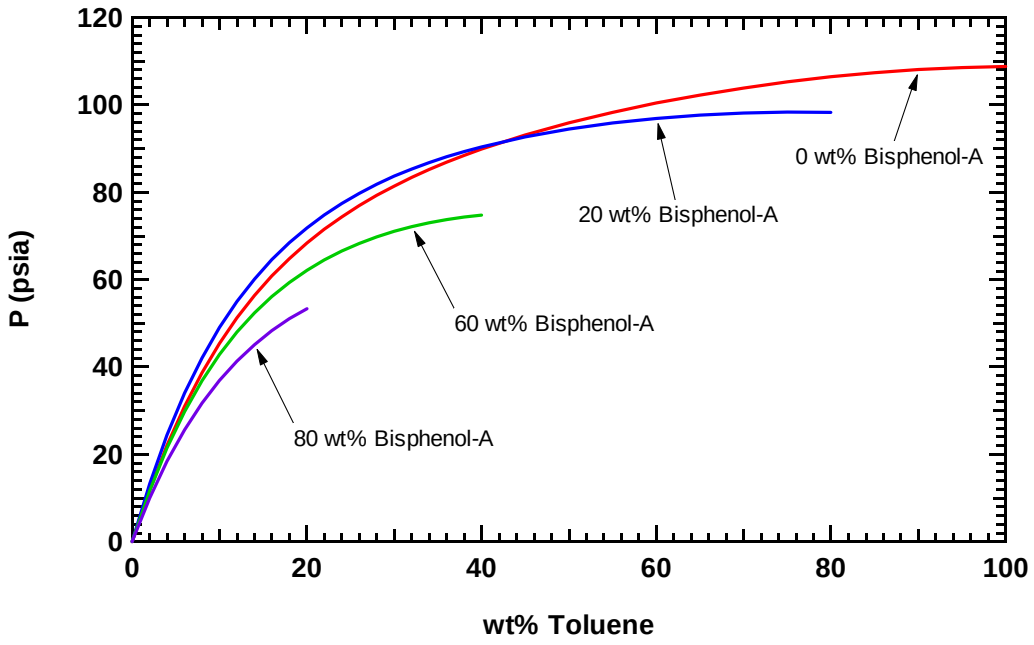

Figure 9.8 Predicted pressures for a system of toluene, bisphenol-A, and polymer-like REF decomposition products at 200ºC using the UNIFAC-FV + PR EOS model with polymer EOS parameters from the new method.

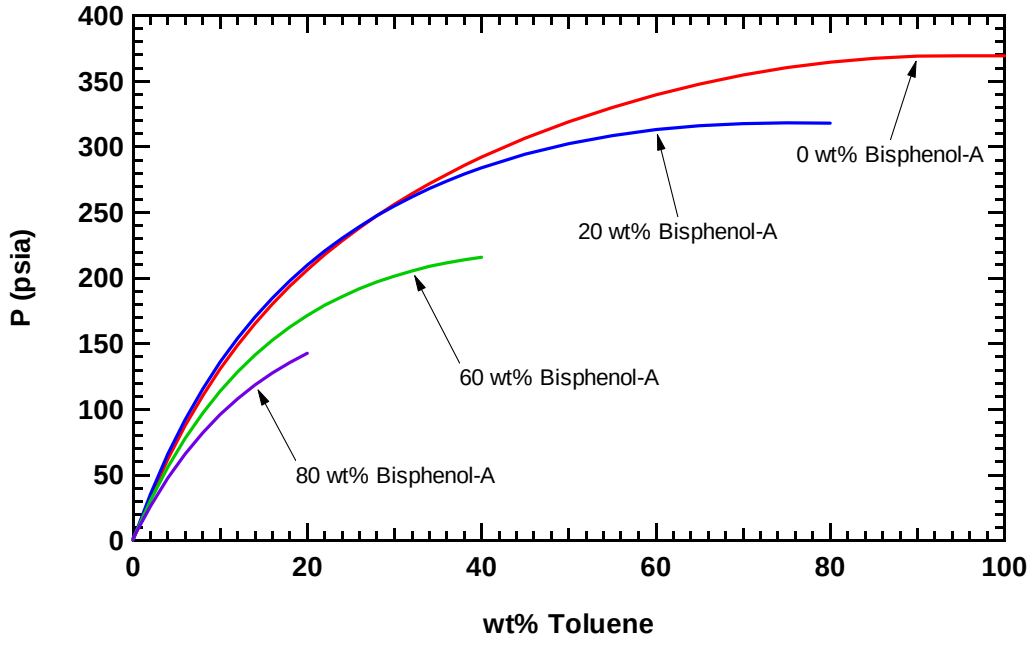

Figure 9.9 Predicted pressures for a system of toluene, bisphenol-A, and polymer-like REF decomposition products at 280ºC using the UNIFAC-FV + PR EOS model with polymer EOS parameters from the new method.

9.6 Summary of Modeling Results

The modeling method presented in the previous chapter was validated by comparing model calculations with literature data for a binary polymer solution and for a ternary mixture of low molecular weight species. These comparisons served to prove the feasibility of using a combined ACM + EOS model and to validate the algorithms used in the multicomponent VLE computer code. The effects of polymer molecular weight on equilibrium pressure calculations were discussed, including the possibility of predicting a liquid phase split.

A comparison of the predictions of the eighteen models with the HT-VLE facility data was then presented. It was found that the combined ACM + EOS models using the polymer EOS parameters from the new method resulted in much lower deviations than from using polymer EOS parameters obtained from the literature method (an average of 7.87% compared to 10.98%). The MEFV ACM was found generally to give the highest deviations from the data. All of the models, however, were able to qualitatively predict the unexpected trends seen in the PEG/IPP data. The overall average deviation between the data and the "ACM alone" models was the lowest of the three model types at 7.17%, but the overall average deviation for the "ACM + EOS Method 2" models, at 7.87%, was not significantly higher. The "ACM + EOS Method 2" models, however, were able to predict a liquid-liquid phase split under some conditions, while this behavior was never predicted by the ACMs alone. Without measurements of the liquid phase compositions from the HT-VLE facility, it was not known whether the liquid phase splitting actually occurred.

For predicting VLE of polymer solutions during decomposition of rigid foams, it was recommended that the UNIFAC-ZM ACM be used alone if the phase splitting behavior is incorrect, but that the UNIFAC-FV + Peng-Robinson EOS model (with polymer EOS parameters from the new method) be used if there is liquid phase splitting under some conditions. Also, using combined ACM + EOS models may have additional advantages over using ACMs alone at the high pressures because ACMs are not functions of pressure.

Finally, some calculations were made of the VLE behavior of a mixture of toluene, bisphenol-A, and the polymer-like decomposition products of REF. The UNIFAC-FV + PR EOS model was used. Calculations were performed over a range of compositions at 200 and at 280ºC. It was found that increasing the bisphenol-A concentration generally resulted in lower equilibrium pressures except at high "polymer" concentrations where the predicted equilibrium pressure for a given toluene concentration was higher at 20 wt% bisphenol-A than at 0 wt% bisphenol-A.

10 Summary and Conclusions

This chapter reviews the achievements of this work and gives a summary of the main conclusions and recommendations. Specifically the completion of each of the objectives of this research is discussed, and suggestions for future work are given.

10.1 Completion of Objectives

The purpose of this research was to measure the vapor-liquid equilibrium behavior at temperatures between 75 and 250ºC of some polymer solutions similar to initial decomposition products of REF and other rigid foams, and to develop a procedure for predicting VLE behavior during thermal decomposition of the actual foams. The accomplishment of each of the three tasks presented earlier is given here.

Task 1. Measurement of VLE Behavior of Representative Solvents and Polymers

During the course of this work, a high-temperature vapor-liquid equilibrium facility was designed and built. After checking and calibrating the thermocouples and pressure transducers, the component measurements of the HT-VLE facility were validated by comparing readings of pure solvent vapor pressures with correlations from the DIPPR database for benzene and furan, and with experimental data in the literature for IPP. The largest average difference was about 3% for the vapor pressure of furan,

while the measured vapor pressures of benzene and IPP were consistently within 1 psi of the DIPPR correlation and literature data, respectively.

An experimental method for measuring the equilibrium pressure of high-temperature polymer solutions was also developed and validated. First, the data were shown to be reproducible through the use of replicate experiments. Next, data collected at 70ºC in the HT-VLE facility for PEG/benzene were compared with data from the literature and were found to be in very good agreement.

Equilibrium pressure data were then collected at temperatures between 75 and 250ºC for the six polymer/solvent systems representative of the initial decomposition products of REF and other rigid foams. The systems were combinations of PS and PEG with each of the three solvents – benzene, furan, and IPP. Data were not previously available in the literature for the benzene systems at temperatures above 70ºC, nor were any data available for the furan or IPP systems. Data trends for most of the systems were consistent with trends seen in literature data for the benzene systems (and other polymer/solvent systems) at lower temperatures. The equilibrium pressures for the PEG/IPP system, however, were closer to being linear over the composition range.

For data reporting purposes, liquid compositions were calculated from the overall compositions of each run. This was done using the volume available to the mixture in the pressure vessel, correlations for the volume of the liquid components, and the Peng-Robinson equation of state for the pure solvents. The amount of solvent in the vapor phase at each temperature was calculated through an iterative process and then subtracted from the overall amount in the vessel to obtain the liquid composition.

Task 2. VLE Submodel Development

Several polymer solution VLE models were selected from the literature for evaluation in comparison with the data collected in this study. The selected models were all free-volume activity coefficient models, which were found from a review of the literature to be generally the most accurate for polymer solutions. The six ACMs examined were the Entropic-FV, Freed-FV, GK-FV, MEFV, UNIFAC-FV, and UNIFAC-ZM models. These ACMs were used alone as well as in combination with the Peng-Robinson equation of state through the Wong-Sandler excess energy mixing rules. Previous studies in the literature have shown that the combination of activity coefficient models with an equation of state through excess energy mixing rules can extend the capabilities of the more accurate ACMs to higher temperatures and pressures as well as reduce the sensitivity of model parameters to changes in temperature and composition. This work is the first time that free-volume activity coefficient models have been combined with an equation of state using the Wong-Sandler mixing rules.

Except for the need for values of pure species liquid volumes, which were required for all but the UNIFAC-ZM model, the models were based on group contributions. This was important because, in the case of decomposing foam networks with large polymer-like fragments, no species-specific information will be available for the polymers besides their structure.

The need for liquid polymer volumes was met through group-contribution volume estimations methods. Two methods used previously in the literature, GCVOL and GCMCM, were subjected to a comprehensive comparison using values of specific volume from various literature sources over wide ranges of pressure and temperature for 14 different polymers, including some with structures similar to the polymer-like

decomposition products of REF. Volumes estimated from the GCMCM method were found to have the lowest overall average deviation from literature values at 5.32%, compared to 7.09% for those estimated from GCVOL. The GCMCM method was also found to be more accurate in its ability to predict the correct temperature sensitivity of polymer volumes, and to be more consistent from species to species in the quality of its predictions.

It was found, however, that GCVOL could be used to estimate liquid volumes for solvent species in cases where they were not available in the DIPPR database or elsewhere. This was the situation with IPP. Volumes estimated using GCVOL for furan, benzene, and two species similar to IPP were compared with correlations from the DIPPR database. For all but furan, for which appropriate group assignments do not exist in GCVOL, the deviations in volume were less than 5% at temperatures up to approximately 80% of the value of the solvent critical temperature. Use of GCVOL at higher temperatures is not recommended because the method fails to reproduce the sharp rise in specific volume as a substance nears its critical point.

A modular computer program was written in order to make predictions of equilibrium pressures and phase compositions using the various models examined in this work. The code was based around a standard bubble point pressure algorithm. Preliminary calculations for two ACMs were compared with binary polymer solution data to show that the ACM + EOS approach was feasible. The algorithms in the program, and specifically the ability to be able to calculate VLE for multicomponent solutions, were validated by comparing calculations with literature data for a mixture of three solvents.

Task 3. Application to Degradation of Rigid Foams

The parameters needed for the models used in this work included the EOS parameters for the pure polymer, as well as k_{ij}, the binary interaction parameters for the Wong-Sandler mixing rules. Polymer EOS parameters were obtained for PEG, PS, and the polymer-like decomposition products of REF following the most recommended method from the literature. A new method for determining these parameters was also developed. Values of k_{ij} were obtained for all of the polymer/solvent systems studied in this work, and also for the binary interactions of the polymer-like decomposition products of REF with toluene and bisphenol-A, by fitting G^{ex}/RT from the ACM + EOS to G^{ex}/RT from the ACM alone over the entire composition range.

The equilibrium pressure data collected from the HT-VLE facility were compared with calculations from 18 different models – the six ACMs mentioned above, each used in three different ways. Calculations were made using the ACMs alone, and using the ACMs combined with the Peng-Robinson equation of state with either the polymer EOS parameters determined from the literature method, or from the new method developed in this work. It was found that the models using the polymer EOS parameters from the new method performed significantly better than the models using the parameters from the literature method, with an overall average deviation from the data of 7.87% compared to 10.98%. The models using the MEFV ACM consistently had the highest deviations from the data. All of the models, though, predicted the unexpected equilibrium pressure trend of the PEG/IPP data, at least qualitatively. The deviations between the data and the models using the ACMs alone (7.17%) were similar to the deviations between the data and the ACM + EOS models using the new polymer EOS parameters (7.87%). The

latter, however, sometimes predicted a liquid-liquid phase split, while this behavior was never predicted by the ACMs alone under the conditions of this study. It was not known whether liquid phase splitting occurred because measurements of phase compositions in the HT-VLE facility were not taken.

For predicting VLE of polymer solutions during decomposition of rigid foams, it was recommended that the UNIFAC-ZM ACM be used alone if the phase splitting behavior is incorrect, and that the UNIFAC-FV + Peng-Robinson EOS model (with polymer EOS parameters from the new method) be used if there is liquid phase splitting under some conditions. Also, using combined ACM + EOS models may have additional advantages over using ACMs alone at the high pressures that may be encountered when actual foams are decomposing. In both cases, liquid volumes of the polymer should be estimated using GCMCM.

Finally, some sample predictions of the VLE behavior of a hypothetical ternary system of REF decomposition products were made using the UNIFAC-FV + PR EOS model. The mixture used in the calculations included the polymer-like products along with toluene and bisphenol-A. Reported results included equilibrium pressures calculated over a range of compositions and at two temperatures.

10.2 Recommendations for Future Work

During the course of this research it was discovered that further work would be necessary in a few areas to improve the recommendations given here. The following is a list of additional work outside the scope of this research and that should be done:

- Perform experiments to determine if liquid phase splitting occurs under the conditions of this study, perhaps by measuring phase compositions.
- Perform additional experiments and model calculations at higher pressures to see if there are more advantages to using a combined ACM + EOS model over the ACM alone at high pressure.
- Examine the use of other excess energy mixing rules, besides those of Wong and Sandler, to determine whether they would result in lower deviations from the HT-VLE facility data.

10.3 Summary of Research Accomplishments

This section summarizes the research accomplishments for this study. First, a high-temperature vapor-liquid equilibrium facility for measuring VLE behavior of polymer solutions was built and its use was validated. Important data were obtained for polymer systems that were not available in the literature and at higher temperatures than existing data. Next, a comprehensive comparison of two existing polymer volume estimation methods was performed, and a recommendation of the best method was made. Also, a new method for obtaining polymer EOS parameters was developed that led to better results than parameters obtained from the most recommended method in the literature. This work was the first to examine the combination of free-volume activity coefficient models with an equation of state through the Wong-Sandler mixing rules. Using the findings of this examination, a procedure for predicting VLE of high-temperature polymer solutions formed during the initial decomposition of REF and other

rigid foams was developed and a computer code was written. Finally, this work forms the basis for future studies with other materials.

11 References

Bawn, C., R. Freeman and A. Kamaliddin, "High polymer solutions Part 1. Vapour pressure of polystyrene solutions," *Transactions of the Faraday Society,* **46**, 677 (1950).

Bogdanic, G. and A. Fredenslund, "Revision of the group-contribution Flory equation of state for phase equilibria calculations in mixtures with polymers: 1. Prediction of vapor-liquid equilibria for polymer solutions," *Industrial & Engineering Chemistry Research,* **33**, 1331-1340 (1994).

Bondi, A., Physical Properties of Molecular Crystals, Liquids, and Glasses, New York, John Wiley & Sons (1968).

Brostow, W., V. M. Castano, G. Martinez-Barrera and D. Pietkiewicz, "Pressure-volume-temperature properties of an epoxy plus fluorinated poly(aryl ether ketone) system," *Physica B-Condensed Matter,* **344**(1-4), 206-213 (2004).

Chen, F., A. Fredenslund and P. Rasmussen, "Group-contribution Flory equation of state for vapor-liquid equilibria in mixtures with polymers," *Industrial & Engineering Chemistry Research,* **29**, 875-882 (1990).

Clayton, D., "Modeling flow effects during polymer decomposition using percolation lattice statistics," Ph.D. Dissertation, Department of Chemical Engineering, Brigham Young University (2002).

Coutinho, J. A. P., S. I. Andersen and E. H. Stenby, "Evaluation of activity coefficient models in prediction of alkane solid-liquid equilibria," *Fluid Phase Equilibria,* **103**, 23-39 (1995).

Coutsikos, P., N. S. Kalospiros and D. P. Tassios, "Capabilities and limitations of the Wong-Sandler mixing rules," *Fluid Phase Equilibria,* **108**, 59-78 (1995).

Dahl, S. and M. L. Michelsen, "High-pressure vapor-liquid equilibrium with a UNIFAC-based equation of state," *AIChE Journal,* **36**(12), 1829-1836 (1990).

Danner, R. P. and M. S. High, Handbook of Polymer Solution Thermodynamics, New York, American Institute of Chemical Engineers (1993).

Dlubek, G., J. Pointeck, M. Q. Shaikh, E. M. Hassan and R. Krause-Rehberg, "Free volume of an oligomeric epoxy resin and its relation to structural relaxation: Evidence from positron lifetime and pressure-volume-temperature experiments," *Physical Review E,* **75**(2), 021802 (2007).

Dudowicz, J., K. F. Freed and W. G. Madden, "Role of molecular structure on the thermodynamic properties of melts, blends, and concentrated polymer solutions. Comparison of Monte Carlo simulations with the cluster theory for the lattice model," *Macromolecules,* **23**, 4803-4819 (1990).

Elbro, H. S., A. Fredenslund and P. Rasmussen, "A new simple equation for the prediction of solvent activities in polymer solutions," *Macromolecules,* **23**, 4707-4714 (1990).

Elbro, H. S., A. Fredenslund and P. Rasmussen, "Group contribution method for the prediction of liquid densities as a function of temperature for solvents, oligomers, and polymers," *Industrial and Engineering Chemistry Research,* **30**, 2576-2582 (1991).

Erickson, K. L., S. M. Trujillo, K. R. Thompson, A. C. Sun, M. L. Hobbs and K. J. Dowding, "Liquefaction and flow behavior of a thermally decomposing removable epoxy foam," Computational Methods in Materials Characterisation, A. Mammoli and C. Brebbia, Santa Fe, NM, WIT Press, **6:** 217-242 (2003).

Fisher, M. E. and J. W. Essam, "Some cluster size and percolation problems," *Journal of Mathematical Physics,* **2**, 609-619 (1961).

Flory, P. J., Principles of Polymer Chemistry, Ithaca, NY, Cornell University Press (1953).

Flory, P. J., "Thermodynamics of polymer solutions," *Discussions of the Faraday Society,* **49**, 7-29 (1970).

Fredenslund, A., R. L. Jones and J. M. Prausnitz, "Group-contribution estimation of activity coefficients in nonideal liquid mixtures," *AIChE Journal,* **21**, 1086-1099 (1975).

Gmehling, J., U. Onken and U. Weidlich, Vapor-Liquid Equilibrium Data Collection - Organic Hydroxy Compounds: Alcohols and Phenols (Supplement 2), Frankfurt, DECHEMA (1982).

Grant, D. M., R. J. Pugmire, T. H. Fletcher and A. R. Kerstein, "Chemical model of coal devolatilization using percolation lattice statistics," *Energy and Fuels,* **3**, 175-186 (1989).

Guggenheim, E. A., Mixtures : the theory of the equilibrium properties of some simple classes of mixtures, solutions and alloys, Oxford, Clarendon Press (1952).

Haghtalab, A. and R. Espanani, "A new model and extension of Wong–Sandler mixing rule for prediction of (vapour + liquid) equilibrium of polymer solutions using EOS/G^E," *Journal of Chemical Thermodynamics,* **36**, 901-910 (2004).

Hansen, H. K., P. Rasmussen, A. Fredenslund, M. Schiller and J. Gmehling, "Vapor-liquid equilibria by UNIFAC group contribution. 5. Revision and extension," *Industrial & Engineering Chemistry Research,* **30**, 2352-2355 (1991).

Hansen, H. K., B. Coto and B. Kuhlmann, "UNIFAC with linearly-dependent group-interaction parameters.," Lyngby, Denmark, Research Engineering Center, Institut for Kemiteknik, The Technical University of Denmark (1992).

Hao, W., H. S. Elbro and P. Alessi, Polymer Solution Data Collection Part 1: Vapor-Liquid Equilibrium, Frankfurt, DECHEMA (1992).

Harismiadis, V. I., G. M. Kontogeorgis, A. Fredenslund and D. P. Tassios, "Application of the van der Waals equation of state to polymers II. Prediction," *Fluid Phase Equilibria,* **96**, 93-117 (1994).

Haynes, C. A., R. A. Beynon, R. S. King, H. W. Blanch and J. M. Prausnitz, "Thermodynamic properties of aqueous polymer solutions: poly(ethylene glycol)/dextran," *Journal of Physical Chemistry,* **93**, 5612-5617 (1989).

High, M. S. and R. P. Danner, "Application of the group contribution lattice-fluid equation of state to polymer solutions," *AIChE Journal,* **36**, 1625-1632 (1990).

Hobbs, M. L., K. L. Erickson and T. Y. Chu, "Modeling decomposition of unconfined rigid polyurethane foam," Albuquerque, NM, Sandia National Laboratories (1999).

Hobbs, M. L., K. L. Erickson, T. Y. Chu, T. T. Borek, K. R. Thompson, K. J. Dowding, D. Clayton and T. H. Fletcher, "CPUF - A chemical-structure-based polyurethane foam decomposition and foam response model," Albuquerque, NM, Sandia National Laboratories (2003).

Hobbs, M. L., "SREF - A simple removable epoxy foam decomposition chemistry model," Albuquerque, NM, Sandia National Laboratories (2003).

Huron, M. J. and J. Vidal, "New mixing rules in simple equations of state for representing vapor-liquid-equilibria of strongly non-ideal mixtures," *Fluid Phase Equilibria,* **3**(4), 255-271 (1979).

Ihmels, E. C. and J. Gmehling, "Extension and revision of the group contribution method GCVOL for the prediction of pure compound liquid densities," *Industrial & Engineering Chemistry Research,* **42**(2), 408-412 (2003).

Jin, G., J. M. Walsh and M. D. Donohue, "A group-contribution correlation for predicting thermodynamic properties with the Perturbed-Soft-Chain Theory," *Fluid Phase Equilibria,* **31**, 123-146 (1986).

Kalospiros, N. S. and D. Tassios, "Prediction of vapor-liquid equilibria in polymer solutions using an equation of state/excess Gibbs free energy model," *Industrial and Engineering Chemistry Research,* **34**, 2117-2124 (1995).

Kontogeorgis, G. M., A. Fredenslund and D. P. Tassios, "Simple activity coefficient model for the prediction of solvent activities in polymer solutions," *Industrial and Engineering Chemistry Research,* **32**, 362-372 (1993).

Kontogeorgis, G. M., V. I. Harismiadis, A. Fredenslund and D. P. Tassios, "Application of the van der Waals equation of state to polymers I. Correlation," *Fluid Phase Equilibria,* **96**, 65-92 (1994a).

Kontogeorgis, G. M., A. Fredenslund, I. G. Economou and D. P. Tassios, "Equations of state and activity coefficient models for vapor-liquid equilibria of polymer solutions," *AIChE Journal*, **40**, 1711-1727 (1994b).

Kontogeorgis, G. M. and P. M. Vlamos, "An interpretation of the behavior of EoS/G^E models for asymmetric systems," *Chemical Engineering Science,* **55**, 2351-2358 (2000).

Kouskoumvekaki, I. A., M. L. Michelsen and G. M. Kontogeorgis, "An improved entropic expression for polymer solutions," *Fluid Phase Equilibria,* **202**, 325-335 (2002).

Lieu, J. G. and J. M. Prausnitz, "Vapor-liquid equilibria for binary solutions of polyisobutylene in C_6 through C_9 n-alkanes," *Polymer,* **40**, 5865-5871 (1999).

Louli, V. and D. Tassios, "Vapor-liquid equilibrium in polymer-solvent systems with a cubic equation of state," *Fluid Phase Equilibria,* **168**, 165-182 (2000).

Maldonado-Santoyo, M., C. Ortiz-Estrada, G. Luna-Barcenas, I. C. Sanchez, L. C. Cesteros, I. Katime and S. M. Nuno-Donlucas, "Miscibility behavior and hydrogen bonding in blends of poly(vinyl phenyl ketone hydrogenated) and poly(2-ethyl-2-oxazoline)," *Journal of Polymer Science Part B-Polymer Physics,* **42**(4), 636-645 (2004).

McElhanon, J. R., E. M. Russick, D. R. Wheeler, D. A. Loy and J. H. Aubert, "Removable foams based upon an epoxy resin incorporating reversible Diels-Alder adducts," *Journal of Applied Polymer Science,* **88**, 1496-1502 (2002).

Michelsen, M. L., "A method for incorporating excess Gibbs energy models in equations of state," *Fluid Phase Equilibria,* **60**, 47-58 (1990a).

Michelsen, M. L., "A modified Huron-Vidal mixing rule for cubic equations of state," *Fluid Phase Equilibria,* **60**, 213-219 (1990b).

Morris, W. O., P. Vimalchand and M. D. Donohue, "Perturbed-soft-chain theory: An equation of state based on the Lennard-Jones potential," *Fluid Phase Equilibria,* **32**, 103-115 (1987).

Nesterova, T. N., A. G. Nazmutdinov, V. S. Tsvetkov, A. M. Rozhnov and I. Y. Roshchupkina, "Vapor-pressures and enthalpies of vaporization of alkylphenols," *Journal of Chemical Thermodynamics,* **22**(4), 365-377 (1990).

Oishi, T. and J. M. Prausnitz, "Estimation of solvent activities in polymer solutions using a group-contribution method," *Industrial & Engineering Chemistry, Process Design and Development,* **17**, 333-339 (1978).

Orbey, H., S. I. Sandler and D. S. H. Wong, "Accurate equation of state predictions at high temperatures and pressures using the existing UNIFAC model," *Fluid Phase Equilibria,* **85**, 41-54 (1993).

Orbey, H. and S. I. Sandler, "On the combination of equation of state and excess free energy models," *Fluid Phase Equilibria,* **111**, 53-70 (1995).

Orbey, H. and S. I. Sandler, "A comparison of Huron-Vidal type mixing rules of mixtures of compounds with large size differences, and a new mixing rule," *Fluid Phase Equilibria,* **132**, 1-14 (1997).

Orbey, H., C.-C. Chen and C. P. Bokis, "An extension of cubic equations of state to vapor-liquid equilibria in polymer-solvent mixtures," *Fluid Phase Equilibria,* **145**, 169-192 (1998a).

Orbey, H., C. P. Bokis and C.-C. Chen, "Polymer-solvent vapor-liquid equilibrium: Equations of state versus activity coefficient models," *Industrial and Engineering Chemistry Research,* **37**, 1567-1573 (1998b).

Orbey, H., C. Balci and G. A. Gürüz, "Phase equilibrium of asymmetric systems by predictive equations of state models," *Industrial and Engineering Chemistry Research,* **41**, 963-967 (2002).

Orbey, N. and S. I. Sandler, "Vapor-liquid equilibrium of polymer solutions using a cubic equation of state," *AIChE Journal,* **40**, 1203-1209 (1994).

Panayiotou, C. and J. H. Vera, "Statistical thermodynamics of r-mer fluids and their mixtures," *Polymer Journal,* **14**(681-694) (1982).

Pappa, G. D., E. C. Voutsas and D. P. Tassios, "Prediction of activity coefficients in polymer and copolymer solutions using simple activity coefficient models," *Industrial & Engineering Chemistry Research,* **38**, 4975-4984 (1999).

Parkinson, A., R. Balling, J. Free, T. Chambers, J. Talbert, D. Davidson, G. Gritton, L. Borup, B. Busaker and D. Warren, "OptdesX," Orem, UT, Design Synthesis Inc. (1994).

Peng, D. and D. B. Robinson, "New two-constant equation of state," *Industrial & Engineering Chemistry Fundamentals,* **15**(1), 59-64 (1976).

Prigogine, I., A. Bellemans and V. Mathot, The Molecular Theory of Solutions, Amsterdam, North-Holland (1957).

Radfarnia, H. R., C. Ghotbi, V. Taghikhani and G. M. Kontogeorgis, "A modified free-volume-based model for predicting vapor-liquid and solid-liquid equilibria for size asymmetric systems," *Fluid Phase Equilibria,* **234**, 94-100 (2005).

Radfarnia, H. R., G. M. Kontogeorgis, C. Ghotbi and V. Taghikhani, "Classical and recent free-volume models for polymer solutions: A comparative evaluation," *Fluid Phase Equilibria,* **257**, 63-69 (2007).

Rodgers, P. A., "Pressure-volume-temperature relationships for polymeric liquids: A review of equations of state and their characteristic parameters for 56 polymers," *Journal of Applied Polymer Science,* **48**, 1061-1080 (1993).

Rodriguez, F., C. Cohen, C. K. Ober and L. A. Archer, Principles of Polymer Systems, New York, Taylor & Francis (2003).

Rowley, R. L., W. V. Wilding, J. L. Oscarson, Y. Yang, T. E. Daubert and R. P. Danner, "DIPPR® Data Compilation of Pure Chemical Properties," Design Institute for Physical Properties, AIChE, New York, NY (2005).

Russick, E. M. and P. B. Rand, "Development and characterization of a new epoxy foam encapsulant as an Ablefoam replacement," Albuquerque, New Mexico, Sandia National Laboratories (1998).

Saeki, S., J. Holste and D. Bonner, "Sorption of organic vapors by polystyrene," *Journal of Polymer Science: Polymer Physics Edition,* **19**, 307-320 (1981).

Sako, T., A. H. Wu and J. M. Prausnitz, "Cubic equation of state for high-pressure phase equilibria of mixtures containing polymers and volatile fluids," *Journal of Applied Polymer Science,* **38**, 1839-1858 (1989).

Sandler, S. I., Chemical and Engineering Thermodynamics, New York, John Wiley & Sons, Inc. (1999).

Sato, Y., H. Hashiguchi, S. Takishima and H. Masuoka, "Prediction of PVT properties of polymer melts with a new group-contribution equation of state," *Fluid Phase Equilibria,* **144**, 427-440 (1998).

Sato, Y., K. Inohara, S. Takishima, H. Masuoka, M. Imaizumi, H. Yamamoto and M. Takasugi, "Pressure-volume-temperature behavior of polylactide, poly(butylene succinate), and poly(butylene succinate-co-adipate)," *Polymer Engineering and Science,* **40**(12), 2602-2609 (2000).

Stryjek, R. and J. H. Vera, "PRSV: An improved Peng-Robinson equation of state for pure compounds and mixtures," *Canadian Journal of Chemical Engineering,* **64**, 323-333 (1986).

Surana, R. K., R. P. Danner, A. B. d. Haan and N. Beckers, "New technique to measure high-pressure and high-temperature polymer-solvent vapor-liquid equilibrium," *Fluid Phase Equilibria,* **139**, 361-370 (1997).

Tanbonliong, J. O. and J. M. Prausnitz, "Vapour-liquid equilibria for some binary and ternary polymer solutions," *Polymer,* **38**, 5775-5783 (1997).

Van Krevelen, D. W. and P. J. Hoftyzer, Properties of Polymers. Correlation with Chemical Structure, Amsterdam, Elsevier Scientific (1972).

Wibawa, G., S. Takishima, Y. Sato and H. Masuoka, "Revision of UNIFAC group interaction parameters of group contribution models to improve prediction results of vapor-liquid equilibria for solvent-polymer systems," *Fluid Phase Equilibria,* **202**, 367-383 (2002).

Wibawa, G., S. Takishima, Y. Sato and H. Masuoka, "An improved prediction result of Entropic-FV model for vapor–liquid equilibria of solvent–polymer systems," *Journal of Applied Polymer Science,* **97**, 1145-1153 (2005).

Wohlfarth, C., Vapor-Liquid Equilibrium Data of Binary Polymer Solutions, Amsterdam, Elsevier (1994).

Wohlfarth, C., CRC Handbook of Thermodynamic Data of Copolymer Solutions, Boca Raton, CRC Press LLC (2001).

Wong, D. S. H. and S. I. Sandler, "A theoretically correct mixing rule for cubic equations of state," *AIChE Journal,* **38**, 671-680 (1992).

Wong, D. S. H., H. Orbey and S. I. Sandler, "Equation of state mixing rule for nonideal mixtures using available activity coefficient model parameters and that allows extrapolation over large ranges of temperature and pressure," *Industrial and Engineering Chemistry Research,* **31**, 2033-2039 (1992).

Zhong, C., Y. Sato, H. Masuoka and X. Chen, "Improvement of predictive accuracy of the UNIFAC model for vapor-liquid equilibria of polymer solutions," *Fluid Phase Equilibria,* **123**, 97-106 (1996).

Zoller, P. and D. J. Walsh, Standard Pressure-Volume-Temperature Data for Polymers, Lancaster, PA, Technomic Pub. Co. (1995).

Appendix A. Model Equations

A.1 Peng-Robinson Equation of State

The Peng-Robinson equation of state (Peng and Robinson, 1976) is a two-parameter cubic equation of state (EOS) that can be written as

$$P = \frac{RT}{V-b} - \frac{a}{V^2 + 2bV - b^2} \qquad \textbf{(A.1)}$$

where P is the pressure, T is the temperature, $\overline{V}$ is the molar volume, and R is the universal gas constant. The equation of state parameters, a and b, are the energy and volume parameters, respectively. For low molecular weight species (i.e. the solvents in a polymer solution), the energy and volume parameters are given by

$$b = 0.077796\frac{RT_c}{P_c} \qquad \textbf{(A.2)}$$

and

$$a = \left(0.457235\frac{R^2T_c^2}{P_c}\right)\alpha \qquad \textbf{(A.3)}$$

where T_c and P_c are the critical temperature and pressure, and α is a function of temperature and the acentric factor, ω:

$$\alpha = \left[1 + \kappa\left(1 - \sqrt{\frac{T}{T_c}}\right)\right]^2 \qquad \textbf{(A.4)}$$

where

$$\kappa = 0.37464 + 1.54226\omega - 0.26992\omega^2 \qquad \textbf{(A.5)}$$

For polymers the EOS parameters must be obtained in a different manner because the critical properties are not known. Several methods for obtaining values for polymer EOS parameters, including a new method, are explained in the body of this dissertation.

The Peng-Robinson equation of state treats mixtures by using energy and volume parameters that represent the properties of the mixtures. Mixing rules are needed to obtain values for these parameters, designated here as a_m and b_m, from the parameters for the pure species. The Wong-Sandler excess energy mixing rules were used in this work and are described below.

A.2 Wong-Sandler Mixing Rules

The Wong-Sandler mixing rules (Wong and Sandler, 1992) were developed by setting the excess Helmholtz energy, A^{ex}, at infinite pressure from an equation of state equal to the excess Gibbs energy, G^{ex}, from an activity coefficient model by making the following assumptions:

$$G^{ex}(P = low) \approx A^{ex}(P = low) \approx A^{ex}(P = \infty) \quad \textbf{(A.6)}$$

The resulting mixing rule equations are

$$b_m = \frac{Q}{1 - D} \quad \textbf{(A.7)}$$

$$a_m = RTQ\frac{D}{1 - D} = RTDb_m \quad \textbf{(A.8)}$$

$$D = \sum_i x_i \frac{a_i}{b_i RT} + \frac{G^{ex}}{cRT} \quad \textbf{(A.9)}$$

$$Q = \sum_i \sum_j x_i x_j \left(b - \frac{a}{RT} \right)_{ij} \quad \textbf{(A.10)}$$

$$\left(b - \frac{a}{RT} \right)_{ij} = \frac{1}{2}\left[\left(b_i - \frac{a_i}{RT} \right) + \left(b_j - \frac{a_j}{RT} \right) \right] \left(1 - k_{ij} \right) \quad \textbf{(A.11)}$$

where x_i is the mole fraction, and a_i and b_i refer to the EOS parameters for each species in the mixture. The constant, *c*, is EOS-dependent, and for the Peng-Robinson EOS is

$$c = \frac{\ln\left(\sqrt{2} - 1\right)}{\sqrt{2}} \quad \textbf{(A.12)}$$

The binary interaction parameter, k_{ij}, is included in Equation A.11. In this work, the value of k_{ij} was determined by fitting the excess Gibbs energy as calculated from the equation of state to the excess Gibbs energy from the activity coefficient model over the entire range of composition, following the suggestion of Wong et al. (1992).

Using these mixing rules, any activity coefficient model can be incorporated into the equation of state by calculating the excess Gibbs energy in Equation A.9 from

$$\frac{G^{ex}}{RT} = \sum_i x_i \ln \gamma_i \qquad \textbf{(A.13)}$$

where γ_i is the activity coefficient for each species.

A.3 Fugacity Coefficient Equations

The fugacity coefficient of a pure species, ϕ_i, is given by

$$\ln \phi_i = \frac{P\overline{V}}{RT} - 1 - \ln \frac{P\overline{V}}{RT} - \frac{1}{RT}\int_{\infty}^{\overline{V}} \left(P - \frac{RT}{\overline{V}} \right) d\overline{V} \qquad \textbf{(A.14)}$$

where P is determined from an equation of state. For the Peng-Robinson equation of state, Equation A.14 becomes

$$\ln \phi_i = \frac{P\overline{V}}{RT} - 1 - \ln\left(\frac{P\left(\overline{V} - b\right)}{RT} \right) + \frac{a}{2\sqrt{2}bRT} \ln\left(\frac{\overline{V} + \left(1 - \sqrt{2}\right)b}{\overline{V} + \left(1 + \sqrt{2}\right)b} \right) \qquad \textbf{(A.15)}$$

To calculate the liquid fugacity coefficient, ϕ_i^L, the liquid molar volume, $\overline{V}_L$, is used in Equation A.15. The vapor fugacity coefficient, ϕ_i^V, is obtained by using the vapor molar volume, $\overline{V}_V$.

The partial fugacity coefficient of a species in a mixture, $\hat{\phi}_i$, is given by

$$\ln \hat{\phi}_i = -\ln \frac{P\overline{V}}{RT} - \frac{1}{RT}\int_{\infty}^{\overline{V}} \left(N \frac{\partial P}{\partial N_i} - \frac{RT}{\overline{V}} \right) d\overline{V} \qquad \textbf{(A.16)}$$

where N is the total number of moles in the mixture, and N_i is the number of moles of species i. For the Peng-Robinson EOS Equation A.16 becomes

$$\begin{aligned} \ln \hat{\phi}_i = {} & \frac{1}{b_m}\left(\frac{\partial (N b_m)}{\partial N_i} \right)\left(\frac{P\overline{V}}{RT} - 1 \right) - \ln\left(\frac{P(\overline{V} - b_m)}{RT} \right) \\ & + \frac{a_m}{2\sqrt{2} b_m RT}\left[\frac{1}{a_m}\left(\frac{\partial (N^2 a_m)}{N \partial N_i} \right) - \frac{1}{b_m}\left(\frac{\partial (N b_m)}{\partial N_i} \right) \right] \ln\left(\frac{\overline{V} + (1-\sqrt{2}) b_m}{\overline{V} + (1+\sqrt{2}) b_m} \right) \end{aligned} \qquad \textbf{(A.17)}$$

Similar to the pure species fugacity coefficient, the partial fugacity coefficient of a species in the liquid or vapor phase is obtained by using the molar volume and composition of the liquid or vapor phase, respectively.

Because Equation A.17 involves partial derivatives of a_m and b_m, the EOS parameters for the mixture, the partial fugacity coefficient is also dependent on the choice of mixing rules. For the Wong-Sandler mixing rules the partial derivatives are evaluated from the following equations:

$$\frac{\partial(Nb_m)}{\partial N_i} = \frac{1}{1-D}\left(\frac{\partial(N^2 Q)}{N\partial N_i}\right) - \frac{Q}{(1-D)^2}\left(1 - \frac{\partial(ND)}{\partial N_i}\right) \quad \textbf{(A.18)}$$

$$\frac{\partial(N^2 a_m)}{N\partial N_i} = RT\left[D\frac{\partial(Nb_m)}{\partial N_i} + b_m\frac{\partial(ND)}{\partial N_i}\right] \quad \textbf{(A.19)}$$

$$\frac{\partial(ND)}{\partial N_i} = \frac{a_i}{b_i RT} + \frac{\ln\gamma_i}{c} \quad \textbf{(A.20)}$$

$$\frac{\partial(N^2 Q)}{N\partial N_i} = 2\sum_j x_j\left(b - \frac{a}{RT}\right)_{ij} \quad \textbf{(A.21)}$$

A.4 Activity Coefficient Models

Activity coefficient models (ACM) often divide the activity coefficient into separate terms resulting from different types of contributions to non-ideality. Generally, they can be written as follows:

$$\ln\gamma = \ln\gamma^{comb} + \ln\gamma^{res} \quad \textbf{(A.22)}$$

where γ^{comb} and γ^{res} are the combinatorial and residual terms, respectively. All of the ACMs used in this work have a combinatorial term that is based on the combinatorial term of the Flory-Huggins (FH) model. The combinatorial term is either modified to

include free-volume effects, or a separate free-volume term is added. All of the ACMs employ the residual term of the original UNIFAC model.

A.4.1 Flory-Huggins

The classical Flory-Huggins model (Flory, 1953) included only a combinatorial term, written as

$$\ln \gamma_i^{comb} = \ln\left(\frac{\phi_i^{vol}}{x_i}\right) + 1 - \frac{\phi_i^{vol}}{x_i} \qquad \textbf{(A.23)}$$

where ϕ_i^{vol} is the volume fraction of each species.

It was later discovered that the combinatorial term was not sufficient, so a van Laar heat of mixing term was added to account for residual effects. For the solvent in a binary solvent(1)-polymer(2) solution this term is

$$\ln \gamma_1^{res} = \chi\left(\phi_2^{vol}\right)^2 \qquad \textbf{(A.24)}$$

The FH energy parameter, χ, is an empirical constant that was found to be nonzero even for nearly athermal solutions (because of free-volume effects that are not accounted for), and to be temperature and composition dependent.

A.4.2 UNIFAC

The UNIQUAC Functional Activity Coefficients (UNIFAC) model was developed by Fredenslund et al. (1975). It is a group-contribution model that requires only a knowledge of the structure of the species in a mixture in order to calculate the activity coefficients. The combinatorial term is similar to that of the FH model, but with a Staverman-Guggenheim shape correction term added:

$$\ln \gamma_i^{comb} = \ln\left(\frac{\phi_i^{vol}}{x_i}\right) + 1 - \frac{\phi_i^{vol}}{x_i} - \frac{z}{2} q_i \left(\ln \frac{\phi_i^{vol}}{\theta_i} + 1 - \frac{\phi_i^{vol}}{\theta_i}\right) \quad \textbf{(A.25)}$$

The volume and surface area fraction of each species, ϕ_i^{vol} and θ_i, as well as the normalized volume and surface area of each species, r_i and q_i, are defined as

$$\phi_i^{vol} = \frac{x_i r_i}{\sum_j x_j r_j} \quad \textbf{(A.26)}$$

$$\theta_i = \frac{x_i q_i}{\sum_j x_j q_j} \quad \textbf{(A.27)}$$

$$r_i = \sum_k \nu_k^{(i)} R_k \quad \textbf{(A.28)}$$

$$q_i = \sum_k \nu_k^{(i)} Q_k \quad \textbf{(A.29)}$$

The UNIFAC group volume and surface area parameters, R_k and Q_k, are given in Appendix E, and $\nu_k^{(i)}$ is the number of groups of type *k* in a molecule of species *i* (for a polymer, this is the total number of each group in the molecule, not the number in the repeat unit). The coordination number in Equation A.25, *z*, is set to 10.

The UNIFAC residual term is given by

$$\ln \gamma_i^{res} = \sum_k \nu_k^{(i)} \left[\ln \Gamma_k - \ln \Gamma_k^{(i)} \right] \qquad \textbf{(A.30)}$$

where Γ_k is the residual activity coefficient of group *k* in the solution, given by

$$\ln \Gamma_k = Q_k \left[1 - \ln\left(\sum_m \Theta_m \Psi_{mk} \right) - \sum_m \frac{\Theta_m \Psi_{km}}{\sum_n \Theta_m \Psi_{nm}} \right] \qquad \textbf{(A.31)}$$

The residual activity coefficient of group *k* in a hypothetical reference solution consisting only of species *i*, $\Gamma_k^{(i)}$, is calculated for each species using Equation A.31 with the summations only being performed for the groups in that species. The surface area fraction of each group, Θ_m, is

$$\Theta_m = \frac{Q_m X_m}{\sum_n Q_n X_n} \qquad \textbf{(A.32)}$$

where X_m is the mole fraction of group *m* in the solution. The interaction of group *m* with group *k* is given by

$$\Psi_{mk} = \exp\left(-a_{mk}/T\right) \tag{A.33}$$

where a_{mn} are the UNIFAC group interaction parameters given in Appendix E.

A.4.3 Entropic-FV Activity Coefficient Model

The Entropic-FV model was proposed by Elbro et al. (1990). It is similar to the UNIFAC model, but takes into account the differences in free-volume between polymers and smaller molecules. The combinatorial term of Equation A.25 is replaced by a combined combinatorial and free-volume term given by

$$\ln \gamma_i^{comb+fv} = \ln\left(\frac{\phi_i^{fv}}{x_i}\right) + 1 - \frac{\phi_i^{fv}}{x_i} \tag{A.34}$$

where ϕ_i^{fv} is the free-volume fraction and v_i^{fv} is the free-volume of component *i*:

$$\phi_i^{fv} = \frac{x_i v_i^{fv}}{\sum_j x_j v_j^{fv}} \tag{A.35}$$

$$v_i^{fv} = v_i - v_i^{hc} \tag{A.36}$$

where v_i and v_i^{hc} are the molar and hard-core volumes of component *i* respectively. The hard-core volume is assumed to be the same as the van der Waals volume which can be calculated from values provided by Bondi (1968). The UNIFAC group volume parameters, R_k, are normalized versions of these hard-core volumes. Thus, the hard-core volume for species *i* can be obtained by multiplying the UNIFAC species volume parameter, r_i, by 15.17 cm^3/mol.

A.4.4 Freed-FV Activity Coefficient Model

The Freed-FV model, developed by Radfarnia et al. (2005) is obtained by adding the following non-randomness factor to the combinatorial/free-volume term of the Entropic-FV model of Equation A.34:

$$r_i\left[\sum_j \beta_{ji}\phi_j^{fv}\left(1-\phi_j^{fv}\right)-0.5\sum_{j\neq i}\sum_{k\neq i}\beta_{jk}\phi_j^{fv}\phi_k^{fv}\right] \qquad \textbf{(A.37)}$$

with

$$\beta_{ji}=\alpha\left(\frac{1}{r_j}-\frac{1}{r_i}\right) \qquad \textbf{(A.38)}$$

where r_i in these equations is the ratio of the free-volume of species *i* to the free-volume of the smallest solvent, and α, the non-randomness parameter, is set to 0.2.

A.4.5 GK-FV Activity Coefficient Model

The GK-FV model of Kontogeorgis et al. (1993) is a modification of the Entropic-FV model. The Staverman-Guggenheim shape correction term used in the original UNIFAC model is kept in the combinatorial/free-volume term. Thus, Equation A.34 of the Entropic-FV model becomes

$$\ln \gamma_i^{comb+fv} = \ln\left(\frac{\phi_i^{fv}}{x_i}\right) + 1 - \frac{\phi_i^{fv}}{x_i} - \frac{z}{2} q_i \left(\ln \frac{\phi_i^{vol}}{\theta_i} + 1 - \frac{\phi_i^{vol}}{\theta_i} \right) \qquad \textbf{(A.39)}$$

where free-volume fractions replace the volume fractions of the UNIFAC model in the Flory-Huggins portion of the combinatorial term, but volume fractions remain in the Staverman-Guggenheim shape correction.

A.4.6 MEFV Activity Coefficient Model

The MEFV model of Kouskoumvekaki et al. (2002) is another modification of the Entropic-FV model. In this case, only the definition of the hard-core volume (used in Equation A.36 to calculate the free-volume) is changed. While in the Entropic-FV model v_i^{hc} is assumed to be equal to the van der Waals volume, in the MEFV model v_i^{hc} is assumed to be equal to 1.2 times the van der Waals volume.

A.4.7 UNIFAC-FV Activity Coefficient Model

The UNIFAC-FV model was proposed by Oishi and Prausnitz (1978). They added a separate free-volume term to the combinatorial and residual terms of the original UNIFAC model. The free-volume term is given by

$$\ln \gamma_i^{fv} = 3c_i \ln\left[\frac{\breve{v}_i^{1/3}-1}{\breve{v}_M^{1/3}-1}\right] - c_i\left[\left(\frac{\breve{v}_i}{\breve{v}_M}-1\right)\left(\frac{1}{1-\frac{1}{\breve{v}_i^{1/3}}}\right)\right] \qquad \textbf{(A.40)}$$

where c_i is a parameter representing one-third of the degrees of freedom and is set to 1.1 for solvents. However, larger values may be needed for solvents that are significantly heavier than benzene, toluene, and hexane. The reduced volume of each species, $\breve{v}_i$, is given by

$$\breve{v}_i = \frac{v_i}{br_i\left(15.17\,cm^3/mol\right)} \qquad \textbf{(A.41)}$$

and is the ratio of the molar volume, v_i, to a definition of the hard-core volume. Oishi and Prausnitz effectively defined the hard-core volume as the van der Waals volume (the species volume parameter, r_i, times 15.17 cm^3/mol) multiplied by *b*, a proportionality constant set to 1.28, which is similar to the value used in the MEFV model.

The reduced volume of the mixture, $\breve{v}_M$, is given by

$$\breve{v}_M = \frac{\sum_j v_j}{b\left(\sum_j r_j x_j\right)\left(15.17\,cm^3/mol\right)} \qquad \textbf{(A.42)}$$

A.4.8 UNIFAC-ZM Activity Coefficient Model

The UNIFAC-ZM model of Zhong et al. (1996) is the only model examined in this study that does not require species liquid volumes. Instead, the volume fractions in the FH portion of the original UNIFAC combinatorial term (but not in the Staverman-Guggenheim portion) are modified so that the volume of a polymer of n repeat units is taken to be $0.6583n$ times the volume of the monomer.

A.5 Volume Estimation Methods

Equations for the GCVOL and GCMCM volume estimation methods are given here.

A.5.1 GCVOL Volume Estimation Method

In the GCVOL volume estimation method of Elbro et al. (1991), the specific volume, $\widetilde{V}$, is given by

$$\widetilde{V} = \frac{\sum_k n_k \left(A_k + B_k T + C_k T^2 \right)}{M_r} \qquad \textbf{(A.43)}$$

where n_k is the number of groups of type k in the polymer repeat unit, and M_r is the molecular weight of the repeat unit. The group parameters A_k, B_k, and C_k are given in Appendix E.

A.5.2 GCMCM Volume Estimation Method

The GCMCM volume estimation method of Sato et al. (1998) is in the form of an equation of state:

$$\frac{\frac{P}{P^*}\frac{\widetilde{V}}{V^*}}{\frac{T}{T^*}} = \frac{\left(\frac{\widetilde{V}}{V^*}\right)^{1/3}}{\left(\frac{\widetilde{V}}{V^*}\right)^{1/3} - 0.8909r} - \frac{2T^*}{T}\left(\frac{1.2045}{\left(\frac{\widetilde{V}}{V^*}\right)^2} - \frac{1.011}{\left(\frac{\widetilde{V}}{V^*}\right)^4}\right) \qquad \textbf{(A.44)}$$

where here r is a correction factor for free-volume whose value is 1.07. The characteristic (starred) variables are

$$P^* = \frac{RT^*}{3M_0V^*} \qquad \textbf{(A.45)}$$

$$V^* = \frac{\sum_k n_k R_k}{M_r} \qquad \textbf{(A.46)}$$

$$T^* = \frac{3(z-2)\varepsilon^*}{R} \qquad \textbf{(A.47)}$$

$$\varepsilon^* = \sum_k \sum_l \theta_k \theta_l \sqrt{e_k e_l} \qquad \textbf{(A.48)}$$

where R, again, is the universal gas constant, the coordination number, z, is set to 12, and

$$M_0 = \frac{M_r}{\sum_k n_k a_k} \tag{A.49}$$

$$\theta_k = \frac{n_k Q_k}{\sum_l n_l Q_l} \tag{A.50}$$

The group parameters R_k, e_k, Q_k, and a_k are given in Appendix E. Then, given temperature, pressure, and the structure of the polymer repeat unit, Equation A.44 can be solved iteratively for the specific volume.

Appendix B. Use of Number-average Molecular Weight

Polymers are not monodisperse components, meaning they do not have a single molecular weight, but rather a distribution of molecular weights. Thus, some form of average molecular weight is needed to describe a polymer. Two commonly used averages are the number-average molecular weight, MW_n, and the weight-average molecular weight, MW_w. If a polymer sample is imagined as a collection of monodisperse components of the same type but of different molecular weights, then the number- and weight-average molecular weights of the sample can be defined as

$$MW_n = \frac{\sum N_i MW_i}{\sum N_i} \qquad \textbf{(B.1)}$$

and

$$MW_w = \frac{\sum N_i MW_i^2}{\sum N_i MW_i} = \frac{\sum W_i MW_i}{\sum W_i} \qquad \textbf{(B.2)}$$

where N_i is the number of molecules of each component i, MW_i is the molecular weight of that component, and W_i is the total mass of that component in the sample. Because of these definitions MW_n is more sensitive to the concentration of low

molecular weight components, whereas MW_w is more sensitive to the concentration of high molecular weight components.

Sometimes confusion exists as to which average molecular weight should be used to describe the polymer. For correlating polymer properties that are affected more by larger molecules, such as viscosity and toughness, MW_w is more useful than MW_n (Rodriguez et al., 2003). In predicting phase equilibria, the need for polymer molecular weights is often eliminated by using equations based on mass fractions. However, if a polymer molecular weight is needed to convert between mass fractions and mole fractions, the correct average molecular weight is MW_n. This can be easily shown. The mass of any species, s, can be converted to the number of moles (this is equivalent to converting mass fractions to mole fractions) through

$$N_s = \frac{W_s}{MW_s} \qquad \textbf{(B.3)}$$

For a polymer sample, again imagined to be a collection of i components of different molecular weights, the total number of moles and the total mass are

$$N_s = \sum N_i \qquad \textbf{(B.4)}$$

$$W_s = \sum W_i = \sum N_i MW_i \qquad \textbf{(B.5)}$$

Solving for MW_s in equation B.3 and inserting equations B.4 and B.5 gives

$$MW_s = \frac{\sum N_i MW_i}{\sum N_i} \qquad \textbf{(B.6)}$$

which is the definition of the number-average molecular weight. This demonstration that MW_n is the correct average may seem obvious, but the wrong average molecular weight is sometimes used in the literature (see, for example, Orbey et al., 1998a).

Appendix C. HT-VLE Facility Information and Data

The calibrations and correlations used to correct the measurements from the high-temperature vapor-liquid equilibrium facility are presented in this appendix. The data for all of the polymer solution runs are also shown.

C.1 Correlations and Calibrations

This section contains the correlation between the gage block temperature and vessel temperature, as well as the coefficients for the pressure transducer calibrations.

C.1.1 Furnace Temperature Correlation

The correlation between the temperature measured by the thermocouple in the gage block and the temperature measured by the thermocouple on the wall of the pressure vessel is

$$T_{vessel} = 0.000129\left(T_{gage}\right)^2 + 0.93067\left(T_{gage}\right) + 0.9916 \qquad \textbf{(C.1)}$$

where T_{gage} and T_{vessel} are the gage block and pressure vessel temperatures, respectively, in ºC. Using this quadratic correlation results in calculated vessel temperatures that are

within 0.2ºC of the temperatures measured by the thermocouple on the pressure vessel wall. The correlation is valid for a furnace cool-down rate of 2ºC.

C.1.2 Pressure Transducer Calibrations

Two sets of calibration tests were conducted for the 0-300 psia pressure transducer (alpha code Z66-96) – one in October 2005 and one in March 2007. The 0-50 psia transducer (alpha code B77-61) was calibrated in March 2008. The pressure transducers were calibrated to a Paroscientific Model 740 Digiquartz digital pressure transducer (see section 4.3.2 for calibration details). The calibration equation used is

$$P_{correct} = c_0 + c_T T + c_P P_{Kulite} \qquad \textbf{(C.2)}$$

where $P_{correct}$ is the corrected pressure in psia; P_{Kulite} is the pressure measured by the Kulite pressure transducer in psia; T is the temperature in ºC (gage block temperature for both of the Z66-96 calibrations, and vessel wall temperature for the B77-61 calibration); and c_0, c_T, and c_P for each calibration are given in Table C.1.

Table C.1 Calibration constants for pressure transducers.

Calibration	c_0	c_T	c_P
2005	9.3839	-0.0074959	0.98856
2007	5.5493	0.0061435	0.98984
2008	-4.2296	-0.0099907	0.96416

C.2 Experimental Data

Plots of all of the polymer solution data collected in the high-temperature vapor-liquid equilibrium facility are shown below in chronological order. Temperature and pressure data were collected every second, but the amount of data was later reduced by taking 21-second time-centered averages at one-minute intervals. Vessel temperatures are reported here either as values calculated from the gage block temperature using the correlation given in section C.1.1 (for the PEG/benzene and PEG/furan systems), or as values measured directly by a thermocouple placed on the pressure vessel wall (for the PS/benzene, PS/furan, PS/IPP, and PEG/IPP systems). Pressures are reported as corrected values using one of the calibrations given in section C.1.2 and a zero-shift if necessary. For each run, the date on which the run started, as well as information about the calibration and zero-shift used, is given in the caption.

C.2.1 PEG/Benzene

The data collected for the PEG/benzene system are shown in the following figures. The first nine PEG/benzene runs occurred before the leak in the cold trap was discovered, so the true compositions are not known. Only data for runs 10 through 15 are valid and are shown here.

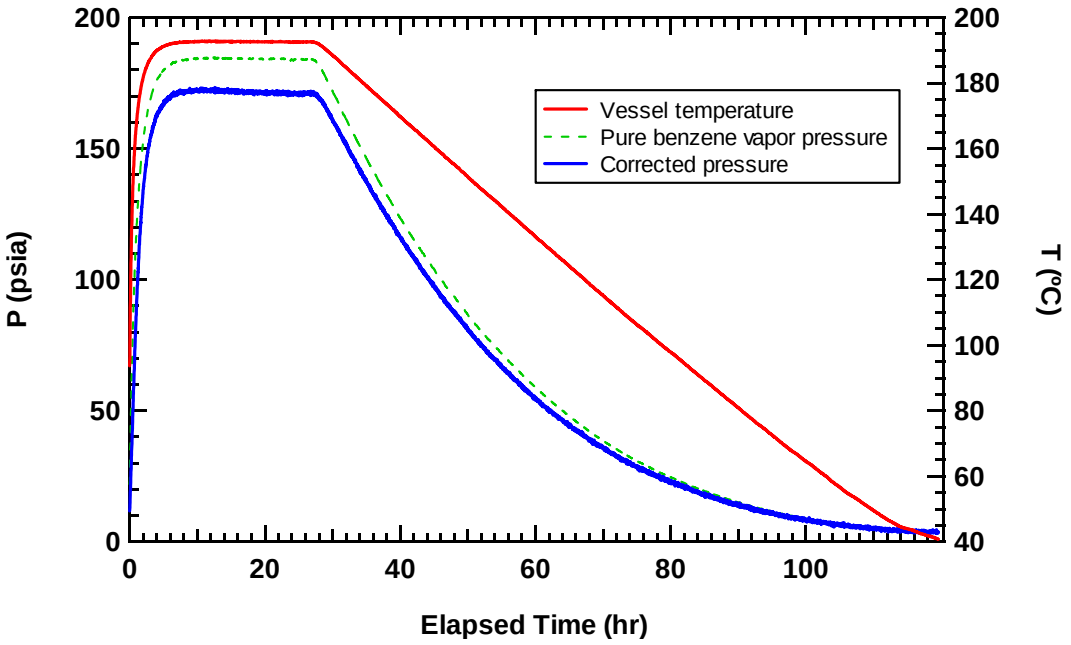

Figure C.1 PEG/benzene run 10 (started on 7/7/06). The overall composition was 59.6 wt% benzene. The Z66-96 pressure transducer was used with the 2005 calibration. A zero-shift of -3.5 psi was applied.

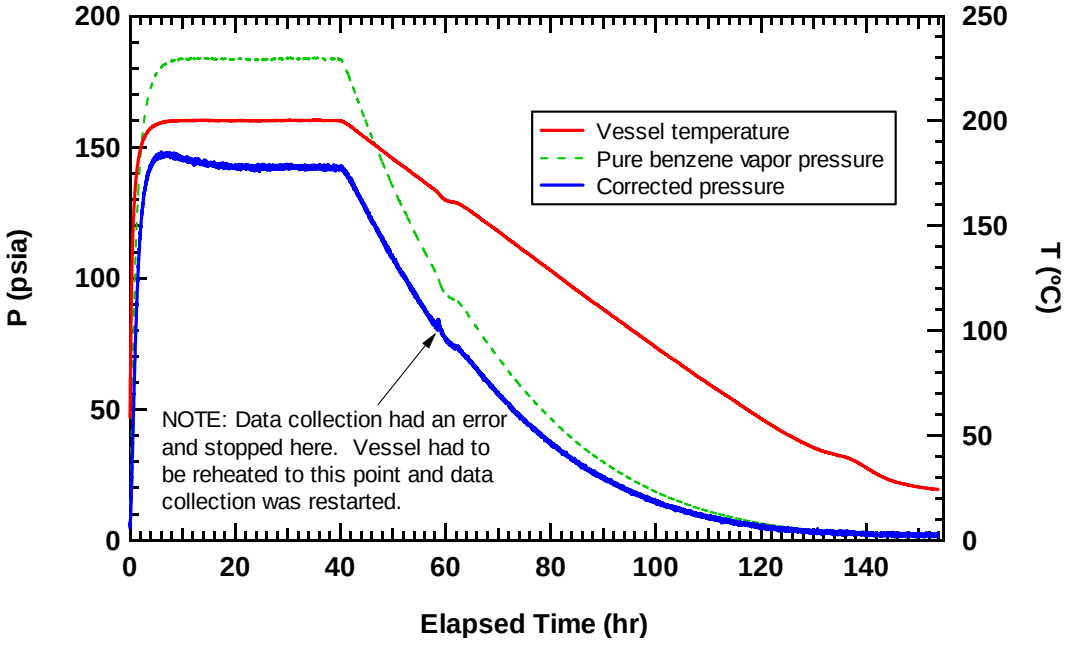

Figure C.2 PEG/benzene run 11 (started on 7/12/06). The overall composition was 40.1 wt% benzene. The Z66-96 pressure transducer was used with the 2005 calibration. A zero-shift of -3.5 psi was applied.

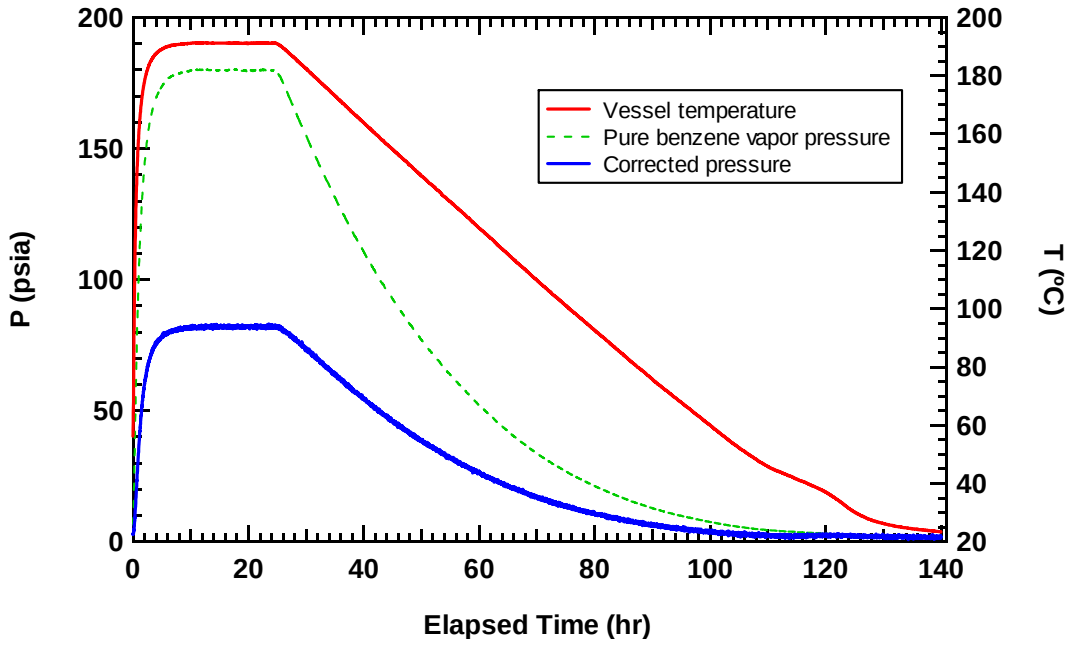

Figure C.3 PEG/benzene run 12 (started on 7/31/06). The overall composition was 19.2 wt% benzene. The Z66-96 pressure transducer was used with the 2005 calibration. A zero-shift of -3.5 psi was applied.

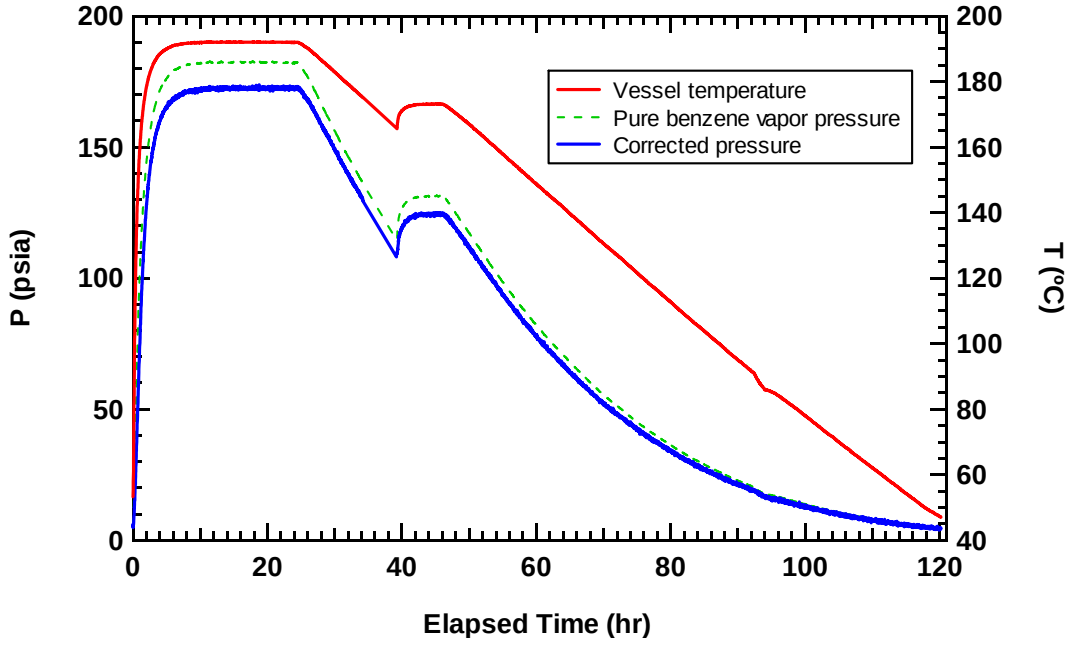

Figure C.4 PEG/benzene run 13 (started on 8/7/06). The overall composition was 73.8 wt% benzene. The Z66-96 pressure transducer was used with the 2005 calibration. A zero-shift of -3.5 psi was applied.

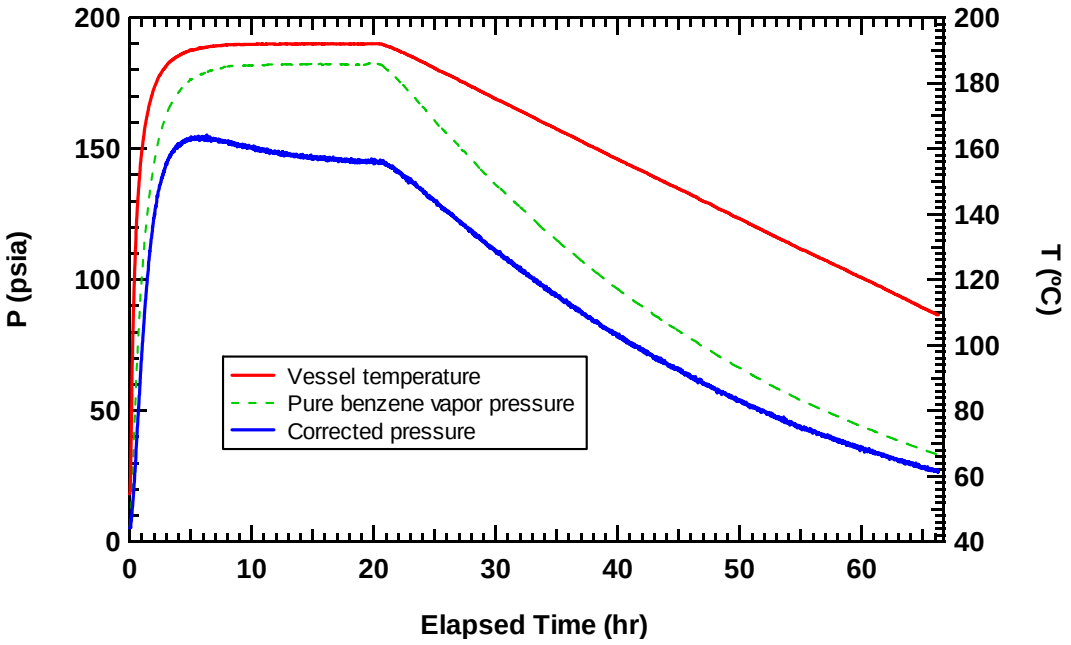

Figure C.5 PEG/benzene run 14 (started on 8/12/06). The overall composition was 41.7 wt% benzene. The Z66-96 pressure transducer was used with the 2005 calibration. A zero-shift of -3.5 psi was applied.

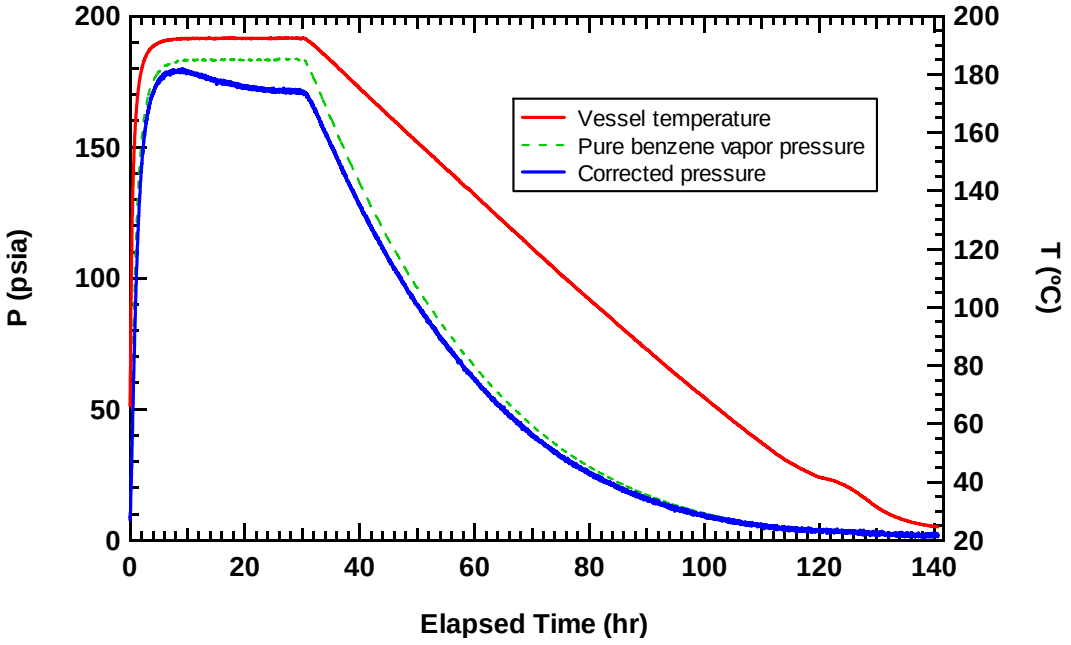

Figure C.6 PEG/benzene run 15 (started on 8/15/06). The overall composition was 59.3 wt% benzene. The Z66-96 pressure transducer was used with the 2005 calibration. A zero-shift of -3.5 psi was applied.

A summary of the points taken from each PEG/benzene run for comparison with model predictions is given in Table C.2. Each point is a 31-minute average centered around the time at which the indicated vessel temperature was reached. Because of the slow cool-down rate, the pressure vs. temperature curve is very linear over a half-hour period, so an arithmetic average is appropriate.

Table C.2 Summary of PEG/benzene at selected temperatures. Solvent weight percents at each temperature represent the calculated liquid composition (see section 5.4.2).

Run	Overall wt% solv	190ºC		150ºC		75ºC	
		wt% solv	P (psi)	wt% solv	P (psi)	wt% solv	P (psi)
12	19.2	16.8	81.2	17.9	42.0	18.9	6.3
11	40.1	37.2	137.9	38.6	67.8	39.8	10.0
14	41.7	39.0	141.3	40.3	68.7	-	-
15	59.3	57.3	165.2	58.3	78.3	59.1	11.4
10	59.6	57.6	165.0	58.6	78.7	59.4	11.7
13	73.8	69.3	167.6	71.8	80.0	73.4	11.7
Benzene	100.0	100.0	174.2	100.0	82.0	100.0	12.0

C.2.2 PEG/Furan

The data collected for the PEG/furan system are shown in the following figures. The last two PEG/furan runs (runs 6 and 7) were the first experimental runs conducted with the step cool-down method instead of the 2ºC/min. cool-down method.

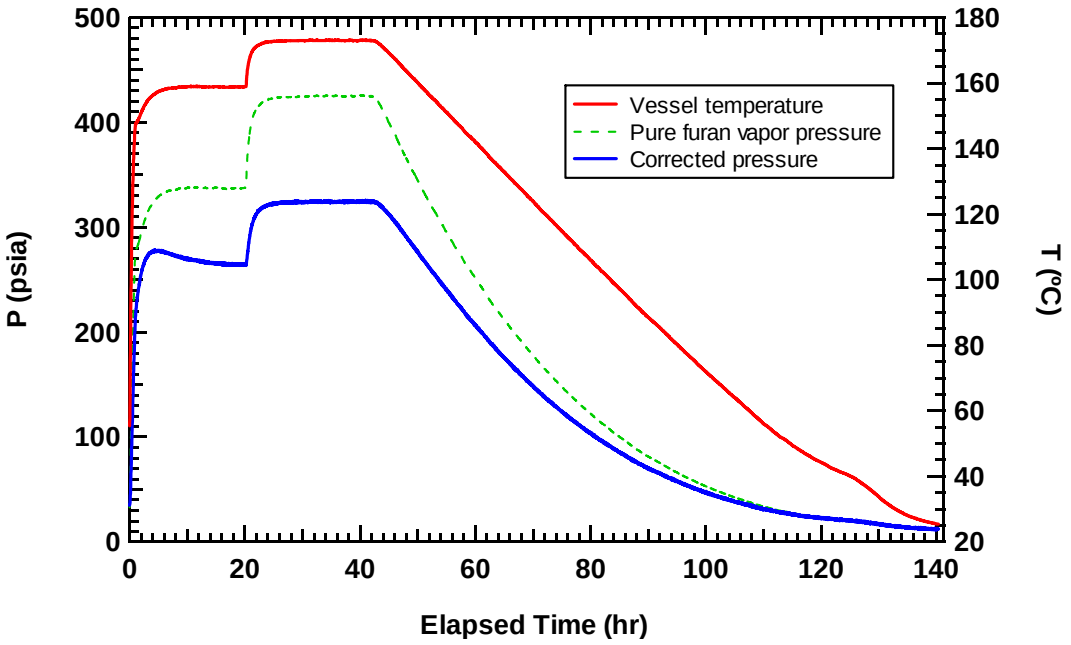

Figure C.7 PEG/furan run 1 (started on 10/31/06). The overall composition was 45.2 wt% furan. The Z66-96 pressure transducer was used with the 2005 calibration. A zero-shift of +0.2 psi was applied.

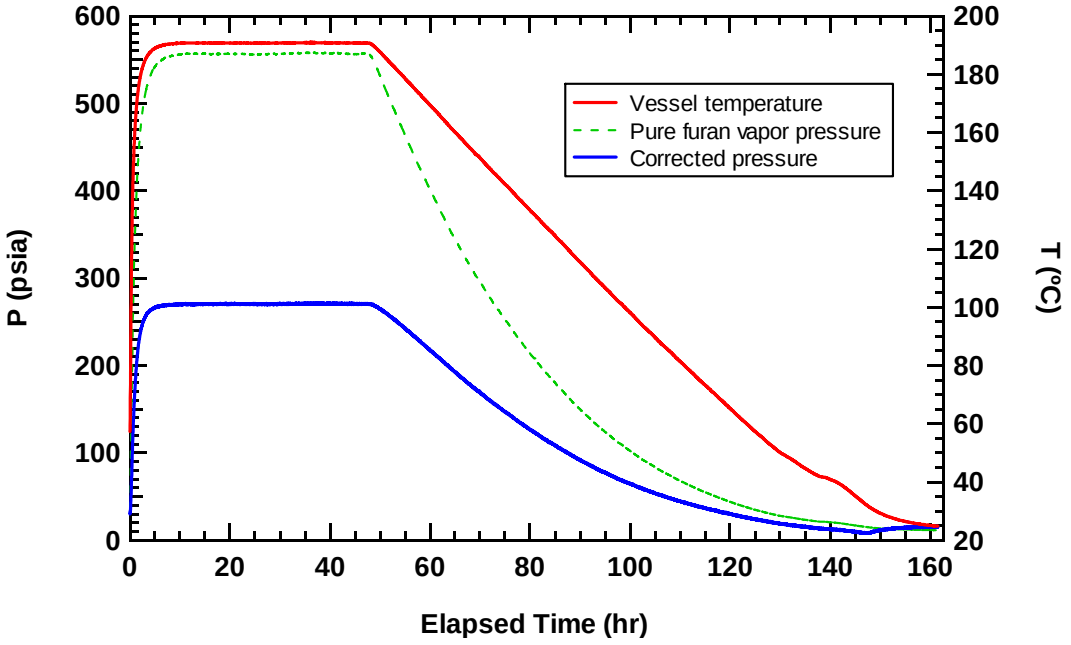

Figure C.8 PEG/furan run 2 (started on 11/7/06). The overall composition was 28.4 wt% furan. The Z66-96 pressure transducer was used with the 2005 calibration. A zero-shift of +0.2 psi was applied.

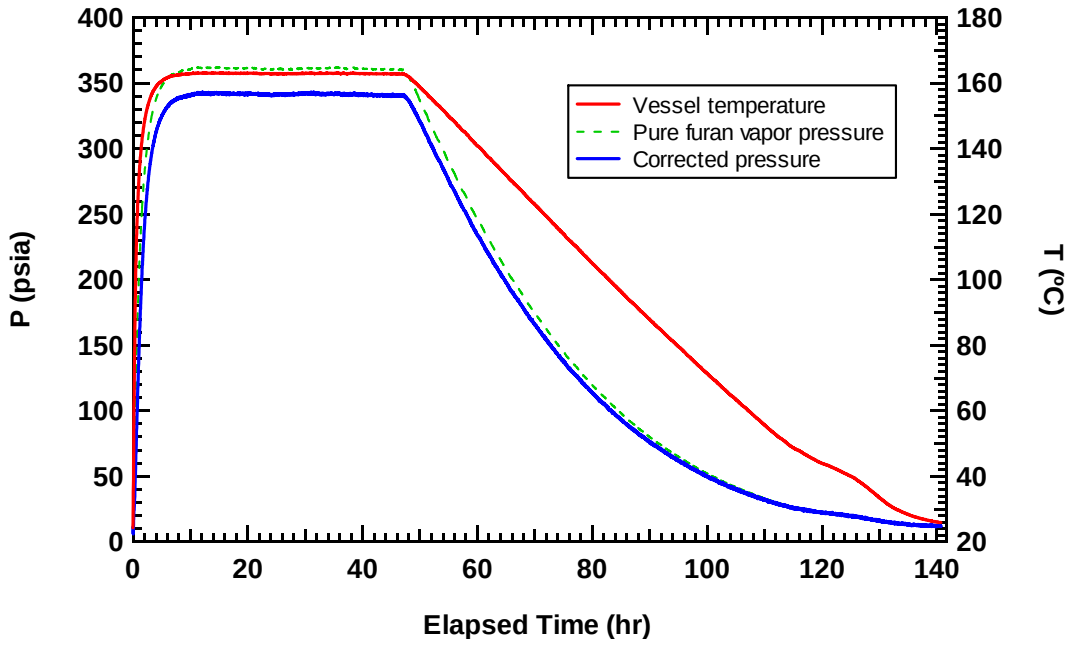

Figure C.9 PEG/furan run 3 (started on 11/22/06). The overall composition was 72.4 wt% furan. The Z66-96 pressure transducer was used with the 2005 calibration. A zero-shift of -3.8 psi was applied.

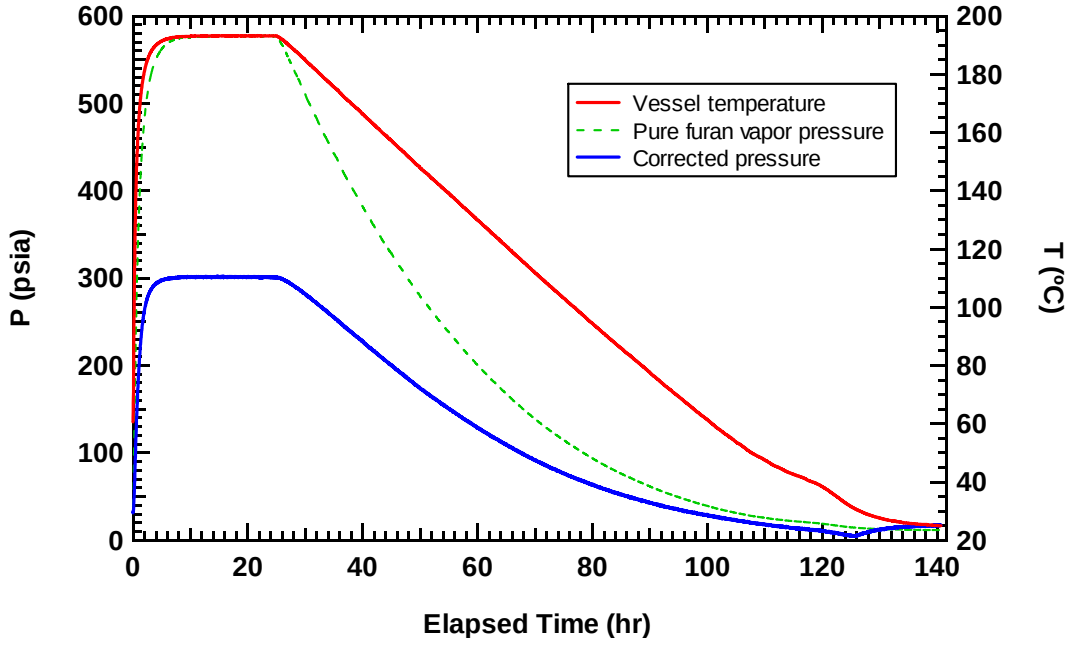

Figure C.10 PEG/furan run 4 (started on 11/27/06). The overall composition was 30.2 wt% furan. The Z66-96 pressure transducer was used with the 2005 calibration. No zero-shift was applied.

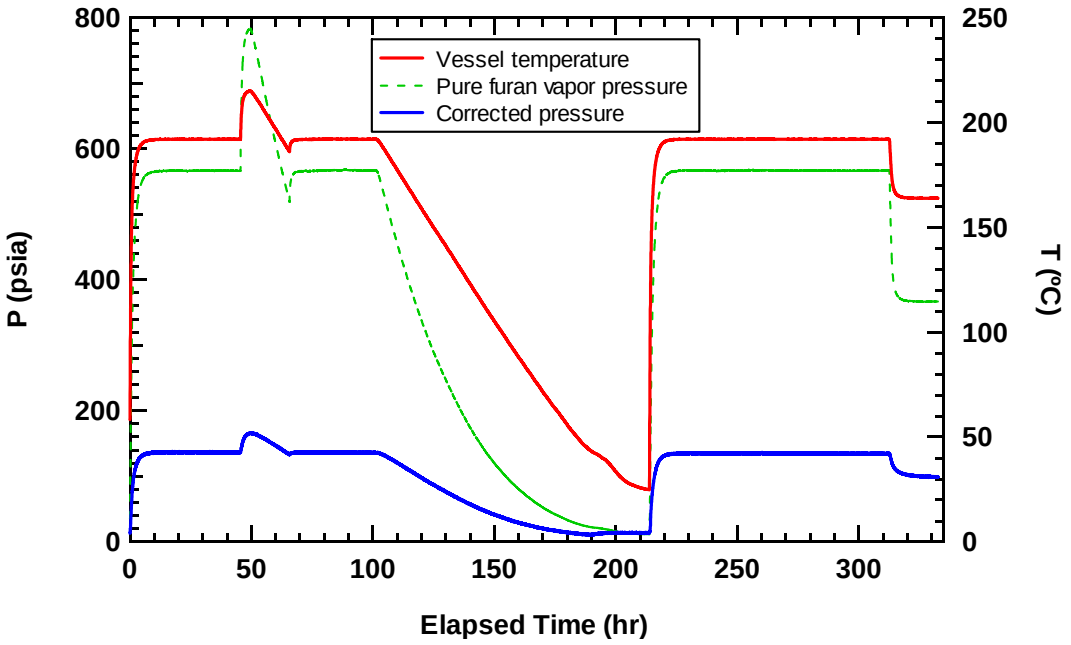

Figure C.11 PEG/furan run 5 (started on 1/9/07). The overall composition was 14.8 wt% furan. The Z66-96 pressure transducer was used with the 2005 calibration. No zero-shift was applied.

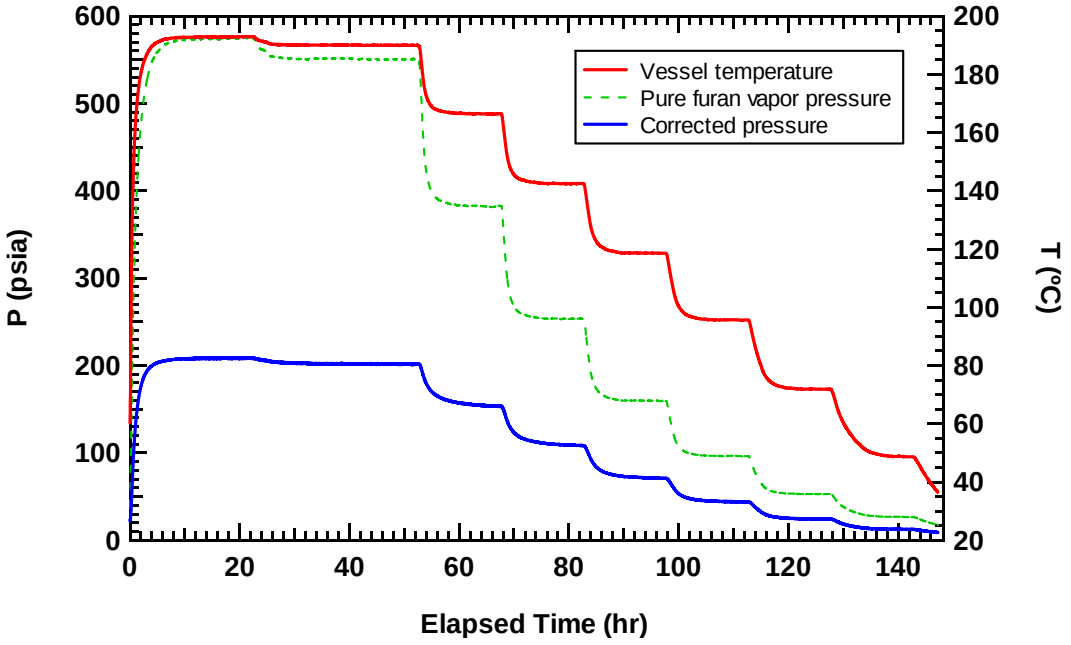

Figure C.12 PEG/furan run 6 (started on 5/2/07). The overall composition was 21.2 wt% furan. The Z66-96 pressure transducer was used with the 2007 calibration. No zero-shift was applied.

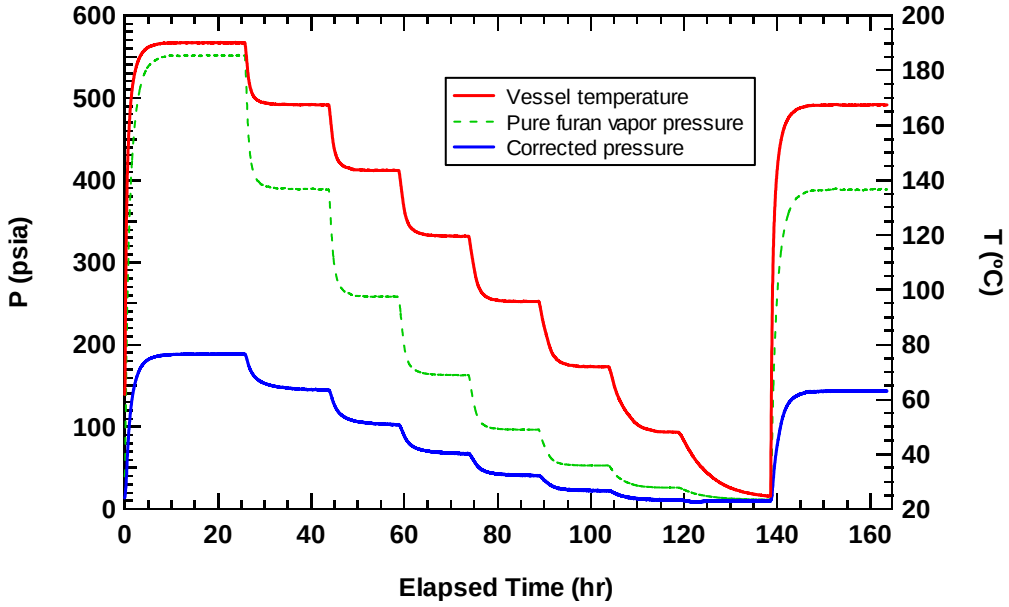

Figure C.13 PEG/furan run 7 (started on 5/14/07). The overall composition was 19.4 wt% furan. The Z66-96 pressure transducer was used with the 2007 calibration. No zero-shift was applied.

A summary of the points taken from each PEG/furan run for comparison with model predictions is given in Table C.3. For runs 1 through 5, each point is a 31-minute average centered around the time at which the indicated vessel temperature was reached. For runs 6 and 7, each point is an average of the last hour of each temperature step.

Table C.3 Summary of PEG/furan at selected temperatures. Solvent weight percents at each temperature represent the calculated liquid composition (see section 5.4.2).

Run	Overall wt% solv	170°C		140°C		75°C	
		wt% solv	P (psi)	wt% solv	P (psi)	wt% solv	P (psi)
5	14.8	11.4	111.5	12.4	75.2	14.0	22.0
7	19.4	15.5	149.5	16.7	97.1	18.6	24.4
6	21.2	16.9	160.5	18.3	104.3	20.4	26.5
2	28.4	22.3	219.1	24.4	141.7	27.3	38.3
4	30.2	23.7	238.3	26.1	153.1	29.1	40.2
1	45.2	37.5	314.9	40.6	199.5	44.0	50.7
3	72.4	-	-	68.6	230.2	71.5	55.1
Furan	100.0	-	-	100.0	234.3	100.0	55.4

C.2.3 PS/Benzene

The data collected for the PS/benzene system are shown in the following figures. Beginning with this system a thermocouple was added to the wall of the pressure vessel to measure the vessel temperature directly, without needing to calculate it from the gage block temperature. Also starting with this system, the zero-shift was determined from the pressure measured while the polymer was being degassed (assuming it should be nearly zero). Equipment problems were experienced during the first run for this system, so only runs 2 through 4 are shown.

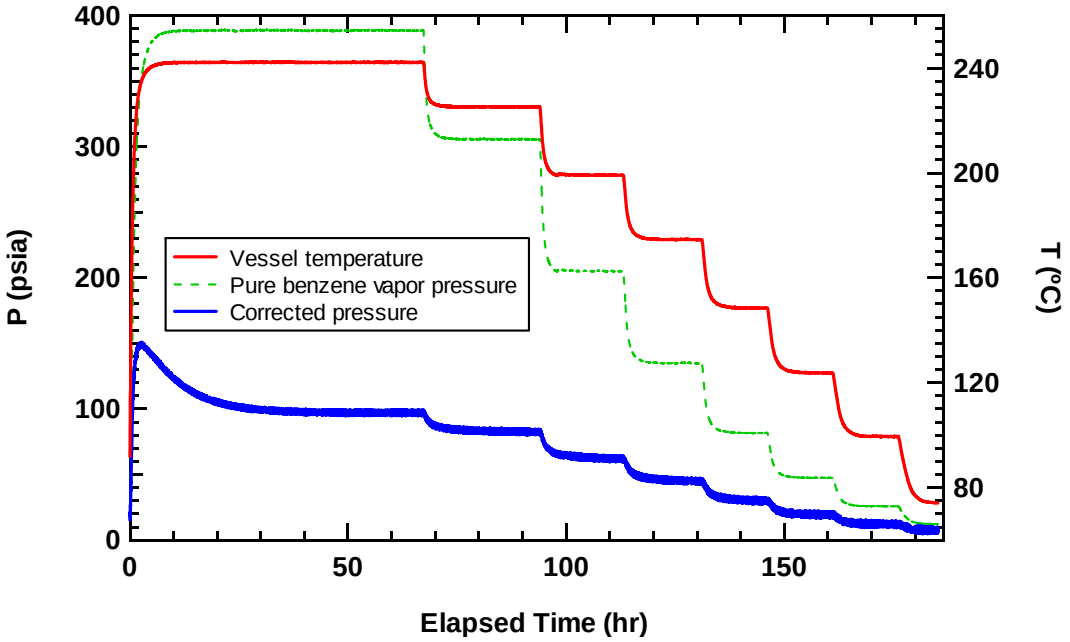

Figure C.14 PS/benzene run 2 (started on 6/29/07). The overall composition was 13.3 wt% benzene. The Z66-96 pressure transducer was used with the 2007 calibration. A zero-shift of +1.7 psi was applied.

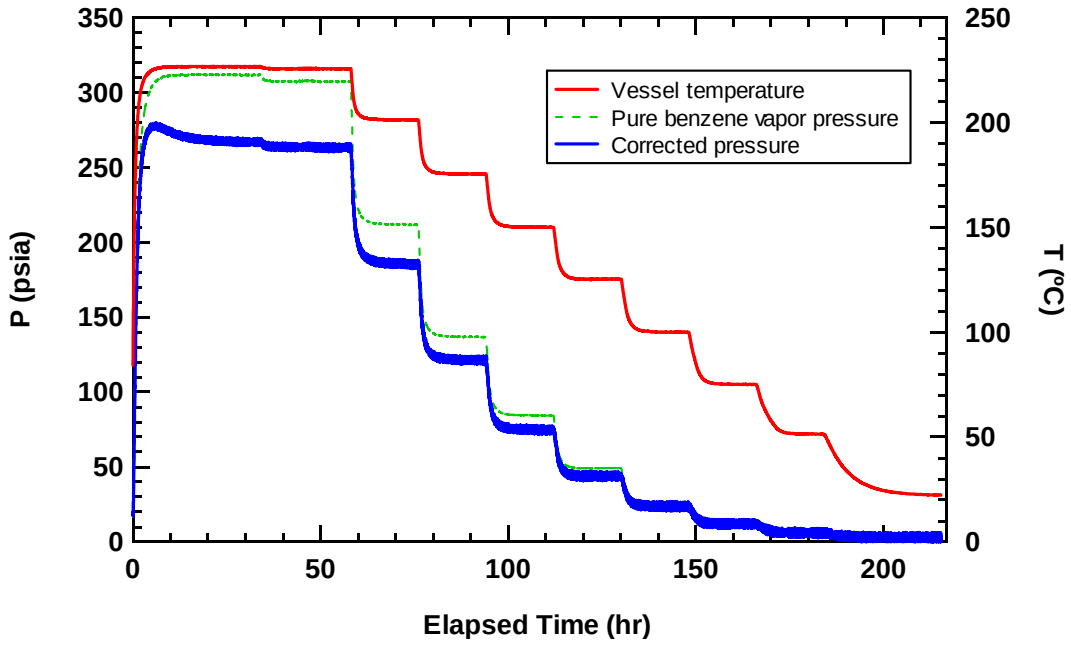

Figure C.15 PS/benzene run 3 (started on 6/29/07). The overall composition was 54.0 wt% benzene. The Z66-96 pressure transducer was used with the 2007 calibration. A zero-shift of +0.4 psi was applied.

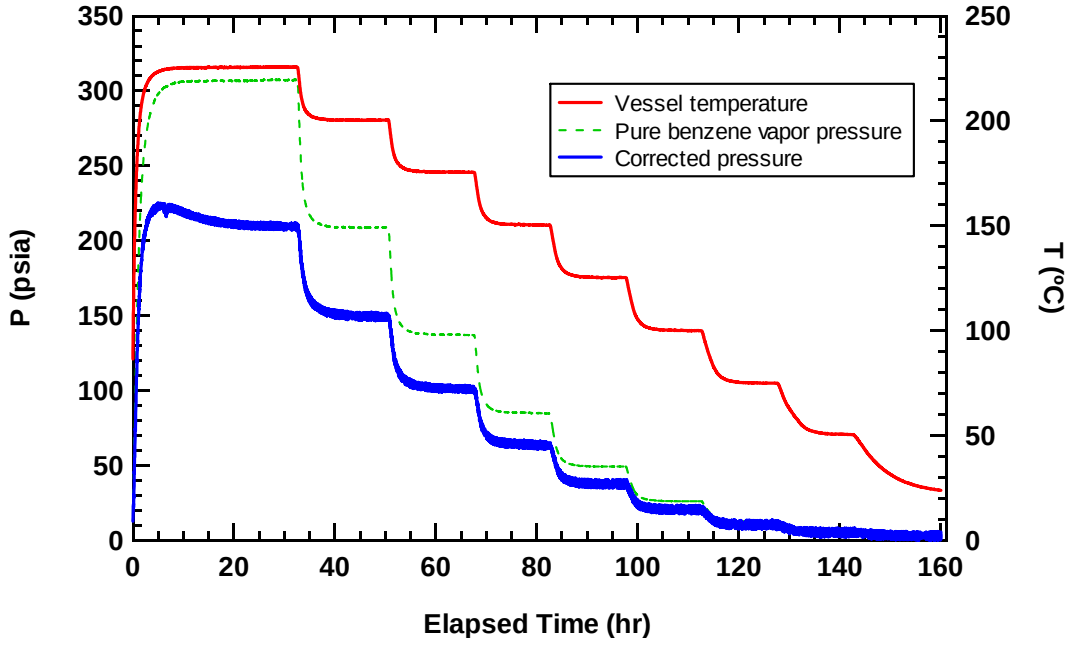

Figure C.16 PS/benzene run 4 (started on 6/29/07). The overall composition was 30.7 wt% benzene. The Z66-96 pressure transducer was used with the 2007 calibration. A zero-shift of +0.4 psi was applied.

A summary of the points taken from each PS/benzene run for comparison with model predictions is given in Table C.4. Each point is an average of the last hour of each temperature step.

Table C.4 Summary of PS/benzene at selected temperatures. Solvent weight percents at each temperature represent the calculated liquid composition (see section 5.4.2).

Run	Overall wt% solv	225ºC		175ºC		100ºC	
		wt% solv	P (psi)	wt% solv	P (psi)	wt% solv	P (psi)
2	13.3	10.9	82.2	11.8	45.4	12.8	12.2
4	30.7	26.4	208.4	28.6	100.4	30.2	20.4
3	54.0	50.2	261.0	52.3	120.8	53.6	24.0
Benzene	100.0	-	-	100.0	136.4	100.0	25.4

C.2.4 PS/Furan

The data collected for the PS/furan system are shown in the following figures. The first run for this system leaked, so only runs 2 through 5 are shown. At two temperature steps in run 2 (175 and 150ºC) it was evident that the pressure did not reach its equilibrium value, so the mixture was reheated in an attempt to find the correct equilibrium pressure at these temperatures. In order to account for pressure loss due to slow leakage over time, the pressure was also measured at 200ºC again. The difference between the pressure at 200ºC in the first and second parts of the run (1.3 psi) was subtracted from the difference between the pressure in the two parts of the run at 175 and 150ºC (4.0 and 3.7 psi, respectively) to get an estimate of the equilibrium pressure at those temperatures without any leakage.

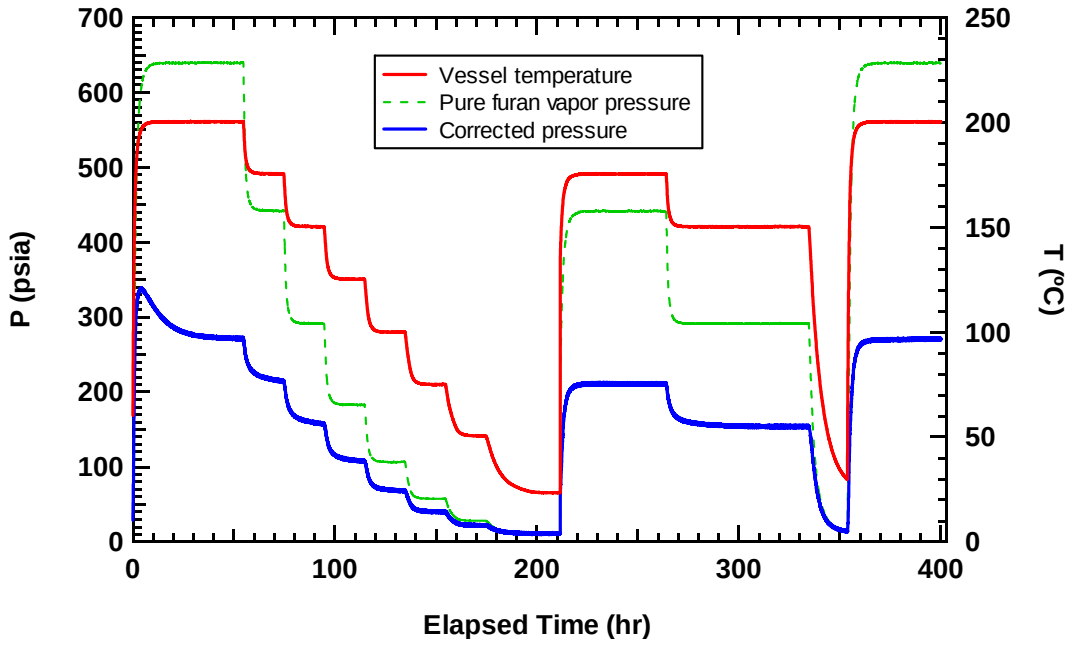

Figure C.17 PS/furan run 2 (started on 8/28/07). The overall composition was 22.1 wt% furan. The Z66-96 pressure transducer was used with the 2007 calibration. A zero-shift of +2.6 psi was applied.

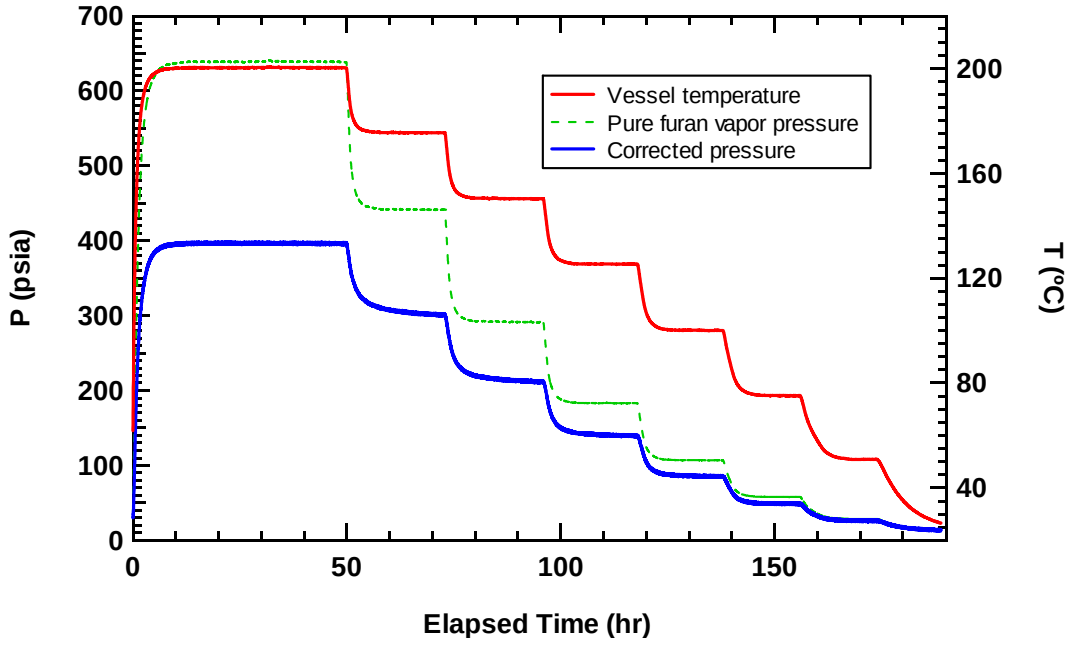

Figure C.18 PS/furan run 3 (started on 10/4/07). The overall composition was 36.1 wt% furan. The Z66-96 pressure transducer was used with the 2007 calibration. A zero-shift of +2.7 psi was applied.

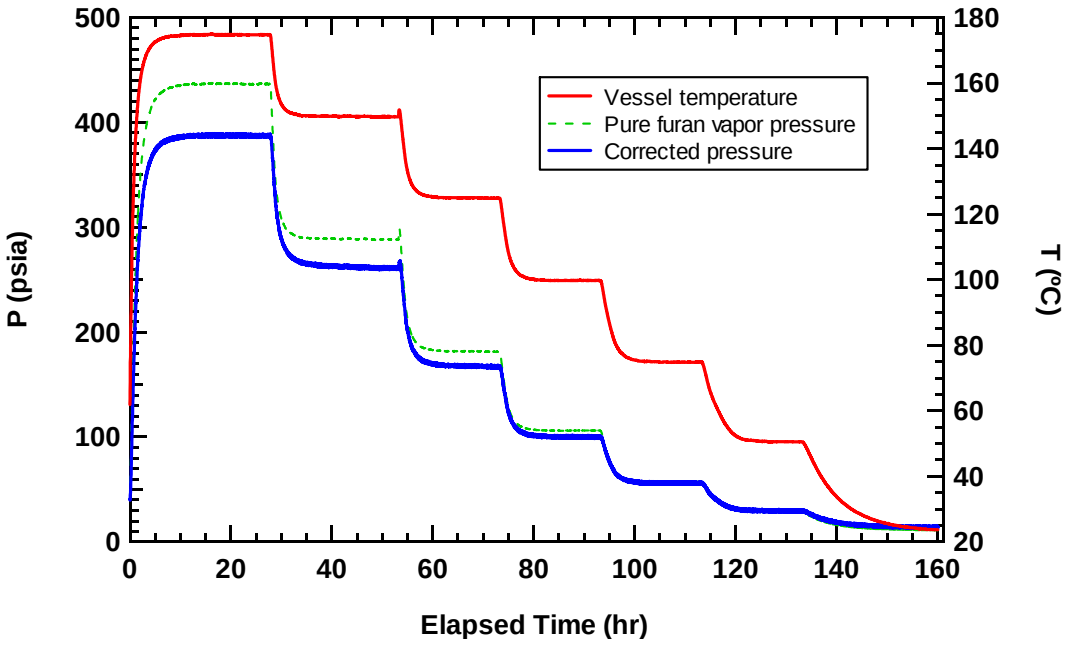

Figure C.19 PS/furan run 4 (started on 10/15/07). The overall composition was 52.0 wt% furan. The Z66-96 pressure transducer was used with the 2007 calibration. A zero-shift of +3.0 psi was applied.

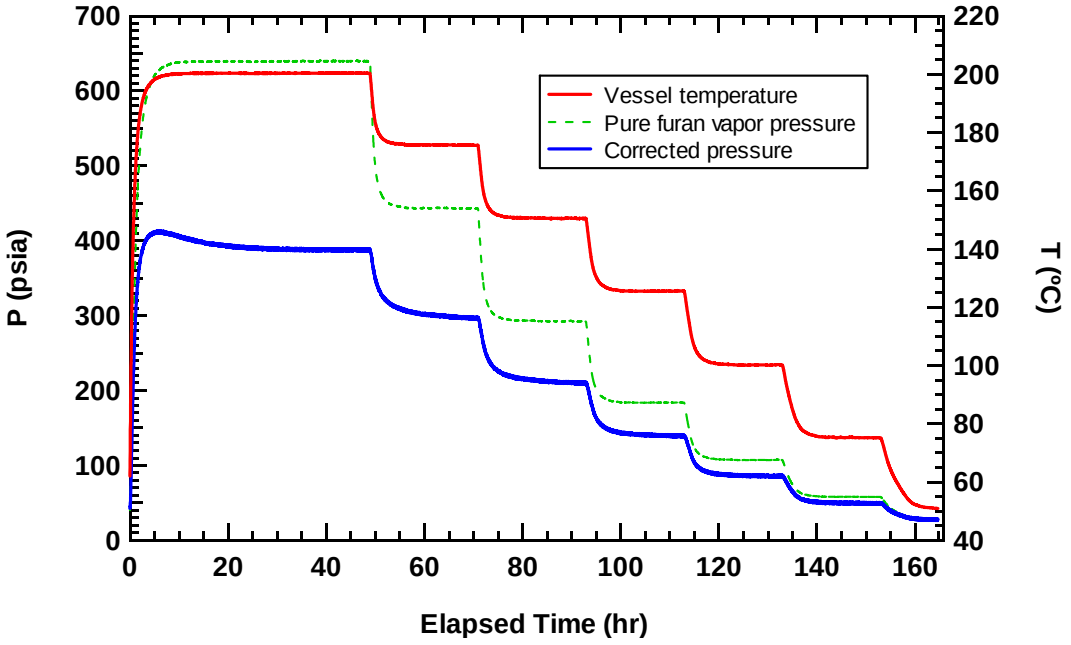

Figure C.20 PS/furan run 5 (started on 10/23/07). The overall composition was 31.8 wt% furan. The Z66-96 pressure transducer was used with the 2007 calibration. A zero-shift of +3.2 psi was applied.

A summary of the points taken from each PS/furan run for comparison with model predictions is given in Table C.5. Each point is an average of the last hour of each temperature step.

Table C.5 Summary of PS/furan at selected temperatures. Solvent weight percents at each temperature represent the calculated liquid composition (see section 5.4.2).

Run	Overall wt% solv	175ºC		150ºC		100ºC	
		wt% solv	P (psi)	wt% solv	P (psi)	wt% solv	P (psi)
2	22.1	16.3	211.2	17.8	154.5	20.1	67.8
5	31.8	25.1	294.4	27.1	208.3	29.9	85.2
3	36.1	30.6	299.3	32.3	210.7	34.5	85.1
4	52.0	45.8	388.8	48.2	262.5	50.6	100.5
Furan	100.0	-	-	100.0	280.9	100.0	103.1

C.2.5 PS/IPP

The data collected for the PS/IPP system are shown in the following figures. Runs 1, 2, and 4 had significant problems with decomposition of the IPP, so only runs 3 and 5 are shown. Run 5 also seemed to start out having problems, but was cooled, evacuated, and reheated, and then it seemed not to have serious problems with decomposition.

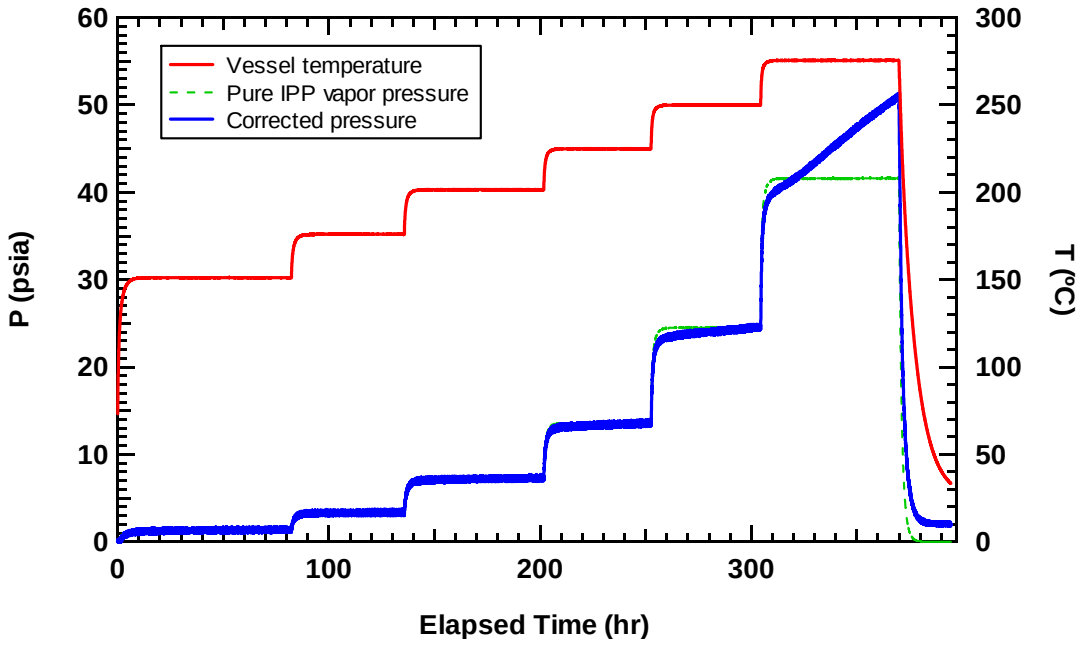

Figure C.21 PS/IPP run 3 (started on 1/5/08). The overall composition was 50.0 wt% IPP. The B77-61 pressure transducer was used with the 2008 calibration. A zero-shift of +3.6 psi was applied.

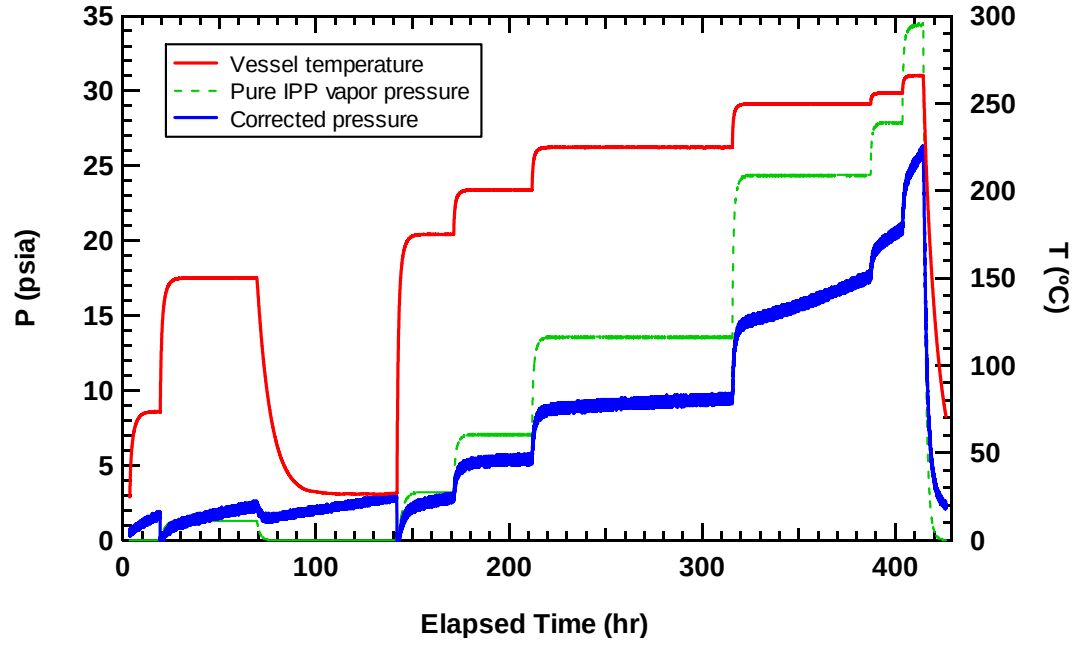

Figure C.22 PS/IPP run 5 (started on 1/29/08). The overall composition was 15.0 wt% IPP. The B77-61 pressure transducer was used with the 2008 calibration. A zero-shift of +2.8 psi was applied.

A summary of the points taken from each PS/IPP run for comparison with model predictions is given in Table C.6. Each point is generally an average of the last hour of each temperature step, except at 250ºC when the average was taken soon after most of the pressure rise for the temperature step had occurred.

Table C.6 Summary of PS/IPP at selected temperatures. Solvent weight percents at each temperature represent the calculated liquid composition (see section 5.4.2).

Run	Overall wt% solv	250ºC		225ºC		200ºC	
		wt% solv	P (psi)	wt% solv	P (psi)	wt% solv	P (psi)
5	15.0	14.5	15.0	14.7	8.9	14.8	5.4
3	50.0	49.5	23.7	49.7	13.3	49.9	7.0
IPP	100.0	100.0	25.8	100.0	14.4	100.0	7.6

C.2.6 PEG/IPP

The data collected for the PEG/IPP system are shown in the following figures. Runs 1, 3, and 4 had significant problems with decomposition of the IPP, so only runs 2 and 5 are shown. For run 5, the pressure vessel was opened to a vacuum line in between each temperature step to remove vapors created by the decomposition of IPP. Assumptions were made that the overall composition did not change significantly upon repeated evacuation of the vessel (because the pressure was relatively low), and that the liquid phase contained only IPP and PEG (even though slow decomposition of the IPP was occurring).

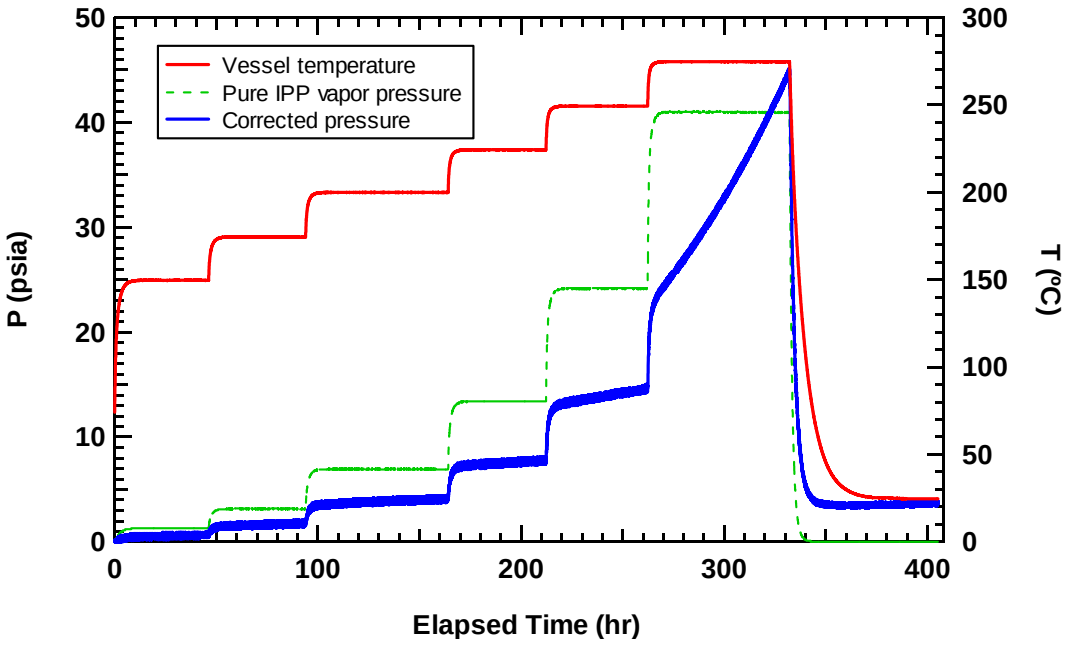

Figure C.23 PEG/IPP run 2 (started on 2/16/08). The overall composition was 30.2 wt% IPP. The B77-61 pressure transducer was used with the 2008 calibration. A zero-shift of +2.3 psi was applied.

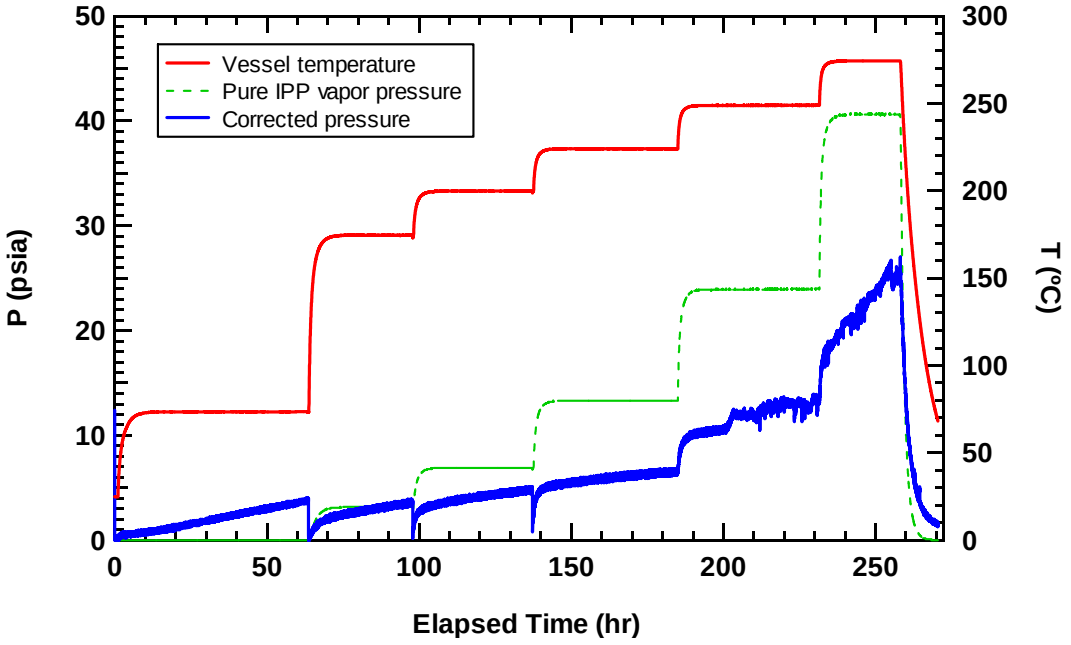

Figure C.24 PEG/IPP run 5 (started on 4/11/08). The overall composition was 18.6 wt% IPP. The B77-61 pressure transducer was used with the 2008 calibration. A zero-shift of +0.3 psi was applied.

A summary of the points taken from each PEG/IPP run for comparison with model predictions is given in Table C.7. Each point is a 1-hour average of the data collected soon after most of the pressure rise for each new temperature step had occurred.

Table C.7 Summary of PEG/IPP at selected temperatures. Solvent weight percents at each temperature represent the calculated liquid composition (see section 5.4.2).

Run	Overall wt% solv	250ºC		225ºC		200ºC	
		wt% solv	P (psi)	wt% solv	P (psi)	wt% solv	P (psi)
5	18.6	18.3	10.6	18.4	5.5	18.5	3.6
2	30.2	29.8	13.5	30.0	7.9	30.2	4.1
IPP	100.0	100.0	25.8	100.0	14.4	100.0	7.6

Appendix D. Model Calculations

This section presents the equilibrium pressures predicted for each polymer/solvent system by the models used in this work. Data from the HT-VLE facility are also given. Each figure shows the results from an activity coefficient model used in three ways.

D.1 PEG/Benzene

PEG/benzene system predictions are shown in Figure D.1 through Figure D.6.

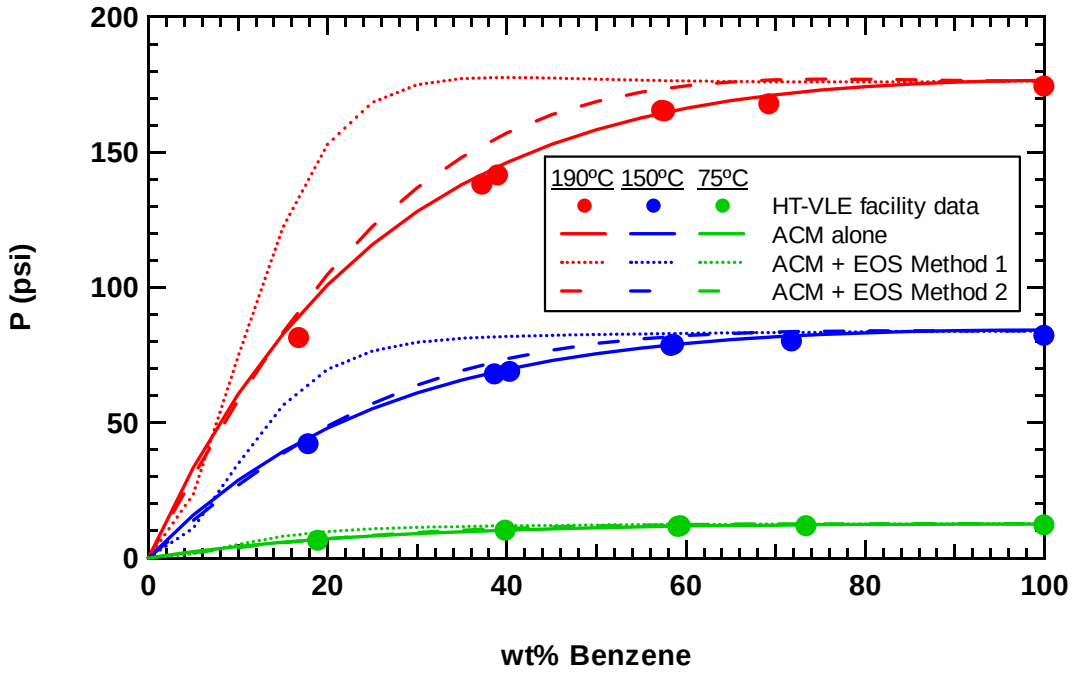

Figure D.1 Predicted pressures for the PEG/benzene system from the models using the Entropic-FV ACM.

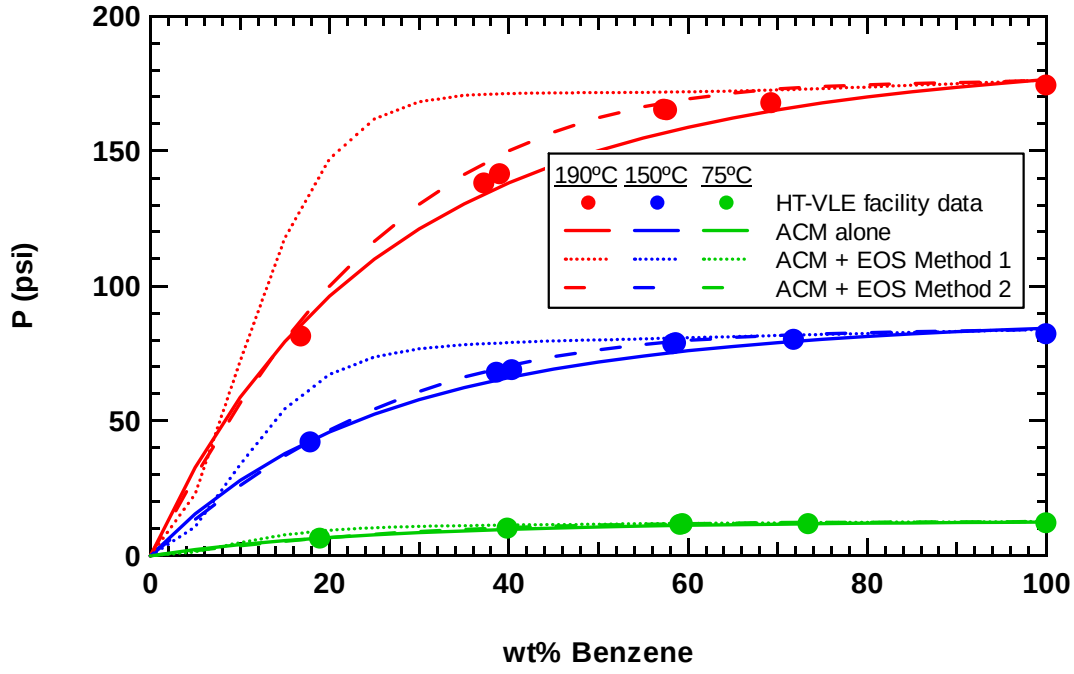

Figure D.2 Predicted pressures for the PEG/benzene system from the models using the Freed-FV ACM.

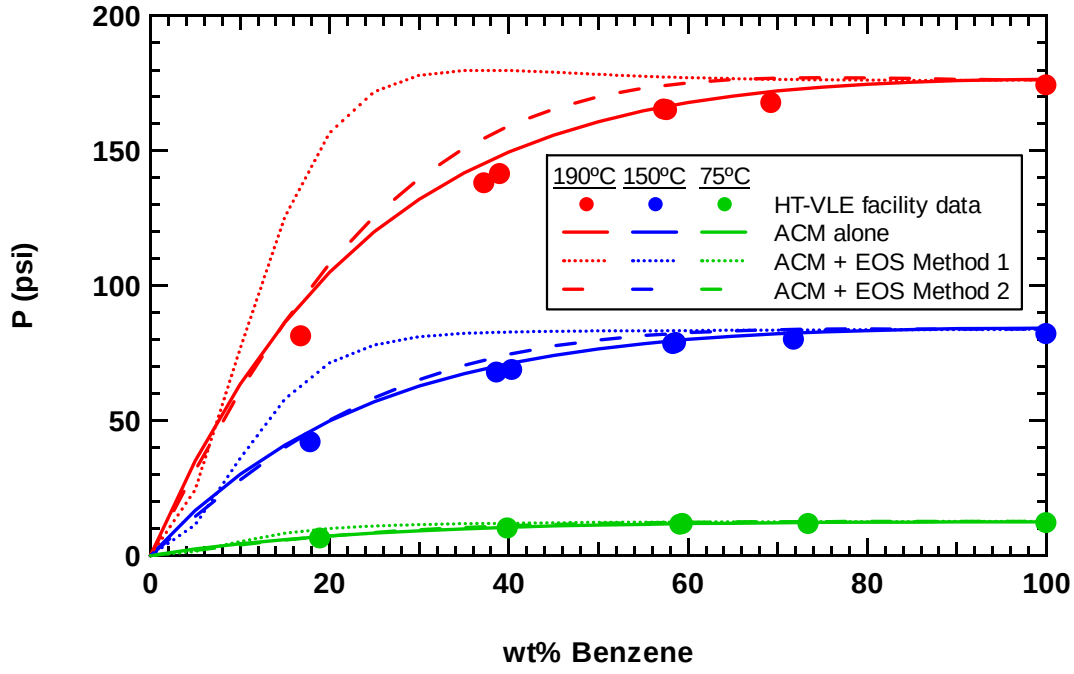

Figure D.3 Predicted pressures for the PEG/benzene system from the models using the GK-FV ACM.

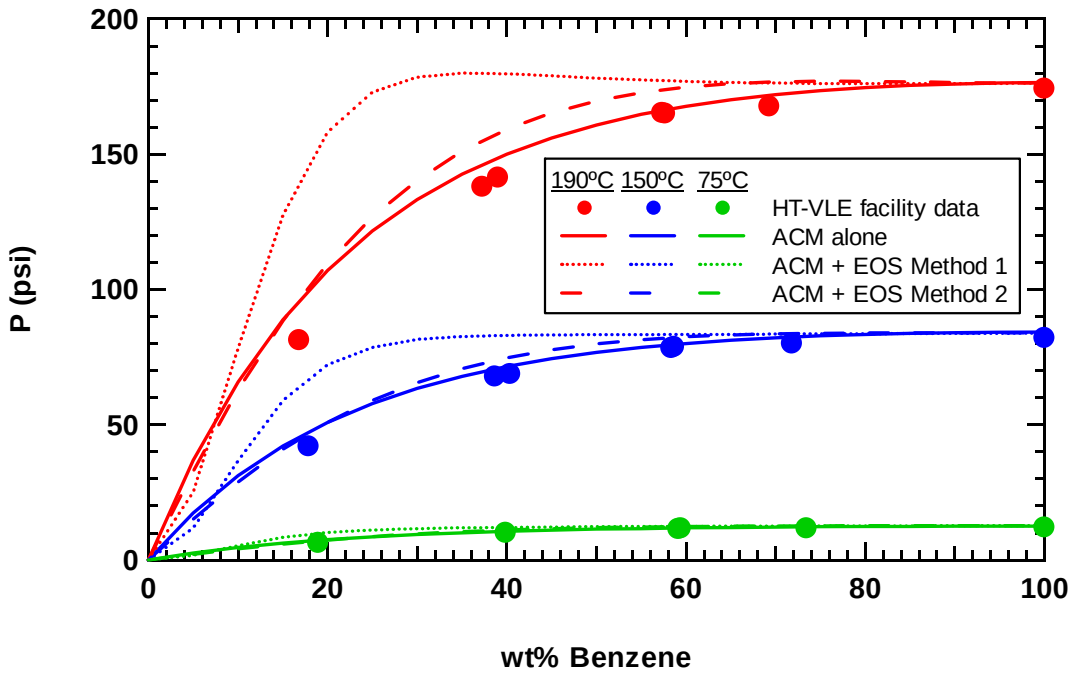

Figure D.4 Predicted pressures for the PEG/benzene system from the models using the MEFV ACM.

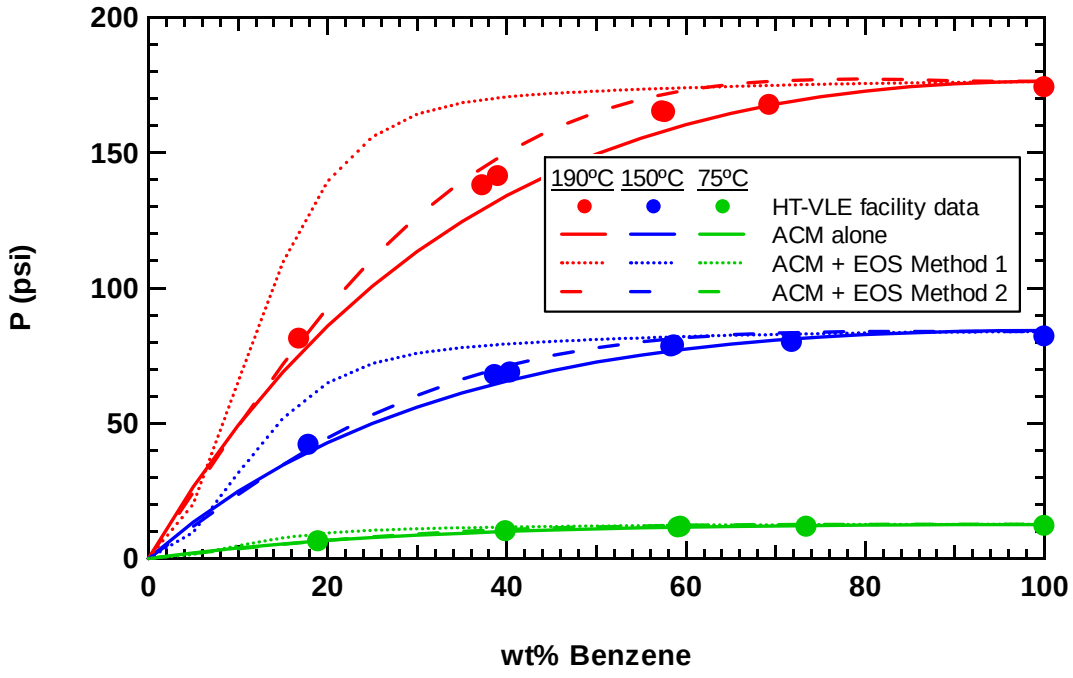

Figure D.5 Predicted pressures for the PEG/benzene system from the models using the UNIFAC-FV ACM.

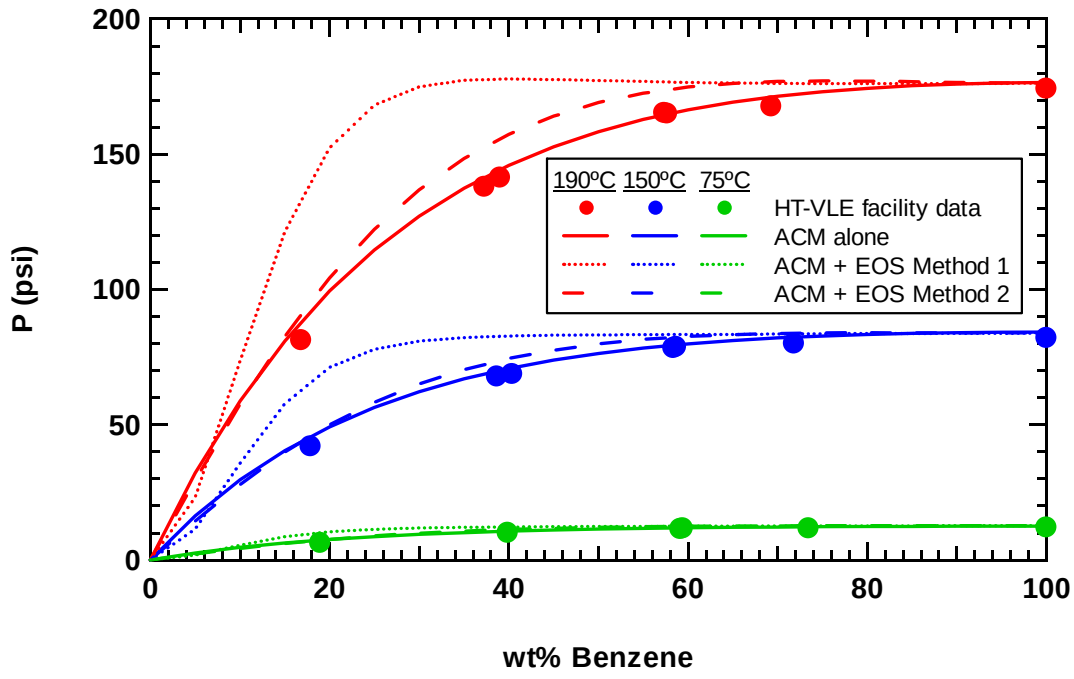

Figure D.6 Predicted pressures for the PEG/benzene system from the models using the UNIFAC-ZM ACM.

D.2 PEG/Furan

PEG/furan system predictions are shown in Figure D.7 through Figure D.12.

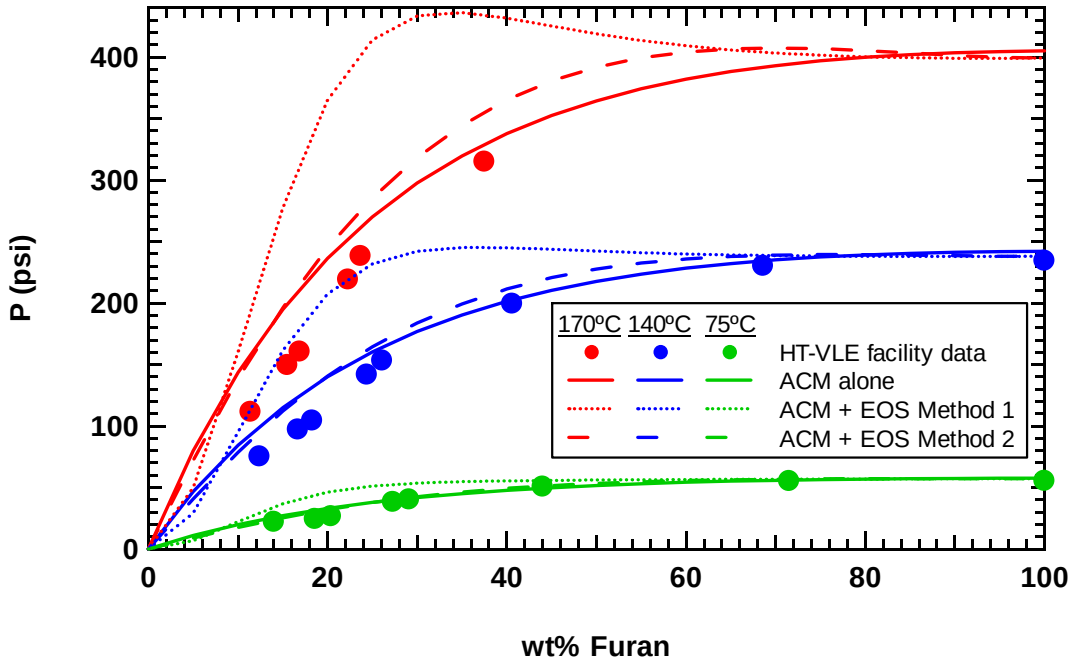

Figure D.7 Predicted pressures for the PEG/furan system from the models using the Entropic-FV ACM.

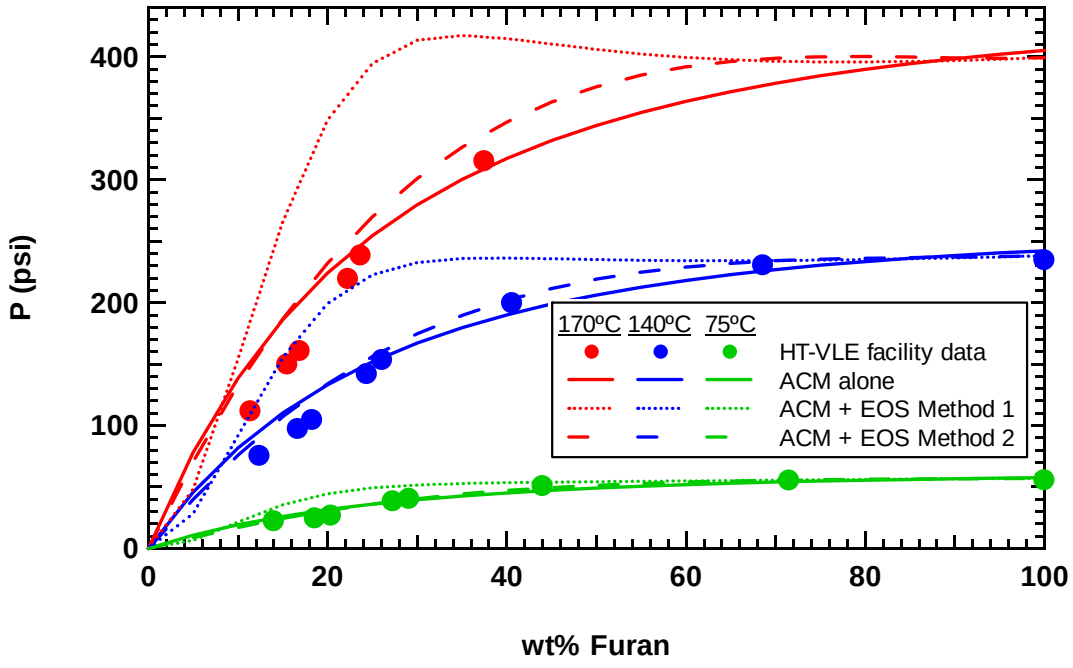

Figure D.8 Predicted pressures for the PEG/furan system from the models using the Freed-FV ACM.

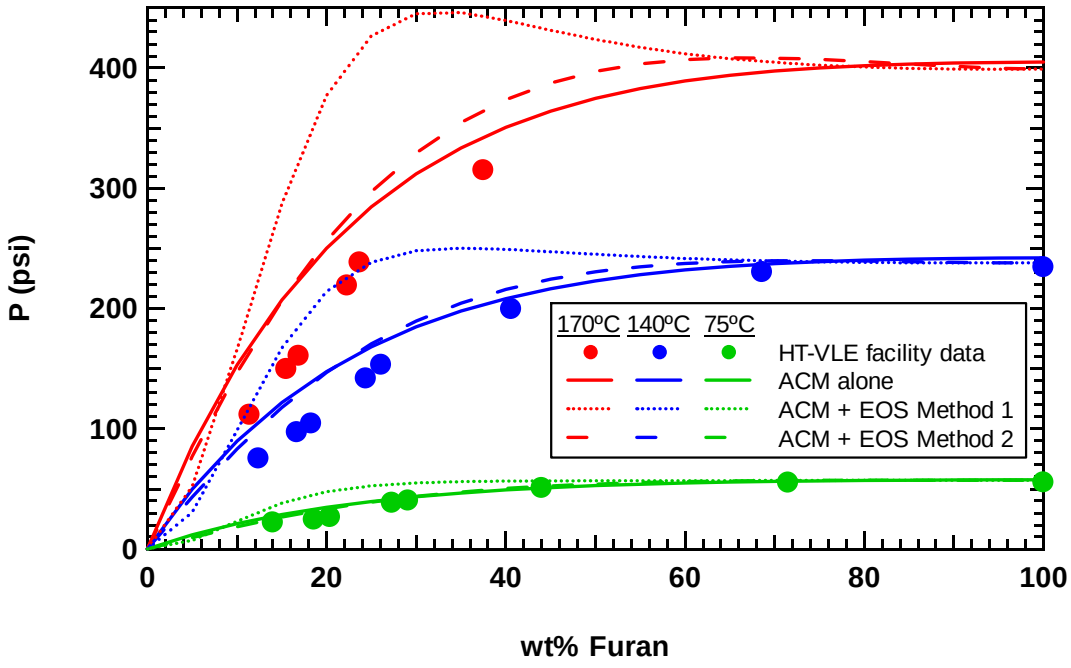

Figure D.9 Predicted pressures for the PEG/furan system from the models using the GK-FV ACM.

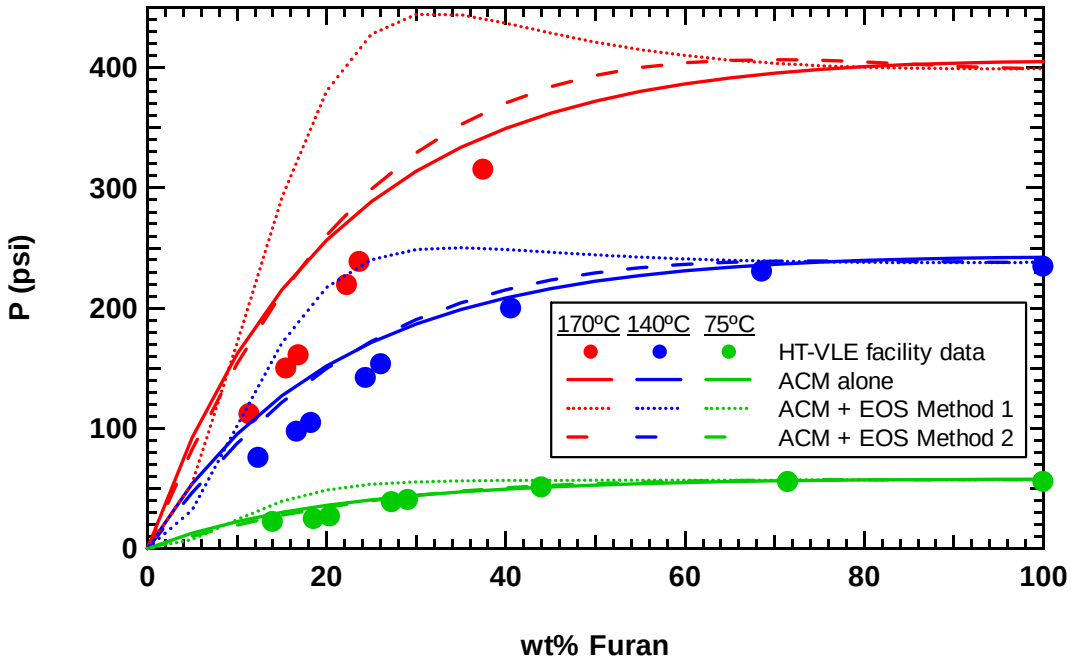

Figure D.10 Predicted pressures for the PEG/furan system from the models using the MEFV ACM.

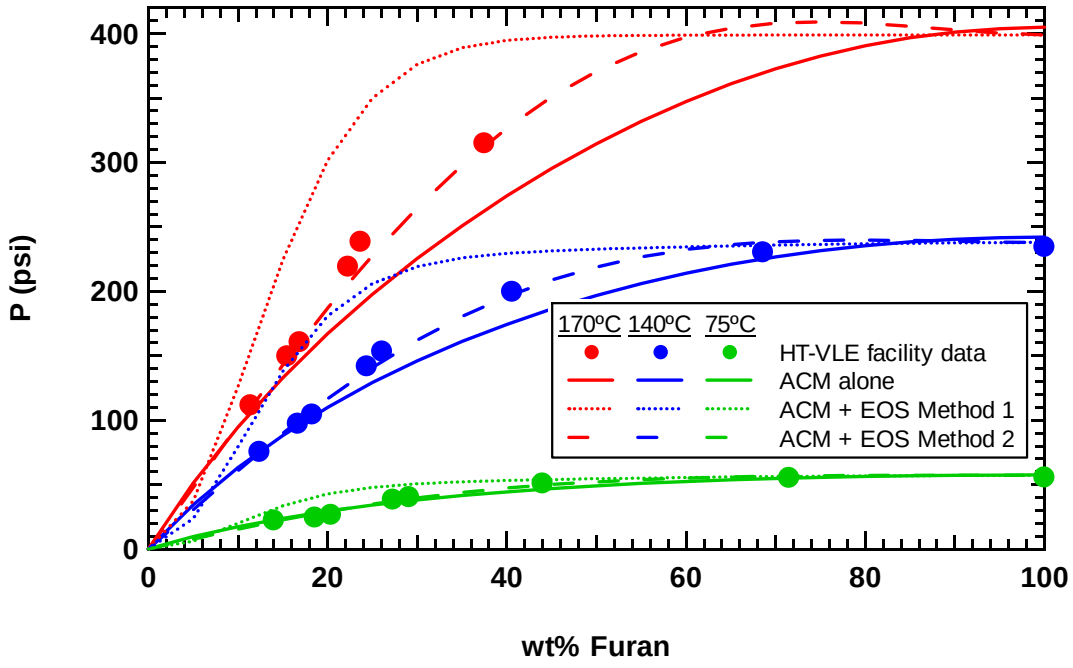

Figure D.11 Predicted pressures for the PEG/furan system from the models using the UNIFAC-FV ACM.

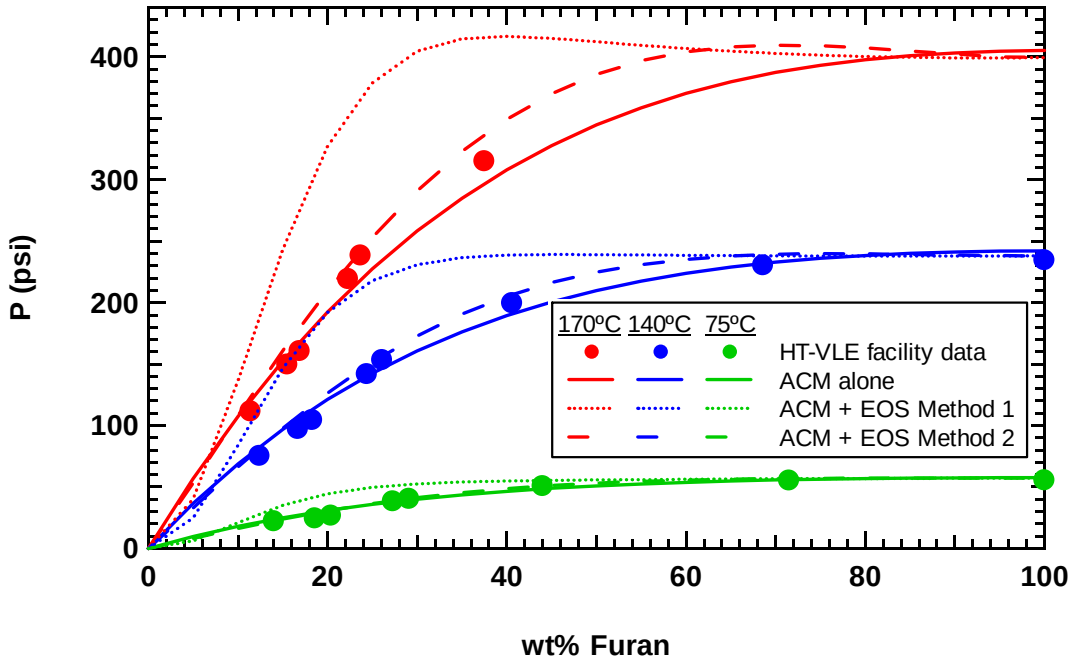

Figure D.12 Predicted pressures for the PEG/furan system from the models using the UNIFAC-ZM ACM.

D.3 PEG/IPP

PEG/IPP system predictions are shown in Figure D.13 through Figure D.18.

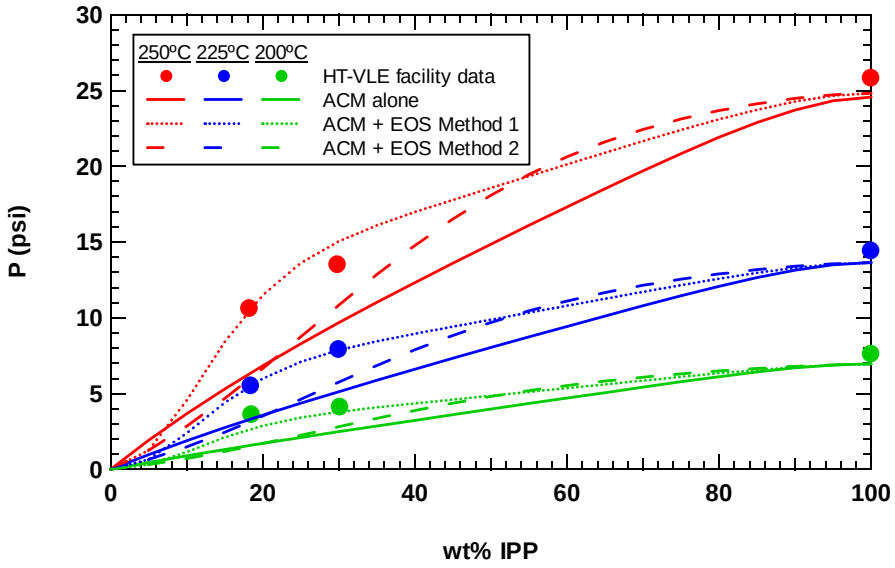

Figure D.13 Predicted pressures for the PEG/IPP system from the models using the Entropic-FV ACM.

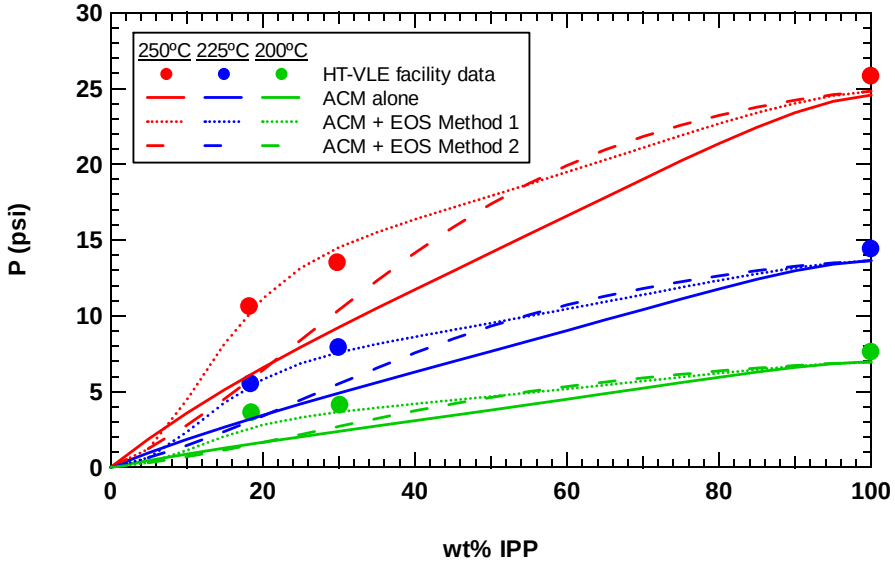

Figure D.14 Predicted pressures for the PEG/IPP system from the models using the Freed-FV ACM.

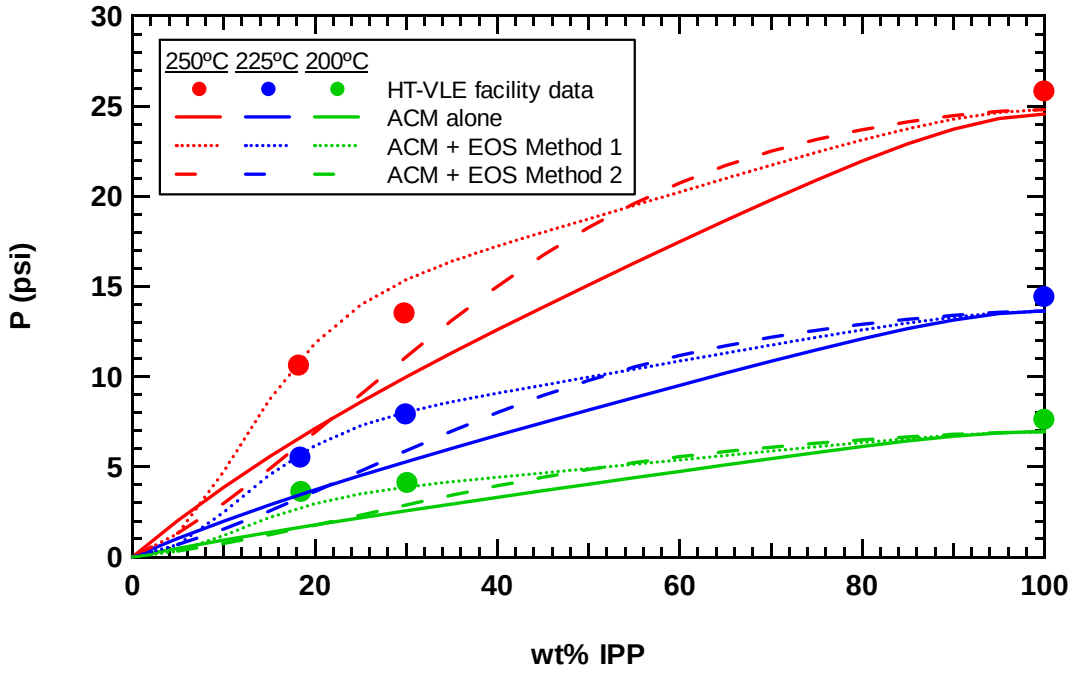

Figure D.15 Predicted pressures for the PEG/IPP system from the models using the GK-FV ACM.

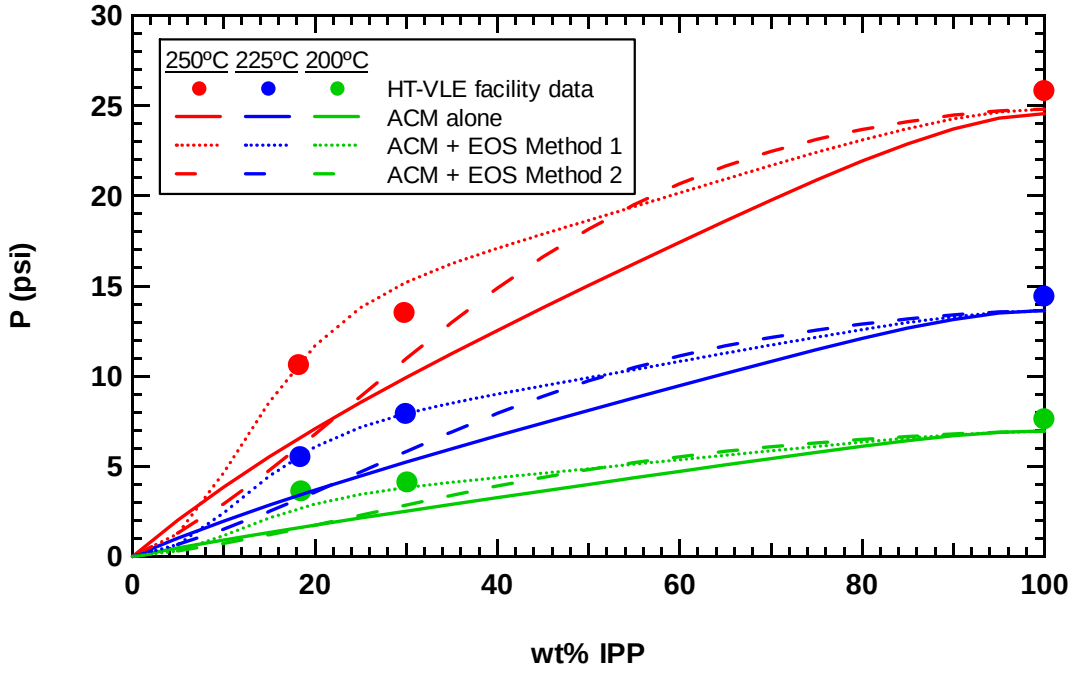

Figure D.16 Predicted pressures for the PEG/IPP system from the models using the MEFV ACM.

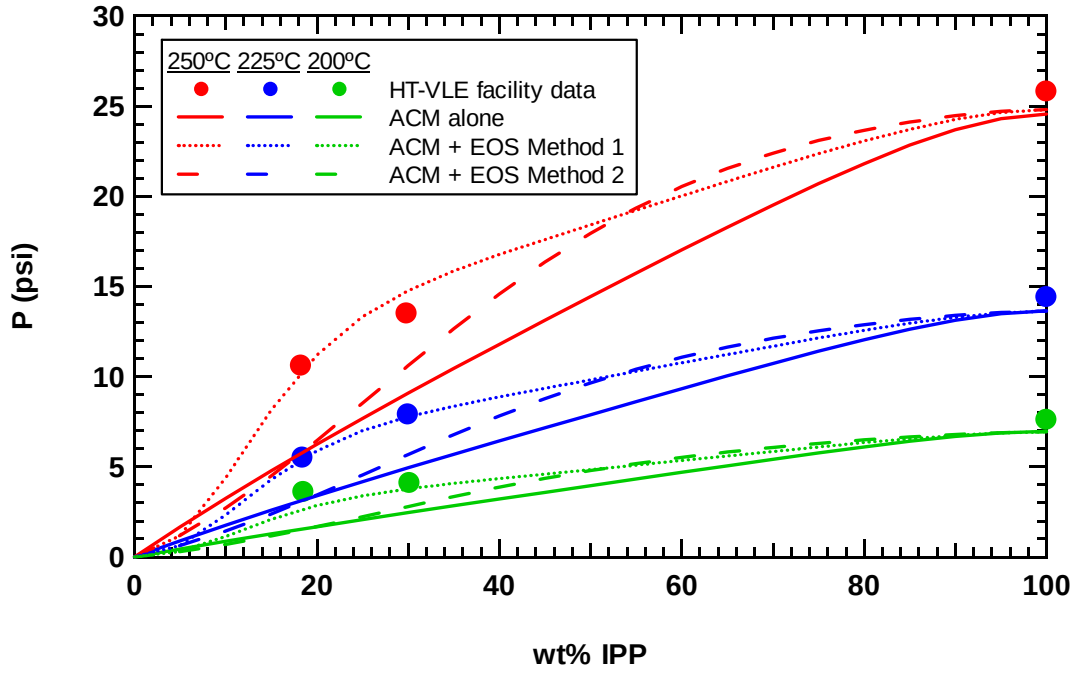

Figure D.17 Predicted pressures for the PEG/IPP system from the models using the UNIFAC-FV ACM.

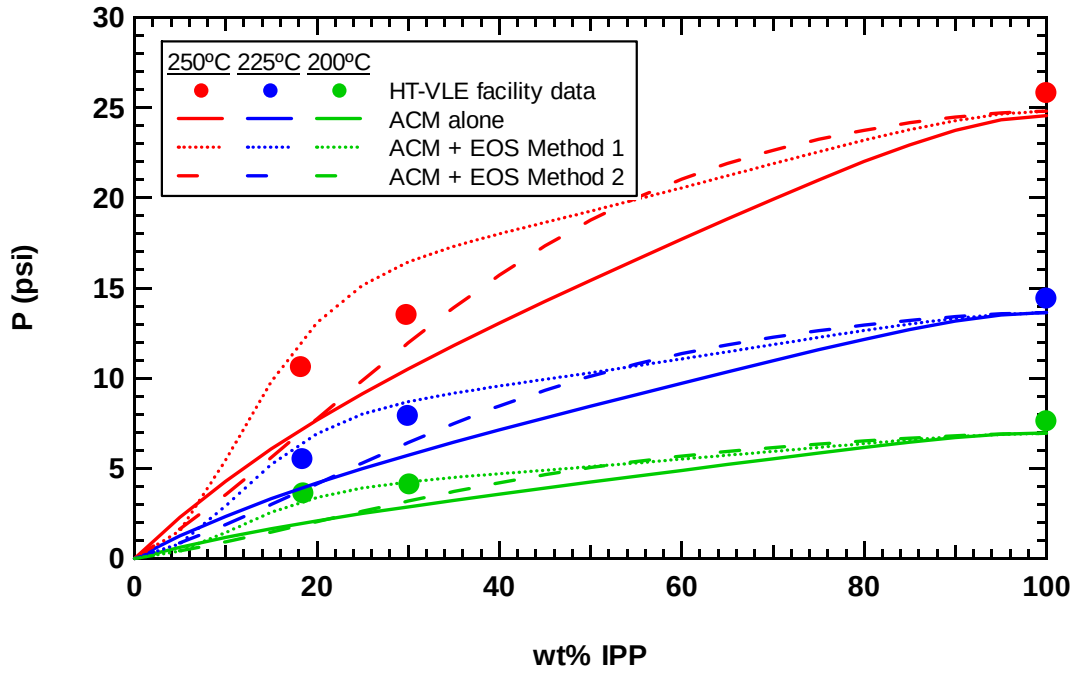

Figure D.18 Predicted pressures for the PEG/IPP system from the models using the UNIFAC-ZM ACM.

D.4 PS/Benzene

PS/benzene system predictions are shown in Figure D.19 through Figure D.24.

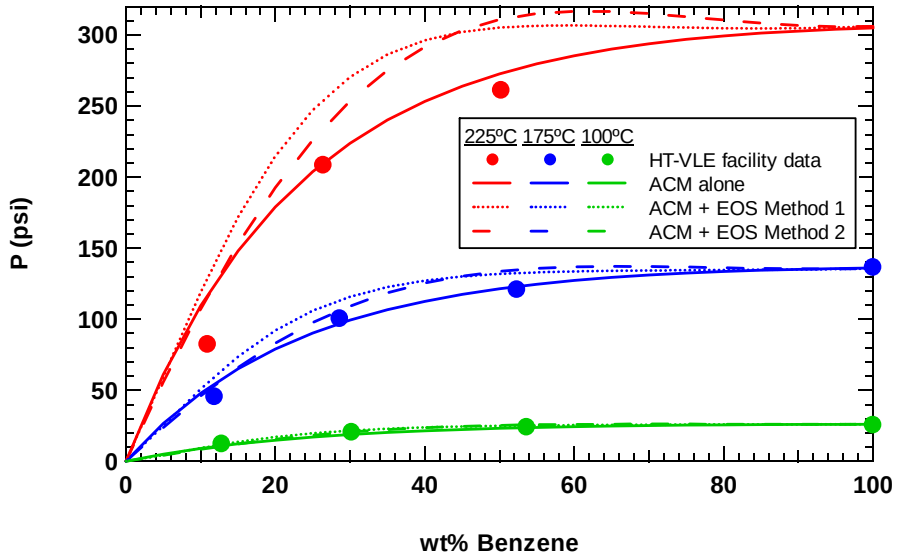

Figure D.19 Predicted pressures for the PS/benzene system from the models using the Entropic-FV ACM.

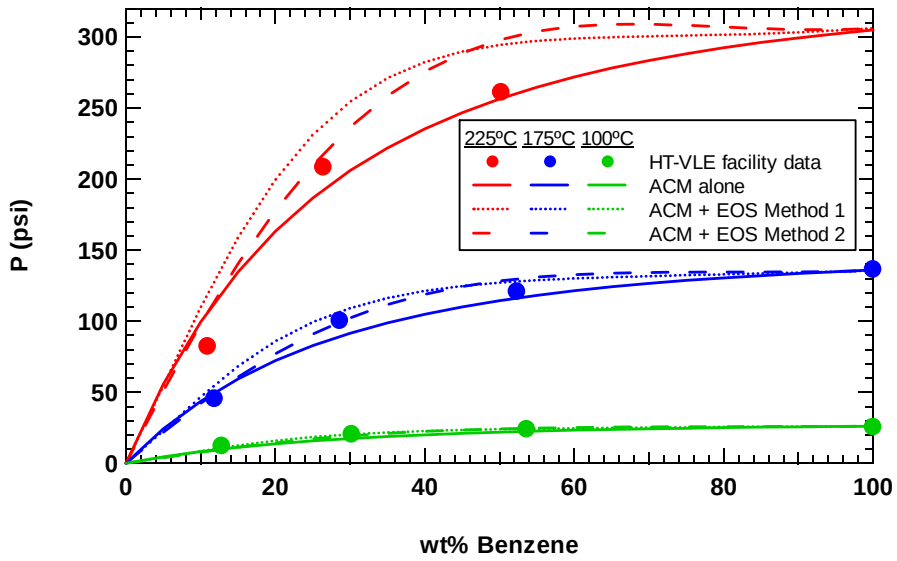

Figure D.20 Predicted pressures for the PS/benzene system from the models using the Freed-FV ACM.

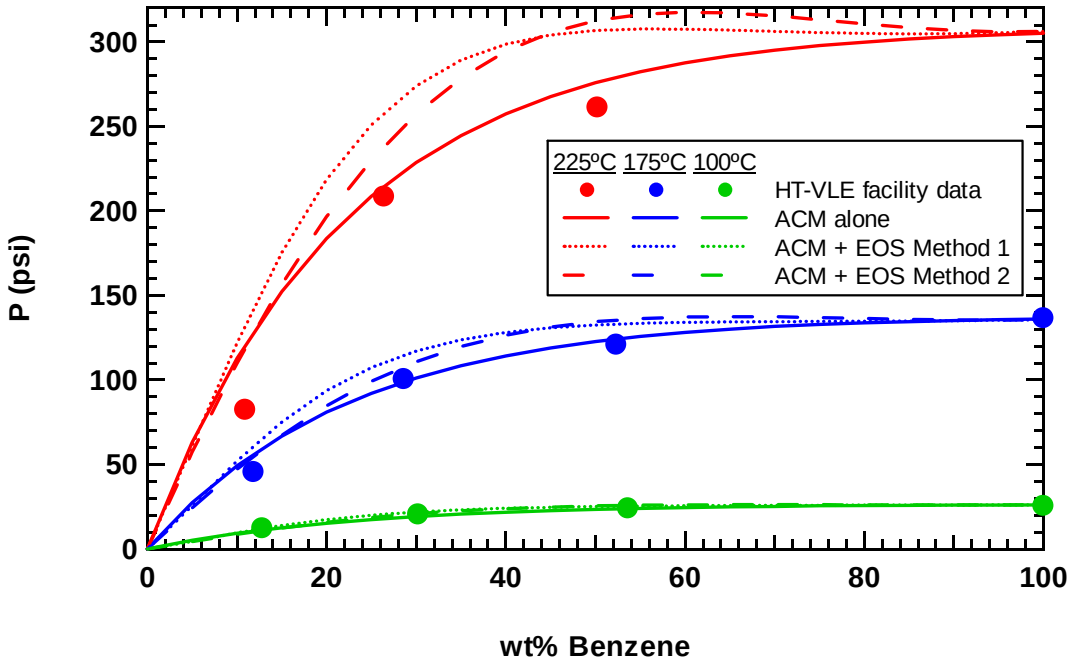

Figure D.21 Predicted pressures for the PS/benzene system from the models using the GK-FV ACM.

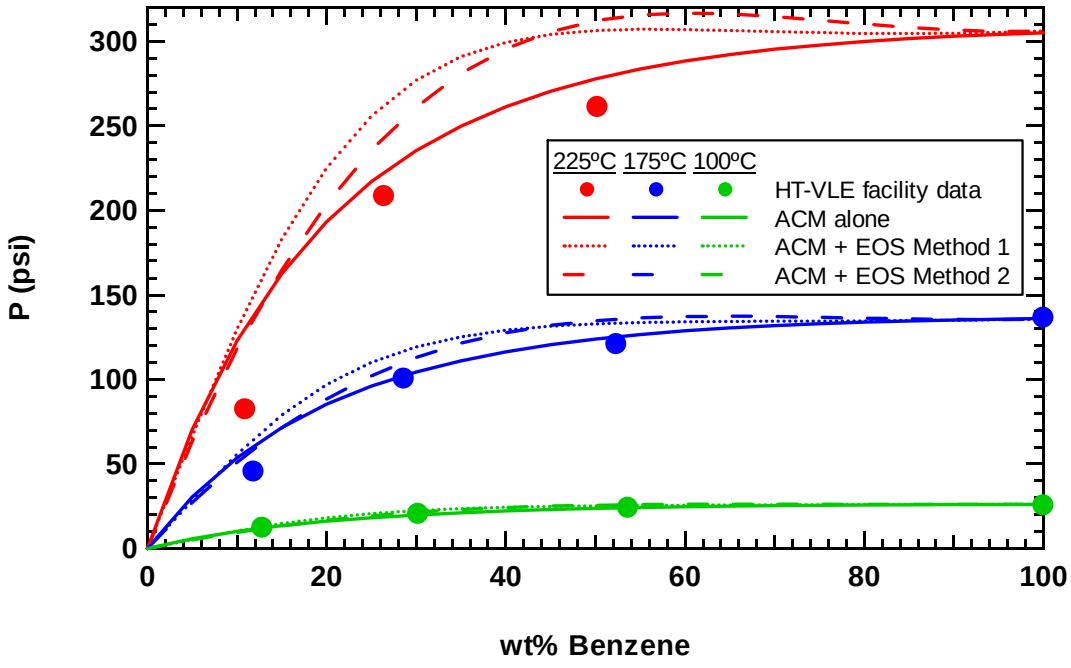

Figure D.22 Predicted pressures for the PS/benzene system from the models using the MEFV ACM.

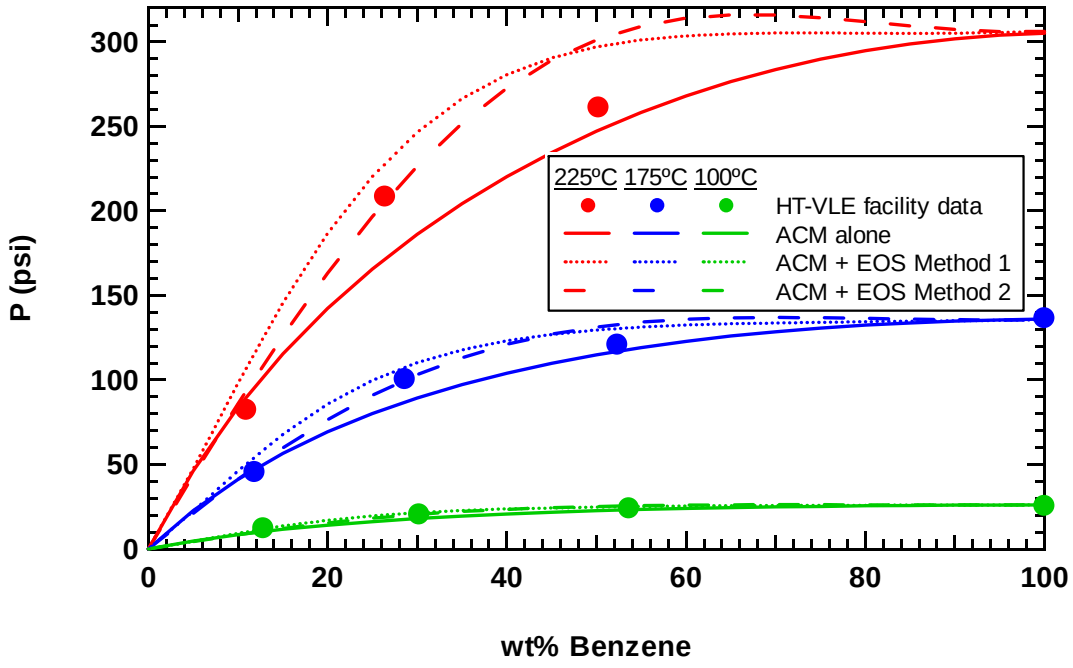

Figure D.23 Predicted pressures for the PS/benzene system from the models using the UNIFAC-FV ACM.

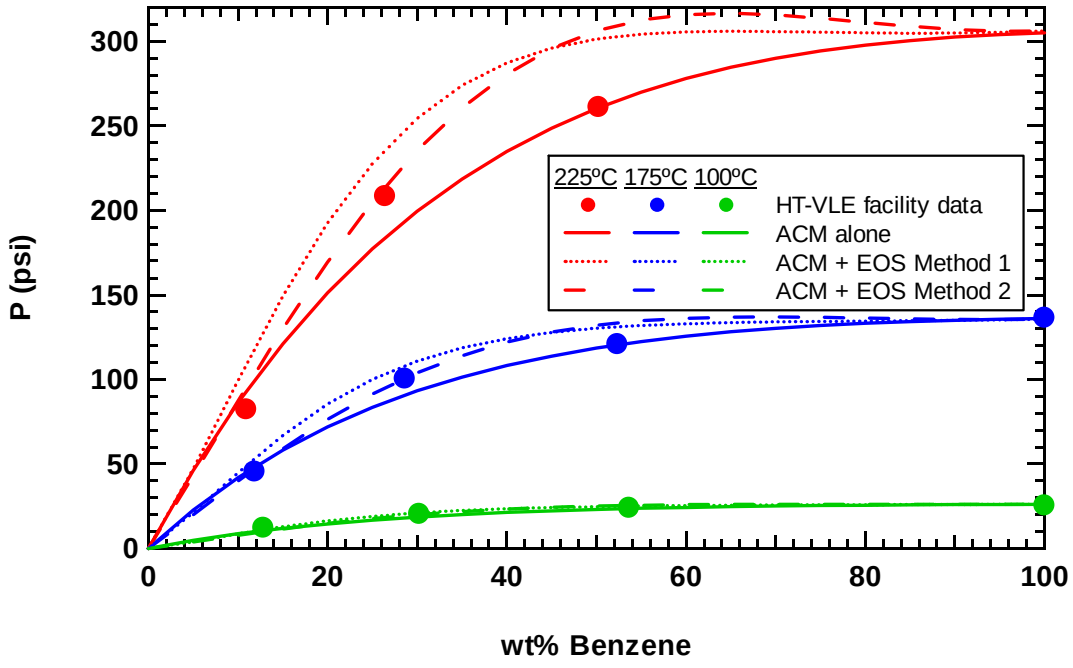

Figure D.24 Predicted pressures for the PS/benzene system from the models using the UNIFAC-ZM ACM.

D.5 PS/Furan

PS/furan system predictions are shown in Figure D.25 through Figure D.30.

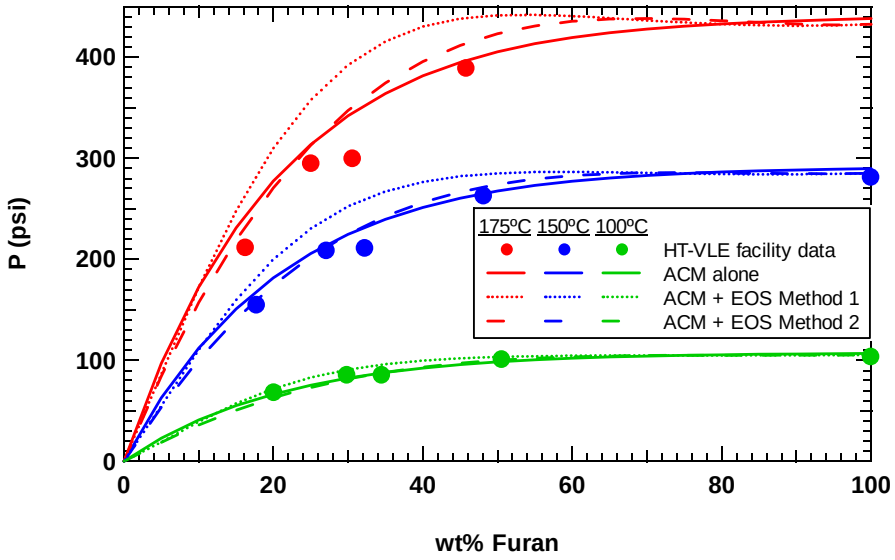

Figure D.25 Predicted pressures for the PS/furan system from the models using the Entropic-FV ACM.

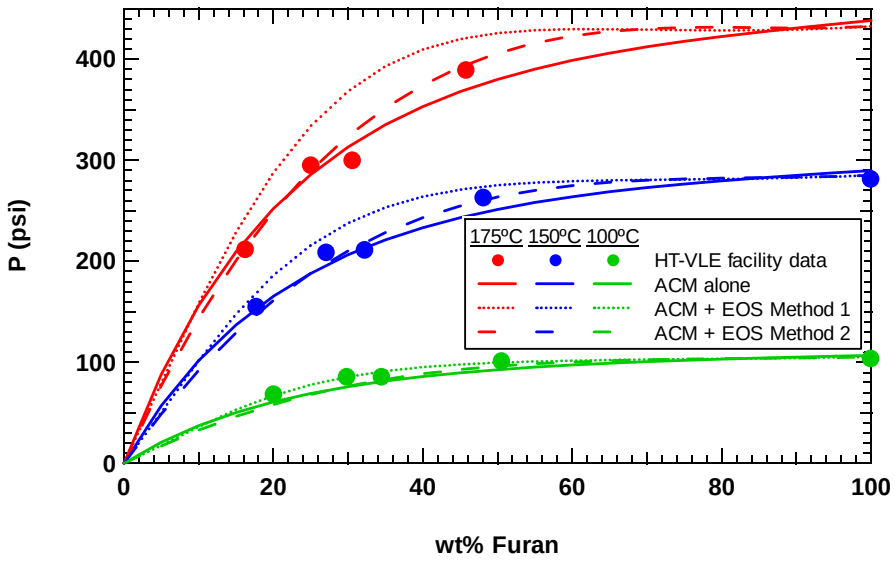

Figure D.26 Predicted pressures for the PS/furan system from the models using the Freed-FV ACM.

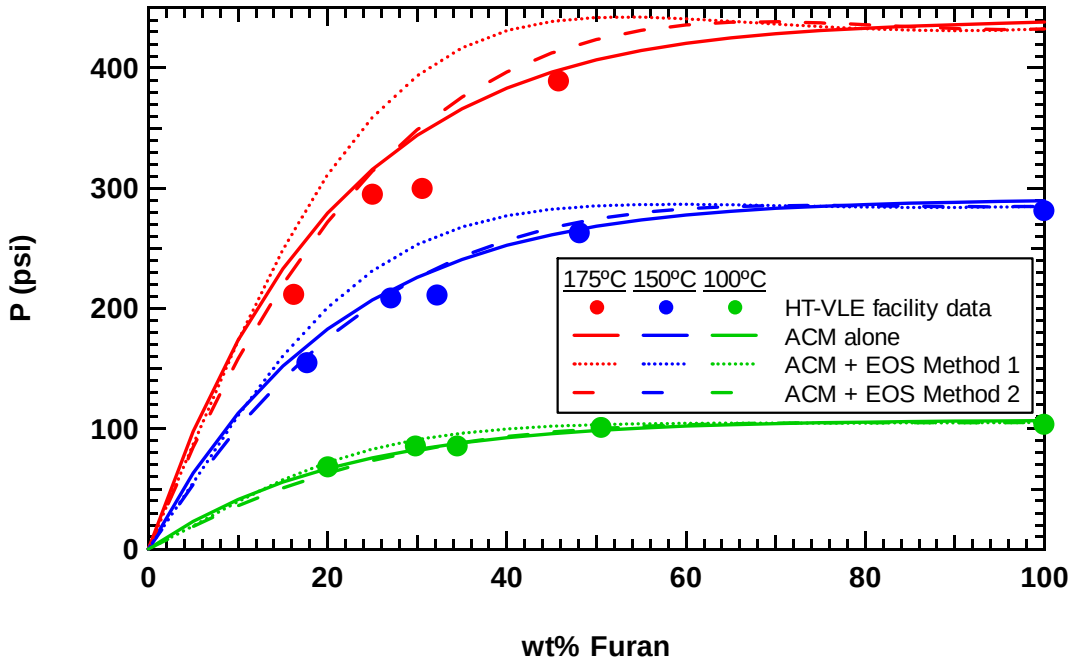

Figure D.27 Predicted pressures for the PS/furan system from the models using the GK-FV ACM.

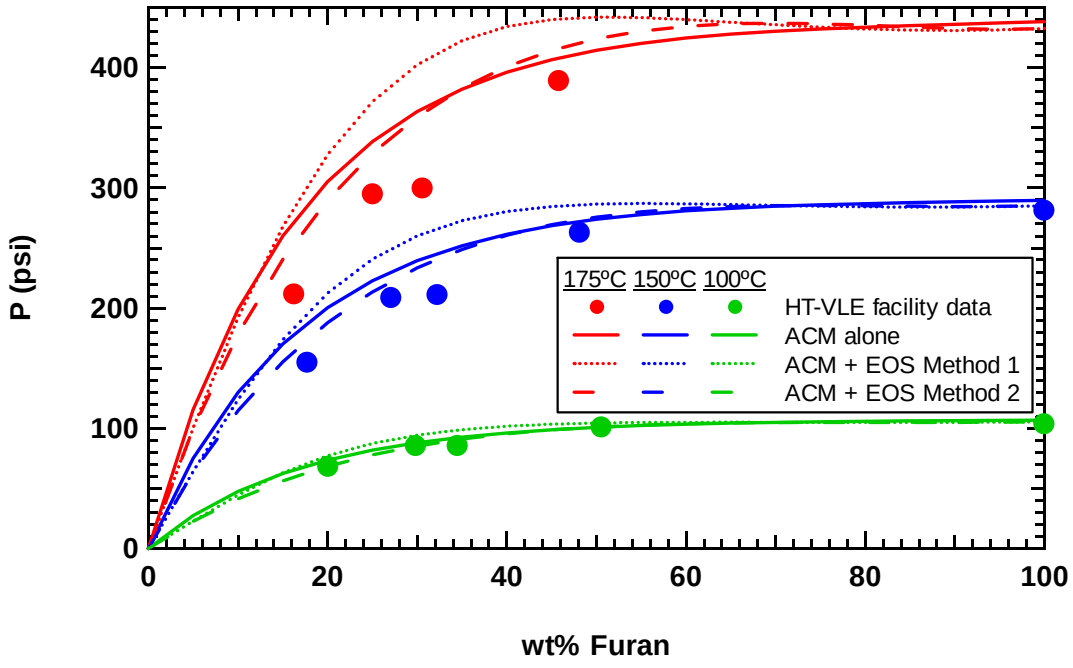

Figure D.28 Predicted pressures for the PS/furan system from the models using the MEFV ACM.

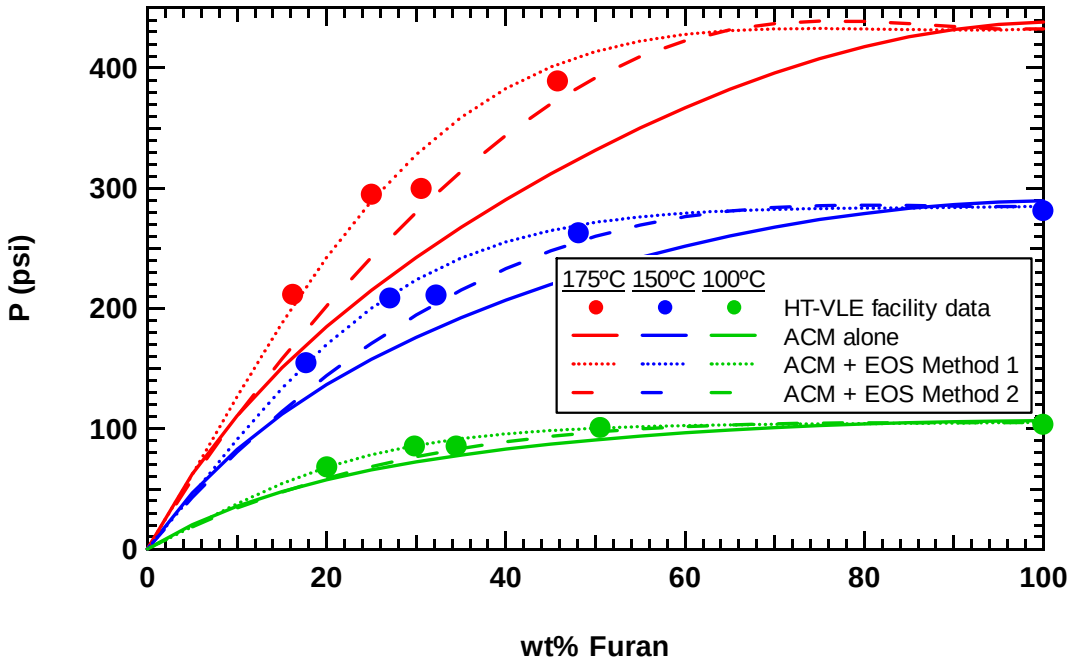

Figure D.29 Predicted pressures for the PS/furan system from the models using the UNIFAC-FV ACM.

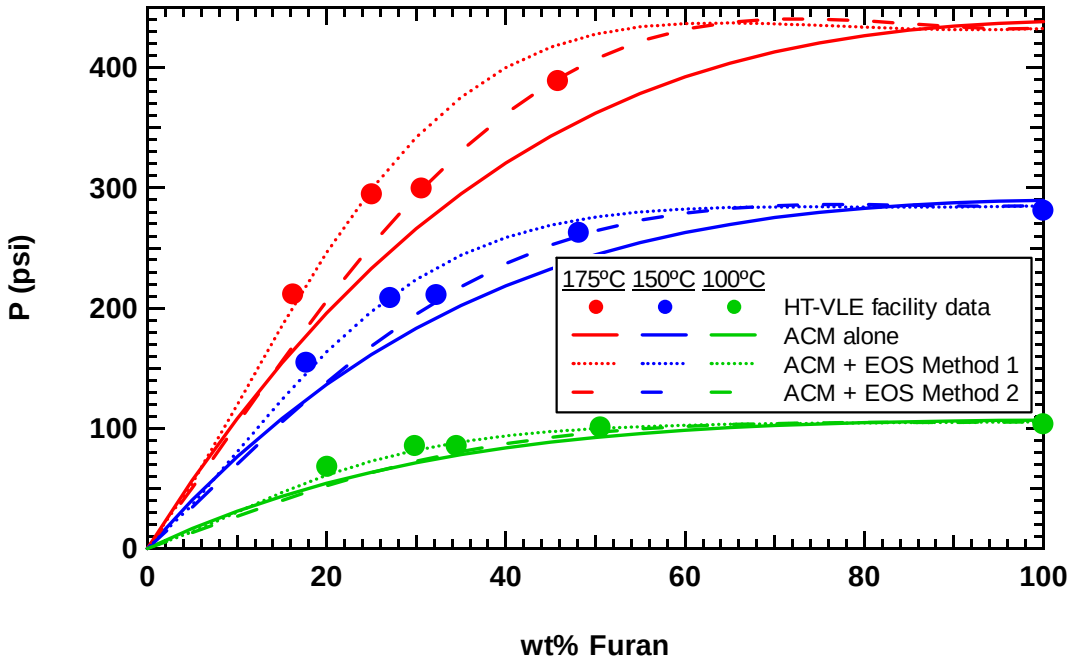

Figure D.30 Predicted pressures for the PS/furan system from the models using the UNIFAC-ZM ACM.

D.6 PS/IPP

PS/IPP system predictions are shown in Figure D.31 through Figure D.36.

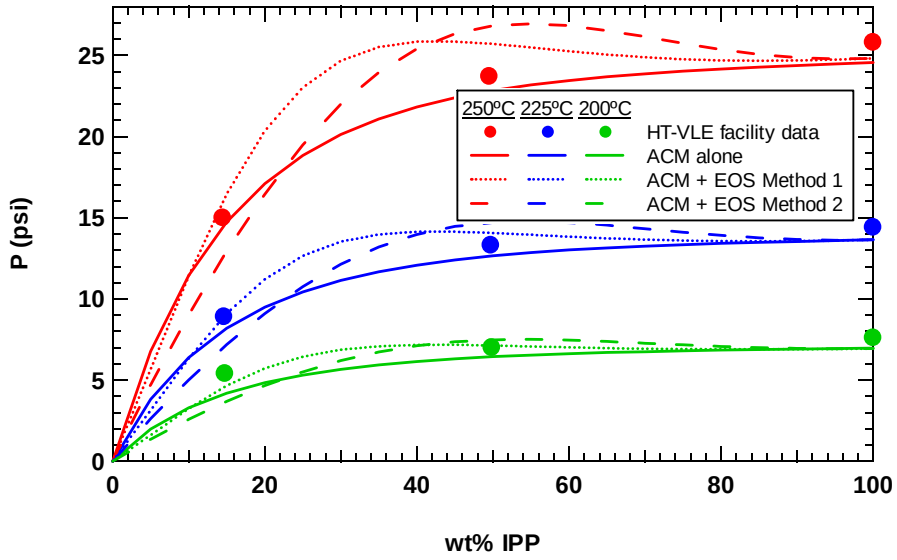

Figure D.31 Predicted pressures for the PS/IPP system from the models using the Entropic-FV ACM.

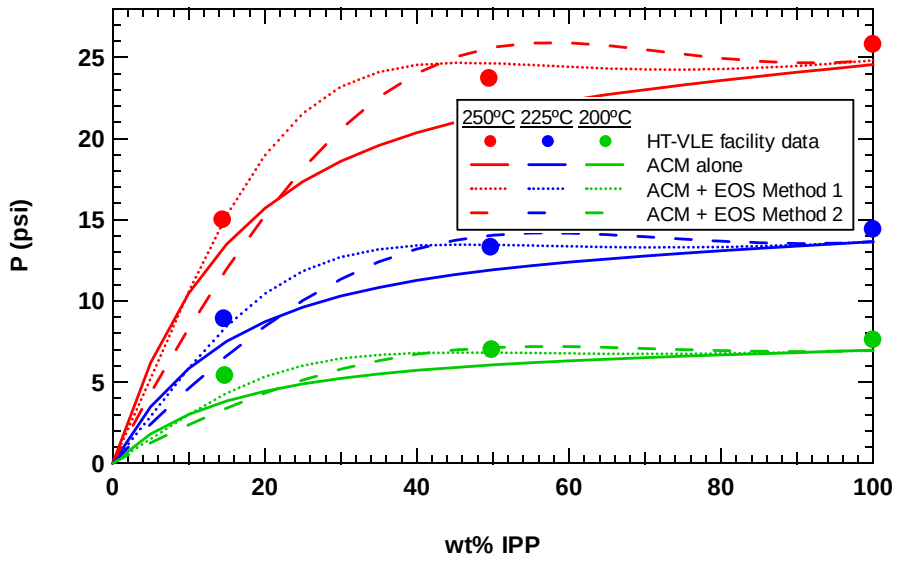

Figure D.32 Predicted pressures for the PS/IPP system from the models using the Freed-FV ACM.

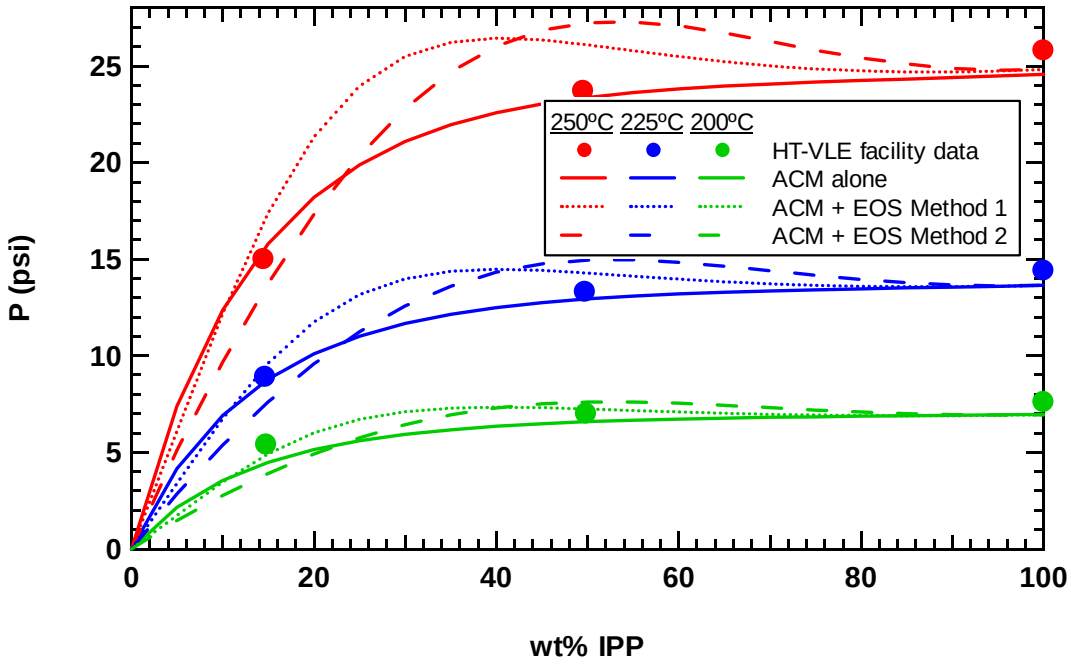

Figure D.33 Predicted pressures for the PS/IPP system from the models using the GK-FV ACM.

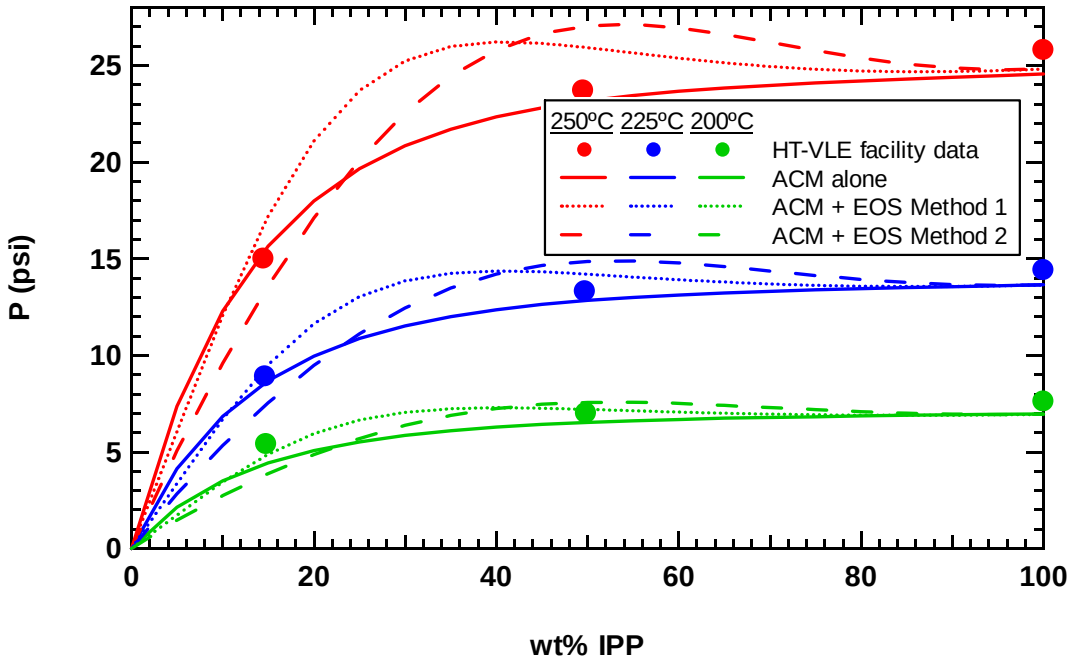

Figure D.34 Predicted pressures for the PS/IPP system from the models using the MEFV ACM.

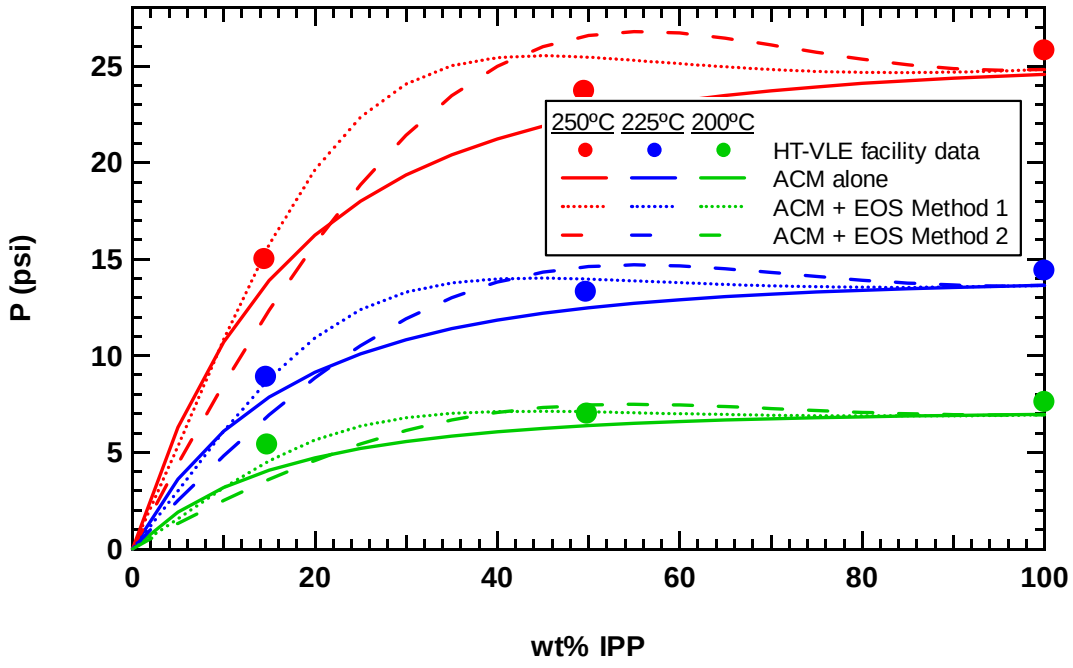

Figure D.35 Predicted pressures for the PS/IPP system from the models using the UNIFAC-FV ACM.

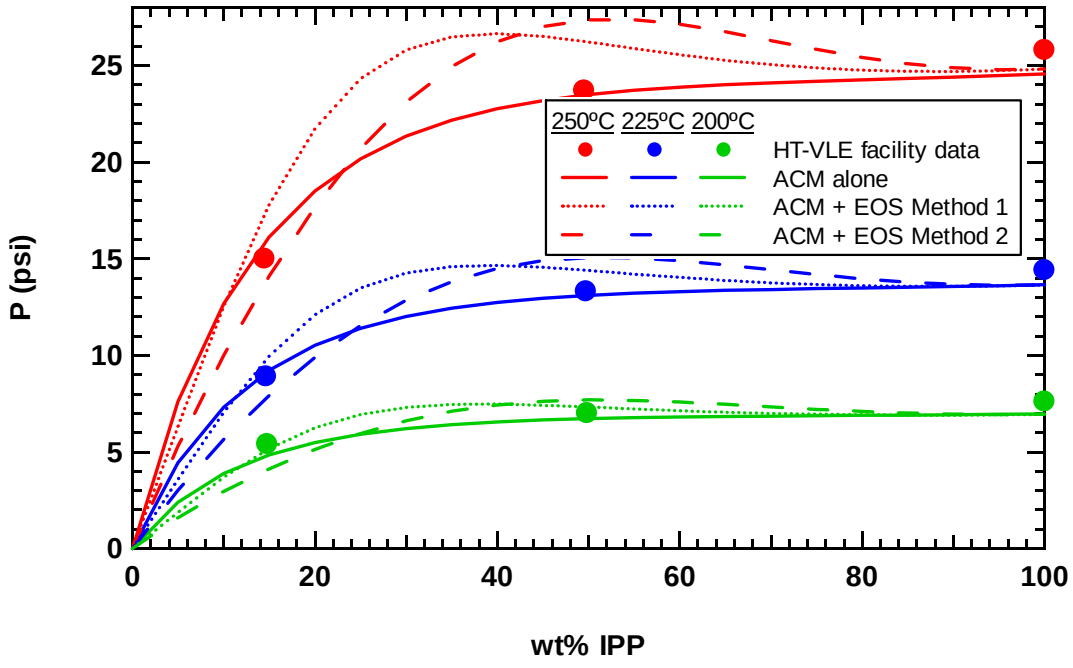

Figure D.36 Predicted pressures for the PS/IPP system from the models using the UNIFAC-ZM ACM.

Appendix E. Parameter Tables

E.1 GCVOL

The group parameters for the GCVOL volume estimation method are given in Table E.1. Aromatic carbons are designated as AC.

Table E.1 GCVOL group parameters from Ihmels and Gmehling (2003).

Group #	Group Description	A_k (cm^3/mol)	$B_k \cdot 10^3$ (cm^3/mol·K)	$C_k \cdot 10^5$ (cm^3/mol·K^2)
1	$–CH_3$	16.43	55.62	0
2	$–CH_2–$ (chain)	12.04	14.10	0
3	>CH– (chain)	7.299	-26.06	0
4	C (chain)	87.80	-619.9	88.22
5	ACH	9.929	17.41	0
6	$AC–CH_3$	24.71	21.11	0
7	$AC–CH_2–$	16.84	-4.642	0
8	AC–CH<	54.39	-290.8	33.01
9	AC–C	39.37	-272.1	24.92
10	$CH_2=$	32.69	-60.14	16.28
11	–CH=	-1.651	93.42	-14.39
12	>C=	-10.93	62.41	-14.13
13	$–CH_2OH$	36.73	-71.25	14.06
14	>CHOH	14.26	-8.187	0
15	AC–OH	46.35	-167.0	22.13
16	CH_3CO (ketone)	30.16	39.19	0
17	CH_2CO (ketone)	53.35	-179.6	28.84

Table E.1 *Continued*.

Group #	Group Description	A_k (cm^3/mol)	$B_k \cdot 10^3$ (cm^3/mol·K)	$C_k \cdot 10^5$ (cm^3/mol·K^2)
18	CHCO (ketone)	33.69	-84.87	0
19	CHO (aldehyde)	-19.91	278.2	-40.87
20	CH_3COO (ester)	53.82	-62.34	18.80
21	CH_2COO (ester)	36.32	-36.46	11.52
22	CHCOO (ester)	38.23	-112.1	16.65
23	COO (ester)	61.15	-248.2	36.81
24	ACCOO (ester)	27.61	-20.77	0
25	CH_3O (ether)	19.87	50.60	0
26	$–CH_2O–$ (ether)	13.57	26.68	0
27	>CHO– (ether)	-103.2	684.3	-105.6
28	CO– (ether)	29.91	-218.5	27.32
29	CH_2Cl	31.47	30.12	0
30	CHCl	52.97	-168.7	26.19
31	CCl	3.070	106.3	-27.09
32	$CHCl_2$	58.25	-85.68	22.37
33	CCl_3	61.39	-16.11	13.81
34	ACCl	19.86	23.09	0
35	Si	144.0	-913.9	144.0
36	SiO	41.93	-142.3	13.76
37	COH (tertiary alcohol)	-95.68	593.5	-94.79
38	–C≡CH (alkyne)	52.71	-177.9	37.37
39	–COOH	20.52	23.39	0
40	=C= (allene)	1.245	-24.51	16.50
41	CH_2 (cyclic)	15.65	5.985	0
42	CH (cyclic)	-52.95	295.6	-31.38
43	C (cyclic)	115.8	-767.0	122.6
44	$–CF_3$	8.659	218.7	-28.30
45	$–CHF_2$	14.57	123.6	-15.26
46	$–CH_2F$	-14.23	276.3	-40.00
47	ACF	10.74	28.18	0
48	–Br	36.89	-83.88	18.30
49	–I	41.02	-60.69	12.12
50	–SH (thiol)	-23.09	294.0	-42.46
51	$–CH_2S–$ (sulfide)	44.12	-105.3	17.25
52	$–CH_2SO_4CH_2–$ (sulfate)	78.77	-84.73	14.52
53	$–CH_2–NH_2$ (amine)	36.93	-67.32	18.82

Table E.1 *Continued*.

Group #	Group Description	A_k (cm^3/mol)	$B_k \cdot 10^3$ (cm^3/mol·K)	$C_k \cdot 10^5$ (cm^3/mol·K^2)
54	>CH–NH_2 (amine)	126.8	-808.7	153.4
55	>NH (secondary amine)	-0.201	63.28	-13.16
56	>N– (tertiary amine)	5.153	-39.31	0
57	AC–NH_2 (amine)	13.00	12.11	0
58	–CH_2NO_2 (nitro)	67.97	-188.2	32.73
59	AC–NO_2 (nitro)	19.92	25.38	0
60	–CN (nitrile)	17.56	20.30	0

E.2 GCMCM

The GCMCM group parameters are given in Table E.2.

Table E.2 GCMCM group parameters from Sato et al. (1998).

Group #	Group Description	$R_k \cdot 10^5$ (m^3/mol)	e_k (J/mol)	a_k	Q_k
1	–CH_3	2.0451	1011.3	0.95738	0.848
2	–CH_2–	1.4791	1581.2	0.45154	0.540
3	>CH–	0.9907	5356.1	-0.32482	0.228
4	C	0.0000	24310.4	-0.76187	0.150
5	CH=CH	2.3107	1207.4	1.43361	0.867
6	C=CH	1.8446	2624.2	0.30665	0.676
7	CO (carbonyl)	0.7641	3476.7	-0.50084	0.640
8	COO (carboxyl)	1.9362	1343.6	1.77578	1.200
9	ACH	0.9967	1599.8	0.48358	0.400
10	ACCH3	2.4136	1577.4	0.87439	0.968
11	ACCH	2.5196	4828.8	-0.26987	0.348
12	AC	1.0582	10481	-0.05594	0.120
13	ACO (ether)	1.6080	730.8	0.82654	0.360
14	ACCO (carbonyl)	1.8924	3432.7	0.76406	0.760
15	NH	0.2271	4032.6	-0.03507	0.396
16	Cl	1.6497	1433.9	1.04182	0.724
17	F	1.1130	411.1	0.63131	0.453
18	SiO	2.3265	1906	0.17246	0.466
19	OH	0.5354	1587.6	3.59353	1.200
20	O (ether)	0.5811	1334.8	0.70931	0.240

E.3 UNIFAC

The UNIFAC group volume and surface area parameters are given in Table E.3.

Table E.3 UNIFAC group volume and surface area parameters (Hansen et al., 1991).

Main Group #	Sub Group #	Group Description	R_k	Q_k
1	1	CH_3	0.9011	0.848
	2	CH_2	0.6744	0.540
	3	CH	0.4469	0.228
	4	C	0.2195	0.000
2	5	CH_2=CH	1.3454	1.176
	6	CH=CH	1.1167	0.867
	7	CH_2=C	1.1173	0.988
	8	CH=C	0.8886	0.676
	9	C=C	0.6605	0.485
3	10	ACH	0.5313	0.400
	11	AC	0.3652	0.120
4	12	$ACCH_3$	1.2663	0.968
	13	$ACCH_2$	1.0396	0.660
	14	ACCH	0.8121	0.348
5	15	OH	1.0000	1.200
6	16	CH_3OH	1.4311	1.432
7	17	H_2O	0.9200	1.400
8	18	ACOH	0.8952	0.680
9	19	CH_3CO (ketone)	1.6724	1.488
	20	CH_2CO (ketone)	1.4457	1.180
10	21	CHO (aldehyde)	0.9980	0.948
11	22	CH_3COO (ester)	1.9031	1.728
	23	CH_2COO (ester)	1.6764	1.420
12	24	HCOO (ester)	1.2420	1.188
13	25	CH_3O (ether)	1.1450	1.088
	26	CH_2O (ether)	0.9183	0.780
	27	CH-O (ether)	0.6908	0.468
	28	tetrahydrofuran	0.9183	1.100
14	29	CH_3NH_2	1.5959	1.544
	30	CH_2NH_2	1.3692	1.236
	31	$CHNH_2$	1.1417	0.924
15	32	CH_3NH	1.4337	1.244
	33	CH_2NH	1.2070	0.936
	34	CHNH	0.9795	0.624
16	35	CH_3N	1.1865	0.940
	36	CH_2N	0.9597	0.632
17	37	$ACNH_2$	1.0600	0.816

Table E.3 *Continued*.

Main Group #	Sub Group #	Group Description	R_k	Q_k
18	38	C_5H_5N (pyridine)	2.9993	2.113
	39	C_5H_4N (pyridine)	2.8332	1.833
	40	C_5H_3N (pyridine)	2.6670	1.553
19	41	CH_3CN (nitrile)	1.8701	1.724
	42	CH_2CN (nitrile)	1.6434	1.416
20	43	COOH (acid)	1.3013	1.224
	44	HCOOH (formic acid)	1.5280	1.532
21	45	CH_2Cl	1.4654	1.264
	46	CHCl	1.2380	0.952
	47	CCl	1.0060	0.724
22	48	CH_2Cl_2	2.2564	1.988
	49	$CHCl_2$	2.0606	1.684
	50	CCl_2	1.8016	1.448
23	51	$CHCl_3$	2.8700	2.410
	52	CCl_3	2.6401	2.184
24	53	CCl_4	3.3900	2.910
25	54	ACCl	1.1562	0.844
26	55	CH_3NO_2	2.0086	1.868
	56	CH_2NO_2	1.7818	1.560
	57	$CHNO_2$	1.5544	1.248
27	58	$ACNO_2$	1.4199	1.104
28	59	CS_2	2.0570	1.650
29	60	CH_3SH (thiol)	1.8770	1.676
	61	CH_2SH (thiol)	1.6510	1.368
30	62	furfural	3.1680	2.481
31	63	$(CH_2OH)_2$ (diol)	2.4088	2.248
32	64	I	1.2640	0.992
33	65	Br	0.9492	0.832
34	66	CH≡C (alkyne)	1.2920	1.088
	67	C≡C (alkyne)	1.0613	0.784
35	68	dimethylsulfoxide	2.8266	2.472
36	69	acrylonitrile	2.3144	2.052
37	70	Cl(C=C)	0.7910	0.724
38	71	ACF	0.6948	0.524
39	72	dimethylformamide	3.0856	2.736
39	73	$HCON(CH_2)_2$	2.6322	2.120
40	74	CF_3	1.4060	1.380
	75	CF_2	1.0105	0.920
	76	CF	0.6150	0.460
41	77	COO (ester)	1.3800	1.200
42	78	SiH_3	1.6035	1.2632
	79	SiH_2	1.4443	1.0063
	80	SiH	1.2853	0.7494
	81	Si	1.0470	0.4099

Table E.3 *Continued*.

Main Group #	Sub Group #	Group Description	R_k	Q_k
43	82	SiH_2O	1.4838	1.0621
	83	SiHO	1.3030	0.7639
	84	SiO	1.1044	0.4657
44	85	N-methylpyrrolidone	3.9810	3.200
45	86	CCl_3F	3.0356	2.644
	87	CCl_2F	2.2287	1.916
	88	$HCCl_2F$	2.4060	2.116
	89	HCClF	1.6493	1.416
	90	$CClF_2$	1.8174	1.648
	91	$HCClF_2$	1.9670	1.828
	92	$CClF_3$	2.1721	2.100
	93	CCl_2F_2	2.6243	2.376
46	94	$CONH_2$	1.4515	1.248
	95	$CONHCH_3$	2.1905	1.796
	96	$CONHCH_2$	1.9637	1.488
	97	$CON(CH_3)_2$	2.8589	2.428
	98	$CONCH_3CH_2$	2.6322	2.120
	99	$CON(CH_2)_2$	2.4054	1.812
47	100	$C_2H_5O_2$ (ethoxyethanol)	2.1226	1.904
	101	$C_2H_4O_2$ (ethoxyethanol)	1.8952	1.592
48	102	CH_3S	1.6130	1.368
	103	CH_2S	1.3863	1.060
	104	CHS	1.1589	0.748
49	105	morpholine	3.4740	2.796
50	106	C_4H_4S	2.8569	2.140
	107	C_4H_3S	2.6908	1.860
	108	C_4H_2S	2.5247	1.580

The UNIFAC group interaction parameters, a_{mn}, are given in Table E.4. The units of the interaction parameters are Kelvins. Parameters for group-group interactions that are unavailable are indicated with a dash.

Table E.4 UNIFAC group interaction parameters, a_{mn}, in Kelvins (Hansen et al., 1991)

Main Group	***n* = 1**	**2**	**3**	**4**	**5**	**6**	**7**	**8**
***m* = 1**	0	86.02	61.13	76.5	986.5	697.2	1318	1333
2	-35.36	0	38.81	74.15	524.1	787.6	270.6	526.1
3	-11.12	3.446	0	167	636.1	637.3	903.8	1329
4	-69.7	-113.6	-146.8	0	803.2	603.2	5695	884.9
5	156.4	457	89.6	25.82	0	-137.1	353.5	-259.7
6	16.51	-12.52	-50	-44.5	249.1	0	-181	-101.7
7	300	496.1	362.3	377.6	-229.1	289.6	0	324.5
8	275.8	217.5	25.34	244.2	-451.6	-265.2	-601.8	0
9	26.76	42.92	140.1	365.8	164.5	108.7	472.5	-133.1
10	505.7	56.3	23.39	106	529	-340.2	480.8	-155.6
11	114.8	132.1	85.84	-170	245.4	249.6	200.8	-36.72
12	329.3	110.4	18.12	428	139.4	227.8	-	-
13	83.36	26.51	52.13	65.69	237.7	238.4	-314.7	-178.5
14	-30.48	1.163	-44.85	296.4	-242.8	-481.7	-330.4	-
15	65.33	-28.7	-22.31	223	-150	-370.3	-448.2	-
16	-83.98	-25.38	-223.9	109.9	28.6	-406.8	-598.8	-
17	1139	2000	247.5	762.8	-17.4	-118.1	-341.6	-253.1
18	-101.6	-47.63	31.87	49.8	-132.3	-378.2	-332.9	-341.6
19	24.82	-40.62	-22.97	-138.4	185.4	162.6	242.8	-
20	315.3	1264	62.32	89.86	-151	339.8	-66.17	-11
21	91.46	40.25	4.68	122.9	562.2	529	698.2	-
22	34.01	-23.5	121.3	140.8	527.6	669.9	708.7	-
23	36.7	51.06	288.5	69.9	742.1	649.1	826.7	-
24	-78.45	160.9	-4.7	134.7	856.3	709.6	1201	10000
25	106.8	70.32	-97.27	402.5	325.7	612.8	-274.5	622.3
26	-32.69	-1.996	10.38	-97.05	261.6	252.6	417.9	-
27	5541	-	1824	-127.8	561.6	-	360.7	-
28	-52.65	16.62	21.5	40.68	609.8	914.2	1081	1421
29	-7.481	-	28.41	19.56	461.6	448.6	-	-
30	-25.31	82.64	157.3	128.8	521.6	-	23.48	-
31	140	-	221.4	150.6	267.6	240.8	-137.4	838.4
32	128	-	58.68	26.41	501.3	431.3	-	-
33	-31.52	174.6	-154.2	1112	524.9	494.7	-	-
34	-72.88	41.38	-	-	68.95	-	-	-
35	50.49	64.07	-2.504	-143.2	-25.87	695	-240	-
36	-165.9	573	-123.6	397.4	389.3	218.8	386.6	-
37	47.41	124.2	395.8	419.1	738.9	528	-	-
38	-5.132	-131.7	-237.2	-157.3	649.7	645.9	-	-
39	-31.95	249	-133.9	-240.2	64.16	172.2	-287.1	-
40	147.3	62.4	140.6	-	-	-	-	-
41	529	1397	317.6	615.8	88.63	171	284.4	-167.3
42	-34.36	-	787.9	-	1913	-	180.2	-
43	110.2	-	234.4	-	-	-	-	-
44	13.89	-16.11	-23.88	6.214	796.9	-	832.2	-234.7
45	30.74	-	167.9	-	794.4	762.7	-	-
46	27.97	9.755	-	-	394.8	-	-509.3	-
47	-11.92	132.4	-86.88	-19.45	517.5	-	-205.7	-
48	39.93	543.6	-	-	-	420	-	-
49	-23.61	161.1	142.9	274.1	-61.2	-89.24	-384.3	-
50	-8.479	-	23.93	2.845	682.5	597.8	-	810.5

Table E.4 *Continued*.

Main Group	*n* = 9	10	11	12	13	14	15	16
***m* = 1**	476.4	677	232.1	507	251.5	391.5	255.7	206.6
2	182.6	448.8	37.85	333.5	214.5	240.9	163.9	61.11
3	25.77	347.3	5.994	287.1	32.14	161.7	122.8	90.49
4	-52.1	586.6	5688	197.8	213.1	19.02	-49.29	23.5
5	84	-203.6	101.1	267.8	28.06	8.642	42.7	-323
6	23.39	306.4	-10.72	179.7	-128.6	359.3	-20.98	53.9
7	-195.4	-116	72.87	-	540.5	48.89	168	304
8	-356.1	-271.1	-449.4	-	-162.9	-	-	-
9	0	-37.36	-213.7	-190.4	-103.6	-	-174.2	-169
10	128	0	-110.3	766	304.1	-	-	-
11	372.2	185.1	0	-241.8	-235.7	-	-73.5	-196.7
12	385.4	-236.5	1167	0	-234	-	-	-
13	191.1	-7.838	461.3	457.3	0	-78.36	251.5	5422
14	-	-	-	-	222.1	0	-107.2	-41.11
15	394.6	-	136	-	-56.08	127.4	0	-189.2
16	225.3	-	2889	-	-194.1	38.89	865.9	0
17	-450.3	-	-294.8	-	-	-15.07	-	-
18	29.1	-	-	554.4	-156.1	-	-	-
19	-287.5	-	-266.6	99.37	38.81	-157.3	-108.5	-
20	-297.8	-165.5	-256.3	193.9	-338.5	-	-	-
21	286.3	-47.51	35.38	-	225.4	131.2	-	-
22	82.86	190.6	-133	-	-197.7	-	-	-141.4
23	552.1	242.8	176.5	235.6	-20.93	-	-	-293.7
24	372	-	129.5	351.9	113.9	261.1	91.13	316.9
25	518.4	-	-171.1	383.3	-25.15	108.5	102.2	2951
26	-142.6	-	129.3	-	-94.49	-	-	-
27	-101.5	-	-	-	-	-	-	-
28	303.7	-	243.8	-	112.4	-	-	-
29	160.6	-	-	201.5	63.71	106.7	-	-
30	317.5	-	-146.3	-	-87.31	-	-	-
31	135.4	-	152	-	9.207	-	-	-
32	138	245.9	21.92	-	476.6	-	-	-
33	-142.6	-	24.37	-	736.4	-	-	-
34	443.6	-	-	-	-	-	-	-
35	110.4	-	41.57	-	-93.51	-	-	-
36	-	354	175.5	-	-	-	-	-
37	-40.9	183.8	611.3	134.5	-217.9	-	-	-
38	-	-	-	-	167.1	-	-198.8	116.5
39	97.04	13.89	-82.12	-116.7	-158.2	49.7	-	-185.2
40	-	-	-	-	-	-	-	-
41	123.4	577.5	-234.9	145.4	-247.8	-	284.5	-
42	992.4	-	-	-	448.5	961.8	1464	-
43	-	-	-	-	-	-125.2	1604	-
44	-	-	-	-	-	-	-	-
45	-	-	-	-	-	-	-	-
46	-	-	-	-	-	-	-	-
47	156.4	-	-3.444	-	-	-	-	-
48	-	-	-	-	-	-	-	-
49	-	-	-	-	-	-	-	-
50	278.8	-	-	-	-	-	-	-

Table E.4 *Continued*.

Main Group	*n* = 17	18	19	20	21	22	23	24
***m* = 1**	920.7	287.8	597	663.5	35.93	53.76	24.9	104.3
2	749.3	280.5	336.9	318.9	-36.87	58.55	-13.99	-109.7
3	648.2	-4.449	212.5	537.4	-18.81	-144.4	-231.9	3
4	664.2	52.8	6096	872.3	-114.1	-111	-80.25	-141.3
5	-52.39	170	6.712	199	75.62	65.28	-98.12	143.1
6	489.7	580.5	53.28	-202	-38.32	-102.5	-139.4	-44.76
7	243.2	459	112.6	-14.09	325.4	370.4	353.7	497.5
8	119.9	-305.5	-	408.9	-	-	-	1827
9	6201	7.341	481.7	669.4	-191.7	-130.3	-354.6	-39.2
10	-	-	-	497.5	751.9	67.52	-483.7	-
11	475.5	-	494.6	660.2	-34.74	108.9	-209.7	54.47
12	-	-233.4	-47.25	-268.1	-	-	-126.2	179.7
13	-	213.2	-18.51	664.6	301.1	137.8	-154.3	47.67
14	-200.7	-	358.9	-	-82.92	-	-	-99.81
15	-	-	147.1	-	-	-	-	71.23
16	-	-	-	-	-	-73.85	-352.9	-262
17	0	89.7	-281.6	-396	287	-	-	822
18	117.4	0	-169.7	-153.7	-	-351.6	-114.7	-205.3
19	777.4	134.3	0	-	4.933	-152.7	-15.62	-54.86
20	493.8	-313.5	-	0	13.41	-44.7	39.63	183.4
21	429.7	-	54.32	519.1	0	108.3	249.6	62.42
22	-	587.3	258.6	543.3	-84.53	0	-	56.33
23	-	18.98	74.04	504.2	-157.1	-	0	-30.1
24	898.2	368.5	492	631	11.8	17.97	51.9	0
25	334.9	-	363.5	993.4	-129.7	-8.309	-0.2266	248.4
26	-	-	0.2827	-	113	-9.639	-	-34.68
27	134.9	2475	-	-	1971	-	-	514.6
28	-	-	335.7	-	-73.09	-	-26.06	-60.71
29	-	-	161	-	-27.94	-	-	-
30	-	-	-	570.6	-	-	48.48	-133.1
31	192.3	-	169.6	-	-	-	-	-
32	-	-	-	616.6	-	-40.82	21.76	48.49
33	-	-42.71	136.9	5256	-262.3	-174.5	-	77.55
34	-	-	329.1	-	-	-	-	-
35	-	-	-	-180.2	-	-215	-343.6	-58.43
36	-	-	-42.31	-	-	-	-	-85.15
37	-	281.6	335.2	898.2	383.2	301.9	-149.8	-134.2
38	-	159.8	-	-	-	-	-	-124.6
39	343.7	-	150.6	-97.77	-	-	-	-186.7
40	-	-	-	-	-	-	-	-
41	-22.1	-	-61.6	1179	182.2	305.4	-193	335.7
42	-	-	-	-	-	-	-	-
43	-	-	-	-	-	-	-	70.81
44	-	-	-	-	-	-	-196.2	-
45	-	-	-	-	-	-	-	-
46	-	-	-	-70.25	-	-	-	-
47	-	-	119.2	-	-	-194.7	-	3.163
48	-	-	-	-	-	-	-363.1	-11.3
49	-	-	-	-	-	-	-	-
50	-	221.4	-	-	-	-	-	-79.34

Table E.4 *Continued*.

Main Group	*n* = 25	26	27	28	29	30	31	32
***m* = 1**	11.44	661.5	543	153.6	184.4	354.6	3025	335.8
2	100.1	357.5	-	76.3	-	262.9	-	-
3	187	168	194.9	52.07	-10.43	-64.69	210.7	113.3
4	-211	3629	4448	-9.451	393.6	48.49	4975	259
5	123.5	256.5	157.1	488.9	147.5	-120.5	-318.9	313.5
6	-28.25	75.14	-	-31.09	17.5	-	-119.2	212.1
7	133.9	220.6	399.5	887.1	-	188	12.72	-
8	6915	-	-	8484	-	-	-687.1	-
9	-119.8	137.5	548.5	216.1	-46.28	-163.7	71.46	53.59
10	-	-	-	-	-	-	-	117
11	442.4	-81.13	-	183	-	202.3	-101.7	148.3
12	24.28	-	-	-	103.9	-	-	-
13	134.8	95.18	-	140.9	-8.538	170.1	-20.11	-149.5
14	30.05	-	-	-	-70.14	-	-	-
15	-18.93	-	-	-	-	-	-	-
16	-181.9	-	-	-	-	-	-	-
17	617.5	-	-139.3	-	-	-	0.1004	-
18	-	-	2845	-	-	-	-	-
19	-4.624	-0.515	-	230.9	0.4604	-	177.5	-
20	-79.08	-	-	-	-	-208.9	-	228.4
21	153	32.73	86.2	450.1	59.02	-	-	-
22	223.1	108.9	-	-	-	-	-	177.6
23	192.1	-	-	116.6	-	-64.38	-	86.4
24	-75.97	490.9	534.7	132.2	-	546.7	-	247.8
25	0	132.7	2213	-	-	-	-	-
26	132.9	0	533.2	320.2	-	-	139.8	304.3
27	-123.1	-85.12	0	-	-	-	-	2990
28	-	277.8	-	0	-	-	-	292.7
29	-	-	-	-	0	-	-	-
30	-	-	-	-	-	0	-	-
31	-	481.3	-	-	-	-	0	-
32	-	64.28	2448	-27.45	-	-	-	0
33	-185.3	125.3	4288	-	-	-	-	-
34	-	174.4	-	-	-	-	-	-
35	-	-	-	-	85.7	-	535.8	-
36	-	-	-	-	-	-	-	-
37	-	379.4	-	167.9	-	-	-	-
38	-	-	-	-	-	-	-	-
39	-	223.6	-	-	-71	-	-191.7	-
40	-	-	-	-	-	-	-	-
41	956.1	-124.7	-	885.5	-	-64.28	-264.3	288.1
42	-	-	-	-	-	-	-	-
43	-	-	-	-	-	-	-	-
44	161.5	-	-	-	-274.1	-	262	-
45	-	844	-	-	-	-	-	-
46	-	-	-	-	-	-	-	-
47	7.082	-	-	-	-	-	515.8	-
48	-	-	-	-	6.971	-	-	-
49	-	-	-	-	-	-	-	-
50	-	176.3	-	-	-	-	-	-

Table E.4 *Continued*.

Main Group	*n* = 33	34	35	36	37	38	39	40
***m* = 1**	479.5	298.9	526.5	689	-4.189	125.8	485.3	-2.859
2	183.8	31.14	179	-52.87	-66.46	359.3	-70.45	449.4
3	261.3	-	169.9	383.9	-259.1	389.3	245.6	22.67
4	210	-	4284	-119.2	-282.5	101.4	5629	-
5	202.1	727.8	-202.1	74.27	225.8	44.78	-143.9	-
6	106.3	-	-399.3	-5.224	33.47	-48.25	-172.4	-
7	-	-	-139	160.8	-	-	319	-
8	-	-	-	-	-	-	-	-
9	245.2	-246.6	-44.58	-	-34.57	-	-61.7	-
10	-	-	-	-339.2	172.4	-	-268.8	-
11	18.88	-	52.08	-28.61	-275.2	-	85.33	-
12	-	-	-	-	11.4	-	308.9	-
13	-202.3	-	128.8	-	240.2	-274	254.8	-
14	-	-	-	-	-	-	-164	-
15	-	-	-	-	-	570.9	-	-
16	-	-	243.1	-	-	-196.3	22.05	-
17	-	-	-	-	-	-	-334.4	-
18	-60.78	-	-	-	160.7	-158.8	-	-
19	-62.17	-203	-	81.57	-55.77	-	-151.5	-
20	-95	-	-463.6	-	-11.16	-	-228	-
21	344.4	-	-	-	-168.2	-	-	-
22	315.9	-	215	-	-91.8	-	-	-
23	-	-	363.7	-	111.2	-	-	-
24	146.6	-	337.7	369.5	1187.1	215.2	498.6	-
25	593.4	-	-	-	-	-	-	-
26	10.17	-27.7	-	-	10.76	-	-223.1	-
27	-124	-	-	-	-	-	-	-
28	-	-	-	-	-47.37	-	-	-
29	-	-	31.66	-	-	-	78.92	-
30	-	-	-	-	-	-	-	-
31	-	-	-417.2	-	-	-	302.2	-
32	-	-	-	-	-	-	-	-
33	0	-	32.9	-	-	-	-	-
34	-	0	-	-	2073	-	-119.8	-
35	-111.2	-	0	-	-	-	-97.71	-
36	-	-	-	0	-208.8	-	-8.804	-
37	-	631.5	-	837.2	0	-	255	-
38	-	-	-	-	-	0	-	-117.2
39	-	6.699	136.6	5.15	137.7	-	0	-5.579
40	-	-	-	-	-	185.6	55.8	0
41	627.7	-	-29.34	-53.91	-198	-	-28.65	-
42	-	-	-	-	-	-	-	-
43	-	-	-	-	-	-	-	-
44	-	-	-	-	-66.31	-	-	-
45	-	-	-	-	-	-	-	-32.17
46	-	-	-	-	-	-	-	-
47	-	-	-	-	-	-	-	-
48	-	-	-	-	148.9	-	-	-
49	-	-	-	-	-	-	-	-
50	-	-	-	-	-	-	-	-

Table E.4 *Continued*.

Main Group	*n* = 41	42	43	44	45
***m* = 1**	387.1	-450.4	252.7	220.3	-5.869
2	48.33	-	-	86.46	-
3	103.5	-432.3	238.9	30.04	-88.11
4	69.26	-	-	46.38	-
5	190.3	-817.7	-	-504.2	72.96
6	165.7	-	-	-	-52.1
7	-197.5	-363.8	-	-452.2	-
8	-494.2	-	-	-659	-
9	-18.8	-588.9	-	-	-
10	-275.5	-	-	-	-
11	560.2	-	-	-	-
12	-122.3	-	-	-	-
13	417	1338	-	-	-
14	-	-664.4	275.9	-	-
15	-38.77	448.1	-1327	-	-
16	-	-	-	-	-
17	-89.42	-	-	-	-
18	-	-	-	-	-
19	120.3	-	-	-	-
20	-337	-	-	-	-
21	63.67	-	-	-	-
22	-96.87	-	-	-	-
23	255.8	-	-	-35.68	-
24	256.5	-	233.1	-	-
25	-71.18	-	-	-209.7	-
26	248.4	-	-	-	-218.9
27	-	-	-	-	-
28	469.8	-	-	-	-
29	-	-	-	1004	-
30	43.37	-	-	-	-
31	347.8	-	-	-262	-
32	68.55	-	-	-	-
33	-195.1	-	-	-	-
34	-	-	-	-	-
35	153.7	-	-	-	-
36	423.4	-	-	-	-
37	730.8	-	-	26.35	-
38	-	-	-	-	-
39	72.31	-	-	-	-
40	-	-	-	-	111.8
41	0	-	-	-	-
42	-	0	-2166	-	-
43	-	745.3	0	-	-
44	-	-	-	0	-
45	-	-	-	-	0
46	-	-	-	-	-
47	101.2	-	-	-	-
48	-	-	-	-	-
49	-	-	-	-	-
50	-	-	-	-	-

Table E.4 *Continued*.

Main Group	*n* = 46	47	48	49	50
***m* = 1**	390.9	553.3	187	216.1	92.99
2	200.2	268.1	-617	62.56	-
3	-	333.3	-	-59.58	-39.16
4	-	421.9	-	-203.6	184.9
5	-382.7	-248.3	-	104.7	57.65
6	-	-	37.63	-59.4	-46.01
7	835.6	139.6	-	407.9	-
8	-	-	-	-	1005
9	-	37.54	-	-	-162.6
10	-	-	-	-	-
11	-	151.8	-	-	-
12	-	-	-	-	-
13	-	-	-	-	-
14	-	-	-	-	-
15	-	-	-	-	-
16	-	-	-	-	-
17	-	-	-	-	-
18	-	-	-	-	-136.6
19	-	16.23	-	-	-
20	-322.3	-	-	-	-
21	-	-	-	-	-
22	-	361.1	-	-	-
23	-	-	565.9	-	-
24	-	423.1	63.95	-	108.5
25	-	434.1	-	-	-
26	-	-	-	-	-4.565
27	-	-	-	-	-
28	-	-	-	-	-
29	-	-	-18.27	-	-
30	-	-	-	-	-
31	-	-353.5	-	-	-
32	-	-	-	-	-
33	-	-	-	-	-
34	-	-	-	-	-
35	-	-	-	-	-
36	-	-	-	-	-
37	-	-	2429	-	-
38	-	-	-	-	-
39	-	-	-	-	-
40	-	122.4	-	-	-
41	-	-	-	-	-
42	-	-	-	-	-
43	-	-	-	-	-
44	-	-	-	-	-
45	-	-	-	-	-
46	0	-	-	-	-
47	-	0	-	-	-
48	-	-	0	-	-
49	-	-	-	0	-
50	-	-	-	-	0

Appendix F. Program Source Code

The source code for the program used in this work is given below following a flowchart of the program, which shows where each subroutine or function is used.

F.1 Program Flowchart

A flowchart of the program is given in Figure F.1.

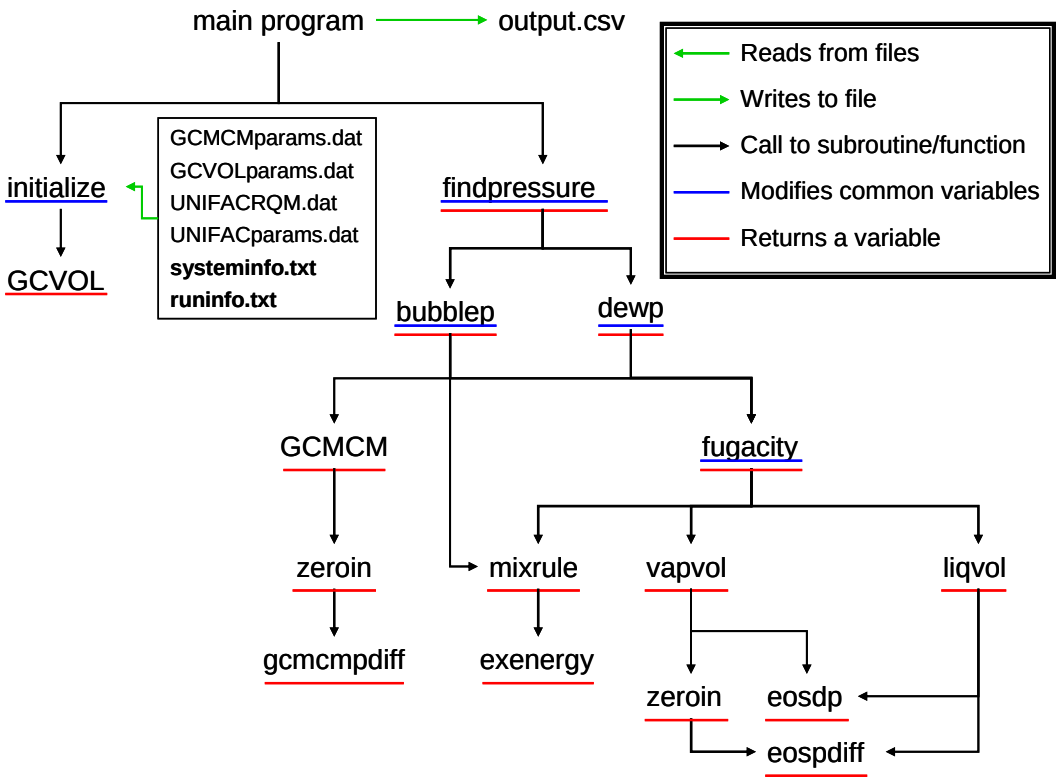

Figure F.1 Flowchart of the program used in this work.

F.2 Source Code for Subroutines and Functions

The source code for each subroutine and function used in the program is given below. The "exenergy" subroutine shown uses the UNIFAC-FV activity coefficient model. There are also two files that contain constants and common block parameters that are used throughout the program and are included in each subroutine. These files are named "constants.inc" and "common.inc."

F.2.1 Main Program

```
   program vlemulti

C-----------------------------------------------------------------------C
C MAIN PROGRAM
C-----------------------------------------------------------------------C
C This program calculates the equilibrium pressure, vapor and liquid
C mole fractions of a closed system containing multiple polymers and
C solvents whose temperature, total volume, and overall species masses
C are specified.

   implicit none

   include 'constants.inc'
   include 'common.inc'

   double precision p

   double precision findpressure

   open (unit = 20, file = outputfile)
   open (unit = 30, file = logfile)
   open (unit = 45, file = pfile)
   open (unit = 55, file = kfile)
   open (unit = 65, file = lfile)
   open (unit = 75, file = xyfile)
   open (unit = 85, file = vfile)

   call initialize ()

   p = findpressure()

   write (20,'(7(F10.7,A),F10.2,4(A,I1))')
&           zmol(1),',',zmol(2),',',xmol(1),',',xmol(2),',',
&           ymol(1),',',ymol(2),',',L,',',p,',',
&           lflag,',',kflag,',',pflag,',',vflag

   close (20)
```

```
   close (30)
   close (45)
   close (55)
   close (65)
   close (75)
   close (85)

   end program vlemulti
```

F.2.2 BubbleP

```
   double precision function bubbleP (mol)

C-----------------------------------------------------------------------C
C Bubble Point Pressure Calculation
C-----------------------------------------------------------------------C
C This function returns the bubble point pressure of the system at the
C specified temperature and at liquid mole fractions equal to the
C specified overall mole fractions.

   implicit none

   include 'constants.inc'
   include 'common.inc'

   integer i, ny, np, maxyiter, maxpiter
   logical yconv, pconv
   double precision p, fracsum, dymax, ytol, ptol
   double precision, dimension(nsmax+1) :: mol, yold, ynorm, zm
   double precision, dimension(nsmax) :: lnphiL, lnphiV

   double precision GCMCM

C Set convergence criteria for vapor mole fracs, pressure, max iters
   ytol = 1.0D-5
   ptol = 1.0D-6
   maxyiter = 30
   maxpiter = 20

C Set liquid mole fractions equal to overall mole fractions
   do i = 1, nc
      xmol(i) = mol(i)
   end do

C Establish initial guess for pressure using Raoult's law
   p= 0.0D0
   do i = 1, ns
      p = p + xmol(i) * psat(i)
   end do

C Recalculate polymer volumes and b parameters at current pressure
   do i = 1, ns
      if (3 == spectype(i)) then
         vmol(i) = GCMCM(i,p)
         b(i) = binfo(i,1) + binfo(i,2) * temp + binfo(i,3) * p
```

```
      end if
   end do

C Calculate initial guess for K, vapor mole fracs using Raoult's law
   do i = 1, ns
      K(i) = psat(i) / p
      yold(i) = K(i) * xmol(i)
      ynorm(i) = yold(i)
   end do
   yold(poly) = 0.0D0

C Pressure loop
   np = 0
   pconv = .false.
   do while (.not. pconv .and. np < maxpiter)
C     Calculate new partial fugacity coefficients for liquid
      call fugacity ('L', p, xmol, lnphiL)

C     Vapor mole fractions loop
      ny = 0
      yconv = .false.
      do while (.not. yconv .and. ny < maxyiter)
C        Calculate new partial fugacity coefficients for vapor
         call fugacity ('V', p, ynorm, lnphiV)

C        Calculate new K values and vapor mole fractions
         dymax = 0.0D0
         fracsum = 0.0D0
         do i = 1, ns
            K(i) = exp(lnphiL(i) - lnphiV(i))
            ymol(i) = xmol(i) * K(i)
            dymax = max(abs(ymol(i) - yold(i)), dymax)
            yold(i) = ymol(i)
            fracsum = fracsum + ymol(i)
         end do

C        Calculate normalized liquid mole fractions
         do i = 1, ns
            ynorm(i) = ymol(i) / fracsum
            ymol(i) = ynorm(i)
         end do

C        Check convergence and increment iteration
         if (dymax < ytol) yconv = .true.
         ny = ny + 1
      end do

C     Calculate new pressure
      p = p * fracsum

C     Recalculate polymer volumes and b parameters at current pressure
      do i = 1, ns
         if (3 == spectype(i)) then
            vmol(i) = GCMCM(i,p)
            b(i) = binfo(i,1) + binfo(i,2) * temp + binfo(i,3) * p
         end if
      end do
```

```
C     Check convergence and increment iteration
      if (abs(fracsum - 1.0D0) < ptol) pconv = .true.
      np = np + 1
   end do

   zm(1) = (mol(1)*MW(1)) / (mol(1)*MW(1)+mol(2)*MW(2)+mol(3)*MW(3))

   if (.not. pconv) then
   write (*,*) 'ERROR: P not converged at zmas(1) = ',zm(1),
&            ', T = ', temp
   end if

   if (.not. yconv) then
   write (*,*) 'ERROR: y not converged at zmas(1) = ',zm(1),
&            ', T = ', temp
   end if

   bubbleP = p

   end function bubbleP
```

F.2.3 DewP

```
   double precision function dewP (mol)

C-----------------------------------------------------------------------C
C Dew Point Pressure Calculation
C-----------------------------------------------------------------------C
C This function returns the dew point pressure of the system at the
C specified temperature and at vapor mole fractions equal to the
C specified overall mole fractions.

   implicit none

   include 'constants.inc'
   include 'common.inc'

   integer i, nx, np, maxxiter, maxpiter
   logical xconv, pconv
   double precision p, fracsum, dxmax, xtol, ptol
   double precision, dimension(nsmax+1) :: xold, xnorm, mol
   double precision, dimension(nsmax) :: lnphiL, lnphiV

   double precision GCMCM

C Set convergence criteria for liquid mole fracs, pressure, max iters
   xtol = 1.0D-5
   ptol = 1.0D-6
   maxxiter = 30
   maxpiter = 10

C Set vapor mole fractions equal to overall mole fractions
   do i = 1, nc
      ymol(i) = mol(i)
```

```
   end do

C Establish initial guess for pressure using Raoult's law
   p= 0.0D0
   do i = 1, ns
      p = p + ymol(i) / psat(i)
   end do
   p = 1.0D0 / p

C Recalculate polymer volumes and b parameters at current pressure
   do i = 1, ns
      if (3 == spectype(i)) then
         vmol(i) = GCMCM(i,p)
         b(i) = binfo(i,1) + binfo(i,2) * temp + binfo(i,3) * p
      end if
   end do

C Establish initial guess for K, liquid mole fracs using Raoult's law
   do i = 1, ns
      K(i) = psat(i) / p
      xold(i) = ymol(i) / K(i)
      xnorm(i) = xold(i)
   end do

C Pressure loop
   np = 0
   pconv = .false.
   do while (.not. pconv .and. np < maxpiter)
C     Calculate new partial fugacity coefficients for vapor
      call fugacity ('V', p, ymol, lnphiV)

C     Liquid mole fractions loop
      nx = 0
      xconv = .false.
      do while (.not. xconv .and. nx < maxxiter)
C        Calculate new partial fugacity coefficients for liquid
         call fugacity ('L', p, xnorm, lnphiL)

C        Calculate new K values and liquid mole fractions
         dxmax = 0.0D0
         fracsum = 0.0D0
         do i = 1, ns
            K(i) = exp(lnphiL(i) - lnphiV(i))
            xmol(i) = ymol(i) / K(i)
            dxmax = max(abs(xmol(i) - xold(i)), dxmax)
            xold(i) = xmol(i)
            fracsum = fracsum + xmol(i)
         end do

C        Calculate normalized liquid mole fractions
         do i = 1, ns
            xnorm(i) = xmol(i) / fracsum
            xmol(i) = xnorm(i)
         end do

C        Check convergence and increment iteration
         if (dxmax < xtol) xconv = .true.
```

```
         nx = nx + 1
      end do

C     Calculate new pressure
      p = p / fracsum

C     Recalculate polymer volumes and b parameters at current pressure
      do i = 1, ns
         if (3 == spectype(i)) then
            vmol(i) = GCMCM(i,p)
            b(i) = binfo(i,1) + binfo(i,2) * temp + binfo(i,3) * p
         end if
      end do

C     Check convergence and increment iteration
      if (abs(fracsum - 1.0D0) < ptol) pconv = .true.
      np = np + 1
   end do

   dewP = p

   end function dewP
```

F.2.4 Eosdp

```
   double precision function eosdp (v)

C-----------------------------------------------------------------------C
C First Derivative of Pressure from Equation of State
C-----------------------------------------------------------------------C
C This subroutine uses the specified temperature, molar volume and
C equation of state parameters to calculate the first derivative of the
C pressure using the:
C
C    - the Peng-Robinson equation of state

   implicit none

   include 'constants.inc'
   include 'common.inc'

   double precision aaa, bbb
   common /eosparams/ aaa, bbb

   double precision v

   eosdp = -rg*temp/(v - bbb)**2 +
&       2.0D0*aaa*(v + bbb)/(v**2 + 2.0D0*bbb*v - bbb**2)**2

   return
   end function eosdp
```

F.2.5 Eospdiff

```
   double precision function eospdiff (v)

C-----------------------------------------------------------------------C
C Pressure from Equation of State
C-----------------------------------------------------------------------C
C This subroutine uses the specified temperature, molar volume and
C equation of state parameters to calculate the difference between the
C pressure contained in ppp and the pressure calculated at v from:
C
C    - the Peng-Robinson equation of state

   implicit none

   include 'constants.inc'
   include 'common.inc'

   double precision aaa, bbb, pspec
   common /eosparams/ aaa, bbb, pspec

   double precision v

   eospdiff = rg*temp/(v-bbb) - aaa/(v**2 + 2.0D0*bbb*v - bbb**2)
   eospdiff = eospdiff - pspec

   return
   end function eospdiff
```

F.2.6 Exenergy

```
   subroutine exenergy (mol, gexrt, lngamma)

C-----------------------------------------------------------------------C
C Excess Gibbs Energy
C-----------------------------------------------------------------------C
C This subroutine uses the:
C
C    - UNIFAC-FV activity coefficient model
C
C to calculate the excess gibbs energy of the mixture and the natural
C logarithm of the activity coefficients for each component.

   implicit none

   include 'constants.inc'
   include 'common.inc'

   integer i, j, kk, m, n
   double precision gexrt
   double precision, dimension(nsmax+1) :: mol, lngamma

   double precision sumxrr, sumxqq, sumxv, sumgr, sumthgr, sum
   double precision sg, vrm
```

```
      double precision, dimension(nsmax+1) :: vr
      double precision, dimension(nsmax+1) :: phi, theta
      double precision, dimension(nsmax+1) :: lngamc, lngamfv, lngamr
      double precision, dimension(nsmax+1) :: rr, qq
      double precision, dimension(ngmax) :: Xgr, thetagr, lncapgam
      double precision, dimension(nsmax+1,ngmax) :: Xgrref, thetagrref
      double precision, dimension(nsmax+1,ngmax) :: lncapgamref
      double precision, dimension(ngmax,ngmax) :: psi
C     z is the coordination number
      double precision, parameter :: z = 10.0D0
C     c is an external degree of freedom
      double precision, parameter :: c = 1.1D0
      double precision, parameter :: third = 1.0D0 / 3.0D0

C Change zero mole fractions to almost zero to avoid later math errors
      do i = 1, ns
         if (0.0D0 == mol(i)) mol(i) = 1.0D-15
      end do

C Calculate group interaction parameters
      do i = 1, ng
         do j = 1, ng
            psi(i,j) = exp(-aij(i,j) / temp)
         end do
      end do

C Calculate volumes and surface areas and their fractions
      sumxrr = 0.0D0
      sumxqq = 0.0D0
      do i = 1, nc
         rr(i) = 0.0D0
         qq(i) = 0.0D0
         do kk = 1, ng
            rr(i) = rr(i) + nu(kk,i) * capR(kk)   !Scaled volumes
            qq(i) = qq(i) + nu(kk,i) * capQ(kk)   !Scaled surface areas
         end do
         sumxrr = sumxrr + mol(i) * rr(i)
         sumxqq = sumxqq + mol(i) * qq(i)
      end do
      do i = 1, nc
         phi(i) = mol(i) * rr(i) / sumxrr    !Volume fractions
         theta(i) = mol(i) * qq(i) / sumxqq  !Surface area fractions
      end do

C Calculate combinatorial portion of activity coefficients
      do i = 1, nc
         sg = -(log( phi(i) / theta(i) ) + 1.0D0 - phi(i) / theta(i))
&          * qq(i) * z / 2.0D0   !Staverman-Guggenheim shape correction
         lngamc(i) = log( phi(i) / mol(i) ) + 1.0D0 - phi(i) / mol(i)
         lngamc(i) = lngamc(i) + sg
      end do

C Calculate free-volume portion of activity coefficients
      sumxv = 0.0D0
      do i = 1, nc
         vr(i) = vmol(i) / 0.01517D-3 / 1.28D0 / rr(i) !Reduced volumes
         sumxv = sumxv + vmol(i) * mol(i)
```

```
      end do
      vrm = sumxv / 0.01517D-3 / 1.28 / sumxrr   !Reduced mixture volume
      do i = 1, nc
         lngamfv(i) = log( (vr(i)**third-1.0D0) / (vrm**third-1.0D0) )
&           * 3.0D0 * c
&           - c * (vr(i)/vrm - 1.0D0) / (1.0D0 - vr(i)**(-third))
      end do

C Calculate group mole fractions
      sumgr = 0.0D0
      do j = 1, nc
         do n = 1, ng
            sumgr = sumgr + nu(n,j) * mol(j)
         end do
      end do
      do m = 1, ng
         Xgr(m) = 0.0D0
         do j = 1, nc
            Xgr(m) = Xgr(m) + nu(m,j) * mol(j)
         end do
         Xgr(m) = Xgr(m) / sumgr   !Group mole fractions
      end do

C Calculate group surface area fractions
      do m = 1, ng
         sumthgr = 0.0D0
         do n = 1, ng
            sumthgr = sumthgr + capQ(n) * Xgr(n)
         end do
         thetagr(m) = capQ(m) * Xgr(m) / sumthgr !Group surface area fracs
      end do

C Calculate group residual activity coefficients
      do kk = 1, ng
         sum = 0.0D0
         do m = 1, ng
            sumthgr = 0.0D0
            do n = 1, ng
               sumthgr = sumthgr + thetagr(n) * psi(n,m)
            end do
            sum = sum + thetagr(m) * psi(kk,m) / sumthgr
         end do
         sumthgr = 0.0D0
         do m = 1, ng
            sumthgr = sumthgr + thetagr(m) * psi(m,kk)
         end do
         lncapgam(kk) = capQ(kk) * (1.0D0 - log(sumthgr) - sum) !Residual
      end do

C Calculate residual activity coefficients in ref solns of each species
      do j = 1, nc
         sumgr = 0.0D0
         do n = 1, ng
            sumgr = sumgr + nu(n,j)
         end do
         do m = 1, ng   !Group mole fractions in ref solns
            Xgrref(j,m) = nu(m,j) / sumgr
```

```
      end do
      sumthgr = 0.0D0
      do n = 1, ng
         sumthgr = sumthgr + capQ(n) * Xgrref(j,n)
      end do
      do m = 1, ng   !Group surface area fractions in ref solns
         thetagrref(j,m) = capQ(m) * Xgrref(j,m) / sumthgr
      end do
      do kk = 1, ng
         sum = 0.0D0
         do m = 1, ng
            sumthgr = 0.0D0
            do n = 1, ng
               sumthgr = sumthgr + thetagrref(j,n) * psi(n,m)
            end do
            sum = sum + thetagrref(j,m) * psi(kk,m) / sumthgr
         end do
         sumthgr = 0.0D0
         do m = 1, ng
            sumthgr = sumthgr + thetagrref(j,m) * psi(m,kk)
         end do   !Group residual in ref solns
         lncapgamref(j,kk) = capQ(kk) * (1.0D0 - log(sumthgr) - sum)
      end do
   end do

C Calculate residual portion of activity coefficients
   do i = 1, nc
      lngamr(i) = 0.0D0
      do kk = 1, ng
         lngamr(i)=lngamr(i)+nu(kk,i)*(lncapgam(kk)-lncapgamref(i,kk))
      end do
   end do

C Sum portions of activity coefficients and calculate excess energy
   gexrt = 0.0D0
   do i = 1, nc
      lngamma(i) = lngamc(i) + lngamfv(i) + lngamr(i)
      gexrt = gexrt + mol(i) * lngamma(i)
   end do

   return
   end subroutine exenergy
```

F.2.7 Findpressure

```
   double precision function findpressure ()

C-----------------------------------------------------------------------C
C Pressure Search
C-----------------------------------------------------------------------C
C This function returns the correct system pressure by comparing the
C specified total volume to the total volume calculated from the
C current pressure guess as well as the temperature, total number of
C moles and overall mole fractions.  It performs bubble point and dew
C point calculations to establish bounds for the two phase region and
```

```
C then uses a successive substitution method to converge on the correct
C pressure.

      implicit none

      include 'constants.inc'
      include 'common.inc'

      integer i, iter, maxiter
      logical molconv
      double precision p, vcalc, nL, nLold, nV
      double precision moltol, errmol, zm
      double precision pbubble, pdew, Vbubble, Vdew, vliq, vvap
      double precision am, bm
      double precision, dimension(nsmax) :: da, db
      double precision, dimension(nsmax+1) :: ntoti, nLi, nVi

      double precision flashvol, bubbleP, dewP, liqvol, vapvol

C Set convergence criteria and max number of iterations
      moltol = 1.0D-5
      maxiter = 40

C Dew point calculation
      pdew = dewP(zmol)
      write (30,'(//,T5,A,F15.3)')'Dew Point Pressure = ', pdew
      call mixrule(zmol,am,bm,da,db)
      Vdew = vapvol(temp,pdew,am,bm) * ntot
      write (30, '(T11,A,G12.5)') 'Dew point volume = ', Vdew
      write (30, '(T11,A,G12.5)') 'Specified volume is ', Vtot
      write (45,*) 'Dew Point,', pdew
      write (85,*) 'Dew Point,', Vdew
      write (75,'(A,40(A,G12.5))') 'Dew Point',
&                       (',', xmol(i), i = 1, nc),
&                       (',', ymol(i), i = 1, nc)

C Bubble point calculation
      pbubble = bubbleP(zmol)
      write (30,'(//,T5,A,F15.3)')'Bubble point pressure = ', pbubble
      call mixrule(zmol,am,bm,da,db)
      Vbubble = liqvol(temp,pbubble,am,bm) * ntot
      write (30, '(T11,A,G12.5)') 'Bubble point volume = ', Vbubble
      write (30, '(T11,A,G12.5)') 'Specified volume is ', Vtot
      write (45,*) 'Bubble Point,', pbubble
      write (85,*) 'Bubble Point,', Vbubble
      write (75,'(A,40(A,G12.5))') 'Bubble Point',
&                       (',', xmol(i), i = 1, nc),
&                       (',', ymol(i), i = 1, nc)

C Check to make sure specified volume is within two phase region
      if (Vtot < Vbubble) then
         write (*,*) 'ERROR: System does not have two phases.'
         write (*,'(T3,A,//)') '- Specified volume is too small.'
         return
      else if (Vtot > Vdew) then
         write (*,*) 'ERROR: System does not have two phases.'
         write (*,'(T3,A,//)') '- Specified volume is too large.'
```

```
      return
   end if

C Calculate overall moles of each component and use that as initial
C guess for liquid composition
   do i = 1, ns
      ntoti(i) = zmol(i) * ntot
      nLi(i) = ntoti(i)
   end do
   nL = ntot
   nV = 0.0D0

C Use bubble point as initial point and loop to find correct liquid
C composition

   iter = 1
   molconv = .false.
   do
      nLold = nL
      do i = 1, ns
         xmol(i) = nLi(i) / nLold
      end do
      p = bubbleP(xmol)
      call mixrule(xmol,am,bm,da,db)
      vliq = liqvol(temp,p,am,bm)
      call mixrule(ymol,am,bm,da,db)
      vvap = vapvol(temp,p,am,bm)
      nV = (Vtot - vliq * nLold) / vvap
      nL = ntot - nV
      do i = 1, ns
         nVi(i) = ymol(i) * nV
         nLi(i) = ntoti(i) - nVi(i)
      end do

C     Check for convergence
      errmol = abs((nL - nLold) / nL)
      if (errmol < moltol) molconv = .true.
      iter = iter + 1

      if (molconv .or. iter > maxiter) exit
   end do

   zm = zmol(1)*MW(1)/(zmol(1)*MW(1) + zmol(2)*MW(2) + zmol(3)*MW(3))

   if (.not. molconv) then
      write (*,*) 'ERROR: Liquid moles not converged.'
      write (*,*) '   T = ', temp
      write (*,*) '   Solvent weight fraction = ', zm
   end if

   findpressure = p

   return
   end function findpressure
```

F.2.8 Fugacity

```
   subroutine fugacity (ph, p, mol, lnphi)

C-----------------------------------------------------------------------C
C Partial Fugacity Coefficients
C-----------------------------------------------------------------------C
C This subroutine uses the specified temperature, pressure, and
C compostion and the:
C
C    - Peng-Robinson equation of state
C
C to calculate the partial fugacity coefficients for each solvent in
C the mixture.

   implicit none

   include 'constants.inc'
   include 'common.inc'

   integer i
   character ph
   double precision rt
   double precision p, vm, am, bm
   double precision, dimension(nsmax+1) :: mol
   double precision, dimension(ns) :: da, db, lnphi
   double precision, parameter :: sqrt2 = 1.41421356237D0

   double precision vapvol
   double precision liqvol

C Calculate mixture parameters
   call mixrule (mol, am, bm, da, db)

C Calculate mixture volume for correct phase
   if (ph .eq. 'l' .or. ph .eq. 'L') then
      vm = liqvol (temp, p, am, bm)
   else if (ph .eq. 'v' .or. ph .eq. 'V') then
      vm = vapvol (temp, p, am, bm)
   else
      write (30, *) "ERROR: Phase not correctly specified"
   end if

C Calculate partial fugacity coefficients
   rt = rg * temp
   do i = 1, ns
      lnphi(i) = db(i) * (p*vm/rt - 1) / bm - log(p*(vm-bm)/rt) +
&             am / (2*sqrt2*bm*rt) * (da(i)/am - db(i)/bm) *
&             log((vm+(1-sqrt2)*bm) / (vm+(1+sqrt2)*bm))
   end do

   return
   end subroutine fugacity
```

F.2.9 GCMCM

```
   double precision function GCMCM (s, p)

C-----------------------------------------------------------------------C
C Specific volume calculation
C-----------------------------------------------------------------------C
C This function calculates the specific volume of species s using the
C group assignments given in gcmcmnu for the:
C
C    - GCMCM method
C
C This function also makes use of the system temperature and the
C pressure.
C
C Units of system variables: temp[K], p[Pa]
C Units of parameters: R[m3/mol], e[J/mol], a[-], Q[-], MWgr[g/mol]
C Units of specific volume output: [m3/mol]

   implicit none

   include 'constants.inc'
   include 'common.inc'
   double precision tred, pred
   common /GCMCMreduced/ tred, pred

   integer s, kk, ll, vredflag
   double precision, dimension(20) :: theta
   double precision p, Mr, Vstar, estar, Tstar, M0, Pstar
   double precision sumR, sumQ, suma
   double precision vred1, vred2, vre, vae
   double precision, parameter :: z = 12
   double precision, parameter :: r = 1.07

   double precision gcmcmpdiff
   external gcmcmpdiff

   Mr = 0.0D0
   sumR = 0.0D0
   sumQ = 0.0D0
   suma = 0.0D0
   do kk = 1, 20
      Mr = Mr + gcmcmnu(kk,s) * gcmcmMWgr(kk)
      sumR = sumR + gcmcmnu(kk,s) * gcmcmR(kk)
      sumQ = sumQ + gcmcmnu(kk,s) * gcmcmQ(kk)
      suma = suma + gcmcmnu(kk,s) * gcmcma(kk)
   end do

C Convert from g/mol to kg/mol
   Mr = Mr * 1.0D-3

   M0 = Mr / suma

   do kk = 1, 20
      theta(kk) = gcmcmnu(kk,s) * gcmcmQ(kk) / sumQ
   end do
```

```
   estar = 0.0D0
   do kk = 1, 20
     do ll = 1, 20
       estar=estar+theta(kk)*theta(ll)*(gcmcme(kk)*gcmcme(ll))**0.5D0
     end do
   end do

   Vstar = sumR / Mr
   Tstar = 3.0D0 * (z - 2.0D0) * estar / rg
   Pstar = rg * Tstar / 3.0D0 / M0 / Vstar
   tred = temp / Tstar
   pred = p / Pstar

   if (temp > 0.1193233 * Tstar) then
      write (*,*) 'ERROR: T too high for GCMCM.'
   end if

   vred1 = (0.8909D0 * r)**3.0D0 + 1.0D-6
   vred2 = 1.7574D0
   vre = 1.0D-6
   vae = 0.0D0
   call zeroin (gcmcmpdiff, vred1, vred2, vre, vae, vredflag)

   if (vredflag > 2) then
      write (*,*) 'ERROR in finding GCMCM root.'
   end if

   GCMCM = vred1 * Vstar * MW(s)

   return
   end function GCMCM
```

F.2.10 Gcmcmpdiff

```
   double precision function gcmcmpdiff (vred)

C-----------------------------------------------------------------------C
C Difference in reduced pressure
C-----------------------------------------------------------------------C
C This function calculates the difference between a specified reduced
C pressure and the reduced pressure calculated from the GCMCM equation
C of state at the system temperature and the reduced volume, vred.
C This function is used with zeroin.f to find the liquid volume root at
C the system temperature and specified pressure.

   implicit none

   include 'constants.inc'
   include 'common.inc'

   double precision vred, tred, pred
   common /GCMCMreduced/ tred, pred

   double precision, parameter :: r = 1.07
```

```
   double precision, parameter :: third = 1.0D0 / 3.0D0

   gcmcmpdiff = -2.0D0/tred*(1.2045D0/vred**2.0D0-1.011/vred**4.0D0)
   gcmcmpdiff = gcmcmpdiff + vred**third / (vred**third - 0.8909D0*r)
   gcmcmpdiff = gcmcmpdiff * tred / vred - pred

   return
   end function gcmcmpdiff
```

F.2.11 GCVOL

```
   double precision function GCVOL (s)

C-----------------------------------------------------------------------C
C Specific volume calculation
C-----------------------------------------------------------------------C
C This function calculates the specific volume of species s using the
C group assignments given in gcvolnu for the:
C
C    - GCVOL method
C
C This function also makes use of the system temperature.
C
C Units of system variables: temp[K]
C Units of parameters:A[cm3/mol],B[cm3/mol·K],C[cm3/mol·K2],MWgr[g/mol]
C Units of specific volume output: [m3/mol]

   implicit none

   include 'constants.inc'
   include 'common.inc'

   integer s, i

C Sum up volume increments
   GCVOL = 0.0D0
   do i = 1, 60
      GCVOL = GCVOL +
&     gcvolnu(i,s) * (gcvolA(i)+gcvolB(i)*temp+gcvolC(i)*temp*temp)
   end do

C Convert from cm3/mol to m3/mol
   GCVOL = GCVOL * 1.0D-6

   return
   end function GCVOL
```

F.2.12 Initialize

```
   subroutine initialize

C-----------------------------------------------------------------------C
C Program Initialization
C-----------------------------------------------------------------------C
C This subroutine reads in the system and run info to set up info
C for the calculations that will be performed.

   implicit none

   include 'constants.inc'
   include 'common.inc'

   integer i, j, kk, ll, m, n, ngr, gr
   character header
   double precision MWunit, tr, kappa, alpha, nutemp
   double precision, dimension(ngmax) :: maingr, subgr
   double precision, dimension(nsmax) :: tc, pc, omega
   double precision, dimension(nsmax) :: AA, BB, CC, DD
   double precision, dimension(nsmax+1) :: wt

   double precision GCVOL

   open (unit = 901, file = 'UNIFACparams.dat', status = 'old')
   open (unit = 902, file = 'UNIFACRQM.dat', status = 'old')
   open (unit = 903, file = 'GCMCMparams.dat', status = 'old')
   open (unit = 904, file = 'GCVOLparams.dat', status = 'old')
   open (unit = 11, file = inputfile1, status = 'old')
   open (unit = 12, file = inputfile2, status = 'old')


C Initialize gcmcmnu and gcvolnu with zeros
   do kk = 1, 20
      do i = 1, nsmax+1
         gcmcmnu(kk,i) = 0.0D0
      end do
   end do
   do kk = 1, 60
      do i = 1, nsmax+1
         gcvolnu(kk,i) = 0.0D0
      end do
   end do

C Read in info from UNIFAC parameter tables
   read (901,*) header
   read (901,*) header
   read (901,*) header
   do m = 1, 50
      read (901,*) (UNIFACamn(m,n), n=1,50)
   end do

   read (902,*) header
   read (902,*) header
   do kk = 1, 108
```

```
      read (902,*) UNIFACR(kk), UNIFACQ(kk), UNIFACMWgr(kk)
   end do

C Read in info from GCMCM parameter table
   read (903,*) header
   read (903,*) header
   read (903,*) header
   do kk = 1, 20
      read (903,*) gcmcmR(kk), gcmcme(kk), gcmcma(kk),
&             gcmcmQ(kk), gcmcmMWgr(kk)
   end do

C Read in info from GCVOL parameter table
   read (904,*) header
   read (904,*) header
   read (904,*) header
   do kk = 1, 60
      read (904,*) gcvolA(kk), gcvolB(kk), gcvolC(kk), gcvolMWgr(kk)
   end do

C Read in system information
   read (11,*) header
   read (11,*) ns
   nc = ns
   poly = nsmax+1  !nc will always be equal to ns, poly not needed
   if (ns > nsmax) write(*,*)'ERROR: Too many species-increase nsmax'
   read (11,*) vtot

C Read in pure component info
   read (11,*) header
   do i = 1, ns
      read (11,*) header
      read (11,*) spectype(i)
      read (11,*) MW(i)
      if (1 == spectype(i)) then
C     Type 1: solvents w/critical info and DIPPR liquid density info
         read (11,*) tc(i)
         read (11,*) pc(i)
         read (11,*) omega(i)
         read (11,*) AA(i)
         read (11,*) BB(i)
         read (11,*) CC(i)
         read (11,*) DD(i)
      else if (2 == spectype(i)) then
C     Type 2: solvents w/critical info and GCVOL group assignments
         read (11,*) tc(i)
         read (11,*) pc(i)
         read (11,*) omega(i)
         read (11,*) header
         read (11,*) header
         read (11,*) ngr
         if (ngr > 60) write (*,*) 'ERROR: Too many GCVOL groups.'
         read (11,*) header
         do kk = 1, ngr
            read (11,*) gr, nutemp
            gcvolnu(gr,i) = nutemp
         end do
```

```
      else if (3 == spectype(i)) then
C     Type 3: polymers w/ a and b info and GCMCM group assignments
         read (11,*) a(i)
         read (11,*) binfo(i,1)
         read (11,*) binfo(i,2)
         read (11,*) binfo(i,3)
         read (11,*) header
         read (11,*) header
         read (11,*) ngr
         if (ngr > 20) write (*,*) 'ERROR: Too many GCMCM groups.'
         read (11,*) header
         do kk = 1, ngr
            read (11,*) gr, nutemp
            gcmcmnu(gr,i) = nutemp
         end do
      else
         write (*,*) 'ERROR: Invalid species type.'
      end if
   end do

C Read in UNIFAC group assignments (repeat unit for polymer)
   read (11,*) header
   read (11,*) header
   read (11,*) header
   read (11,*) ng
   if (ng > ngmax) write(*,*)'ERROR: Too many groups-increase ngmax.'
   read (11,*) header
   do kk = 1, ng
      read (11,*) maingr(kk),subgr(kk),(nu(kk,i),i=1,ns)
   end do

C Read in interaction parameters and copy (kji = kij)
   read (11,*) header
   do i = 1, nc-1
      do j = i+1, nc
         read (11,*) kij(i,j)
         kij(i,i) = 0.0D0
         kij(j,i) = kij(i,j)
      end do
   end do
   kij(nc,nc) = 0.0D0

C Read in temperature, vapor pressures and composition
   read (12,*) header
   read (12,*) temp
   do i = 1, ns
      read (12,*) header
      read (12,*) psat(i)
      read (12,*) wt(i)
   end do

C Create condensed R, Q, and aij arrays for UNIFAC groups
   do kk = 1, ng
      capR(kk) = UNIFACR(subgr(kk))
      capQ(kk) = UNIFACQ(subgr(kk))
      do ll = 1, ng
         aij(kk,ll) = UNIFACamn(maingr(kk),maingr(ll))
```

```
      end do
   end do

C Calculate overall moles and mole fractions
   ntot = 0.0D0
   do i = 1, ns
      ntot = ntot + wt(i) / MW(i)
   end do
   do i = 1, ns
      zmol(i) = wt(i) / MW(i) / ntot
   end do

C Calculate solvent EOS parameters and liquid volumes, set UNIFAC-ZM
C multipliers, adjust nu for polymers
   do i = 1, ns
      if (1 == spectype(i)) then
         vexc(i) = 1.0D0
         tr = temp / tc(i)
         kappa = 0.37464D0+1.54226D0*omega(i)-0.26992D0*omega(i)**2
         alpha = ( 1.0D0 + kappa * (1 - tr**0.5D0) )**2
         a(i) = 0.457235D0 * rg * rg * tc(i) * tc(i) * alpha /pc(i)
         b(i) = 0.077796D0 * rg * tc(i) / pc(i)
         vmol(i) = BB(i)**(1.0D0+(1.0D0-temp/CC(i))**DD(i))/AA(i)
      else if (2 == spectype(i)) then
         vexc(i) = 1.0D0
         tr = temp / tc(i)
         kappa = 0.37464D0+1.54226D0*omega(i)-0.26992D0*omega(i)**2
         alpha = ( 1.0D0 + kappa * (1 - tr**0.5D0) )**2
         a(i) = 0.457235D0 * rg * rg * tc(i) * tc(i) * alpha /pc(i)
         b(i) = 0.077796D0 * rg * tc(i) / pc(i)
         vmol(i) = GCVOL(i)
      else if (3 == spectype(i)) then
         vexc(i) = 0.6583D0
         MWunit = 0.0D0
         do kk = 1, ng
            MWunit = MWunit+nu(kk,i)*UNIFACMWgr(subgr(kk))*1.0D-3
         end do
         do kk = 1, ng
            nu(kk,i) = nu(kk,i) * MW(i) / MWunit
         end do
      end if
   end do

C Set up output file headers
   write (45,'(A)') 'np,P'
   write (55,'(A,20(A,I1,A))') 'nk', (',K(', i, ')', i = 1, ns)
   write (65,'(A)') 'nk,L'
   write (75,'(A,40(A,I1,A))') 'nk', (',x(', i, ')', i = 1, nc),
&                                    (',y(', i, ')', i = 1, nc)
   write (85,'(A)') 'np,Vcalc'

   close(901)
   close(902)
   close(903)
   close(904)
   close(11)
   close(12)
```

```
   return
   end subroutine initialize
```

F.2.13 Liqvol

```
   double precision function liqvol (temp, p, a, b)

C-----------------------------------------------------------------------C
C Liquid Molar Volume
C-----------------------------------------------------------------------C
C This subroutine uses the specified temperature, pressure and equation
C of state parameters to calculate the liquid molar volume using:
C
C    - the Peng-Robinson equation of state
C    - the bisection method

   implicit none

   include 'constants.inc'

   double precision aaa, bbb, pspec
   common /eosparams/ aaa, bbb, pspec

   integer n, nmax
   double precision temp, p, a, b
   double precision vleft, vright, vmid, pleft, pright, pmid
   double precision mult, vre

   double precision eospdiff, eosdp

C Set values of aaa, bbb, and pspec for use in eospdiff and eosdp
   aaa = a
   bbb = b
   pspec = p

C Set convergence criteria and max steps
   vre = 1.0D-7
   nmax = 500

C Find bounds for bisection method
   mult = 1.0D0 + 1.0D-10
   vleft = b * mult
   pleft = eospdiff(vleft)
   if (pleft < 0.0D0) write (*,*)'ERROR: Bound not close enough to b'
   mult = mult + 0.1D0
   vright = b * mult
   pright = eospdiff(vright)
100   n = 0
   do while (pleft*pright > 0.0D0 .and. n < nmax)
      mult = mult + 0.1D0
      vright = b * mult
      pright = eospdiff(vright)
      n = n + 1
      if (eosdp(vright) > 0.0D0) exit
```

```
   end do
   if (n == nmax) write (*,*) 'ERROR: n > nmax in liqvol.'

C Find root and check it
   do while ((vright-vleft)/vleft > vre)
      vmid = (vright+vleft) * 0.5D0
      pmid = eospdiff(vmid)
      if (pleft*pmid > 0.0D0) then
         vleft = vmid
         pleft = pmid
      else
         vright = vmid
         pright = pmid
      end if
   end do

   liqvol = (vright+vleft) * 0.5D0

   if (eosdp(liqvol) > 0.0D0) then
      write (*,*) 'ERROR: Found middle root instead of liquid root.'
      vright = vleft
      pright = pleft
      vleft = b * (1.0D0 + 1.0D-10)
      pleft = eospdiff(vleft)
      goto 100
   end if
   if ( vright > ((2.0D0*b*b + a/p)**0.5D0 - b) ) then
      write (*,*) 'ERROR: Found vapor root instead of liquid root.'
   end if

   return
   end function liqvol
```

F.2.14 Mixrule

```
   subroutine mixrule (mol, am, bm, da, db)

C-----------------------------------------------------------------------C
C Mixing Rules
C-----------------------------------------------------------------------C
C This subroutine uses the:
C
C    - Wong-Sandler (WS) mixing rules
C    - with the constant for the Peng-Robinson equation of state
C
C to calculate the mixture co-volume and energy parameters for the
C composition and temperature specified in the input.  It also
C calculates the partial molar derivatives of these parameters.

   implicit none

   include 'constants.inc'
   include 'common.inc'

   integer i, j
```

```
   double precision rt
   double precision am, bm, Q, D, gexrt
   double precision, dimension(nsmax+1) :: mol, lngamma
   double precision, dimension(nsmax+1,nsmax+1) :: bart
   double precision, dimension(nsmax) :: da, db, dQ, dD
C The parameter "c", below, is a constant for the WS mixing rules. Its
C value is specific to the PR EoS.  Equal to log(sqrt(2)-1)/sqrt(2).
   double precision, parameter :: c = -0.62322524D0

C Calculate excess gibbs energy and activity coefficients
   call exenergy (mol, gexrt, lngamma)

C Calculate the mixture parameters
   rt = rg * temp
   Q = 0.0D0
   D = 0.0D0
   do i = 1, nc
      do j = 1, nc
         bart(i,j) = (b(i) - a(i)/rt + b(j) - a(j)/rt) *
     1                   (1 - kij(i,j)) / 2.0D0
         Q = Q + mol(i) * mol(j) * bart(i,j)
       end do
      D = D + mol(i) * a(i) / b(i)
   end do
   D = D/rt + gexrt/c
   bm = Q/(1 - D)
   am = rt * D * bm

C Calculate the partial derivatives of the mixture parameters
   do i = 1, ns
      dQ(i) = 0.0D0
      do j = 1, nc
         dQ(i) = dQ(i) + mol(j) * bart(i,j)
      end do
      dQ(i) = dQ(i) * 2.0D0
      dD(i) = a(i) / b(i) / rt + lngamma(i) / c
      db(i) = dQ(i)/(1 - D) - (1 - dD(i)) * Q/(1 - D)**2
      da(i) = rt * (D * db(i) + bm * dD(i))
   end do

   return
   end subroutine mixrule
```

F.2.15 Vapvol

```
   double precision function vapvol (temp, p, a, b)

C-----------------------------------------------------------------------C
C Vapor Molar Volume
C-----------------------------------------------------------------------C
C This subroutine uses the specified temperature, pressure and equation
C of state parameters to calculate the vapor molar volume using:
C
C    - the Peng-Robinson equation of state
C    - zeroin.f
```

```
   implicit none

   include 'constants.inc'

   double precision aaa, bbb, pspec
   common /eosparams/ aaa, bbb, pspec

   integer flag
   double precision temp, p, a, b
   double precision v1, v2, vre, vae

   double precision eospdiff, eosdp
   external eospdiff

C Set values of aaa and bbb for use in eospdiff, and eosdp
   aaa = a
   bbb = b
   pspec = p

C Set convergence criteria and bounds
   vre = 1.0D-7
   vae = 0.0D0
   v1 = (2.0D0*b*b + a/p)**0.5D0 - b
   v2 = rg*temp/p + b

   if ( rg*temp/(v1-b) < 2.0D0*a/(v1*v1+2.0D0*b*v1-b*b) ) then
      write (*,*) 'ERROR: Vapor root not bounded.'
   end if

C Find root and check it
   call zeroin (eospdiff, v1, v2, vre, vae, flag)

   if (flag > 2) write (*,*) 'ERROR: Vapor root not found.'

   if (eosdp(v1) > 0.0D0) write (*,*) 'ERROR: Root is not vapor root'

   vapvol = v1

   return
   end function vapvol
```

F.2.16 Zeroin

```
      SUBROUTINE ZEROIN(F,B,C,RE,AE,IFLAG)
      IMPLICIT DOUBLE PRECISION (A-H,O-Z)
C##
      EXTERNAL F
C##
C
C     SANDIA MATHEMATICAL PROGRAM LIBRARY
C     APPLIED MATHEMATICS DIVISION 2646
C     SANDIA LABORATORIES
C     ALBUQUERQUE, NEW MEXICO  87185
C     CONTROL DATA 6600/7600  VERSION 8.1  AUGUST 1980
```

```
C                  ************************
C                  *       ISSUED BY      *
C                  *  SANDIA LABORATORIES, *
C                  *   A PRIME CONTRACTOR  *
C                  ********     TO THE     *
C                         *  UNITED STATES *
C                         *   DEPARTMENT   *
C                         *       OF       *
C                         *     ENERGY     *
C      *********************  ---NOTICE---  *********************
C      *THIS REPORT WAS PREPARED AS AN ACCOUNT OF WORK SPONSORED*
C      *  BY THE UNITED STATES GOVERNMENT.  NEITHER THE UNITED  *
C      *   STATES NOR THE UNITED STATES DEPARTMENT OF ENERGY,   *
C      *               NOR ANY OF THEIR EMPLOYEES,              *
C      * NOR ANY OF THEIR CONTRACTORS, SUBCONTRACTORS, OR THEIR *
C      * EMPLOYEES, MAKES ANY WARRANTY, EXPRESS OR IMPLIED, OR  *
C      * ASSUMES ANY LEGAL LIABILITY OR RESPONSIBILITY FOR THE  *
C      *          **********    ACCURACY,   **********          *
C      *          *        *  COMPLETENESS  *        *          *
C      *          *        *  OR USEFULNESS *        *          *
C      *          *        *     OF ANY     *        *          *
C      *          *        *  INFORMATION,  *        *          *
C      *          *        *   APPARATUS,   *        *          *
C      *       ****        *     PRODUCT    *        ****       *
C      *       *           *    OR PROCESS   *           *       *
C      *       *           *    DISCLOSED,   *           *       *
C      *       *           *   OR REPRESENTS *           *       *
C      *       *          **     THAT ITS    **          *       *
C      *       *          **   USE WOULD NOT **          *       *
C      *********          **     INFRINGE    **          *********
C                         **     PRIVATELY   **
C                         **       OWNED     **
C                         **      RIGHTS.    **
C                         **                 **
C                         **                 **
C                         **                 **
C                         ********************
C
C     BASED ON A METHOD BY T J DEKKER
C     WRITTEN BY L F SHAMPINE AND H A WATTS
C     MODIFIED FOR THE MATH LIBRARY BY C B BAILEY
C
C     ABSTRACT
C        ZEROIN SEARCHES FOR A ZERO OF A FUNCTION F(X) BETWEEN
C        THE GIVEN VALUES B AND C UNTIL THE WIDTH OF THE INTERVAL
C        (B,C) HAS COLLAPSED TO WITHIN A TOLERANCE SPECIFIED BY
C        THE STOPPING CRITERION, ABS(B-C) .LE. 2.*(RW*ABS(B)+AE).
C        THE METHOD USED IS AN EFFICIENT COMBINATION OF BISECTION AND
C        THE SECANT RULE.  IN ORDER TO INSURE THAT ZEROIN WILL CONVERGE
C        TO A ZERO, THE USER SHOULD PICK VALUES FOR B AND C AT WHICH
C        THE FUNCTION DIFFERS IN SIGN.
C
C     DESCRIPTION OF ARGUMENTS
C     F,B,C,RE AND AE ARE INPUT PARAMETERS
C     B,C AND IFLAG ARE OUTPUT PARAMETERS
C        F     - NAME OF THE REAL VALUED EXTERNAL FUNCTION.  THIS NAME
C                MUST BE IN AN EXTERNAL STATEMENT IN THE CALLING
```

```
C                PROGRAM.  F MUST BE A FUNCTION OF ONE REAL ARGUMENT.
C       B      - ONE END OF THE INTERVAL (B,C).  THE VALUE RETURNED FOR
C                B USUALLY IS THE BETTER APPROXIMATION TO A ZERO OF F.
C       C      - THE OTHER END OF THE INTERVAL (B,C)
C       RE     - RELATIVE ERROR USED FOR RW IN THE STOPPING CRITERION.
C                IF THE REQUESTED RE IS LESS THAN MACHINE PRECISION,
C                THEN RW IS SET TO APPROXIMATELY MACHINE PRECISION.
C       AE     - ABSOLUTE ERROR USED IN THE STOPPING CRITERION.  IF THE
C                GIVEN INTERVAL (B,C) CONTAINS THE ORIGIN, THEN A
C                NONZERO VALUE SHOULD BE CHOSEN FOR AE.
C       IFLAG  - A STATUS CODE.  USER MUST CHECK IFLAG AFTER EACH CALL.
C                CONTROL RETURNS TO THE USER FROM ZEROIN IN ALL CASES.
C                XERROR DOES NOT PROCESS DIAGNOSTICS IN THESE CASES.
C                 1 B IS WITHIN THE REQUESTED TOLERANCE OF A ZERO.
C                   THE INTERVAL (B,C) COLLAPSED TO THE REQUESTED
C                   TOLERANCE, THE FUNCTION CHANGES SIGN IN (B,C), AND
C                   F(X) DECREASED IN MAGNITUDE AS (B,C) COLLAPSED.
C                 2 F(B) = 0.  HOWEVER, THE INTERVAL (B,C) MAY NOT HAVE
C                   COLLAPSED TO THE REQUESTED TOLERANCE.
C                 3 B MAY BE NEAR A SINGULAR POINT OF F(X).
C                   THE INTERVAL (B,C) COLLAPSED TO THE REQUESTED
C                   TOLERANCE AND THE FUNCTION CHANGES SIGN IN (B,C)BUT
C                   F(X) INCREASED IN MAGNITUDE AS (B,C) COLLAPSED,I.E.
C                     ABS(F(B OUT)) .GT. MAX(ABS(F(B IN)),ABS(F(C IN)))
C                 4 NO CHANGE IN SIGN OF F(X) WAS FOUND ALTHOUGH THE
C                   INTERVAL (B,C) COLLAPSED TO THE REQUESTED TOLERANCE
C                   THE USER MUST EXAMINE THIS CASE AND DECIDE WHETHER
C                   B IS NEAR A LOCAL MINIMUM OF F(X), OR B IS NEAR A
C                   ZERO OF EVEN MULTIPLICITY, OR NEITHER OF THESE.
C                 5 TOO MANY (.GT. 500) FUNCTION EVALUATIONS USED.
C
C     REFERENCES
C       1.  L F SHAMPINE AND H A WATTS, ZEROIN, A ROOT-SOLVING CODE,
C           SC-TM-70-631, SEPT 1970.
C       2.  T J DEKKER, FINDING A ZERO BY MEANS OF SUCCESSIVE LINEAR
C           INTERPOLATION, *CONSTRUCTIVE ASPECTS OF THE FUNDAMENTAL
C           THEOREM OF ALGEBRA*, EDITED BY B DEJON AND P HENRICI, 1969.
C
C
C     ER IS TWO TIMES THE COMPUTER UNIT ROUNDOFF VALUE WHICH IS
C     DEFINED HERE BY THE FUNCTION BBMACH (REPLACES D1MACH).
C
      ER = 2.0D0 * BBMACH()
C
C     INITIALIZE
      RW=DMAX1(RE,ER)
      AW=DMAX1(AE,0.0D0)
      IC=0
      ACBS=DABS(B-C)
      A=C
      T=A
      FA=F(T)
      T=B
      FB=F(T)
      FC=FA
      KOUNT=2
      FX=DMAX1(DABS(FB),DABS(FC))
```

```
C
    1 IF (DABS(FC) .GE. DABS(FB)) GO TO 2
C     PERFORM INTERCHANGE
      A=B
      FA=FB
      B=C
      FB=FC
      C=A
      FC=FA
C
    2 IF (FB .EQ. 0.0D0) GO TO 11
      CMB=0.5D0*(C-B)
      ACMB=DABS(CMB)
      TOL=RW*DABS(B)+AW
C
C     TEST STOPPING CRITERION
      IF (ACMB .LE. TOL) GO TO 10
C
C     CALCULATE NEW ITERATE IMPLICITLY AS B+P/Q
C     WHERE WE ARRANGE P .GE. 0.
C     THE IMPLICIT FORM IS USED TO PREVENT OVERFLOW.
      P=(B-A)*FB
      Q=FA-FB
      IF (P .GE. 0.0D0) GO TO 3
      P=-P
      Q=-Q
C
C     UPDATE A AND CHECK FOR SATISFACTORY REDUCTION
C     IN THE SIZE OF OUR BOUNDING INTERVAL.
    3 A=B
      FA=FB
      IC=IC+1
      IF (IC .LT. 4) GO TO 4
      IF (8.0D0*ACMB .GE. ACBS) GO TO 6
      IC=0
      ACBS=ACMB
C
C     TEST FOR TOO SMALL A CHANGE
    4 IF (P .GT. DABS(Q)*TOL) GO TO 5
C
C     INCREMENT BY TOLERANCE
      B=B+DSIGN(TOL,CMB)
      GO TO 7
C
C     ROOT OUGHT TO BE BETWEEN B AND (C+B)/2.0D0
    5 IF (P .GE. CMB*Q) GO TO 6
C
C     INTERPOLATE
      B=B+P/Q
      GO TO 7
C
    6 B=0.5D0*(C+B)
C     BISECT
C
C     HAVE COMPLETED COMPUTATION FOR NEW ITERATE B
    7 T=B
      FB=F(T)
```

```
      IF (FB .EQ. 0.0D0) GO TO 11
C
C     DECIDE WHETHER NEXT STEP IS INTERPOLATION OR EXTRAPOLATION
      IF (DSIGN(1.0D0,FB) .NE. DSIGN(1.0D0,FC)) GO TO 8
      C=A
      FC=FA
    8 KOUNT=KOUNT+1
      IF (KOUNT .GT. 500) GO TO 15
      GO TO 1
C
C
C     FINISHED. PROCESS RESULTS FOR PROPER SETTING OF IFLAG
C
   10 IF (DSIGN(1.0D0,FB) .EQ. DSIGN(1.0D0,FC)) GO TO 13
      IF (DABS(FB) .GT. FX) GO TO 12
      IFLAG = 1
      RETURN
   11 IFLAG = 2
      RETURN
   12 IFLAG = 3
      RETURN
   13 IFLAG = 4
      RETURN
   15 IFLAG = 5
      RETURN
      END
      DOUBLE PRECISION FUNCTION BBMACH ()
C------------------------------------------------------------------------
C THIS ROUTINE COMPUTES THE UNIT ROUNDOFF OF THE MACHINE IN DOUBLE
C PRECISION.  THIS IS DEFINED AS THE SMALLEST POSITIVE MACHINE NUMBER
C U SUCH THAT  1.0D0 + U .NE. 1.0D0 (IN DOUBLE PRECISION).
C------------------------------------------------------------------------
      DOUBLE PRECISION U, COMP
      U = 1.0D0
 10   U = U*0.5D0
      COMP = 1.0D0 + U
      IF (COMP .NE. 1.0D0) GO TO 10
      BBMACH = U*2.0D0
      RETURN
C---------------------- END OF FUNCTION BBMACH ----------------------
      END
```

F.2.17 Common.inc

```
C Declare variables
      integer ng, ns, nc, poly, lflag, kflag, pflag, vflag
      integer, dimension(nsmax+1) :: spectype
      double precision temp, Vtot, ntot, L
      double precision, dimension(nsmax+1) :: psat, vmol, K
      double precision, dimension(nsmax+1) :: zmol, xmol, ymol, a, b,MW
      double precision, dimension(nsmax+1,nsmax+1) :: kij
      double precision, dimension(nsmax+1,3) :: binfo
      double precision, dimension(ngmax) :: capR, capQ
      double precision, dimension(ngmax,ngmax) :: aij
      double precision, dimension(ngmax,nsmax+1) :: nu
```

```
      double precision, dimension(nsmax+1) :: vexc

      double precision, dimension(108) :: UNIFACR, UNIFACQ, UNIFACMWgr
      double precision, dimension(50,50) :: UNIFACamn
      double precision, dimension(20) :: gcmcmR, gcmcme, gcmcma, gcmcmQ
      double precision, dimension(20) :: gcmcmMWgr
      double precision, dimension(20,nsmax+1) :: gcmcmnu
      double precision, dimension(60) :: gcvolA, gcvolB, gcvolC
      double precision, dimension(60) :: gcvolMWgr
      double precision, dimension(60,nsmax+1) :: gcvolnu

C Set up common blocks
      common /indexinfo/ ng, ns, nc, poly
      common /flaginfo/ lflag, kflag, pflag, vflag
      common /sysinfo/ temp, Vtot, ntot, zmol, kij
      common /pureinfo/ psat, vmol, a, b, MW, spectype, binfo
      common /flashinfo/ L, K, xmol, ymol
      common /ACMinfo/ capR, capQ, aij, nu
      common /UZMinfo/ vexc

      common /UNIFACinfo/ UNIFACR, UNIFACQ, UNIFACMWgr, UNIFACamn
      common /GCMCMinfo/ gcmcmR,gcmcme,gcmcma,gcmcmQ,gcmcmMWgr,gcmcmnu
      common /GCVOLinfo/ gcvolA, gcvolB, gcvolC, gcvolMWgr, gcvolnu
```

F.2.18 Contants.inc

```
C Specify names of external files
      character*40 inputfile1, inputfile2
      character*20 outputfile, logfile
      character*20 pfile, kfile, lfile, xyfile, vfile
      parameter (inputfile1 = 'systeminfo.txt')
      parameter (inputfile2 = 'runinfo.txt')
      parameter (outputfile = 'output.csv')
      parameter (logfile = 'log.txt')
      parameter (pfile = '01p.csv')
      parameter (kfile = '02k.csv')
      parameter (lfile = '03l.csv')
      parameter (xyfile = '04xy.csv')
      parameter (vfile = '05v.csv')

C Set values of constants
      double precision, parameter :: rg = 8.314472D0
      double precision, parameter :: pi = 3.14159265358979D0

C Specify maximum number of components
      integer, parameter :: nsmax = 5
      integer, parameter :: ngmax = 20
```

F.3 Example Input Files

Examples of the two input files used by the program, "systeminfo.txt" and "runinfo.txt" are shown below. The examples are for a mixture of toluene, bisphenol-A, and the polymer-like REF decomposition product at 200ºC.

F.3.1 Systeminfo.txt

```
***System Information
3           !Total number of species in system
29.25D-6    !Total volume of system (m3)
***Pure Component Information
**Species 1 (toluene)
1           !Species type (1:DIPPR solvent, 2:other solvent, 3:polymer)
92.1384D-3  !Molecular weight (kg/mol)
591.75D0    !Critical temperature (K)
4.1080D6    !Critical pressure (Pa)
0.264012D0  !Acentric factor
0.8792D3    !Info for DIPPR liquid density correlation - A (mol/m3)
0.27136D0   !Info for DIPPR liquid density correlation - B (-)
591.75D0    !Info for DIPPR liquid density correlation - C (K)
0.29241D0   !Info for DIPPR liquid density correlation - D (-)
**Species 2 (bisphenol-A)
1           !Species type (1:DIPPR solvent, 2:other solvent, 3:polymer)
228.2863D-3 !Molecular weight (kg/mol)
849.00D0    !Critical temperature (K)
2.9300D6    !Critical pressure (Pa)
0.945495D0  !Acentric factor
0.3773D3    !Info for DIPPR liquid density correlation - A (mol/m3)
0.25331D0   !Info for DIPPR liquid density correlation - B (-)
849.00D0    !Info for DIPPR liquid density correlation - C (K)
0.2671D0    !Info for DIPPR liquid density correlation - D (-)
**Species 3 (REF "polymer")
3           !Species type (1:DIPPR solvent, 2:other solvent, 3:polymer)
7500D-3     !Molecular weight (kg/mol)
1.40625D4   !PR-EOS energy parameter, a, for polymer (Pa·m6/mol2)
5.35125D-3  !Info for PR-EOS co-volume, b-intercept (m3/mol)
4.14750D-6  !Info for PR-EOS co-volume, b-T sensitivity (m3/mol·K)
-4.4625D-12 !Info for PR-EOS co-volume, b-P sensitivity (m3/mol·Pa)
*GCMCM group assignments
*Parameters from Sato et al., Fluid Ph Eq, 144 (1998), 427-440
11          !Number of different GCMCM groups in this species
Grp#  nu
1     7
2     43
3     16
4     2
8     3
9     18
12    4
```

```
13    4
15    4
19    5
20    2
***UNIFAC group assignments for all species
**Parameters from Hansen et al., Ind Eng Chem Res, 30 (1991), 2352-2355
**Columns after first two are species (solvents, polymer repeat unit)
16          !Total number of different UNIFAC groups
Main# Sub#  nu1   nu2   nu3
1     1     0     2     7
1     2     0     0     31
1     3     0     0     15
1     4     0     1     2
3     10    5     8     12
3     11    0     2     4
4     12    1     0     0
4     13    0     0     2
5     15    0     0     5
8     18    0     2     0
11    23    0     0     3
13    26    0     0     2
15    33    0     0     1
15    34    0     0     1
16    36    0     0     2
30    62    0     0     2
***Interaction parameters for WS mixing rules
0.19D0                  !k12
0.965D0                 !k13
0.942D0                 !k23
```

F.3.2 Runinfo.txt

```
***Composition and temperature information
473.15D0    !Temperature of system
***Species 1
2500000     !Vapor pressure at temp of system (Pa) (for initial guess)
1.431D-3    !Mass of species
***Species 2
1.0D-10     !Vapor pressure at temp of system (Pa) (for initial guess)
3.572D-3    !Mass of species
***Species 3
1.0D-10     !Vapor pressure at temp of system (Pa) (for initial guess)
3.572D-3    !Mass of species
```